MycoKeys 90: 1–18 (2022)
doi: 10.3897/mycokeys.90.83829
https://mycokeys.pensoft.net

RESEARCH ARTICLE

A peer-reviewed open-access journal
MycoKeys
Launched to accelerate biodiversity research

Four new species of Trichomonascaceae (Saccharomycetales, Saccharomycetes) from Central China

Chun-Yue Chai[1,2], Wan-Li Gao[1], Zhen-Li Yan[3], Feng-Li Hui[1,2]

1 *School of Life Science and Agricultural Engineering, Nanyang Normal University, Nanyang 473061, China* **2** *Research Center of Henan Provincial Agricultural Biomass Resource Engineering and Technology, Nanyang 473061, China* **3** *State Key Laboratory of Motor Vehicle Biofuel Technology, Henan Tianguan Enterprise Group Co., Ltd., Nanyang 473000, China*

Corresponding author: Feng-Li Hui (fenglihui@yeah.net)

Academic editor: Paul Cannon | Received 15 March 2022 | Accepted 9 May 2022 | Published 25 May 2022

Citation: Chai C-Y, Gao W-L, Yan Z-L, Hui F-L (2022) Four new species of Trichomonascaceae (Saccharomycetales, Saccharomycetes) from Central China. MycoKeys 90: 1–18. https://doi.org/10.3897/mycokeys.90.83829

Abstract

Trichomonascaceae is the largest family of ascomycetous yeast in the order Saccharomycetales. In spite of the extensive body of research on Trichomonascaceae in China, there remain new species to be discovered. Here, we describe four new species isolated from several rotting wood samples from Henan Province, Central China. Phylogenetic analysis of a combined ITS and nrLSU dataset with morphological studies revealed four new species in the Trichomonascaceae: *Diddensiella luoyangensis*, *Sugiyamaella cylindrica*, *Su. robnettiae*, and *Zygoascus detingensis*. Clustering in the *Diddensiella* clade, *D. luoyangensis*' closest neighbour was *D. transvaalensis*. Meanwhile, *Su. cylindrica* clustered in the *Sugiyamaella* clade closest to *Su. marilandica* and *Su. qingdaonensis.* Also clustering in the *Sugiyamaella* clade, *Su. robnettiae* was most closely related to *Su. chuxiongensis.* Finally, *Z. detingensis* occupied a distinct and separated basal branch from the other species of the genus *Zygoascus*. These results indicate a high species diversity of Trichomonascaceae.

Keywords

New taxa, phylogenetics, taxonomy, Trichomonascaceae, yeasts

Introduction

The family of Trichomonascaceae was described by Kurtzman and Robnett (2007) to accommodate the genera *Sugiyamaella* Kurtzman and Robnett, *Trichomonascus* (H.S. Jackson) Kurtzman and Robnett, *Wickerhamiella* van der Walt, *Zygoascus* M.Th. Smith and related anamorphs based on multigene phylogenetic analysis (Kurtzman 2011a). Subsequently, two new genera, *Spencermartinsiella* Péter, Dlauchy, Tornai-Lehoczki, M. Suzuki & Kurtzman and *Diddensiella* Péter, Dlauchy and Kurtzman were included based on multi-locus DNA sequences (Péter et al. 2011; Péter et al. 2012). This was followed by Kurtzman and Robnett (2014) in which eight genera were accepted into Trichomonascaceae while the other anamorphic species such as *Candida glaebosa* clade of the family are currently members of the polyphyletic genus *Candida* (Lachance et al. 2011; Daniel et al. 2014). The majority of taxa included in the family Trichomonascaceae form septate hyphae, but members of the genus *Wickerhamiella* do not (Kurtzman and Robnett 2007; Lachance and Kurtzman 2011) and instead the genus *Spencermartinsiella* with the type species *Spencermartinsiella europaea* form blastoconidia on small denticles (Péter et al. 2011). With the exception of *Trichomonascus farinosus* (de Hoog, Rantio-Lehtimäki & M.Th. Smith) Kurtzman & Robnett, all teleomorphic species that form septate hyphae are also heterothallic (Kurtzman and Robnett 2007; Smith et al. 2011a; Péter et al. 2012).

Members of Trichomonascaceae occur on a wide range of substrates in terrestrial and marine environments worldwide (Sakpuntoon et al. 2020), and some have ecological distribution patterns that may imply close relationships with insects. Species have been isolated either directly from insects or insect related substrates. Furthermore, the species of Trichomonascaceae are of economic importance to fields of food production, cosmetics, environment, medicine, and agriculture. For instance, several species of *Blastobotrys* von Klopotek play vital roles in production of lipids (Smith et al. 2011b; Thomas et al. 2019), while some species of *Wickerhamiella* are pathogens of humans (Lachance and Kurtzman 2011; Avchar et al. 2019; Belloch et al. 2020). Additionally, some members of *Sugiyamaella*, including *Su. bahiana* L.M. Sena et al., *Su. bonitensis* L.M. Sena et al., *Su. boreocaroliniensis* (Kurtzman) H. Urbina & M. Blackw, *Su. lignohabitans* (Kurtzman) H. Urbina & M. Blackw, *Su. valenteae* L.M. Sena et al., *Su. xylanicola* Morais, Lachance & Rosa and *Su. xylolytica* L.M. Sena et al., possess the ability to ferment D-xylose into ethanol, and three species: *Su. xylanicola*, *Su. lignohabitans*, and *Su. valenteae* are capable of producing highly active xylanases. (Kurtzman 2011b; Morais et al. 2013a, b; Sena et al. 2017). Therefore, the discovery of novel yeasts in Trichomonascaceae is of both fundamental and applied importance. Moreover, increasing our knowledge and understanding of this group of yeast may provide useful information for their sustainable utilization and conservation of natural resources.

Rotting wood, which contains diverse and abundant assimilable carbon compounds, is known to be a rich habitat for yeast species. In the past few years, thirteen species of Trichomonascaceae, including *Blastobotrys*, *Spencermartinsiella*, and *Sugiyamaella*, were obtained from rotting wood in China, which includes six new species and seven

known species (Wang et al. 2010; Guo et al. 2012; Huang et al. 2018; Chai et al. 2020; Shi et al. 2021). Although the samples of rotting wood were collected in a relatively small geographical area in China, the Trichomonascaceae species are diverse in this rich ecological environment.

During extensive investigations on the diversity of yeast inhabiting rotting wood from China, several unknown yeast strains were collected from Henan Province, and their morphology suggested species of *Diddensiella*, *Sugiyamaella*, and *Zygoascus*. To investigate their taxonomy further, phylogenetic analyses, based on combined ITS and nrLSU sequences, were carried out. Both morphological characteristics and molecular evidence demonstrate that these yeasts represent four new species of Trichomonascaceae, which are described here.

Materials and methods

Sample collection and yeast isolation

Samples of rotting wood were collected in the Tianchi Mountain National Forest Park (34°33'N, 112°28'E) located near Luoyang City, Henan Province, China. The national forest park is at 850 m above sea level (MASL) and has a continental monsoon climate. The average annual temperature is between 14 °C and 16 °C, and the average annual rainfall is greater than 800 mm. Forty samples of decaying wood were collected between September and October in 2020. Samples were stored in sterile plastic bags and transported under refrigeration to the laboratory within 24 hours. Yeast strains were isolated from rotting wood samples according to previously described methods (Huang et al. (2018) and Shi et al. (2021). One gram of each sample was added to 20 mL sterile yeast extract-malt extract (YM) broth (0.3% yeast extract, 0.3% malt extract, 0.5% peptone, 1% glucose, pH 5.0 ± 0.2), supplemented with 0.025% sodium propionate and 200 mg/L chloramphenicol in a 150 mL Erlenmeyer flask, and then cultured for 3–10 days at 180 rpm on a rotary shaker. Subsequently, 0.1 mL aliquots of the enrichment culture and appropriate decimal serial dilutions were plated on YM agar plates and incubated at 25 °C for 3–4 days. Different yeast colony morphotypes were then isolated via repeated plating on YM agar. Isolates were stored on YM agar slants at 4 °C or in 15% glycerol at −80 °C. All isolates were stored in Microbiology Lab of Nanyang Normal University (NYNU; Nanyang, China), and ex-type cultures of novel yeast were deposited in the fungal collection at Westerdijk Fungal Biodiversity Institute (CBS; Utrecht, The Netherlands). Species nomenclature and descriptions were registered in MycoBank (www.mycobank.org, accessed on February 9, 2022).

Morphological and physiological investigation

Morphological and physiological properties were determined according to methods previously described in Kurtzman et al. (2011). Carbon and nitrogen assimilation

tests were performed using liquid media and growth was observed for up to 4 weeks. Carbon fermentation was tested in yeast extract peptone (YP) base media (1% yeast extract and 2% peptone, pH 5.0 ± 0.2), and Durham tubes were used to visualise carbon dioxide production. Growth rates at a range of temperatures (30 °C, 35 °C, 37 °C, and 40 °C) were assessed by streaking cells on to yeast extract peptone glucose (YPD) agar (1% yeast extract, 2% peptone, 2% glucose, 2% agar, pH 5.0 ± 0.2) plates and incubating them for~2 weeks. Formation of true hyphae and pseudohyphae were investigated using the Dalmau plate method on both cornmeal (CM) and 5% malt extract (ME) agar plates. Induction of the sexual stage was tested by incubating single or mixed cultures of the each of the two strains on PDA agar, cornmeal (CM) agar, 5% malt extract (ME) agar, V8 (1:9) agar, Gorodkowa agar, or yeast carbon base plus 0.01% ammonium sulfate (YCBAS) agar at 25 °C for 2 months (Kurtzman 2011b; Péter et al. 2012; Nagatsuka et al. 2016).

DNA amplification and sequencing

Genomic DNA was extracted from each of the yeasts using the Ezup Column Yeast Genomic DNA Purification Kit according to the manufacturer's protocol (Sangon Biotech, China). The rDNA ITS1-5.8S-ITS2 (ITS) region was amplified using the primer pair ITS1/ITS4 (White et al. 1990). The D1/D2 domain of nrLSU rDNA (nrLSU) was amplified using the primer pair NL1/NL4 (Kurtzman and Robnett 1998). The following parameters were used to amplify the ITS and nrLSU regions: an initial denaturation step of 2 min at 95 °C, followed by 35 cycles of 30 s at 95 °C, 30 s at 51 °C, and 40 s at 72 °C, and a final extension of 10 min at 72 °C (Shi et al. 2021). PCR products were directly purified and sequenced by Sangon Biotech Inc. (Shanghai, China). The identity and quality of the newly-obtained sequences were assessed by comparing them to sequences in GenBank and assembling them with BioEdit (Hall 1999). Sequences were then submitted to GenBank (https://www. ncbi.nlm.nih.gov/genbank/; Table 1).

Phylogenetic analyses

Species in the family Trichomonascaceae with high similarity to the new species described here were selected as references in the phylogenetic analyses. *Tortispora caseinolytica* CBS 7781^{T} and *Tor. ganteri* CBS 12581^{T} were used as outgroup. NCBI accession numbers of sequences used in the phylogenetic tree are listed in Table 1. Initial alignment of the combined ITS + nrLSU dataset was performed using the online version MAFFT 6.0 (Katoh and Toh 2010) followed by manual evaluations and adjustments in BioEdit as needed to obtain reliable and high quality results (Hall 1999). The best-fit nucleotide substitution models for separate and combined nucleotide sequences were selected using jModelTest v2.1.7 (Darriba et al. 2012) according to the Akaike Information Criterion (AIC). The final concatenated sequence alignment was deposited in TreeBase (http://www.treebase.org; submission ID S29358).

Table 1. DNA sequences used in the molecular phylogenetic analysis.

Species	Strain	Locality	Sample	ITS	D1/D2
Blastobotrys indianensis	CBS 9600^{T}	USA	White fungus	NR_153638	NG_055333
Diddensiella caesifluorescens	CBS 12613^{T}	Hungary	Rotten wood	JF895509	GU195654
D. santjacobensis	CBS 8183^{T}	USA	Fallen trunk	NR_151808	NG_058985
D. transvaalensis	CBS 6663^{T}	South Africa	Forest litter	N/A	DQ442702
D. luoyangensis	**NYNU 201062^{T}**	**China**	**Rotten wood**	**MW374289**	**MW362346**
D. luoyangensis	**NYNU 201074**	**China**	**Rotten wood**	**MW374461**	**MW374460**
Middelhovenomyces petrohuensis	CBS 8173^{T}	Chile	Rotten trunk	NR_156314	NG_055211
Middelhovenomyces tepae	CBS 5115^{T}	Chile	Decaying tepa tree	NR_154200	NG_055181
Spencermartinsiella cellulosicola	CBS 11952^{T}	China	Rotten wood	NR_151783	NG_055207
Sp. europaea	CBS 11730^{T}	Hungary	Rotten wood	NR_111481	NG_042528
Sp. ligniputridi	CBS 12585^{T}	Hungary	Rotten wood	NR_155842	NG_055382
Sp. silvicola	CBS 11952^{T}	Brazil	Rotting wood	KT222943	KC906243
Sugiyamaella americana	CBS 10352^{T}	USA	Frass	NR_137759	DQ438193
Su. Ayubii	CBS 14108^{T}	Brazil	Rotting wood	NR_155796	KR184132
Su. Bahiana	CBS 13474^{T}	Brazil	Rotting wood	NR_155810	KC959941
Su. Bonitensis	CBS 14270^{T}	Brazil	Rotting wood	NR_155798	KT006004
Su. Boreocaroliniensis	NRRL YB-1835^{T}	USA	Frass	NR_165963	DQ438221
Su. Bullrunensis	CBS 11840^{T}	USA	Insect	NR_111543	HM208601
Su. Castrensis	NRRL Y-17329^{T}	Chile	Rotting wood	NR_111229	DQ438195
Su. Carassensis	CBS 14107^{T}	Brazil	Rotting wood	NR_155808	KX550111
Su. Chiloensis	CBS 8168^{T}	Chile	Rotted wood	DQ911454	DQ438217
Su. Chuxiongensis	NYNU 181038^{T}	China	Rotting wood	MK682800	MK682795
Su. cylindrica	**NYNU 201067^{T}**	**China**	**Rotting wood**	**MW368732**	**MW368731**
Su. Cylindrica	**NYNU 201034**	**China**	**Rotting wood**	**OM501585**	**OM501589**
Su. Floridensis	NRRL YB-3827^{T}	USA	Frass	NR_111230	DQ438222
Su. grinbergsii	NRRL Y-27117^{T}	Chile	Insect	KY102116	DQ438199
Su. Japonica	CBS 10354^{T}	Japan	Frass	NR_111239	DQ438202
Su. Ligni	CBS 13482^{T}	Brazil	Rotting wood	KX550112	KX550112
Su. lignohabitans	NRRL YB-1473^{T}	USA	Decayed log	NR_119622	DQ438198
Su. marionensis	NRRL YB-1336^{T}	USA	Decayed log	NR_111237	DQ438197
Su. marilandica	NRRL YB-1847^{T}	USA	Frass	NR_165965	DQ438219
Su. mastotermitis	CBS 14182^{T}	Berlin	Termite	NR_156606	KU883286
Su. neomexicana	CBS 10349^{T}	USA	Frass	NR_165966	DQ438201
Su. novakii	NRRL Y-27346^{T}	Hungary	Rotting wood	NR_111235	DQ438196
Su. paludigena	NRRL Y-12697^{T}	Russia	Peat	NR_111236	DQ438194
Su. pinicola	CBS 10348^{T}	USA	Frass	NR_165967	DQ438200
Su. qingdaonensis	CBS 11390^{T}	China	Rotting wood	NR_151806	FJ613527
Su. robnettiae	**NYNU 201066^{T}**	**China**	**Rotting wood**	**MW368730**	**MW368701**
Su. robnettiae	**NYNU 201005**	**China**	**Rotting wood**	**OM501584**	**OM501586**
Su. smithiae	CBS 7522.2^{T}	Brazil	Soil	DQ911455	DQ438218
Su. trypani	CBS 15876^{T}	Poland	Soil	MK388412	MK387312
Su. valdiviana	NRRL Y-7791^{T}	Chile	Rotting wood	NR_111544	DQ438220
Su. valenteae	CBS 14109^{T}	Brazil	Rotting wood	NR_155797	KT005999
Su. xiaguanensis	NYNU 161041^{T}	China	Rotting wood	KY213802	KY213817
Su. xylanicola	CBS 12683^{T}	Brazil	Rotting wood	KC493642	KC493642
Su. xylolytica	CBS 13493^{T}	Brazil	Rotting wood	KU214874	KF889433
Su. yunnanensis	NYNU 161059^{T}	China	Rotting wood	MT257259	MT257257
Tortispora ganteri	CBS 12581^{T}	Mexico	Necrotic plant tissue	NR_154483	KC681893
Tortispora caseinolytica	CBS 7781^{T}	USA	Necrotic plant tissue	NR_154482	NG_055343
Trichomonascus petasosporus	CBS 9602^{T}	USA	Frass	NR_155940	NG_055332
Zygoascus biomembranicola	CBS 14157^{T}	Japan	Viscous gel	NR_156007	LC060997
Z. bituminiphila	CBS 8813^{T}	Canada	Tar	NR_137545	NG_055308
Z. hellenicus	CBS 5839^{T}	Germany	Mastitic bovine udder	NR_111258	NG_055323

Species	Strain	Locality	Sample	ITS	D1/D2
Z. meyerae	CBS 4099^{T}	Greece	Fermenting grape must	AY447022	DQ438189
Z. ofunaensis	CBS 8129^{T}	Japan	Soil	N/A	NG_066348
Z. polysorbophila	CBS 7317^{T}	Japan	Viscous gel	NR_160311	NG_064312
Z. tannicola	CBS 6065^{T}	France	Vegetable tanning fluid	KY106018	NG_058446
Z. detingensis	**NYNU 201087^{T}**	**China**	**Rotting wood**	**MW374088**	**MW368733**
Z. detingensis	**NYNU 201011**	**China**	**Rotting wood**	**OM501590**	**OM501591**

Notes: Metabolically inactive ex-type strains are indicated by "T" after the species name; "N/A" means that sequences were not available; Bold indicates strains that were isolated in this study.

Maximum likelihood (ML) and Bayesian inference (BI) analyses were used for the phylogenetic analyses. The ML analysis was carried out using RAxmL v.7.2.8 with a GTR + G + I, model of site substitution including estimation of Gamma-distributed rate heterogeneity and a proportion of invariant sites (Stamatakis 2006). Branch support was evaluated using bootstrapping with 1000 replicates (Hillis and Bull 1993). The BI analysis was performed using MrBayes v3.2 (Ronquist et al. 2012), for two independent runs, each with four Markov chains Monte Carlo (MCMC) independent runs for 5 $\times 10^6$ generations (split frequencies = 0.011). The first 25% of trees were discarded as "burn-in" of each analysis and the remaining 75% were then used to calculate Bayesian posterior probabilities of the majority rule consensus tree.

Phylogenetic trees from the ML and BI analyses were visualised with FigTree v1.4.3 (Rambaut 2016) and edited in Adobe Illustrator CS6. Branches that received bootstrap support for maximum likelihood (BS) and Bayesian posterior probabilities (BPP) greater than or equal to 50% (BS) and 0.95 (BPP) were considered to be significantly supported.

Results

Molecular phylogenetic analysis

The combined ITS and nrLSU dataset was analysed to infer the phylogenetic relationships of the family Trichomonascaceae and the new Chinese isolates. The dataset consisted of 59 sequences including the outgroup, *Tortispora caseinolytica* CBS 7781^{T} and *Tor. ganteri* CBS 12581^{T}. A total of 943 characters including gaps (376 for ITS and 567 for nrLSU) were included in the phylogenetic analysis. GTR + I + G was inferred as the best-fit model for the combined nrLSU and ITS nucleotide sequences according to the AIC in jModelTest v2.1.7 (Darriba et al. 2012). The topologies of the phylogenetic tree of ML and BI analyses are identical, and only the ML tree with a final optimisation likelihood value of –12097.50 is shown in Fig. 1. RAxML bootstrap support values (BS) ≥ 50% and Bayesian posterior probability values (BPP) ≥ 0.95 are shown above the branches and indicated with bolded lines.

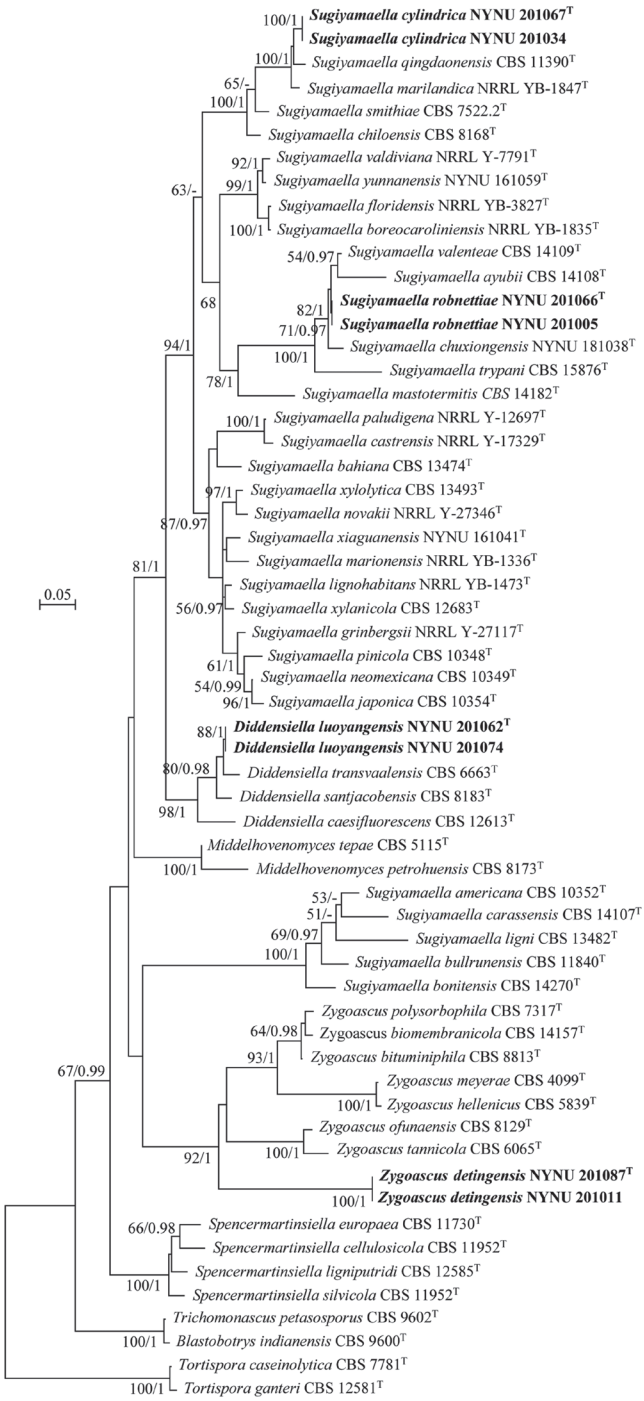

Figure 1. Maximum-likelihood phylogenetic tree based on ITS and nrLSU nucleotide sequences. Bootstrap values (BP) ≥ 50% from ML analysis and Bayesian posterior probabilities (BPP) ≥ 0.95 are shown on the branches. Newly described species are indicated in bold and their metabolically inactive ex-type strains are indicated by "T" after the species name.

In the phylogeny (Fig. 1), newly generated strains in this study nested in the genera *Diddensiella*, *Sugiyamaella*, and *Zygoascus* within the Trichomonascaceae. *D. luoyangensis* clustered in the *Diddensiella* clade with an affinity to *D. santjacobensis* (C. Ramírez & A. González) Péter, Dlauchy & Kurtzman and *D. transvaalensis* (Kurtzman) Péter, Dlauchy & Kurtzman. *Su. cylindrica* and *Su. robnettiae* clustered in the *Sugiyamaella* clade with close similarity to the type species *Su. smithiae* (Giménez-Jurado) Kurtzman and Robnett (2007), and to other related species with high bootstrap support (BS = 94%; BPP = 1.0). Additionally, *Su. cylindrica* clustered together with *Su. marilandica* (Kurtzman) H. Urbina & M. Blackw and *Su. qingdaonensis* (F.L. Li & S.A. Wang) Handel, Wang, Yurkov & König with strong bootstrap support (BS 100%, BPP 1.0), while *Su. robnettiae* formed a separate lineage within *Sugiyamaella* that included *Su. ayubii* L.M. Sena et al., *Su. chuxiongensis* C.Y. Chai & F.L. Hui, and *Su. valenteae* L.M. Sena et al. *Z. detingensis* formed a unique branch of the tree which was clearly distinct and diverged from other species of *Zygoascus*.

Taxonomy

Diddensiella luoyangensis **C.Y. Chai & F.L. Hui, sp. nov.**
MycoBank No: 842899
Fig. 2

Etymology. The specific epithet *luoyangensis* refers to the geographic origin of the type strain: Luoyang City, Henan.

Type. China, Henan Province, Luoyang City, Song County, the Tianchi Mountain National Forest Park, in rotting wood, October 2020, J.Z. Li & Z.T. Zhang (holotype NYNU 201062^{T}, ex-type CBS 16659 = CICC 33512, holotype and ex-type are preserved in a metabolically inactive state).

Description. In YM broth after 3 days at 25 °C, cells are ovoid (2–3 × 3–5 μm) and occur singly or in pairs. Budding is multilateral. Sediment is formed after a month, but a pellicle is not observed. On YM agar after 3 days at 25 °C, colonies are white to cream- coloured, convex, butyrous, and smooth with entire margins. In Dalmau plate culture on corn meal agar, pseudohyphae and true hyphae are formed. Asci or signs of conjugation are not observed on sporulation media. Fermentation of sugars is absent. Glucose, galactose, L-sorbose, glucosamine, D-ribose, D-xylose, L-arabinose, D-arabinose, L-rhamnose, sucrose, maltose, trehalose, methyl α- D-glucoside, cellobiose, salicin, melibiose, lactose, raffinose, melezitose, inulin, glycerol, erythritol, ribitol, D-glucitol, D-mannitol, galactitol, *myo*-inositol, D-glucono-1, 5-lactone, 2-keto-D-gluconate, 5-keto-D-gluconate, D-gluconate, D-glucuronate, DL-lactate succinate, citrate, and ethanol are assimilated as sole carbon sources. Methanol is not assimilated. L-lysine, creatine, glucosamine, and D-tryptophan are assimilated as sole nitrogen sources, while nitrate, nitrite, ethylamine, cadaverine, creatinine, and imidazole are not assimilated. Minimum growth temperature is 15 °C, and maximum growth temperature is 37 °C. Growth in the presence of 0.1% cycloheximide is present, but growth in the presence

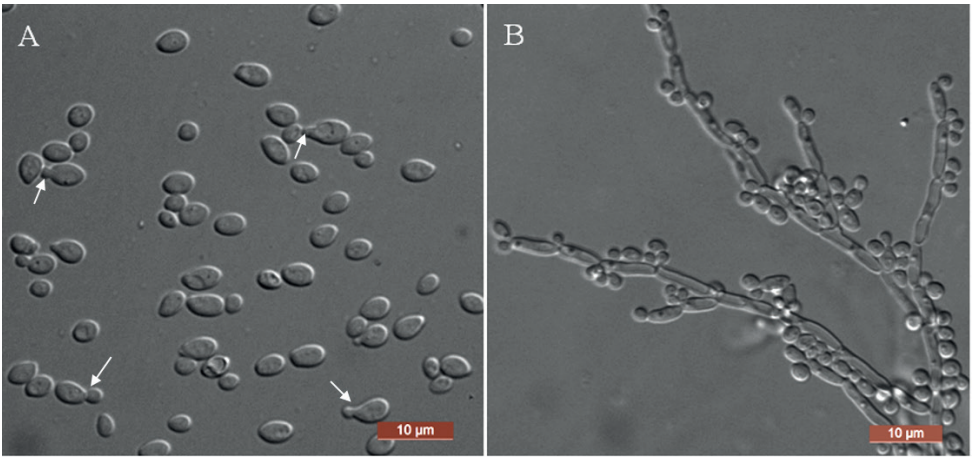

Figure 2. Morphology of *D. luoyangensis* (NYNU 201062, holotype) **A** budding cells were indicated by arrows in YM broth after 3 d **B** pseudohyphae and true hyphae on CM agar after 14 d. Scale bars: 10 μm.

of 10% NaCl plus 5% glucose and 1% acetic acid is absent. Starch-like compounds are not produced. Urease activity and diazonium blue B reactions are negative.

Additional isolate examined. China, Henan Province, Luoyang City, Song County, the Tianchi Mountain National Forest Park, in rotting wood, October 2020, J.Z. Li & Z.T. Zhang (NYNU 201074).

Notes. Two strains were collected from two different substrates, representing *D. luoyangensis*, clustered in the *Diddensiella* clade which is sister to species *D. transvaalensis*. *D. luoyangensis* differed from *D. transvaalensis* by 1.6% substitutions in the D1/D2 domain. Furthermore, we were unable to align the ITS sequence of *D. luoyangensis* with the *D. transvaalensis* type strain, because the ITS sequence of *D. transvaalensis* is not currently available from either the NCBI GenBank or CBS databases. Physiologically, *D. luoyangensis* differs from its closely related species, *D. transvaalensis* (Lachance et al. 2011), based on growth in L-rhamnose, lactose, inulin, D-gluconate and growth at 37 °C, which are present for *D. luoyangensis* and absent for the latter species. Moreover, *D. transvaalensis* ferments glucose and galactose, while this new species does not.

Sugiyamaella cylindrica **C.Y. Chai & F.L. Hui, sp. nov.**
MycoBank No: 842900
Fig. 3

Etymology. The specific epithet *cylindrica* refers to the cylindrical vegetative cells of the type strain.

Type. China, Henan Province, Luoyang City, Song County, the Tianchi Mountain National Forest Park, in rotting wood, October 2020, J.Z. Li & Z.T. Zhang

(holotype NYNU 201067^{T}, ex-type CBS 16662 = CICC 33514, holotype and ex-type are preserved in a metabolically inactive state).

Description. In YM broth after 3 days at 25 °C, cells are cylindrical (2–3 × 5–7 μm) and occur singly or in pairs. Budding is multilateral. Sediment is formed after a month, but a pellicle is not observed. On YM agar after 3 days at 25 °C, colonies are white to cream-coloured, butyrous, convex and smooth with entire margins. In Dalmau plate culture on corn meal agar, rudimentary pseudohyphae are formed. Asci or signs of conjugation are not observed on sporulation media. Glucose and trehalose are weakly fermented, but, galactose, maltose sucrose, melibiose, lactose, cellobiose, melezitose, raffinose, inulin and xylose are not fermented. Glucose, galactose, L-sorbose, glucosamine, D-ribose, D-xylose, L-arabinose, D-arabinose, L-rhamnose, sucrose, maltose, trehalose, methyl α-D-glucoside, cellobiose, salicin, melibiose, raffinose, melezitose, inulin, glycerol, erythritol, ribitol, D-glucitol, D-mannitol, galactitol, *myo*-inositol, D-glucono-1, 5-lactone, 2-keto-D-gluconate, 5-keto-D-gluconate, D-glucuronate, DL-lactate succinate, and ethanol are assimilated as sole carbon sources. Lactose, D-gluconate, citrate and methanol are not assimilated. Nitrate, nitrite, L-lysine, creatine, glucosamine, and D-tryptophan are assimilated as sole nitrogen sources. Ethylamine, cadaverine, creatinine, and imidazole are not assimilated. Minimum growth temperature is 15 °C, and maximum growth temperature is 35 °C. Growth in the presence of 0.1% cycloheximide is present, but growth in the presence of 1% acetic acid and 10% NaCl plus 5% glucose is absent. Starch-like compounds are not produced. Urease activity and diazonium blue B reactions are negative.

Additional isolate examined. China, Henan Province, Luoyang City, Song County, the Tianchi Mountain National Forest Park, in rotting wood, October 2020, J.Z. Li & Z.T. Zhang (NYNU 201034).

Notes. Two strains were collected from two different substrates, representing *Su. cylindrica*, clustered in the *Sugiyamaella* clade and are closely related to

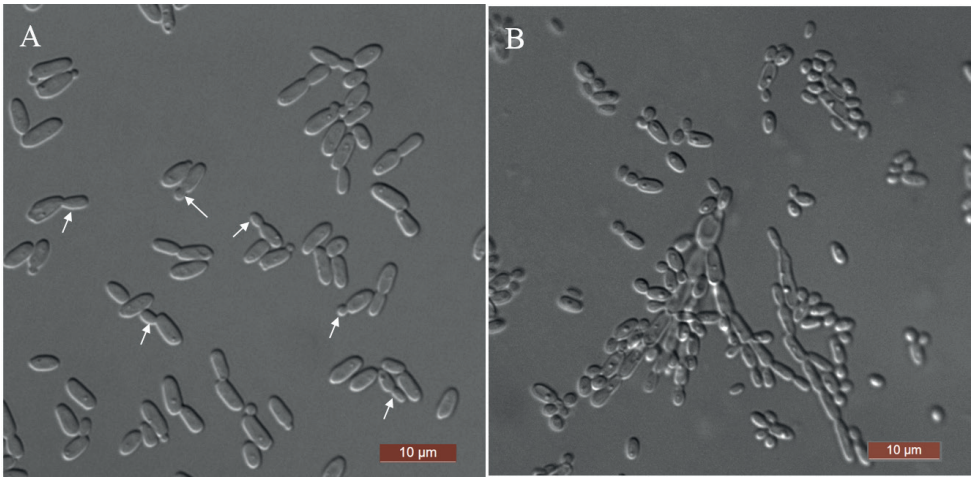

Figure 3. Morphology of *Su. cylindrica* (NYNU 201067, holotype) **A** budding cells were indicated by arrows in YM broth after 3 d **B** rudimentary pseudohyphae on CM agar after 14 d. Scale bars: 10 μm.

Su. marilandica and *Su. qingdaonensis*. The nucleotide differences between the new species and the close relatives *Su. marilandica* and *Su. qingdaonensis* are 1.1–1.4% substitutions in the D1/D2 domain and 5.0–5.9% substitutions in the ITS region, respectively. Physiologically, *Su. cylindrica* differs from the closely related species *Su. marilandica* and *Su. qingdaonensis* (Wang et al. 2010; Kurtzman 2011b) in its ability to assimilate glycerol and DL-lactate and to grow at 35 °C. Additionally, the new species ferments trehalose, while *Su. marilandica and Su.qingdaonensis* do not.

***Sugiyamaella robnettiae* C.Y. Chai & F.L. Hui, sp. nov.**
MycoBank No: 842901
Fig. 4

Etymology. The specific epithet *robnettiae* named in honour of Christie J. Robnett for her proposal of the genus *Sugiyamaella*.

Type. China, Henan Province, Luoyang City, Song County, the Tianchi Mountain National Forest Park, in rotting wood, October 2020, J.Z. Li & Z.T. Zhang (holotype NYNU 201066^{T}, ex-type CBS 16663 = CICC 33513, holotype and ex-type are preserved in a metabolically inactive state).

Description. In YM broths after 3 days at 25 °C, the cells are ellipsoidal to elongate (2–4 × 2–8 μm) and occur singly or in pairs. Budding is multilateral. Sediment is formed after a month, but a pellicle is not observed. On YM agar after 3 days at 25 °C, colonies are white to cream-coloured, convex, buttery and smooth with entire margins. In Dalmau plate culture on corn meal agar, pseudohyphae and true hyphae are formed. Asci or signs of conjugation are not observed on sporulation media. Fermentation of sugars is absent. Glucose, galactose, L-sorbose, glucosamine, D-xylose, L-arabinose, D-arabinose, L-rhamnose, sucrose, maltose, trehalose, methyl α-D-glucoside, cellobiose, salicin, arbutin, lactose, inulin, glycerol, erythritol, ribitol, xylitol, D-glucitol, D-mannitol, galactitol, D-glucono-1, 5-lactone, 2-keto-D-gluconate, 5-keto-D-gluconate, succinate, citrate, and ethanol are assimilated as sole carbon sources. D-ribose, melibiose, raffinose, melezitose, *myo*-inositol, D-gluconate, DL-lactate, and methanol are not assimilated. Nitrate, nitrite, creatine, glucosamine, and D-tryptophan are assimilated as sole nitrogen sources. Ethylamine, L-lysine, creatinine, and imidazole are not assimilated. Minimum growth temperature is 15 °C, and maximum growth temperature is 35 °C. Growth in the presence of 0.1% cycloheximide is present, but growth in the presence of 10% NaCl plus 5% glucose and 1% acetic acid is absent. Starch-like compounds are not produced. Urease activity and diazonium blue B reactions are negative.

Additional isolates examined. China, Henan Province, Luoyang City, Song County, the Tianchi Mountain National Forest Park, in rotting wood, October 2020, J.Z. Li & Z.T. Zhang (NYNU 201005).

Notes. Two strains were collected from two different substrates, formed a well-supported group related to *Su. chuxiongensis*, representing a new species, *Su. robnettiae. Su. robnettiae* differs from *Su. chuxiongensis* by 1.9% substitutions in the D1/D2 domain

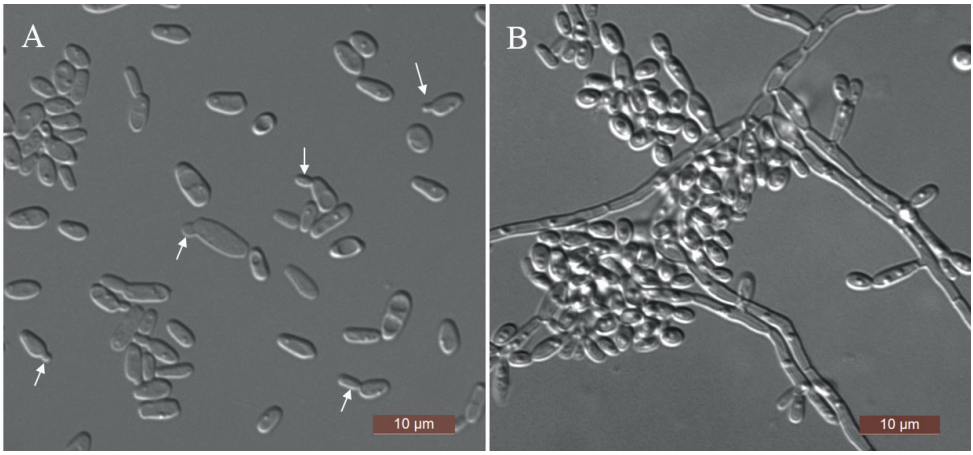

Figure 4. Morphology of *Su. robnettiae* (NYNU 201066, holotype) **A** budding cells were indicated by arrows in YM broth after 3 d **B** pseudohyphae and true hyphae on CM agar after 14 d. Scale bars: 10 μm.

and 6.4% substitutions in the ITS region. Physiologically, unlike *Su. chuxiongensis* (Shi et al., 2021), *Su. robnettiae* is unable to assimilate D-ribose, melibiose, raffinose, or melezitose but is able to assimilate glycerol and lactose.

Zygoascus detingensis **C.Y. Chai & F.L. Hui, sp. nov.**
MycoBank No: 842902
Fig. 5

Etymology. The specific epithet *detingensis* refers to the geographic origin of the type strain, Deting Town, Henan.

Type. China, Henan Province, Luoyang City, Song County, the Tianchi Mountain National Forest Park, in rotting wood, October 2020, J.Z. Li & Z.T. Zhang (holotype NYNU 201087 ^{T}, ex-type CBS 16667 = CICC 33516, holotype and ex-type preserved in a metabolically inactive state).

Description. In YM broth after 3 days at 25 °C, cells are subglobosal to globosal (2–3 × 2–4 μm) and occur singly or in pairs. Budding is multilateral. Sediment is formed after a month, but a pellicle is not observed. On YM agar after 3 days at 25 °C, colonies are cream, smooth, opalescent, convex and glistening. In Dalmau plate culture on corn meal agar, pseudohyphae and true hyphae are formed. Asci or signs of conjugation are not observed on sporulation media. Fermentation of sugars is absent. Glucose, galactose (weak), glucosamine, D-ribose (weak), D-xylose, D-arabinose (weak), L-arabinose (weak), L-rhamnose (weak), sucrose (weak), maltose (weak), trehalose, methyl α-D-glucoside (weak), cellobiose (weak), salicin, melibiose, lactose (weak), raffinose, melezitose (weak), inulin (weak), glycerol (weak),

erythritol, ribitol (weak), xylitol (weak), D-glucitol (weak), D-mannitol (weak), galactitol (weak), *myo*-inositol (weak), D-glucono-1, 5-lactone, 2-keto-D-gluconate, D-gluconate (weak), D-glucuronate (weak), DL-lactate (weak), succinate (weak), and ethanol are assimilated as sole carbon sources. L-sorbose, citrate, and methanol are not assimilated. Ethylamine, glucosamine, and L-lysine are assimilated as sole nitrogen sources. Nitrate, nitrite, cadaverine, creatine, creatinine, imidazole, and D-tryptophan are not assimilated. Minimum growth temperature is 15 °C, and maximum growth temperature is 37 °C. Growth in the presence of 0.1% cycloheximide is present, but growth in the presence of 10% NaCl plus 5% glucose and 1% acetic acid is absent. Starch-like compounds are not produced. Urease activity and diazonium blue B reactions are negative.

Additional isolate examined. China, Henan Province, Luoyang City, Song County, the Tianchi Mountain National Forest Park, in rotting wood, October 2020, J.Z. Li & Z.T. Zhang (NYNU 201011).

Notes. Two strains were collected from two different substrates, both representing *Z. detingensis*, branched separately from the *Zygoascus* clade. *Z. detingensis* differed from the other *Zygoascus* species by more than 9.7% substitutions in the D1/D2 domain and 11.5% substitutions in the ITS region, respectively. Physiologically, *Z. detingensis* differs from its closely related species, *Z. bituminiphila* (V. Robert, B. Bonjean, Karutz, Paschold, W. Peeters & Wubbolts) Nagatsuka, Kiyuna & Sugiyama (Nagatsuka et al. 2016), in its inability to assimilate L-sorbose and its ability to assimilate L-rhamnose, methyl α-D-glucoside, melibiose, lactose, inulin melezitose, erythritol, and 2-keto-D-gluconate. Moreover, *Z. bituminiphila* ferments glucose, galactose, trehalose, and cellobiose, while *Z. detingensis* does not.

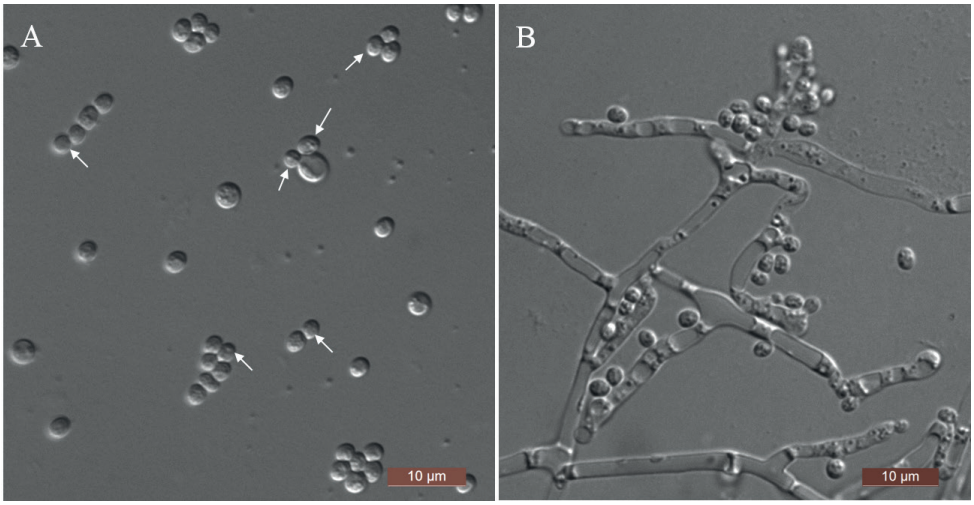

Figure 5. Morphology of *Z. detingensis* (NYNU 201087, holotype) **A** budding cells were indicated by arrows in YM broth after 3 d **B** pseudohyphae and true hyphae on CM agar after 14 d. Scale bars: 10 μm.

Discussion

In the present study, we collected rotting wood from the Tianchi Mountain National Forest Park located near Luoyang City in Henan Province of China. From these samples, we isolated several yeast strains. Some of these yeasts are known species, such as *Metschnikowia henanensis*, *Saturnispora galanensis*, *Wickerhamomyces menglaensis* and *Deakozyma yunnanensis*. Here, we recovered eight isolates from eight rotting woods of *Trichomonascaceae* yeast representing four new species belonging to the genera *Diddensiella*, *Sugiyamaella*, and *Zygoascus*. We described these new species as *D. luoyangensis*, *Su. cylindrica*, *Su. Robnettiae*, and *Z. detingensis* based on molecular phylogenetic and morphological evidence. A thorough and comprehensive phylogenetic analysis of the family *Trichomonascaceae* based on the combined ITS and the D1/D2 domains of the LSU rRNA gene sequences is provided, including almost all GenBank representatives and newly generated sequences, which may serve as a reference for the field. This study provides information on the species delimitation of the family *Trichomonascaceae* based on morphological and phylogenetic evidence.

Our phylogenetic analyses, based on ITS and the D1/D2 domains of the LSU rRNA gene sequences, are in concordance with previous studies (Morais et al. 2013b; Sena et al. 2017; Shi et al. 2021). However, the genus *Sugiyamaella* of *Trichomonascaceae* is not a monophyletic group. Morais et al. (2013b) indicated that *Sugiyamaella* is polyphyletic, where the species are intertwined with representatives of the genera *Diddensiella* and *Spencermartinsiella*. From the latter study, the genus could be divided into two main clades, which were later supported by Sena et al. (2017) and Shi et al. (2021). In this study, all species of *Sugiyamaella* and related genera were used to refine our understanding of the evolutionary relationships of this family, based on the ITS and nrLSU dataset. As shown in Fig. 1, all genera of *Trichomonascaceae* formed monophyletic groups with the exception of *Sugiyamaella* in which two main clades were reconstructed: (i) *Su. smithiae* (the type species), *Su. lignohabitans*, and *Su. valdiviana* and their related species and (ii) *Su. americana*, *Su. bullrunensis*, (S.O. Suh, Houseknecht & J.J. Zhou) H. Urbina & M. Blackw, *Su. carassensis* L.M. Sena et al. and *Su. ligni* L.M. Sena et al.

In recent years, more than 40 yeast species have been identified from rotting wood in China (Wang et al. 2010; Guo et al. 2012; Gao et al. 2017; Zheng et al. 2017; Huang et al. 2018; Chai et al. 2020; Lv et al. 2020; Shi et al. 2021). Among them, at least 16 species of *Trichomonascaceae* have been isolated from rotting wood in China, including six new species previously obtained from China (*Bla. xishuangbannaensis*, *Sp. cellulosicola*, *Su. qingdaonensis*, *Su. xiaguanensis*, *Su. Chuxiong*, and *Su. yunanensis*) (Wang et al. 2010; Guo et al. 2012; Huang et al. 2018; Chai et al. 2020; Shi et al. 2021), new records of six species not known to occur in China (*Su. americana*, *Su. ayubii*, *Su. novakii*, *Su. paludigena*, *Su. Valenteae*, and *Su. valdiviana*) (Shi et al. 2021), and four novel species identified in this study (*D. luoyangensis*, *Su. cylindrica*, *Su. robnettiae*, and *Z. detingensis*). In China, there remain species to be discovered, such as those sequences of the D1/D2 domains of the LSU rRNA gene listed under GenBank accessions JN581115 and JN581116. To date, including the four new

species described in this study, there are more than 100 species of *Trichomonascaceae* worldwide (www.mycobank.org). Although the taxonomy of *Trichomonascaceae* has been a focus of research in the past, many regions are under-sampled and more novel indigenous *Trichomonascaceae* species will undoubtedly be discovered in the future.

Acknowledgements

The authors are very grateful to their colleagues at School of Life Science and Agricultural Engineering, Nanyang Normal University, including Jing-Zhao Li, Sou Zhou, and Zheng-Tian Zhang for providing specimens. This project was supported by Grant No. 31570021 from the National Natural Science Foundation of China (NSFC), P. R. China, Grant No. 2018001 from the State Key Laboratory of Motor Vehicle Biofuel Technology, Henan Tianguan Enterprise Group Co., Ltd., China, and Key specialized research and development breakthrough program in Henan province (grant no. 212102110261)

References

Avchar R, Groenewald M, Baghela A (2019) *Wickerhamiella shivajii* sp. nov., a thermotolerant yeast isolated from distillery effluent. International Journal of Systematic and Evolutionary Microbiology 69(10): 3262–3267. https://doi.org/10.1099/ijsem.0.003616

Belloch C, Pelaez AI, Sánchez J, Kurtzman C (2020) *Wickerhamiella verensis* f.a. sp. nov., a novel yeast species isolated from subsoil groundwater contaminated with hydrocarbons and from a human infection. International Journal of Systematic and Evolutionary Microbiology 70(4): 2420–2425. https://doi.org/10.1099/ijsem.0.004053

Chai CY, Jia RR, Chen CY, Hui FL (2020) *Blastobotrys baotianmanensis* sp. nov. and *Blastobotrys xishuangbannaensis* f.a., sp. nov., two novel yeast species associated with insects and rotting wood. International Journal of Systematic and Evolutionary Microbiology 70(7): 4217–4223. https://doi.org/10.1099/ijsem.0.004275

Daniel HM, Lachance MA, Kurtzman CP (2014) On the reclassification of species assigned to *Candida* and other anamorphic ascomycetous yeast genera based on phylogenetic circumscription. Antonie van Leeuwenhoek International Journal of General and Molecular Microbiology 106(1): 67–84. https://doi.org/10.1007/s10482-014-0170-z

Darriba D, Taboada GL, Doallo R, Posada D (2012) jModelTest 2: More models, new heuristics and parallel computing. Nature Methods 9(8): e772. https://doi.org/10.1038/nmeth.2109

Gao WL, Liu TT, Zheng J, Hui FL (2017) *Kodamaea neixiangensis* f.a., sp. nov. and *Kodamaea jinghongensis* f.a., sp. nov., two yeast species isolated from rotting wood. International Journal of Systematic and Evolutionary Microbiology 67(9): 3358–3362. https://doi.org/10.1099/ijsem.0.002117

Guo XY, Zhu HK, Bai FY (2012) *Candida cellulosicola* sp. nov., a xylose-utilizing anamorphic yeast from rotten wood. International Journal of Systematic and Evolutionary Microbiology 62(1): 242–245. https://doi.org/10.1099/ijs.0.031351-0

Hall TA (1999) Bioedit: A user-friendly biological sequence alignment editor and analysis program for Windows 95/98/NT. Nucleic Acids Symposium Series 41: 95–98.

Hillis DM, Bull JJ (1993) An empirical test of bootstrapping as a method for assessing confidence in phylogenetic analysis. Systematic Biology 42(2): 182–192. https://doi.org/10.1093/sysbio/42.2.182

Huang LN, Xi ZW, Li Y, Hui FL (2018) *Sugiyamaella xiaguanensis* f.a., sp. nov., a yeast species isolated from rotting wood. International Journal of Systematic and Evolutionary Microbiology 68(10): 3307–3310. https://doi.org/10.1099/ijsem.0.002988

Katoh K, Toh H (2010) Parallelization of the MAFFT multiple sequence alignment program. Bioinformatics (Oxford, England) 26(15): 1899–1900. https://doi.org/10.1093/bioinformatics/btq224

Kurtzman CP (2011a) Discussion of teleomorphic and anamorphic ascomycetous yeasts and yeast-like taxa. In: Kurtzman CP, Fell JW, Boekhout T (Eds) The Yeasts – a Taxonomic Study, 5th edn., Vol. 2. Elsevier, Amsterdam, 293–307. https://doi.org/10.1016/B978-0-444-52149-1.00013-6

Kurtzman CP (2011b) *Sugiyamaella* Kurtzman & Robnett (2007). In: Kurtzman CP, Fell JW, Boekhout T (Eds) The Yeasts – a Taxonomic Study, 5th edn., Vol. 2. Elsevier, Amsterdam, 817–822. https://doi.org/10.1016/B978-0-444-52149-1.00072-0

Kurtzman CP, Robnett CJ (1998) Identification and phylogeny of ascomycetous yeasts from analysis of nuclear large subunit (26S) ribosomal DNA partial sequences. Antonie van Leeuwenhoek International Journal of General and Molecular Microbiology 73(4): 331–371. https://doi.org/10.1023/A:1001761008817

Kurtzman CP, Robnett CJ (2007) Multigene phylogenetic analysis of the *Trichomonascus*, *Wickerhamiella* and *Zygoascus* yeast clades, and the proposal of *Sugiyamaella* gen. nov. and 14 new species combinations. FEMS Yeast Research 7(1): 141–151. https://doi.org/10.1111/j.1567-1364.2006.00157.x

Kurtzman CP, Robnett CJ (2014) Three new anascosporic genera of the Saccharomycotina: *Danielozyma* gen. nov., *Deakozyma* gen. nov. and *Middelhovenomyces* gen. nov. Antonie van Leeuwenhoek International Journal of General and Molecular Microbiology 105(5): 933–942. https://doi.org/10.1007/s10482-014-0149-9

Kurtzman CP, Fell JW, Boekhout T, Robert V (2011) Methods for isolation, phenotypic characterization and maintenance of yeasts. In: Kurtzman CP, Fell JW, Boekhout T (Eds) The Yeasts – a Taxonomic Study, 5th edn., vol. 1. Elsevier, Amsterdam, 87–110. https://doi.org/10.1016/B978-0-444-52149-1.00007-0

Lachance MA, Kurtzman CP (2011) *Wickerhamiella* van der Walt (1973). In: Kurtzman CP, Fell JW, Boekhout T (Eds) The Yeasts – a Taxonomic Study, 5th edn., Vol. 2. Elsevier, Amsterdam, 891–897. https://doi.org/10.1016/B978-0-444-52149-1.00079-3

Lachance MA, Boekhout T, Scorzetti G, Fell JW, Kurtzman CP (2011) *Candida* Berkhout (1923). In: Kurtzman CP, Fell JW, Boekhout T (Eds) The Yeasts – a Taxonomic Study, 5th Edn., Vol. 2. Elsevier, Amsterdam, 987–1278. https://doi.org/10.1016/B978-0-444-52149-1.00090-2

Lv SL, Chai CY, Wang Y, Yan ZL, Hui FL (2020) Five new additions to the genus *Spathaspora* (Saccharomycetales, Debaryomycetaceae) from southwest China. MycoKeys 75: 31–49. https://doi.org/10.3897/mycokeys.75.57192

Morais CG, Lara CA, Marques S, Fonseca C, Lachance MA, Rosa CA (2013a) *Sugiyamaella xylanicola* sp. nov., a xylan-degrading yeast species isolated from rotting wood. International Journal of Systematic and Evolutionary Microbiology 63(Pt_6): 2356–2360. https://doi.org/10.1099/ijs.0.050856-0

Morais CG, Cadete RM, Uetanabaro APT, Rosa LH, Lachance MA, Rosa CA (2013b) D-xylose-fermenting and xylanase producing yeast species from rotting wood of two Atlantic rainforest habitats in Brazil. Fungal Genetics and Biology 60: 19–28. https://doi.org/10.1016/j.fgb.2013.07.003

Nagatsuka Y, Ninomiya S, Kiyuna T, Kigawa R, Sano C, Sugiyama J (2016) *Yamadazyma kitorensis* f.a., sp. nov. and *Zygoascus biomembranicola* f.a., sp. nov., novel yeasts from the stone chamber interior of the Kitora tumulus, and five novel combinations in *Yamadazyma* and *Zygoascus* for species of *Candida.* International Journal of Systematic and Evolutionary Microbiology 66(4): 1692–1704. https://doi.org/10.1099/ijsem.0.000930

Péter G, Dlauchy D, Tornai-Lehoczki J, Suzuki M, Kurtzman CP (2011) *Spencermartinsiella europaea* gen. nov., sp. nov., a new member of the family Trichomonascaceae. International Journal of Systematic and Evolutionary Microbiology 61(4): 993–1000. https://doi.org/10.1099/ijs.0.023804-0

Péter G, Dlauchy D, Price NPJ, Kurtzman CP (2012) *Diddensiella caesifluorescens* gen. nov., sp. nov., a riboflavin-producing yeast species of the family Trichomonascaceae. International Journal of Systematic and Evolutionary Microbiology 62(Pt_12): 3081–3087. https://doi.org/10.1099/ijs.0.042895-0

Rambaut A (2016) FigTree, version 1.4.3. University of Edinburgh, Edinburgh.

Ronquist F, Teslenko M, van der Mark P, Ayres DL, Darling A, Hohna S, Larget B, Liu L, Suchard MA, Huelsenbeck JP (2012) MrBayes 3.2: Efficient Bayesian phylogenetic inference and model choice across a large model space. Systematic Biology 61(3): 539–542. https://doi.org/10.1093/sysbio/sys029

Sakpuntoon V, Angchaun J, Boonmak C, Chang CF, Limtong S, Srisuk N (2020) *Wickerhamiella osmotolerans* sp. nov. and *Wickerhamiella tropicalis* sp. nov., novel ascomycetous yeast in the family Trichomonascaceae. International Journal of Systematic and Evolutionary Microbiology 70(4): 2596–2601. https://doi.org/10.1099/ijsem.0.004075

Sena LMF, Morais CG, Lopes MR, Santos RO, Uetanabaro APT, Morais PB, Vital MJS, de Morais Jr MA, Lachance MA, Carlos A Rosa CA (2017) D-Xylose fermentation, xylitol production and xylanase activities by seven new species of *Sugiyamaella.* Antonie van Leeuwenhoek International Journal of General and Molecular Microbiology 110(1): 53–67. https://doi.org/10.1007/s10482-016-0775-5

Shi CF, Zhang KH, Chai CY, Yan ZL, Hui FL (2021) Diversity of the genus *Sugiyamaella* and description of two new species from rotting wood in China. MycoKeys 77: 27–39. https://doi.org/10.3897/mycokeys.77.60077

Smith MT, Hoog GSD, Malloch D, Kurtzman CP (2011a) *Trichomonascus* H.S. Jackson emend. Kurtzman & Robnett (2007). In: Kurtzman CP, Fell JW, Boekhout T (Eds) The Yeasts – a Taxonomic Study, 5th edn., Vol. 2. Elsevier, Amsterdam, 891–897. https://doi.org/10.1016/B978-0-444-52149-1.00076-8

Smith MT, de Hoog GS, Statzell-Tallman A, Kurtzman CP (2011b) *Blastobotrys* von Klopotek (1967). In: Kurtzman CP, Fell JW, Boekhout T (Eds) The Yeasts – a Taxonomic Study, 5th

edn., Vol. 2. Elsevier, Amsterdam, 959–977. https://doi.org/10.1016/B978-0-444-52149-1.00087-2

Stamatakis A (2006) RAxML-VI-HPC: maximum likelihood-based phylogenetic analysis with thousands of taxa and mixed models. Bioinformatics 22: 2688–2690. https://doi.org/10.1093/bioinformatics/btl446

Thomas S, Sanya DRA, Fouchard F, Nguyen HV, Kunze G, Neuvéglise C, Anne-Marie Crutz-Le Coq AM (2019) *Blastobotrys adeninivorans* and *B. raffinosifermentans*, two sibling yeast species which accumulate lipids at elevated temperatures and from diverse sugars. Biotechnology for Biofuels 12(1): e154. https://doi.org/10.1186/s13068-019-1492-x

Wang SA, Li FL, Bai FY (2010) *Candida laoshanensis* sp. nov. and *Candida qingdaonensis* sp. nov., anamorphic, ascomycetous yeast species isolated from decayed wood. International Journal of Systematic and Evolutionary Microbiology 60(7): 1697–1701. https://doi.org/10.1099/ijs.0.015230-0

White TJ, Bruns T, Lee S, Taylor J (1990) Amplification and direct sequencing of fungal ribosomal RNA genes for phylogenetics. In: Innis MA, Gelfand DH, Sninsky JJ, White TJ (Eds) PCR Protocols: A Guide to Methods and Applications. Academic Press, 315–322. https://doi.org/10.1016/B978-0-12-372180-8.50042-1

Zheng J, Liu KF, Liu XJ, Zhang L, Hui FL (2017) *Deakozyma yunnanensis* sp. nov., a novel yeast species isolated from rotten wood. International Journal of Systematic and Evolutionary Microbiology 67(7): 2436–2439. https://doi.org/10.1099/ijsem.0.001978

MycoKeys 90: 19–30 (2022)
doi: 10.3897/mycokeys.90.84562
https://mycokeys.pensoft.net

RESEARCH ARTICLE

A peer-reviewed open-access journal
MycoKeys
Launched to accelerate biodiversity research

Dendrocorticiopsis orientalis gen. et sp. nov. of the Punctulariaceae (Corticiales, Basidiomycota) revealed by molecular data

Chia-Ling Wei[1], Che-Chih Chen[1,2,3], Shuang-Hui He[4], Sheng-Hua Wu[1,2]

1 *Department of Biology, National Museum of Natural Science, Taichung 40453, Taiwan* **2** *Department of Plant Pathology, National Chung Hsing University, Taichung 40227, Taiwan* **3** *Biodiversity Research Center, Academia Sinica, Taipei 11529, Taiwan* **4** *School of Ecology and Nature Conservation, Beijing Forestry University, Beijing 100083, China*

Corresponding authors: Shuang-Hui He (heshuanghui@bjfu.edu.cn); Sheng-Hua Wu (shwu@mail.nmns.edu.tw)

Academic editor: R. Henrik Nilsson | Received 29 March 2022 | Accepted 8 May 2022 | Published 31 May 2022

Citation: Wei C-L, Chen C-C, He S-H, Wu S-H (2022) *Dendrocorticiopsis orientalis* gen. et sp. nov. of the Punctulariaceae (Corticiales, Basidiomycota) revealed by molecular data. MycoKeys 90: 19–30. https://doi.org/10.3897/mycokeys.90.84562

Abstract

Dendrocorticiopsis orientalis is presented in this study as a new genus and new species based on morphological and phylogenetic evidence. This new taxon is characterized by resupinate, smooth and membranaceous basidiomata, monomitic hyphal system with clamps, colorless dendrohyphidia, variable presence of cystidia, and ellipsoid to ovoid basidiospores measuring 5–7 × 3.2–5.2 µm. The phylogenetic analyses based on the ITS1-5.8S-ITS2 (ITS) + nuclear 28S rDNA (28S) dataset of Corticiales indicated that the new taxon is nested in Punctulariaceae, separated from other genera with strong support values. Descriptions, specimen photo, and illustrations of the new taxon are provided in this study. A morphological comparison of the four genera of Punctulariaceae is given.

Keywords

Corticioid fungi, East Asia, phylogeny, taxonomy, wood-decaying fungi

Introduction

Corticiales K.H. Larss. is a small order of corticioid fungi with four families: Corticiaceae Herter, Dendrominiaceae Ghobad-Nejhad, Punctulariaceae Donk, and Vuilleminiaceae Maire ex Lotsy. The members of the order show a variety of nutritional

ecologies, including lignicolous saprobes, foliicolous species, plant pathogens, and lichenicolous species (Ghobad-Nejhad et al. 2010, 2021). Species of Punctulariaceae are mainly saprobic on angiosperm trees, causing white rot. Morphologically, they are characterized by having effused to effused-reflexed basidiomata, smooth to tuberculate hymenial surface, a monomitic hyphal system with clamped generative hyphae, mostly absence of cystidia, sparsely to regularly branched dendrohyphidia, and ellipsoid to subglobose basidiospores which are negative in Melzer's reagent and acyanophilous in cotton blue. When Donk (1964) established this family, he adopted Talbot's suggestion (Talbot 1958) and designated *Punctularia* Pat. as the type genus. Ghobad-Nejhad et al. (2010) were the first to use a phylogenetic approach to analyze Punctulariaceae, and they recognized three genera, viz., *Dendrocorticium* M.J. Larsen & Gilb., *Punctularia*, and *Punctulariopsis* Ghobad-Nejhad. This arrangement was generally accepted by mycologists (Hibbett et al. 2014; He et al. 2019; Wijayawardene et al. 2020).

Most of the previous studies of Punctulariaceae focused on European species (Bernicchia and Gorjón 2010; Gorjón and Bernicchia 2017), although species from other continents received attention as well (Ghobad-Nejhad et al. 2010; Baltazar et al. 2013; Ariyawansa et al. 2015). However, the study of this family in Asia is insufficient and needs an update (Petch 1916; Cooke 1956; Guan et al. 2021). During surveys of corticioid fungi in East Asian regions, we found an unknown species morphologically similar to *Dendrocorticium* spp. Phylogenetic analyses were conducted by using ITS+28S sequences to evaluate the generic placement of the target taxon, and the results indicated that it represents a new genus and a new species of the Punctulariaceae.

Materials and methods

Morphological studies

Descriptions and illustrations are based on dried specimens deposited at the herbaria of the National Museum of Natural Science (**TNM**) and Beijing Forestry University (**BJFC**). Specimens were sliced into thin sections under stereo microscope (Nikon SMZ645) and mounted in 5% KOH with 1% phloxine in preparation for observations and measurements. Melzer's reagent (IKI) and cotton blue were applied to detect amyloidity or dextrinoidity, and cyanophily, respectively. Microscopic studies were carried out under 1,000× magnification using an optical microscope (Olympus BX43). For presenting the range of basidiospore dimensions, 5% values of minimum and maximum are given in parentheses.

DNA extraction and sequencing

DNA was extracted from dried specimens using the Plant Genomic DNA Extraction Miniprep System (Viogene Biotek corporation, New Taipei City, Taiwan), following the manufacturer's protocol. ITS1-5.8S-ITS2 and partial 28S regions were amplified with the primer pairs ITS1/ITS4 (White et al. 1990) and LR0R/LR5 (Vilgalys and Hester 1990). The PCR protocols for ITS and 28S followed Chen et al. (2020). PCR

products were purified and sequenced by MB Mission Biotech company (Taipei City, Taiwan). New sequences were assembled and adjusted using BioEdit v7.2.5 (Hall 1999) and subsequently submitted to GenBank (Table 1).

Table 1. Information of species and strains used in phylogenetic analyses, including their localities, voucher numbers, and GenBank accession numbers (ITS and 28S). Newly generated sequences are shown in bold. Voucher number of holotypes are marked with an asterisk (*).

Species	Locality	Voucher no.	GenBank accession no.	
			ITS	28S
Australovuilleminia coccinea Ghobad-Nejhad & Hallenb.	New Zealand	PDD:94158*	HM046875	HM046930
Basidiodesertica hydei	Oman	DST2020a_ SQUCC15289*	MW077150	MW077159
Corticium roseum	China	Ghobad-Nejhad 2428	MW805872	MW805836
C. thailandicum	Thailand	Ghobad-Nejhad 3012	MW805868	MW805831
Cytidia salicina (Fr.) Burt	Finland	Haikonen 24631	GU590881	HM046921
Dendrocorticiopsis orientalis Sheng H. Wu, C.L. Wei & S.H. He	Taiwan	WEI 20-166*	**MW580922**	**MW580924**
D. orientalis	Taiwan	WEI 20-173	**MW580925**	**MW580927**
D. orientalis	Taiwan	BCRC 36235	EU232219	EU232303
D. orientalis	China	He 4195	**MW580926**	**MW580921**
Dendrocorticium polygonioides (P. Karst.) M.J. Larsen & Gilb.	France	CBS 106.56	MH857525	MH869062
D. roseocarneum (Schwein.) M.J. Larsen & Gilb.	South Korea	KUC20121109-32	KJ668559	KJ668413
Dendrominia dryina (Pers.) Ghobad-Nejhad & Duhem	France	Duhem 5283	JX892936	JX892937
D. ericae (Duhem) Ghobad-Nejhad & Duhem	France	Duhem 4840*	JX892938	JX892939
Disporotrichum dimorphosporum	USA	CBS 433.85	MH861895	MH873584
D. dimorphosporum	Netherlands	CBS 419.70*	MH859776	MH871538
Erythricium hypnophilum	France	MG169	MW805858	MW805823
E. laetum	—	Kotiranta 21287	GU590875	GU590878
Gloeophyllum abietinum (Bull.) P. Karst.	Switzerland	H 22988	JX524619	KC782733
L. fuciformis	Netherlands	CBS 182.49	MH856485	MH868023
L. roseipellis	—	CBS 299.82	EU622846	EU622844
'*Lawreymyces palicei*'	—	Palice 4369*	AY542865	AY542865
'*Lawreymyces palicei*'	—	Palice 2509	AY542864	AY542864
Marchandiomyces aurantioroseus (P. Karst.) Ghobad-Nejhad	Sweden	Hallenberg 8186	KP864659	HM046929
M. corallinus	—	JL128-98	AY583327	AY583331
Mycobernardia incrustans	France	Duhem 3613	MW805860	MW805825
M. incrustans	Canada	CBS172.36	MH855759	MH867272
Punctularia atropurpurascens (Berk. & Broome) Petch	Taiwan	WEI 17-662	**MW570883**	**MW570888**
P. bambusicola C.L. Zhao	China	CLZhao 9098*	MW559983	MW559985
P. strigosozonata (Schwein.) P.H.B. Talbot	—	HHB-11897-sp	DQ398958	AF518642
Punctulariopsis efibulata (M.J. Larsen & Nakasone) Ghobad-Nejhad	USA	Burdsall 8824*	KR494276	KR494277
P. obducens (Hjortstam & Ryvarden) Ghobad-Nejhad	Ethiopia	Ryvarden 28131	HM046918	HM046933
P. subglobispora (Hallenb. & Hjortstam) Ghobad-Nejhad	Argentina	Hallenberg 12761*	HM046917	HM046932
Veluticeps abietina (Pers.) Hjortstam & Tellería	Sweden	KHL 12474	EU118619	EU118619
Vuilleminia comedens (Nees) Maire	—	T-583	DQ398959	AF518666
V. coryli Boidin, Lanq. & Gilles	Turkmenistan	Parmasto 54999	JN387996	JN388005
V. cystidiata Parmasto	South Korea	KUC20131022-26	KJ668433	KJ668285
V. erastii Ghobad-Nejhad	Canada	DAOM 199025*	JN387998	JN388007
V. macrospora (Bres.) Hjortstam	France	Duhem 4860	JX892940	JX892941
V. megalospora Bres.	Italy	Ryvarden 43185	HM046887	HM046926
V. nilsii Ghobad-Nejhad & Duhem	France	Duhem 4847*	JX892947	JX892948
V. pseudocystidiata Boidin, Lanq. & Gilles	France	Boidin 14838*	HM046888	HM046928
Waitea circinata	USA	CBS472.82	MH861518	MH873265
W. guianensis	French Guiana	GUY13-110	MW449090	MW449101

Phylogenetic analyses

The selection of species and samples for the ITS+28S dataset was inspired by Ghobad-Nejhad and Duhem (2014) and Guan et al. (2021). The dataset contained 43 samples from 37 species, including 35 ingroup species from 17 genera of the four families in Corticiales and 2 outgroup species from Gloeophyllales [*Gloeophyllum abietinum* (Bull.) P. Karst. and *Veluticeps abietina* (Pers.) Hjortstam & Tellería, Table 1]. Sequences were aligned in MAFFT v.7 (Katoh and Standley 2013). Partitioned phylogenetic analyses were carried out for the ITS+28S dataset based on maximum likelihood (ML) and Bayesian inference (BI) methods, using MrBayes v. 3.2.6. (Ronquist et al. 2012) and RaxML Black Box (Stamatakis 2014) at the CIPRES Science Gateway (http://www.phylo.org/). For the BI analysis, jModeltest 2.1.10 (Darriba et al. 2012) was first executed to estimate the best-fit substitution model based on Akaike Information Criterion (AIC). The GTR+G+I was used as the substitution model for the ITS1, ITS2 and 28S regions, while K80 was used for 5.8S region. The parameter settings for ML and BI analyses followed Wu et al. (2018). Only the phylogram inferred from the ML analysis is shown since the BI and ML analyses produced similar topologies. The statistical support values are presented above the branches of the ML tree when bootstrap values (BS) ≥ 70 and BI posterior probability (PP) ≥ 0.9. The complete phylogenetic trees and alignment were submitted to TreeBASE (submission number 29602; www.treebase.org).

Results

Phylogenetic inference

The final alignment of 43 sequences contained 1,647 sites (including gaps) of which 724 sites were from the ITS region and 923 sites from the 28S gene. Totally, 565 (34%) sites were parsimony informative. The ML tree (Fig. 1) shows the four highly supported families also recovered in previous studies (Ghobad-Nejhad and Duhem 2014; Ariyawansa et al. 2015; Ghobad-Nejhad et al. 2021; Guan et al. 2021). The four samples of the new species *Dendrocorticiopsis orientalis* formed a monophyletic group in Punctulariaceae with strong support values (BS = 100%; PP = 1), well separated from the other genera, viz., *Dendrocorticium*, *Punctularia*, and *Punctulariopsis* (Fig. 1). Therefore, *Dendrocorticiopsis* is treated as the fourth genus of Punctulariaceae.

Taxonomy

Dendrocorticiopsis **Sheng H. Wu, C.L. Wei & S.H. He, gen. nov.**
MycoBank: MB838902

Diagnosis. *Dendrocorticiopsis* differs from other genera by having strictly resupinate basidiomata, ivory hymenphore, a compact texture, a monomitic hyphal system, nodose-septate hyphae, encrusted cystidia, dendrohyphidia and ellipsoid to ovoid basidiospores.

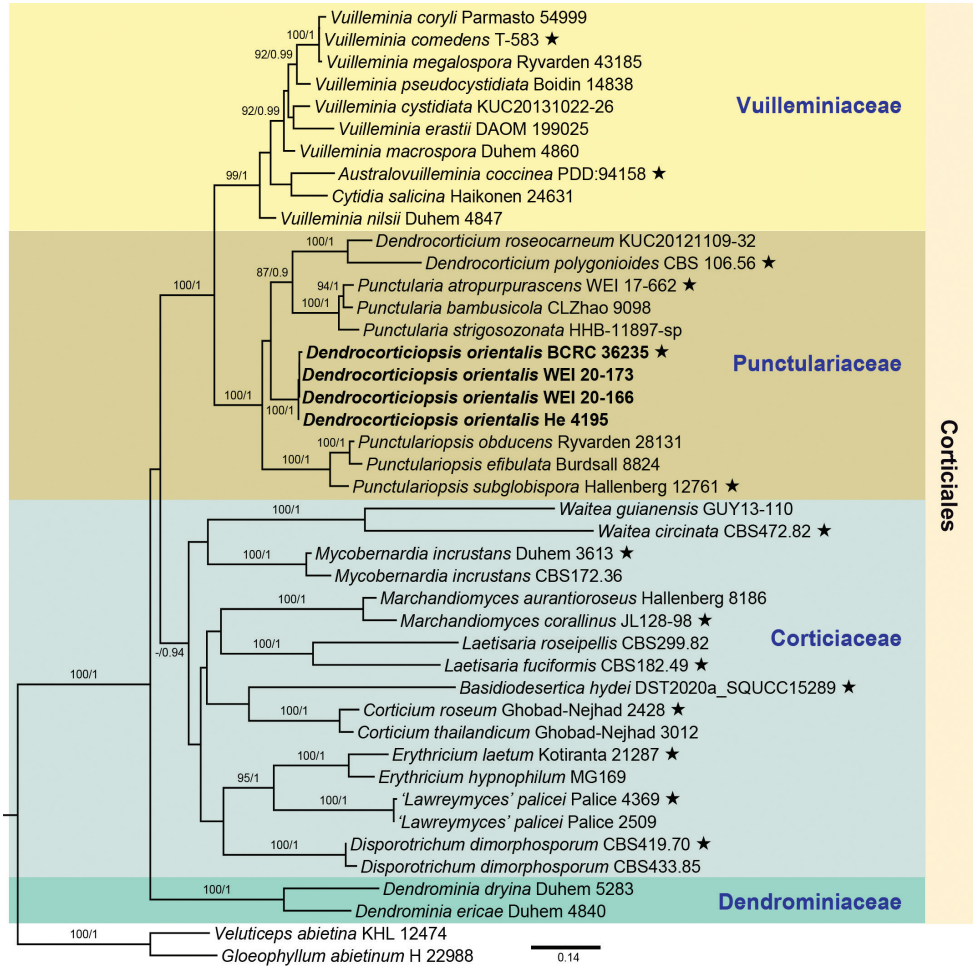

Figure 1. The phylogram of Corticiales inferred from ML analysis using the combined ITS+28S dataset shows the position of *Dendrocorticiopsis orientalis* (shown in bold) in Punctulariaceae. Numbers above branches indicate statistical support of BS ≥ 70% and PP ≥ 0.9. Black stars (é) indicate strains of generic species.

Description. Basidiomata resupinate, effused, adnate, membranaceous. Hymenial surface brownish ivory, grayish ivory to lilac ivory, smooth. Hyphal system monomitic; generative hyphae nodose-septate, colorless, slightly thick- to thick-walled. Subiculum uniform, with compact texture, usually with crystal masses; hyphae fairly horizontal. Hymenial layer thickening, with compact texture, usually with oily materials, hyphae more or less vertical. Dendrohyphidia numerous, thick-walled toward base, colorless. Cystidia clavate, apically with resinous materials. Basidia clavate to subclavate, 4-sterigmata, thick-walled toward base. Basidiospores ellipsoid to ovoid, sometimes broadly ellipsoid, smooth, thin-walled or occasionally slightly thick-walled, negative in Melzer's reagent, acyanophilous.

Type species. *Dendrocorticiopsis orientalis*.

Etymology. *Dendrocorticiopsis* refers to the morphological resemblance to *Dendrocorticium*.

Dendrocorticiopsis orientalis **Sheng H. Wu, C.L. Wei & S.H. He, sp. nov.**
MycoBank: MB838903
Figs 2, 3

Diagnosis. The noteworthy features of *Dendrocorticiopsis orientalis* are: (1) subiculum composed of a basal layer, with compact texture; (2) oily materials usually present in hymenial layer; (3) cystidia with resinous materials at apices; (4) shortly clavate to subclavate basidia; (5) ellipsoid to ovoid basidiospores measuring 5–7 × 3.2–5.2 µm.

Typification. Taiwan, Taichung City, Heping District, near trailhead of Mt. Tangmadan Trail, 24°09'53.0"N, 120°57'26.4"E, 670 m asl., on dead angiosperm trunk, 20 Aug 2020, leg. C.L. Wei, WEI 20-166 (holotype, TNM F34448). GenBank: ITS = MW580922; 28S = MW580924.

Etymology. The epithet refers to the Eastern world, where the specimens were collected.

Description. Basidiomata annual, resupinate, effused, adnate, membranaceous, 50–100 µm thick in section. Hymenial surface brownish ivory, grayish ivory to lilac ivory, smooth, finely cracked; margin concolourous, slightly pruinose, rather determinate. Hyphal system monomitic; generative hyphae nodose-septate. Subiculum fairly uniform, composed of a basal layer, with fairly compact texture, usually with crystal masses; up to 30 µm thick, sometimes indistinct; hyphae mainly horizontal, colorless, fairly straight, 3–4 µm diam, with walls slightly thickened up to 1 µm. Hymenial layer thickening, with more or less compact texture, usually with oily materials, 50–70 µm

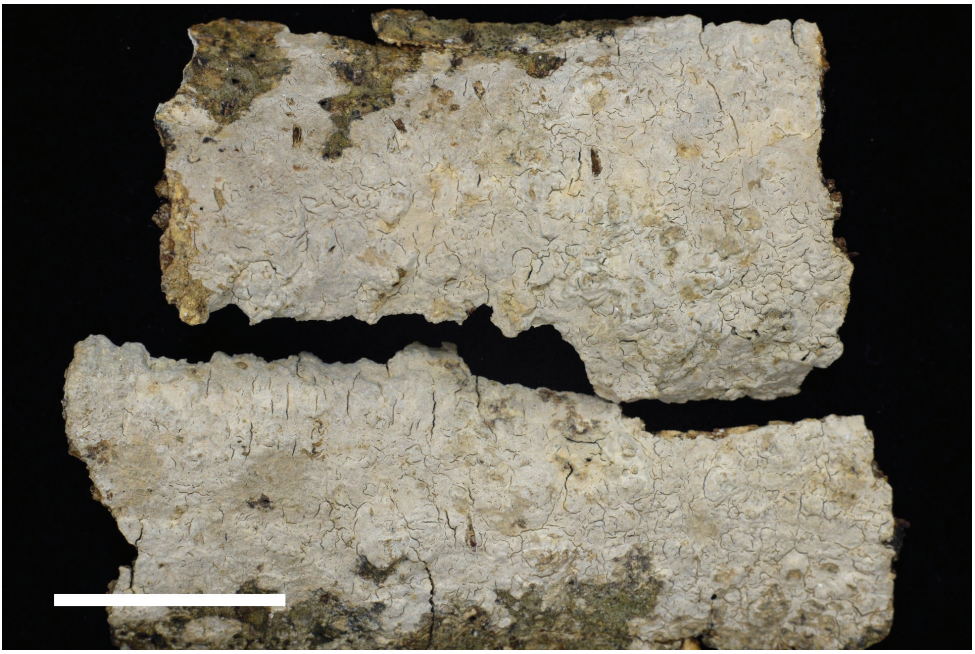

Figure 2. Basidiomata of *Dendrocorticiopsis orientalis* (holotype, WEI 20-166). Scale bar: 1 cm.

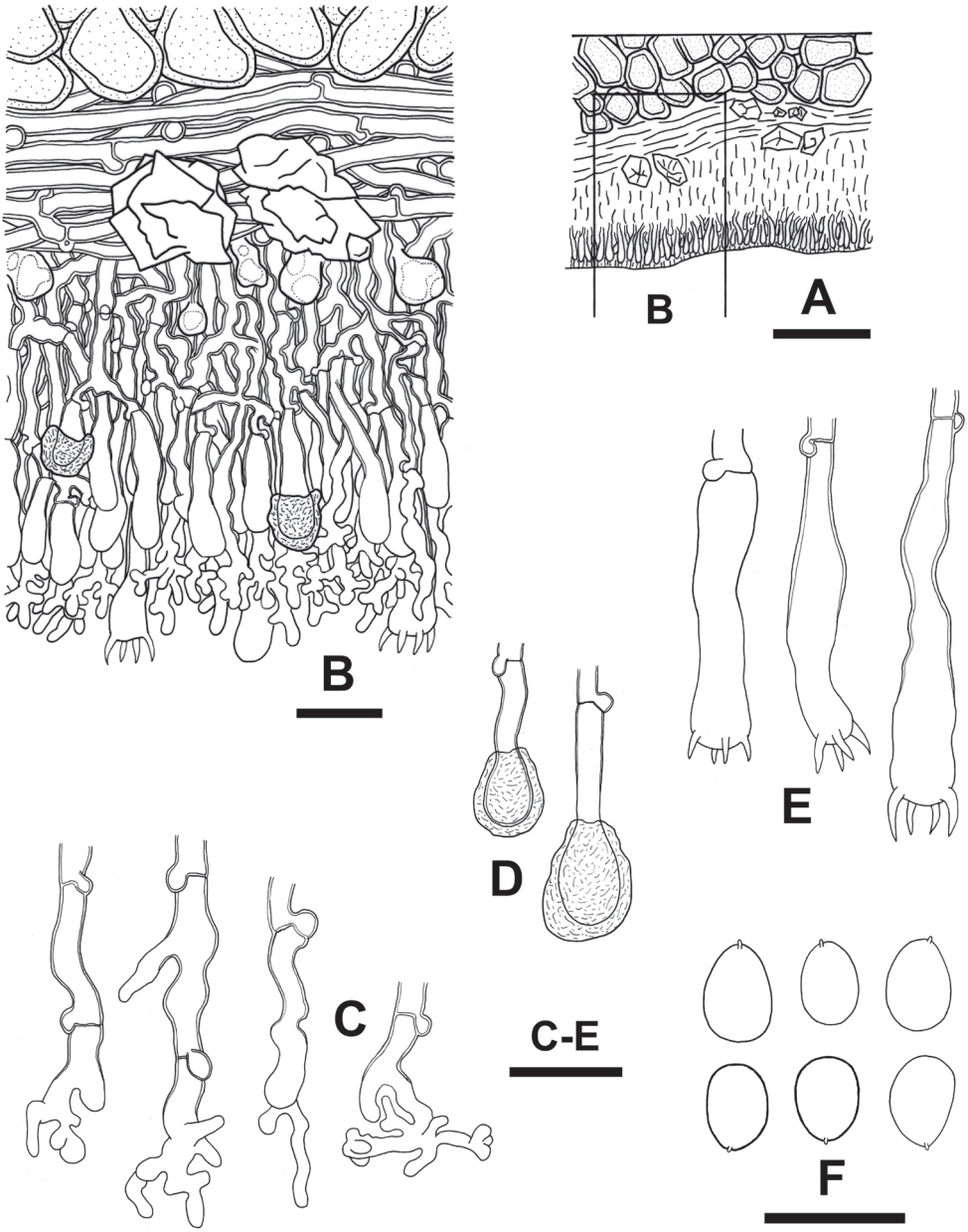

Figure 3. Micromorphological features of *Dendrocorticiopsis orientalis* (holotype, WEI 20-166) **A** profile of basidioma section **B** basidioma section **C** dendrohyphidia **D** cystidia **E** basidia **F** basidiospores. Scale bars: 50 μm (**A**); 10 μm (**B–F**).

thick; hyphae more or less vertical, colorless, 2–4 μm diam, with walls slightly thickened up to 1 μm. Dendrohyphidia numerous, 12–28 × 2–3 μm, thick-walled toward base, with walls up to 1 μm thick, colorless. Cystidia clavate, apically with resinous

materials, gradually dissolving in KOH, 10–20 × 3.5–5.5 µm, slightly thick-walled, or thickening toward base, with walls up to 1 µm thick. Basidia clavate to subclavate, usually broadened at basal or middle parts, 18–35 × 5–7 µm, 4-sterigmata, thickening toward base, with walls up to 1 µm thick. Basidiospores ellipsoid to ovoid, or broadly ellipsoid, smooth, colorless, with homogenous contents, thin-walled or occasionally slightly thick-walled, negative in Melzer's reagent, acyanophilous, mostly 5–7 × 3.2–5.2 µm. (5.5)6–7(7.5) × 4.2–5.2(5.5) µm, L = 6.50±0.42 µm, W = 4.66±0.32 µm, Q = 1.40 (n = 30) (holotype, WEI 20-166). (5.7)6.2–7(7.5) × (4.2)4.5–5(5.2) µm, L = 6.61±0.43 µm, W = 4.77±0.25 µm, Q = 1.39 (n = 30) (WEI 20-173). (4.2)5–6.8(7) × (3)3.2–5(5.2) µm, L = 5.8 µm, W = 4.2 µm, Q = 1.38 (He 4195).

Habitat. On dead angiosperm wood (e.g., *Acacia* and *Castanopsis*), occurring in August.

Distribution. In subtropical regions, known from China: Jiangxi and Taiwan.

Additional specimens examined (paratypes). China, Jiangxi Province, Yichun City, Yifeng County, Guanshan National Nature Reserve, 500 m asl., on dead *Castanopsis* wood, 9 Aug 2016, leg. S.H. He, He 4195 (BJFC 023637). Taiwan, Taichung City, Heping District, near trailhead of Mt. Tangmadan Trail, 24°09'53.0"N, 120°57'26.4"E, 670 m asl., on dead angiosperm trunk, 20 Aug 2020 leg. C.L. Wei, WEI 20-173 (TNM F0034449).

Notes. Both of the ITS and 28S sequences BLAST results showed that *Dendrocorticiopsis orientalis* is close to the strain BCRC 36235 that is annotated as *Ganoderma applanatum* (Pers.) Pat. in GenBank. According to personal communication with Bioresource Collection and Research Center (BCRC, Taiwan), the strain BCRC 36235 was indeed isolated from a *Ganoderma* specimen collected by Dr. Jin-Torng Peng in Nantou, Central Taiwan, on wood of *Acacia confusa* Merr. However, as suggested by Suldbold (2017), the ITS (EU232219) and 28S (EU232303) sequences of the strain BCRC 36235 are not true *G. applanatum*, and we supposed that the strain could be contaminated by *D. orientalis*, which is known to grow on *Acacia*. The specimen He 4195 collected on *Castanopsis* (Fagaceae) from Jiangxi Province has slightly smaller basidiospores (L = 5.8 µm, W = 4.2 µm) than the holotype.

Discussion

A comparison of morphological characteristics for distinguishing the four genera in Punctulariaceae is provided in Table 2. *Dendrocorticiopsis* is morphologically similar to *Dendrocorticium*, however, the latter has longer and narrowly clavate to tubular basidia usually longer than 45 µm, whereas *Dendrocorticiopsis* has clavate to subclavate basidia shorter than 35 µm. *Punctularia* differs from *Dendrocorticiopsis* by having resupinate or effused-reflexed basidiomata with a tuberculate hymenophore, colored dendrohyphidia, and through its lack of cystidia, while *Punctulariopsis* can be distinguished from *Dendrocorticiopsis* by possessing longer basidia and basidiospores, and mostly lacking cystidia.

Table 2. Morphological characteristics used for distinguishing the four genera in Punctulariaceae.

	Dendrocorticiopsis	***Dendrocorticium***	***Punctularia***	***Punctulariopsis***
basidiomata	resupinate	resupinate or effused-reflexed	resupinate or effused-reflexed	resupinate
hymenial surface	smooth	smooth	tuberculate	smooth
dendrohyphidia	colourless	mostly colourless (yellowish in *D. roseolum*); some species with encrustations	yellowish to brown or pink to rose	colourless
cystidia	clavate, apically with resinous materials	mostly absent (*D. roseolum* with halocystidia; *D. piceinum* with leptocystidia)	absent	mostly absent (*P. obducens* with leptocystidia)
basidia	clavate to subclavate; < 35 µm long	narrowly clavate to tubular; mostly > 45 µm long	narrowly clavate to tubular; 35–45 µm long	narrowly clavate to tubular; > 45 µm long
basidiospores	ellipsoid to ovoid; < 10 µm long	broadly ellipsoid to subglobose; usually < 10 µm long	ellipsoid; < 10 µm long	broadly ellipsoid to subglobose; > 10 µm long
distributions	subtropical regions	temperate or tropical regions	tropical to subtropical regions	tropical to subtropical regions

Dendrocorticium violaceum H.S. Jacks. ex M.J. Larsen & Gilb. and *D. polygonioides* (P. Karst.) M.J. Larsen & Gilb. have similar-sized basidiospores to *Dendrocorticiopsis orientalis* [4–6.5 × 3–5 µm in *D. violaceum*, 6–9 × 4–6 µm in *D. polygonioides* (Larsen and Gilbertson 1977)]. However, *D. violaceum* is distributed in Canada, has a reflexed basidiomata margin (closely adnate in *Dendrocorticiopsis orientalis*), and grows mainly on deciduous wood. *Dendrocorticium polygonioides* is mainly distributed in Europe and has a whitish to violaceous surface, large basidia (50–60 × 5–7 µm), and usually encrusted dendrohyphidia (Larsen and Gilbertson 1977).

Acknowledgements

This study was supported by a Grant-in-Aid for Scientific Research (no. 109-08.1-SB-18) from the Council of Agriculture, Executive Yuan, ROC and the National Natural Science Foundation of China (No. 31750001). We are grateful to Miss Shin-Yi Ke for DNA extraction and PCR works, and to Miss Siou-Zhen Chen for managing studied specimens.

References

Ariyawansa HA, Hyde KD, Jayasiri SC, Buyck B, Chethana KWT, Dai DQ, Dai YC, Daranagama DA, Jayawardena RS, Lücking R, Ghobad-Nejhad M, Niskanen T, Thambugala KM, Voigt K, Zhao RL, Li G-J, Doilom M, Boonmee S, Yang ZL, Cai Q, Cui Y-Y, Bahkali AH, Chen J, Cui BK, Chen JJ, Dayarathne MC, Dissanayake AJ, Ekanayaka AH, Hashimoto

A, Hongsanan S, Jones EBG, Larsson E, Li WJ, Li Q-R, Liu JK, Luo ZL, Maharachchikumbura SSN, Mapook A, McKenzie EHC, Norphanphoun C, Konta S, Pang KL, Perera RH, Phookamsak R, Phukhamsakda C, Pinruan U, Randrianjohany E, Singtripop C, Tanaka K, Tian CM, Tibpromma S, Abdel-Wahab MA, Wanasinghe DN, Wijayawardene NN, Zhang J-F, Zhang H, Abdel-Aziz FA, Wedin M, Westberg M, Ammirati JF, Bulgakov TS, Lima DX, Callaghan TM, Callac P, Chang C-H, Coca LF, Dal-Forno M, Dollhofer V, Fliegerová K, Greiner K, Griffith GW, Ho H-M, Hofstetter V, Jeewon R, Kang JC, Wen T-C, Kirk PM, Kytövuori I, Lawrey JD, Xing J, Li H, Liu ZY, Liu XZ, Liimatainen K, Lumbsch HT, Matsumura M, Moncada B, Nuankaew S, Parnmen S, de Azevedo Santiago ALCM, Sommai S, Song Y, de Souza CAF, de Souza-Motta CM, Su HY, Suetrong S, Wang Y, Wei S-F, Wen TC, Yuan HS, Zhou LW, Réblová M, Fournier J, Camporesi E, Luangsa-ard JJ, Tasanathai K, Khonsanit A, Thanakitpipattana D, Somrithipol S, Diederich P, Millanes AM, Common RS, Stadler M, Yan JY, Li XH, Lee HW, Nguyen TTT, Lee HB, Battistin E, Marsico O, Vizzini A, Vila J, Ercole E, Eberhardt U, Simonini G, Wen H-A, Chen X-H, Miettinen O, Spirin V, Hernawati (2015) Fungal diversity notes 111–252—Taxonomic and phylogenetic contributions to fungal taxa. Fungal Diversity 75(1): 27–274. https://doi.org/10.1007/s13225-015-0346-5

Baltazar JM, Da Silveira RMB, Rajchenberg M (2013) *Asterostromella roseola* Bres. ex Rick is combined in *Dendrocorticium* (Corticiaceae, Agaricomycetes). Phytotaxa 104(1): 49–52. https://doi.org/10.11646/phytotaxa.104.1.7

Bernicchia A, Gorjón SP (2010) Fungi Europaei 12: Corticiaceae s.l. Edizioni Candusso, Lomazzo.

Chen CC, Chen CY, Lim YW, Wu SH (2020) Phylogeny and taxonomy of *Ceriporia* and other related taxa and description of three new species. Mycologia 112(1): 64–82. https://doi.org/10.1080/00275514.2019.1664097

Cooke WB (1956) The genus *Phlebia*. Mycologia 48(3): 386–405. https://doi.org/10.1080/00275514.1956.12024546

Darriba D, Taboada GL, Doallo R, Posada D (2012) jModelTest 2: More models, new heuristics and parallel computing. Nature Methods 9(8): 772–772. https://doi.org/10.1038/nmeth.2109

Donk MA (1964) A conspectus of the families of Aphyllophorales. Persoonia 3: 199–324.

Ghobad-Nejhad M, Duhem B (2014) Novelties in the Corticiales: *Vuilleminia nilsii* sp. nov. and *Dendrominia* gen. nov. (Basidiomycota). Mycological Progress 13(1): 1–11. https://doi.org/10.1007/s11557-012-0881-3

Ghobad-Nejhad M, Nilsson RH, Hallenberg N (2010) Phylogeny and taxonomy of the genus *Vuilleminia* (Basidiomycota) based on molecular and morphological evidence, with new insights into Corticiales. Taxon 59(5): 1519–1534. https://doi.org/10.1002/tax.595016

Ghobad-Nejhad M, Langer E, Nakasone K, Diederich P, Nilsson RH, Rajchenberg M, Ginns J (2021) Digging Up the Roots: Taxonomic and Phylogenetic Disentanglements in Corticiaceae ss (Corticiales, Basidiomycota) and Evolution of Nutritional Modes. Frontiers in Microbiology 2320: e704802. https://doi.org/10.3389/fmicb.2021.704802

Gorjón SP, Bernicchia A (2017) *Dendrocorticium pinsapineum* (Corticiales, Basidiomycota), second world distributional area in Italy. Nova Hedwigia 105(3–4): 341–346. https://doi.org/10.1127/nova_hedwigia/2017/0415

Guan QX, Zhao W, Zhao CL (2021) A new species of *Punctularia* (Punctulariaceae, Basidiomycota) from southwest China. Phytotaxa 489(3): 285–292. https://doi.org/10.11646/phytotaxa.489.3.5

Hall TA (1999) BioEdit: A user-friendly biological sequence alignment editor and analysis program for windows 95/98/NT. Nucleic Acids Symposium Series 41: 95–98.

He MQ, Zhao RL, Hyde KD, Begerow D, Kemler M, Yurkov A, McKenzie EHC, Raspé O, Kakishima M, Sánchez-Ramírez S, Vellinga EC, Halling R, Papp V, Zmitrovich IV, Buyck B, Ertz D, Wijayawardene NN, Cui B-K, Schoutteten N, Liu X-Z, Li T-H, Yao Y-J, Zhu X-Y, Liu A-Q, Li G-J, Zhang M-Z, Ling Z-L, Cao B, Antonín V, Boekhout T, da Silva BDB, De Crop E, Decock C, Dima B, Dutta AK, Fell JW, Geml J, Ghobad-Nejhad M, Giachini AJ, Gibertoni TB, Gorjón SP, Haelewaters D, He S-H, Hodkinson BP, Horak E, Hoshino T, Justo A, Lim YW, Menolli Jr N, Mešić A, Moncalvo J-M, Mueller GM, Nagy LG, Nilsson RH, Noordeloos M, Nuytinck J, Orihara T, Ratchadawan C, Rajchenberg M, Silva-Filho AGS, Sulzbacher MA, Tkalčec Z, Valenzuela R, Verbeken A, Vizzini A, Wartchow F, Wei T-Z, Weiß M, Zhao C-L, Kirk PM (2019) Notes, outline and divergence times of Basidiomycota. Fungal Diversity 99(1): 105–367. https://doi.org/10.1007/s13225-019-00435-4

Hibbett DS, Bauer R, Binder M, Giachini AJ, Hosaka K, Justo A, Larsson E, Larsson KH, Lawrey JD, Miettinen O, Nagy LG, Nilsson RH, Weiss M, Thorn RG (2014) 14 Agaricomycetes. In: McLaughlin D, Spatafora J (Eds) Systematics and evolution. Part A. The Mycota, vol 7, 2nd edn. Springer-Verlag, Berlin, Heidelberg, 373–429. https://doi.org/10.1007/978-3-642-55318-9_14

Katoh K, Standley DM (2013) MAFFT Multiple sequence alignment software version 7: Improvements in performance and usability. Molecular Biology and Evolution 30(4): 772–780. https://doi.org/10.1093/molbev/mst010

Larsen MJ, Gilbertson RL (1977) Studies in *Laeticorticium* (Aphyllophorales, Corticiaceae) and related genera. Nordic Journal of Botany 24: 99–121.

Petch T (1916) Revisions of Ceylon fungi (Part IV). Annals of the Royal Botanic Gardens (Peradeniya) 6: 153–183.

Ronquist F, Teslenko M, van der Mark P, Ayres DL, Darling A, Höhna S, Larget B, Liu L, Suchard MA, Huelsenbeck JP (2012) MrBayes 3.2: Efficient Bayesian phylogenetic inference and model choice across a large model space. Systematic Biology 61(3): 539–542. https://doi.org/10.1093/sysbio/sys029

Stamatakis A (2014) RAxML version 8: A tool for phylogenetic analysis and post-analysis of large phylogenies. Bioinformatics (Oxford, England) 30(9): 1312–1313. https://doi.org/10.1093/bioinformatics/btu033

Suldbold J (2017) Taxonomic re-evaluation of medicinal wood-decaying fungi: *Abundisporus*, *Fomitopsis*, and *Ganoderma* in Korea. Dissertation, Seoul National University.

Talbot PHB (1958) Studies of some South African resupinate Hymenomycetes. Part II. Bothalia 7(1): 131–187. https://doi.org/10.4102/abc.v7i1.1652

Vilgalys R, Hester M (1990) Rapid genetic identification and mapping of enzymatically amplified ribosomal DNA from several *Cryptococcus* species. Journal of Bacteriology 172(8): 4238–4246. https://doi.org/10.1128/jb.172.8.4238-4246.1990

White TJ, Bruns T, Taylor LS (1990) Amplification and direct sequencing of fungal ribosomal RNA genes for phylogenetics. In: Innis MA, Gelfand DH, Sninsky JJ, White TJ (Eds)

PCR protocols: a guide to methods and application. Academic Press, San Diego, 322–315. https://doi.org/10.1016/B978-0-12-372180-8.50042-1

Wijayawardene NN, Hyde KD, Al-Ani LKT, Tedersoo L, Haelewaters D, Rajeshkumar KC, Zhao RL, Aptroot A, Leontyev DV, Saxena RK, Tokarev YS, Dai DQ, Letcher PM, Stephenson SL, Ertz D, Lumbsch HT, Kukwa M, Issi IV, Madrid H, Phillips AJL, Selbmann L, Pfliegler WP, Horváth E, Bensch K, Kirk PM, Kolaříková K, Raja HA, Radek R, Papp V, Dima B, Ma J, Malosso E, Takamatsu S, Rambold G, Gannibal PB, Triebel D, Gautam AK, Avasthi S, Suetrong S, Timdal E, Fryar SC, Delgado G, Réblová M, Doilom M, Dolatabadi S, Pawłowska JZ, Humber RA, Kodsueb R, Sánchez-Castro I, Goto BT, Silva DKA, de Souza FA, Oehl F, da Silva GA, Silva IR, Błaszkowski J, Jobim K, Maia LC, Barbosa FR, Fiuza PO, Divakar PK, Shenoy BD, Castañeda-Ruiz RF, Somrithipol S, Lateef AA, Karunarathna SC, Tibpromma S, Mortimer PE, Wanasinghe DN, Phookamsak R, Xu J, Wang Y, Tian F, Alvarado P, Li DW, Kušan I, Matočec N, Mešić A, Tkalčec Z, Maharachchikumbura SSN, Papizadeh M, Heredia G, Wartchow F, Bakhshi M, Boehm E, Youssef N, Hustad VP, Lawrey JD, Santiago ALCMA, Bezerra JDP, Souza-Motta CM, Firmino AL, Tian Q, Houbraken J, Hongsanan S, Tanaka K, Dissanayake AJ, Monteiro JS, Grossart HP, Suija A, Weerakoon G, Etayo J, Tsurykau A, Vázquez V, Mungai P, Damm U, Li QR, Zhang H, Boonmee S, Lu YZ, Becerra AG, Kendrick B, Brearley FQ, Motiejūnaitė J, Sharma B, Khare R, Gaikwad S, Wijesundara DSA, Tang LZ, He MQ, Flakus A, Rodriguez-Flakus P, Zhurbenko MP, McKenzie EHC, Stadler M, Bhat DJ, Liu JK, Raza M, Jeewon R, Nassonova ES, Prieto M, Jayalal RGU, Erdoğdu M, Yurkov A, Schnittler M, Shchepin ON, Novozhilov YK, Silva-Filho AGS, Gentekaki E, Liu P, Cavender JC, Kang Y, Mohammad S, Zhang LF, Xu RF, Li YM, Dayarathne MC, Ekanayaka AH, Wen TC, Deng CY, Pereira OL, Navathe S, Hawksworth DL, Fan XL, Dissanayake LS, Kuhnert E, Grossart HP, , Thines M, (2020) Outline of Fungi and fungus-like taxa. Mycosphere: Journal of Fungal Biology 11(1): 1060–1456. https://doi.org/10.5943/mycosphere/11/1/8

Wu SH, Chen CC, Wei CL (2018) Three new species of *Phanerochaete* (Polyporales, Basidiomycota). MycoKeys 41: 91–106. https://doi.org/10.3897/mycokeys.41.29070

Supplementary material 1

Alignments to TreeBase

Authors: Chia-Ling Wei, Che-Chih Chen, Shuang-Hui He, Sheng-Hua Wu

Data type: Alignments (fas. file)

Explanation note: We have uploaded the alignments to TreeBase and here is the link and the file. http://purl.org/phylo/treebase/phylows/study/TB2:S29602?x-accesscode=cdd27042a420e43e26dd8e62ea382799&format=html.

Link: https://doi.org/10.3897/mycokeys.90.84562.suppl1

MycoKeys 90: 31–51 (2022)
doi: 10.3897/mycokeys.90.84717
https://mycokeys.pensoft.net

RESEARCH ARTICLE

A peer-reviewed open-access journal
MycoKeys
Launched to accelerate biodiversity research

Taxonomy and molecular phylogeny of *Trametopsis* (Polyporales, Basidiomycota) with descriptions of two new species

Shun Liu[1], Yi-Fei Sun[1], Yan Wang[1], Tai-Min Xu[1], Chang-Ge Song[1], Yuan-Yuan Chen[2], Bao-Kai Cui[1]

1 *Institute of Microbiology, School of Ecology and Nature Conservation, Beijing Forestry University, Beijing 100083, China* **2** *College of Forestry, Henan Agricultural University, Zhengzhou, Henan 450002, China*

Corresponding author: Bao-Kai Cui (cuibaokai@bjfu.edu.cn)

Academic editor: María P. Martín | Received 1 April 2022 | Accepted 17 May 2022 | Published 31 May 2022

Citation: Liu S, Sun Y-F, Wang Y, Xu T-M, Song C-G, Chen Y-Y, Cui B-K (2022) Taxonomy and molecular phylogeny of *Trametopsis* (Polyporales, Basidiomycota) with descriptions of two new species. MycoKeys 90: 31–51. https://doi.org/10.3897/mycokeys.90.84717

Abstract

Trametopsis is a worldwide genus belonging to Irpicaceae in the phlebioid clade, which can cause a white decay of wood. Previously, only three species were ascribed to the genus. In this study, we performed a morphological and phylogenetic study of *Trametopsis*. Molecular phylogenetic analyses of multiple loci included the internal transcribed spacer (ITS) regions, the large subunit nuclear ribosomal RNA gene (nLSU), the largest subunit of RNA polymerase II (RPB1), the second largest subunit of RNA polymerase II (RPB2) and the translation elongation factor 1-α gene (TEF1). Phylogenetic trees were inferred from the combined datasets of ITS+nLSU sequences and ITS+nLSU+RPB1+RPB2+TEF1 sequences by using maximum parsimony, maximum likelihood and Bayesian inference analyses. Combined with molecular data, morphological characters and ecological traits, two new species of *Trametopsis* are discovered. *Trametopsis abieticola* is characterised by its pileate, solitary or imbricate basidiomata, buff to buff-yellow pileal surface when fresh, becoming pinkish buff to clay-buff when dry, cream to buff pore surface when fresh, becoming pinkish buff to greyish brown upon drying, round to angular and large pores (0.5–1 per mm), cylindrical basidiospores (5.8–7.2 × 1.9–2.6 µm), distributed in the high altitude of mountains and grows on *Abies* sp. *Trametopsis tasmanica* is characterised by its resupinate basidiomata, cream to pinkish-buff pore surface when fresh, becoming honey-yellow to snuff brown upon drying, cylindrical basidiospores (5.2–6.3 × 1.8–2.2 µm), and by growing on *Eucalyptus* sp. Detailed descriptions and illustrations of the two novel species are provided.

Keywords

Irpicaceae, macrofungi, multi-gene phylogeny, new species, white-rot fungi

Introduction

Trametopsis Tomšovský was established by Tomšovský (2008) with *T. cervina* (Schwein.) Tomšovský as type species. The morphological characteristics of *Trametopsis* are as follows: Basidiomata annual, sessile to effused-reflexed or rarely resupinate. Pileal surface pinkish buff to cinnamon or clay-buff, hirsute to strigose. Pore surface concolorous with pileal surface; pores irregular, daedaloid to irpicoid; dissepiments thin and lacerate. Context pale buff, fibrous. Tubes concolorous with the context, corky. Hyphal system dimitic; generative hyphae clamped. Cystidia absent; fusoid cystidioles occasionally present. Basidia clavate, bearing four sterigmata and a basal clamp connection. Basidiospores cylindrical, hyaline, thin-walled, smooth, IKI–, CB– (Tomšovský 2008).

Gómez-Montoya et al. (2017) evaluated the species of *Trametopsis* in the Neotropics based on phylogenetic evidences and morphological analyses. The phylogenetic analyses showed that *Trametopsis* is an independent genus; furthermore, one new species, *T. aborigena* Gómez-Mont. & Robledo, and the two new combinations, *T. brasiliensis* (Ryvarden & de Meijer) Gómez-Mont. & Robledo and *T. luteocontexta* (Ryvarden & de Meijer) Gómez-Mont., Robledo & Drechsler-Santos were presented. Westphalen et al. (2019) summarised *Antrodiella* Ryvarden & I. Johans. and related genera from the Neotropics, and *T. luteocontexta* was transferred to *Aegis* Gómez-Mont., Rajchenb. & Robledo according to morphological and molecular data. Recent phylogenetic studies have shown that *Trametopsis* belongs to Irpicaceae Spirin & Zmitr in the phlebioid clade (Justo et al. 2017; Chen et al. 2021). So far, three species are accepted in *Trametopsis*, viz., *T. aborigena*, *T. brasiliensis* and *T. cervina*.

During our investigations of wood-decay fungi, some specimens of the phlebioid clade were collected. These specimens possess glabrous or velutinate to strigose pileal surface, round to angular, irregular, daedaleoid to irpicoid pores, saprophytic on dead wood and causing white rot. Preliminary morphological observations showed that these specimens may belong to *Trametopsis*. To determine the phylogenetic positions of these specimens, we performed phylogenetic analyses of Irpicaceae with emphasis on *Trametopsis* based on the combined sequences datasets of ITS+nLSU and ITS+nLSU+RPB1+RPB2+TEF1. Combining morphological and molecular evidence, two new species, viz., *T. abieticola* and *T. tasmanica* are described and illustrated.

Materials and methods

Morphological studies

The examined specimens were deposited at the herbarium of the Institute of Microbiology, Beijing Forestry University (BJFC). Morphological descriptions and abbreviations used in this study follow Cui et al. (2019) and Song et al. (2021).

Molecular studies and phylogenetic analysis

The procedures for DNA extraction and polymerase chain reaction (PCR) used in this study were the same as described by Liu et al. (2021a) and Sun et al. (2022). The ITS regions were amplified with the primer pairs ITS4 and ITS5, the nLSU regions were amplified with the primer pairs LR0R and LR7, RPB1 was amplified with primer pairs RPB1-Af and RPB1-Cr, RPB2 gene was amplified with the primer pairs fRPB2-f5F and bRPB2-7.1R, and TEF1 gene was amplified with the primer pairs EF1-983F and EF1-1567R (White et al. 1990; Rehner 2001; Matheny et al. 2002; Matheny 2005).

The PCR cycling schedules for different DNA sequences of ITS, nLSU, RPB1, RPB2 and TEF1 genes used in this study followed those used in Liu et al. (2021b, 2022) with some modifications. The PCR products were purified and sequenced at Beijing Genomics Institute, China, with the same primers. All newly generated sequences were submitted to GenBank and were listed in Table 1.

Sequences were aligned with additional sequences downloaded from GenBank (Table 1) using ClustalX (Thompson et al. 1997). Alignment was manually adjusted to allow maximum alignment and to minimise gaps in BioEdit (Hall 1999). Sequence alignment was deposited to TreeBase (https://treebase.org/treebase-web; submission ID 29580). In phylogenetic reconstructions, the sequences of *Phanerochaete albida* Sheng H. Wu and *P. alnea* (Fr.) P. Karst. obtained from GenBank were used as outgroups. The reason for choosing these two species as outgroup taxa is that they belong to *Phanerochaete* in Phanerochaetaceae, and are closely related to Irpicaceae (Chen et al. 2021), which conforms to the outgroup selection rules. Furthermore, species of *Phanerochaete* were also selected as outgroups in other phylogenetic studies of Irpicaceae, such as in El-Gharabawy et al (2021).

Phylogenetic analyses approaches used in this study followed Sun et al. (2020) and Ji et al. (2022). The congruencies of the 2-gene (ITS and nLSU) and 5-gene (ITS, nLSU, RPB1, RPB2 and TEF1) were evaluated with the incongruence length difference (ILD) test (Farris et al. 1994) implemented in PAUP* 4.0b10 (Swofford 2002), under heuristic search and 1000 homogeneity replicates. Maximum parsimony (MP) analysis was performed in PAUP* version 4.0b10 (Swofford 2002). Clade robustness was assessed using a bootstrap (BT) analysis with 1000 replicates (Felsenstein 1985). Descriptive tree statistics tree length (TL), consistency index (CI), retention index (RI), rescaled consistency index (RC), and homoplasy index (HI) were calculated for each Most Parsimonious Tree (MPT) generated. Maximum Likelihood (ML) analysis was performed in RAxML-HPC v. 8.2.3 with a GTR+G+I model (Stamatakis 2014). Bayesian inference (BI) was calculated by MrBayes 3.1.2 (Ronquist and Huelsenbeck 2003) with a general time reversible (GTR) model of DNA substitution and a gamma distribution rate variation across sites determined by MrModeltest 2.3 (Posada and Crandall 1998; Nylander 2008). The branch support was evaluated with a bootstrapping method of 1000 replicates (Hillis and Bull 1993).

Trees were viewed in FigTree v1.4.4 (http://tree.bio.ed.ac.uk/software/figtree/). Branches that received bootstrap supports for maximum parsimony (MP), maximum likelihood (ML) and Bayesian posterior probabilities (BPP) greater than or equal to 75% (MP and ML) and 0.95 (BPP) were considered as significantly supported, respectively.

Table 1. A list of species, specimens, and GenBank accession number of sequences used for phylogenetic analyses in this study.

Species	Sample no.	Locality	GenBank accessions					References
			ITS	nLSU	RPB1	RPB2	TEF1	
Byssomerulius corium	FCUG 2701	Russia	MZ636931	GQ470630	MZ748415	OK136068	MZ913668	Wu et al. (2010); Chen et al. (2021)
B. corium	Wu 1207-55	China	MZ636932	MZ637096	—	—	—	Chen et al. (2021)
B. corium	FP-102382	USA	KP135007	KP135230	KP134802	KP134921	—	Floudas and Hibbett (2015)
Ceriporia bubalinomarginata	Dai 11327	China	JX623953	JX644045	—	—	—	Jia et al. (2014)
C. bubalinomarginata	Dai 12499	China	JX623954	JX644044	—	—	—	Jia et al. (2014)
C. viridans	Spirin 5909	Finland	KX236481	KX236481	—	—	—	Spirin et al. (2016)
C. viridans	Miettinen 11701	Netherlands	KX752600	KX752600	—	—	—	Miettinen et al. (2016)
Crystallicutis cf. *serpens*	Wu 1608-130	China	MZ636946	MZ637108	—	—	—	Chen et al. (2021)
C. cf. *serpens*	Wu 1608-81	China	MZ636947	MZ637109	MZ748435	OK136094	MZ913699	Chen et al. (2021)
C. serpens	HHB-15692	USA	KP135031	KP135200	KP134785	KP134914	—	Floudas and Hibbett (2015)
C. sp.	FP-101245	USA	KP135029	—	—	—	—	Floudas and Hibbett (2015)
Cytidiella albida	GB-1833	Spain	KY948748	KY948889	KY948960	OK136069	MZ913675	Justo et al. (2017); Chen et al. (2021)
C. albomarginata	Wei 18-474	China	MZ636948	MZ637110	MZ748429	OK136070	MZ913678	Chen et al. (2021)
C. albomarginata	Wu 0108-86	China	MZ636949	MZ637111	MZ748430	OK136071	MZ913677	Chen et al. (2021)
C. albomellea	FP-102339	USA	MZ636950	MZ637112	MZ748431	—	—	Chen et al. (2021)
C. nitidula	T-407	USA	KY948747	MZ637113	KY948961	OK136072	MZ913676	Justo et al. (2017); Chen et al. (2021)
Efibula gracilis	FD-455	USA	KP135027	MZ637116	KP134804	OK136077	MZ913679	Floudas and Hibbett (2015); Chen et al. (2021)
E. gracilis	FP-102052	USA	KP135028	—	—	—	—	Floudas and Hibbett (2015)
E. matsuensis	Wu 1011-18	China	MZ636956	MZ637119	MZ748418	OK136078	MZ913680	Chen et al. (2021)
E. matsuensis	Wu 1011-19	China	MZ636957	MZ637120	—	—	—	Chen et al. (2021)
E. tropica	Chen 3596	China	MZ636966	MZ637128	—	—	—	Chen et al. (2021)
E. tropica	Wei 18-149	China	MZ636967	MZ637129	MZ748419	OK136079	MZ913681	Chen et al. (2021)
E. yunnanensis	Wu 880515-1	China	MZ636977	GQ470672	MZ748420	OK136080	MZ913682	Wu et al. (2010); Chen et al. (2021)
E. yunnanensis	Wu 0910-104	China	MZ636976	MZ637138	—	—	—	Chen et al. (2021)
Gloeoporus orientalis	Wei 16-485	China	MZ636980	MZ637141	MZ748443	OK136095	MZ913709	Chen et al. (2021)
G. pannocinctus	L-15726	USA	KP135060	KP135214	KP134867	KP134973	—	Floudas and Hibbett (2015)
Irpex flavus	Wu 0705-1	China	MZ636988	MZ637149	MZ748432	OK136087	MZ913683	Chen et al. (2021)
I. flavus	Wu 0705-2	China	MZ636989	MZ637150	—	—	—	Chen et al. (2021)
I. hacksungii	F 2008	South Korea	FJ750851	—	—	—	—	Lee et al. (2008)
I. hydnoides	KUC 20121109-01	South Korea	KJ668510	KJ668362	—	—	—	Jang et al. (2016)
I. lacerates	WHC 1372	China	MZ636990	MZ637151	—	—	—	Chen et al. (2021)

Species	Sample no.	Locality	GenBank accessions					References
			ITS	nLSU	RPB1	RPB2	TEF1	
I. lacteus	DO 421	Sweden	JX109852	JX109852	—	JX109882	—	Binder et al. (2013)
I. lacteus	FD-93	USA	KP135025	—	—	—	—	Floudas and Hibbett (2015)
I. latemarginatus	FP-55521-T	USA	KP135024	KP135202	KP134805	KP134915	—	Floudas and Hibbett (2015)
I. latemarginatus	Dai 7165	China	KY131834	KY131893	—	—	—	Wu et al. (2017)
I. lenis	Wu 1608-14	China	MZ636991	MZ637152	MZ748434	—	MZ913685	Chen et al. (2021)
I. lenis	Wu 1608-22	China	MZ636992	MZ637153	—	—	—	Chen et al. (2021)
I. rosettiformis	LR40855	USA	JN649347	JN649347	—	—	—	Sjökvist et al. (2012)
I. rosettiformis	Meijer3729	Brazil	JN649346	JN649346	—	JX109875	JX109904	Sjökvist et al. (2012); Binder et al. (2013)
Leptoporus mollis	LE BIN 3849	Russia	MG735341	—	—	—	—	Psurtseva (2010)
L. mollis	RLG-7163	USA	KY948794	MZ637155	KY948956	OK136101	MZ913693	Justo et al. (2017); Chen et al. (2021)
Meruliopsis albostramineus	HHB 10729	USA	KP135051	KP135229	KP134787	—	—	Floudas and Hibbett (2015)
M. crassitunicata	CHWC 1506-46	China	LC427010	LC427034	—	—	—	Chen et al. (2020)
M. leptocystidiata	Wu 1708-43	China	LC427013	LC427033	LC427070	—	—	Chen et al. (2020)
M. parvispora	Wu 1209-58	China	LC427017	LC427039	LC427065	—	—	Chen et al. (2020)
M. taxicola	GC 1704-60	China	LC427028	LC427050	LC427063	—	—	Chen et al. (2020)
Phanerochaete albida	GC 1407-14	China	MZ422788	MZ637179	MZ748384	OK136013	MZ913704	Chen et al. (2021)
P. alnea	FP-151125	USA	KP135177	MZ637181	MZ748385	OK136014	MZ913641	Floudas and Hibbett (2015); Chen et al. (2021)
Phanerochaetella angustocystidiata	Wu 9606-39	China	MZ637020	GQ470638	MZ748422	OK136082	MZ913687	Wu et al. (2010); Chen et al. (2021)
P. angustocystidiata	GC 1501-20	China	MZ637017	MZ637225	—	—	—	Chen et al. (2021)
P. exilis	HHB-6988	USA	KP135001	KP135236	KP134799	KP134918	—	Floudas and Hibbett (2015)
P. formosana	Chen 479	China	MZ637023	GQ470650	MZ748424	OK136084	MZ913718	Wu et al. (2010); Chen et al. (2021)
P. formosana	Chen 3468	China	MZ637022	MZ637229	—	—	—	Chen et al. (2021)
P. leptoderma	Chen 1362	China	MZ637025	GQ470646	MZ748423	OK136083	MZ913689	Wu et al. (2010); Chen et al. (2021)
P. leptoderma	Wu 1703-9	China	MZ637027	MZ637232	—	—	—	Wu et al. (2010)
P. xerophila	HHB-8509	USA	KP134996	KP135259	KP134800	KP134919	MZ913688	Floudas and Hibbett (2015); Chen et al. (2021)
P. xerophila	KKN-172	USA	KP134997	—	—	—	—	Floudas and Hibbett (2015)
Raduliporus aneirinus	HHB-15629	USA	KP135023	KP135207	KP134795	—	—	Floudas and Hibbett (2015)
R. aneirinus	Wu 0409-199	China	MZ637068	MZ637267	—	OK136096	MZ913712	Chen et al. (2021)
R. pseudogilvescens	Wu 9508-54	China	MZ637069	MZ637269	—	—	—	Chen et al. (2021)
Resiniporus pseudogilvescens	Wu 1209-46	China	KY688203	MZ637268	MZ748436	OK136097	MZ913713	Chen et al. (2018); Chen et al. (2021)
R. resinascens	BRNM 710169	Czech Republic	FJ496675	FJ496698	—	—	—	Tomšovský et al. (2010)
Trametopsis abieticola	**Cui 18363**	**China**	**ON041038**	**ON041054**	**ON099403**	**ON099411**	**ON083777**	**Present study**
T. abieticola	**Cui 18383**	**China**	**ON041039**	**ON041055**	**ON099404**	**ON099412**	**ON083778**	**Present study**

Species	Sample no.	Locality	GenBank accessions					References
			ITS	nLSU	RPB1	RPB2	TEF1	
T. aborigena	Robledo 1236	Argentina	KY655336	KY655338	—	—	—	Gómez-Montoya et al. (2017)
T. aborigena	Robledo 1238	Argentina	KY655337	KY655339	—	—	—	Gómez-Montoya et al. (2017)
T. brasiliensis	Meijer 3637	Brazil	JN710510	JN710510	—	—	—	Miettinena et al. (2012)
T. cervina	**Cui 17712**	**China**	**ON041040**	**ON041056**	—	**ON099413**	**ON083779**	**Present study**
T. cervina	**Cui 18017**	**China**	**ON041041**	**ON041057**	—	**ON099414**	**ON083780**	**Present study**
T. cervina	**Cui 18019**	**China**	**ON041042**	**ON041058**	**ON099405**	**ON099415**	**ON083781**	**Present study**
T. cervina	**Dai 21818**	**China**	**ON041043**	**ON041059**	**ON099406**	—	**ON083782**	**Present study**
T. cervina	**Dai 21820**	**China**	**ON041044**	**ON041060**	**ON099407**	**ON099416**	**ON083783**	**Present study**
T. cervina	**Dai 22804**	**China**	**ON041045**	**ON041061**	—	**ON099417**	**ON083784**	**Present study**
T. cervina	**Dai 23454**	**China**	**ON041046**	**ON041062**	—	—	**ON083785**	**Present study**
T. cervina	**He 6863**	**China**	**ON041047**	**ON041063**	**ON099408**	**ON099418**	**ON083786**	**Present study**
T. cervina	MG 299	Iran	KU213592	KU213594	—	—	—	—
T. cervina	TJV-93-216T	USA	JN165020	JN164796	JN164839	JN164877	JN164882	Justo and Hibbett (2011)
T. tasmanica	**Cui 16606**	**Australia**	**ON041048**	**ON041064**	**ON099409**	**ON099419**	**ON083787**	**Present study**
T. tasmanica	**Cui 16607**	**Australia**	**ON041049**	**ON041065**	**ON099410**	**ON099420**	**ON083788**	**Present study**

Newly generated sequences for this study are shown in bold.

Results

Phylogeny

The combined 2-gene (ITS+nLSU) sequences dataset had an aligned length of 1893 characters, including gaps (619 characters for ITS, 1274 characters for nLSU), of which 1307 characters were constant, 105 were variable and parsimony-uninformative, and 481 were parsimony-informative. MP analysis yielded 26 equally parsimonious trees (TL = 2150, CI = 0.409, RI = 0.776, RC = 0.317, HI = 0.591). The best-fit evolutionary models applied in Bayesian analyses were selected by MrModeltest2 v. 2.3 for each region of the two genes, the model for ITS was GTR+I+G with equal frequency of nucleotides, while the model for nLSU was SYM+I+G with equal frequency of nucleotides. ML analysis resulted in a similar topology as MP and Bayesian analyses, and only the ML topology is shown in Fig. 1.

The combined 5-gene (ITS+nLSU+RPB1+RPB2+TEF1) sequences dataset had an aligned length of 4609 characters, including gaps (619 characters for ITS, 1274 characters for nLSU, 1170 characters for RPB1, 1001 characters for RPB2, 545 characters for TEF1), of which 2675 characters were constant, 272 were variable and parsimony-uninformative, and 1662 were parsimony-informative. MP analysis yielded 36 equally parsimonious trees (TL = 9247, CI = 0.362, RI = 0.652, RC = 0.236, HI = 0.638). The best-fit evolutionary models applied in Bayesian analyses were selected by MrModeltest2 v. 2.3 for each region of the two genes, the model for ITS, RPB1, RPB2 and TEF1was GTR+I+G with equal frequency of nucleotides, while the model for nLSU was SYM+I+G with equal frequency of nucleotides. ML analysis resulted in a similar topology as MP and Bayesian analyses, and only the ML topology is shown in Fig. 2.

The phylogenetic trees inferred from ITS+nLSU and ITS+nLSU+RPB1+RPB2+TEF1 gene sequences were all obtained from 78 fungal samples representing 42 taxa of Irpicaceae and two taxa of Phanerochaetaceae within the phlebioid clade (Figs 1, 2). Phylogenetic analyses showed that *Trametopsis abieticola*, *T. aborigena*, *T. brasiliensis*, *T. cervina* and *T. tasmanica* grouped together within *Trametopsis* by high support (100% ML, 100% MP, 1.00 BPP; Figs 1, 2).

Taxonomy

Trametopsis abieticola **B.K. Cui & Shun Liu, sp. nov.**
MycoBank No: 844097
Figs 3, 4

Diagnosis. *Trametopsis abieticola* is distinguished from *T. tasmanica* by larger pores (0.5–1 per mm) and basidiospores (5.8–7.2 × 1.9–2.6 μm), and by being distributed in the high altitude of mountains and growing on *Abies* sp.

Holotype. China. Xizang Autonomous Region (Tibet), Mangkang County, Mangkang Mountain, on fallen trunk of *Abies* sp., 8 September 2020, Cui 18383 (holotype BJFC 035242).

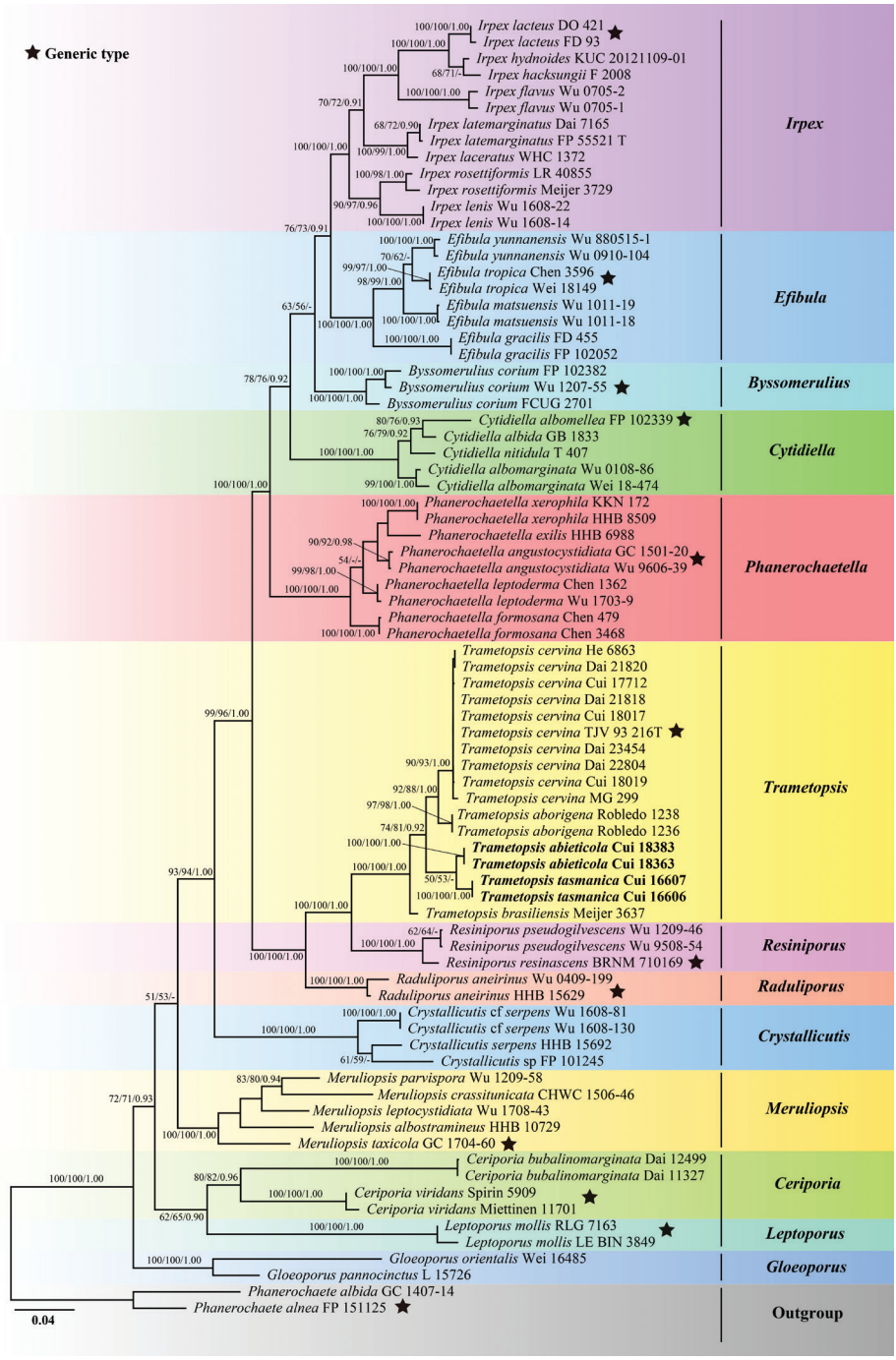

Figure 1. Maximum likelihood tree illustrating the phylogeny of *Trametopsis* based on the combined sequences dataset of ITS+nLSU. Branches are labelled with maximum likelihood bootstrap higher than 50%, parsimony bootstrap proportions higher than 50% and Bayesian posterior probabilities more than 0.90 respectively. Bold names = New species.

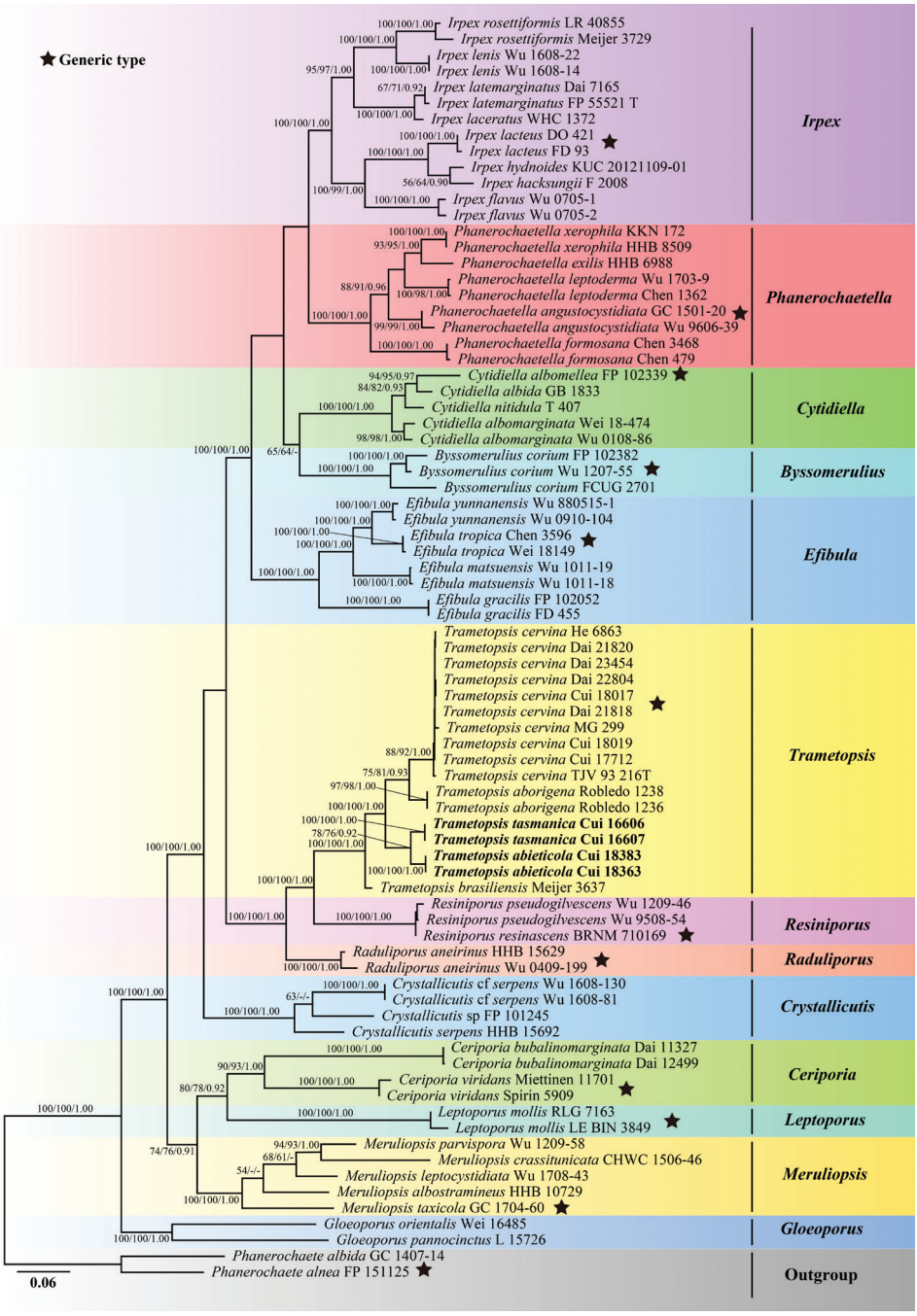

Figure 2. Maximum likelihood tree illustrating the phylogeny of *Trametopsis* based on the combined sequences dataset of ITS+nLSU+RPB1+RPB2+TEF1. Branches are labelled with maximum likelihood bootstrap higher than 50%, parsimony bootstrap proportions higher than 50% and Bayesian posterior probabilities more than 0.90 respectively. Bold names = New species.

Figure 3. Basidiomata of *Trametopsis abieticola* (Holotype, Cui 18383). Scale bar: 3 cm.

Etymology. *Abieticola* (Lat.): referring to the species grows on *Abies* sp.

Fruiting body. Basidiomata annual, pileate, solitary or imbricate, soft corky to corky, without odour or taste when fresh, becoming corky and light in weight upon drying. Pilei applanate to flabelliform, projecting up to 9.5 cm long, 5.5 cm wide, and

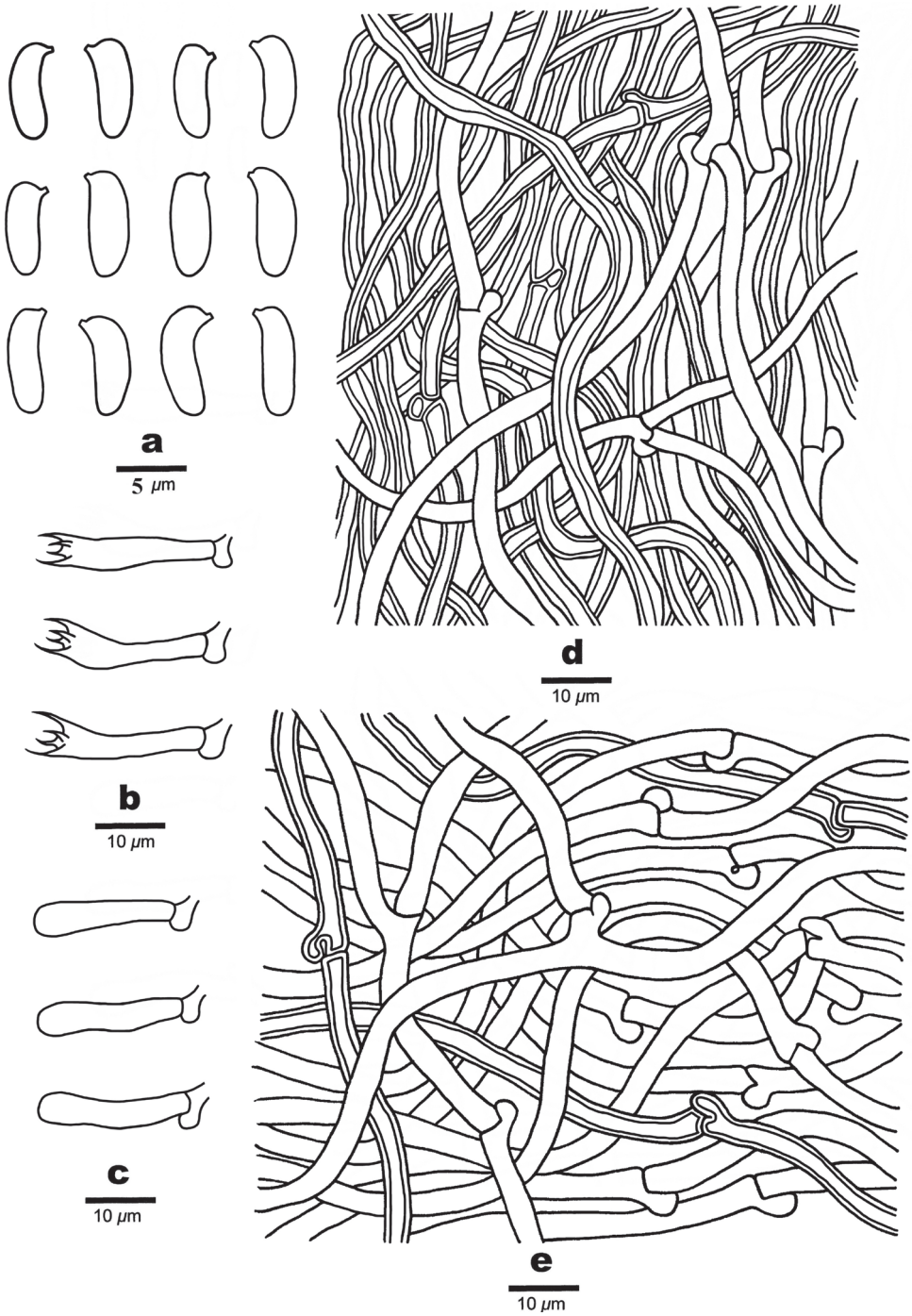

Figure 4. Microscopic structures of *Trametopsis abieticola* (Holotype, Cui 18383) **a** basidiospores **b** basidia **c** basidioles **d** hyphae from trama **e** hyphae from context.

2 cm thick at base. Pileal surface buff to buff-yellow when fresh, becoming pinkish buff to clay-buff when dry, strigose or glabrous; margin white to cream when fresh, becoming cream to buff-yellow when dry, obtuse to acute. Pore surface cream to buff when fresh, becoming pinkish buff to greyish brown upon drying; pores round to angular, 0.5–1 per mm; dissepiments slightly thick, entire to lacerate. Context corky, cream to buff yellow, up to 8 mm thick. Tubes concolorous with pore surface, corky, up to 7 mm long.

Hyphal structure. Hyphal system monomitic in context, dimitic in trama; generative hyphae with clamp connections; skeletal hyphae IKI–, CB–; tissues unchanged in KOH.

Context. Generative hyphae hyaline, thin- to slightly thick-walled, occasionally branched, loosely interwoven, 2.8–4.2 μm in diam.

Tubes. Generative hyphae frequent, hyaline, thin- to slightly thick-walled, occasionally branched, 1.8–3.5 μm in diam.; skeletal hyphae dominant, hyaline, thick-walled with a wide to narrow lumen, occasionally branched, more or less straight, interwoven, 2–4.5 μm in diam. Cystidia and cystidioles absent. Basidia clavate, bearing four sterigmata and a basal clamp connection, 17.8–22.5 × 4.3–5.5 μm; basidioles dominant, similar to basidia but smaller.

Spores. Basidiospores cylindrical, hyaline, thin-walled, smooth, IKI–, CB–, (5.7–)5.8–7.2 × (1.8–)1.9–2.6(–2.8) μm, L = 6.57 μm, W = 2.22 μm, Q = 2.75–3.26 (n = 60/2).

Type of rot. White rot.

Additional specimen (paratype) examined. China. Sichuan Province, Yajiang County, Kangbahanzi Village, on fallen trunk of *Abies* sp., 7 September 2020, Cui 18363 (BJFC 035222).

Trametopsis tasmanica **B.K. Cui & Shun Liu, sp. nov.**
MycoBank No: 844098
Figs 5, 6

Diagnosis. *Trametopsis tasmanica* is distinguished from *T. abieticola* by resupinate basidiomata, smaller pores (2–4 per mm) and basidiospores (5.2–6.3 × 1.8–2.2 μm), and by growing on *Eucalyptus* sp.

Holotype. Australia. Tasmania, Hobart, Mount Wellington, on rotten wood of *Eucalyptus* sp., 13 May 2018, Cui 16606 (holotype BJFC 029905).

Etymology. *Tasmanica* (Lat.): referring to the species collected from Tasmania in Australia.

Fruiting body. Basidiomata annual, resupinate, not easily separated from the substrate, without odour or taste when fresh, becoming corky to fragile and light in weight upon drying; up to 5.5 cm long, 2 cm wide, and 7 mm thick at centre. Pore surface cream to pinkish-buff when fresh, becoming honey-yellow to snuff brown upon drying; pores round to angular, 2–4 per mm; dissepiments slightly thick, entire to lacerate. Context very thin, corky, cream to buff, up to 2 mm thick. Tubes concolorous with pore surface, corky, up to 4 mm long.

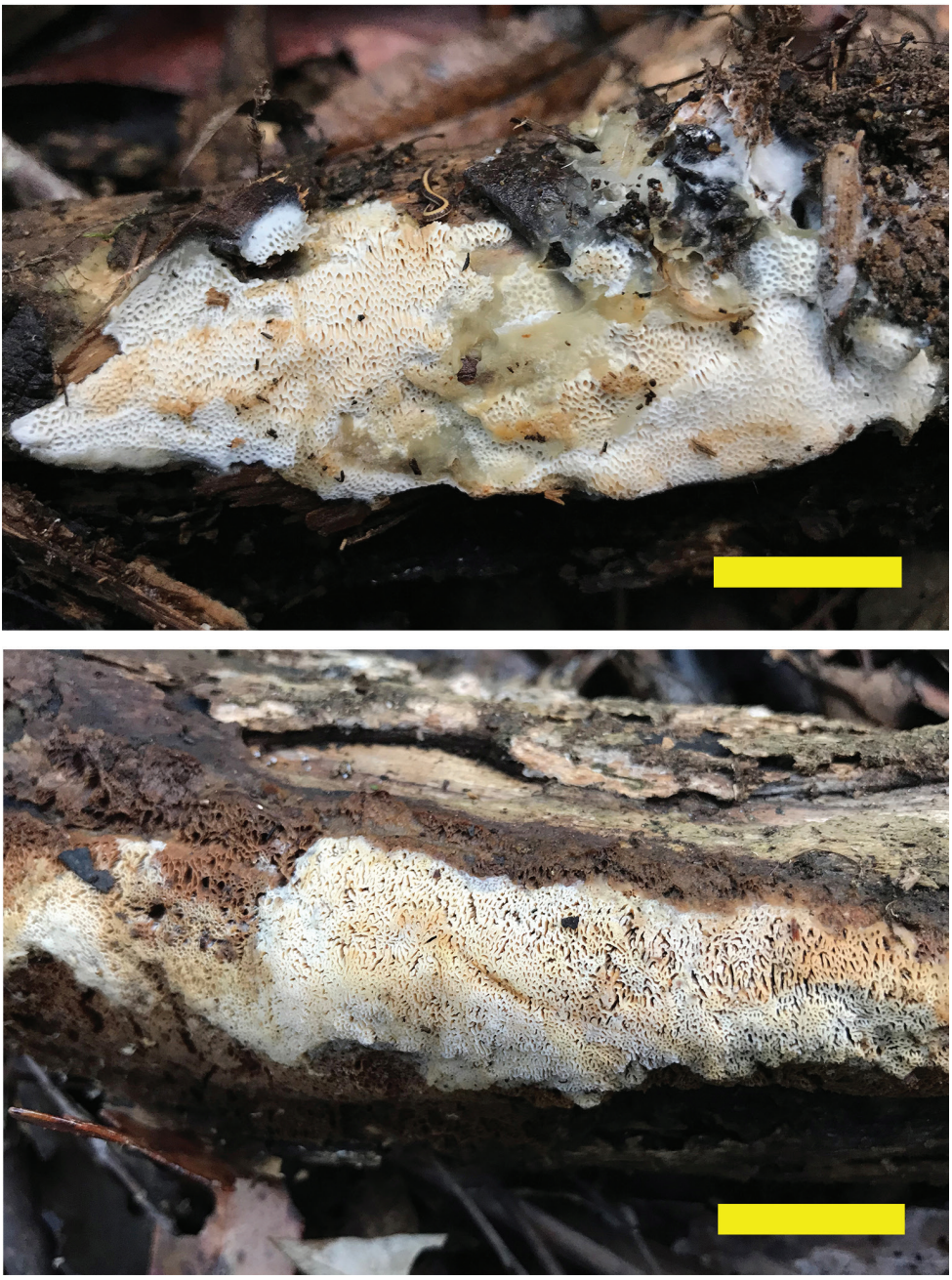

Figure 5. *Trametopsis tasmanica* (Holotype, Cui 16606 and paratype, Cui 16607). Scale bar: 1 cm.

Hyphal structure. Hyphal system monomitic in context, dimitic in trama; generative hyphae with clamp connections; skeletal hyphae IKI–, CB–; tissues unchanged in KOH.

Context. Generative hyphae hyaline, thin- to slightly thick-walled with a wide lumen, occasionally branched, loosely interwoven, 2.7–4 µm in diam.

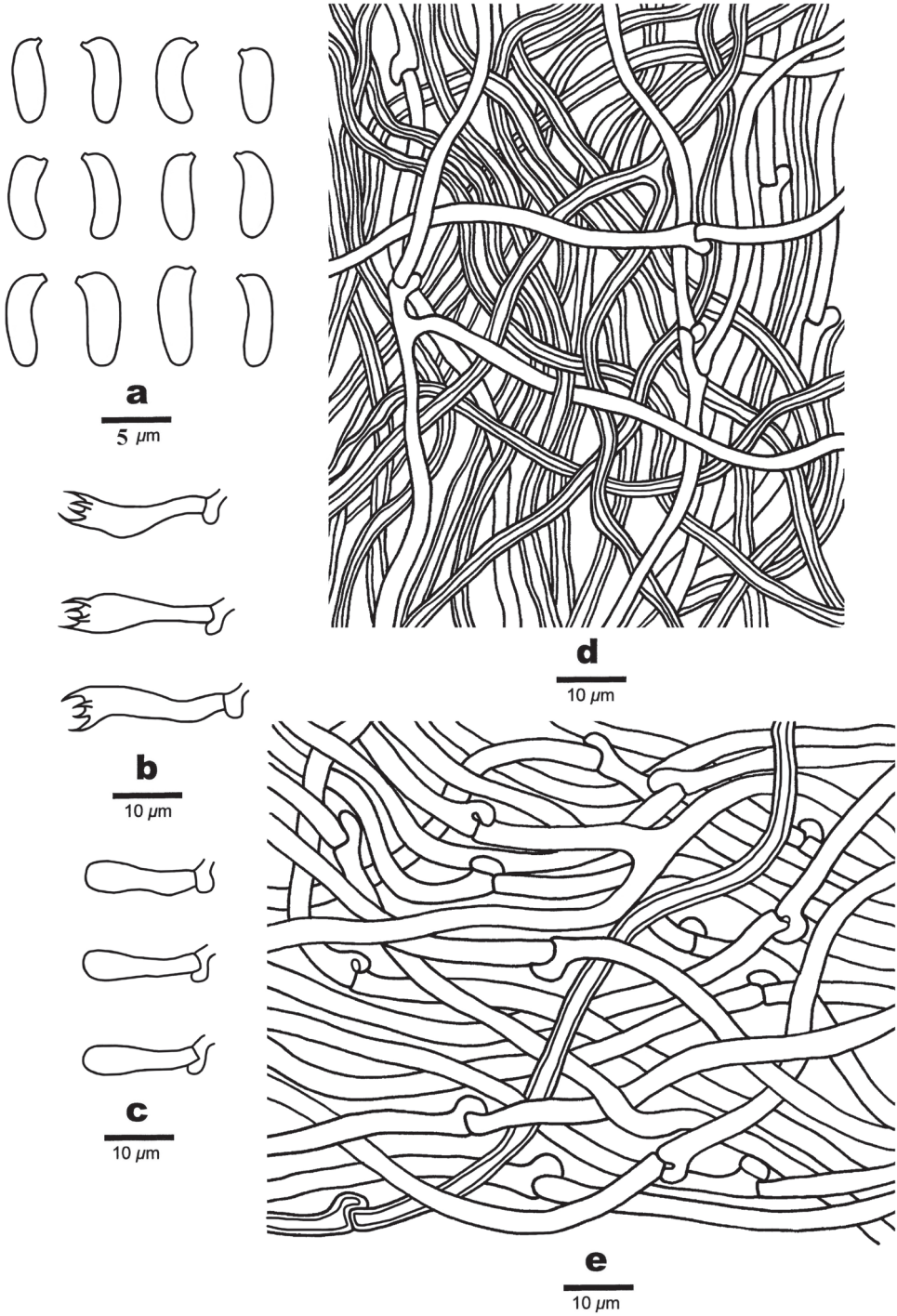

Figure 6. Microscopic structures of *Trametopsis tasmanica* (Holotype, Cui 16606) **a** Basidiospores **b** Basidia **c** Basidioles **d** Hyphae from trama **e** Hyphae from context.

Tubes. Generative hyphae frequent, hyaline, thin-walled, occasionally branched, 2–3 μm in diam.; skeletal hyphae dominant, hyaline, thick-walled with a wide to narrow lumen, occasionally branched, more or less straight, interwoven, 2–3.7 μm in diam. Cystidia and cystidioles absent. Basidia clavate, bearing four sterigmata and a basal clamp connection, 16–19.5 × 3.7–5 μm; basidioles dominant, similar to basidia but smaller.

Spores. Basidiospores cylindrical, hyaline, thin-walled, smooth, IKI–, CB–, (5–)5.2–6.3 × (1.7–)1.8–2.2(–2.4) μm, L = 5.84 μm, W = 2.02 μm, Q = 2.66–3.13 (n = 60/2).

Type of rot. White rot.

Additional specimen (paratype) examined. Australia. Tasmania, Hobart, Mount Wellington, on rotten branch of *Eucalyptus* sp., 13 May 2018, Cui 16607 (BJFC 029906).

Discussion

In this study, the phylogenetic analyses of *Trametopsis* and related genera are inferred from the combined datasets of ITS+nLSU sequences (Fig. 1) and ITS+nLSU+RPB1+RPB2+TEF1 sequences (Fig. 2). The genera; *Raduliporus* Spirin & Zmitr., *Resiniporus* Zmitr. and *Trametopsis* grouped together and formed a highly supported lineage (Figs 1 and 2), which was called the *Trametopsis* lineage by Chen et al. (2021). Morphologically, *Raduliporus* and *Resiniporus* differ from *Trametopsis* by having a monomitic hyphal system and ellipsoid basidiospores (Chen et al. 2021). Phylogenetically, *T. abieticola* and *T. tasmanica* clustered with other *Trametopsis* species (Figs 1, 2) with high supports (100% MP, 100% ML, 1.00 BPP; Figs 1, 2). The main morphological characters and ecological habits of species in *Trametopsis* are provided in Table 2. The geographical locations of the *Trametopsis* species distributed in the world are indicated on the map (Fig. 7).

Trametopsis abieticola is distributed in high altitude areas of the Hengduan Mountains (altitude > 3500 m) and grows on *Abies* sp. In the phylogenetic trees, *T. abieticola* is closely related to *T. tasmanica* (Figs 1, 2). Morphologically, *T. tasmanica* differs from *T. abieticola* in having resupinate basidiomata, smaller pores (2–4 per mm) and basidiospores (5.2–6.3 × 1.8–2.2 μm), being distributed in Australia and growing on *Eucalyptus* sp. *Trametopsis cervina* can also distributed in high altitude areas of the Hengduan Mountains (according to our investigations), but *T. cervina* differs from *T. abieticola* by its smaller pores (2–4 per mm), longer basidiospores (6–9 × 2–3 μm; Tomšovský 2008), and usually growing on angiosperm trees. *Trametopsis aborigena*, *T. brasiliensis* and *T. abieticola* share an annual growth habit, a monomitic hyphal system in context, dimitic in trama and clamped generative hyphae; but *T. aborigena* differs from *T. abieticola* by having light pale brown to pale yellowish pileal surface with yellowish red to dark yellowish brown radial veins, smaller pores (1–3 per mm) and basidiospores (5–7 × 1–2 μm), and being distributed in neotropical regions of Argentina

Table 2. The main morphological characters and ecological habits of species in *Trametopsis*. New species are shown in bold.

Species name	Distribution	Climate zone	Host	Fruiting body	Pores (per mm)	Basidia (µm)	Basidiospores (µm)	References
Trametopsis abieticola	**Asia (China)**	**Alpine plateau**	**Gymnosperm (*Abies*)**	**Pileate**	**0.5–1**	**17.8–22.5 × 4.3–5.5**	**5.8–7.2 × 1.9–2.6**	**Present study**
T. aborigena	South America (Argentina)	Neotropical	Angiosperm (Undetermined)	Pileate, effused-reflexed or occasionally resupinate	1–3	19–22 × 5–6	5–7 × 1–2.5	Gómez-Montoya et al. (2017)
T. brasiliensis	South America (Brazil)	Neotropical	Angiosperm (*Dicotyledonous*)	Pileate	1–2	15–20 × 4–5	4.5–5.5 × 1.8–2.2	Ryvarden and Meijer (2002); Gómez-Montoya et al. (2017)
T. cervina	Africa (Burundi, Rwanda, Tanzania), Asia (China, Iran), Europe (Austria, Belgium, Czech, France, Greece, Italy, Slovakia, Poland, Ukraine, Russia, etc.), and North America (Canada, USA)	Alpine plateau, temperate to tropical	Angiosperm (*Acer*, *Alnus*, *Betula*, *Carpinus*, *Elaeocarpus*, *Fagus*, *Juglans*, *Liquidambar*, *Populus*, *Quercus*, *Salix*, etc.); Gymnosperm (*Larix*, *Pinus*)	Effused-reflexed to pileate or occasionally resupinate	2–4	20–25 × 5–7	6–9 × 2–3	Tomšovský (2008); Gómez-Montoya et al. (2017); present study
T. tasmanica	**Oceania (Australia)**	**Temperate marine climate**	**Angiosperm (*Eucalyptus*)**	**Resupinate**	**2–4**	**16–19.5 × 3.7–5**	**5.2–6.3 × 1.8–2.2**	**Present study**

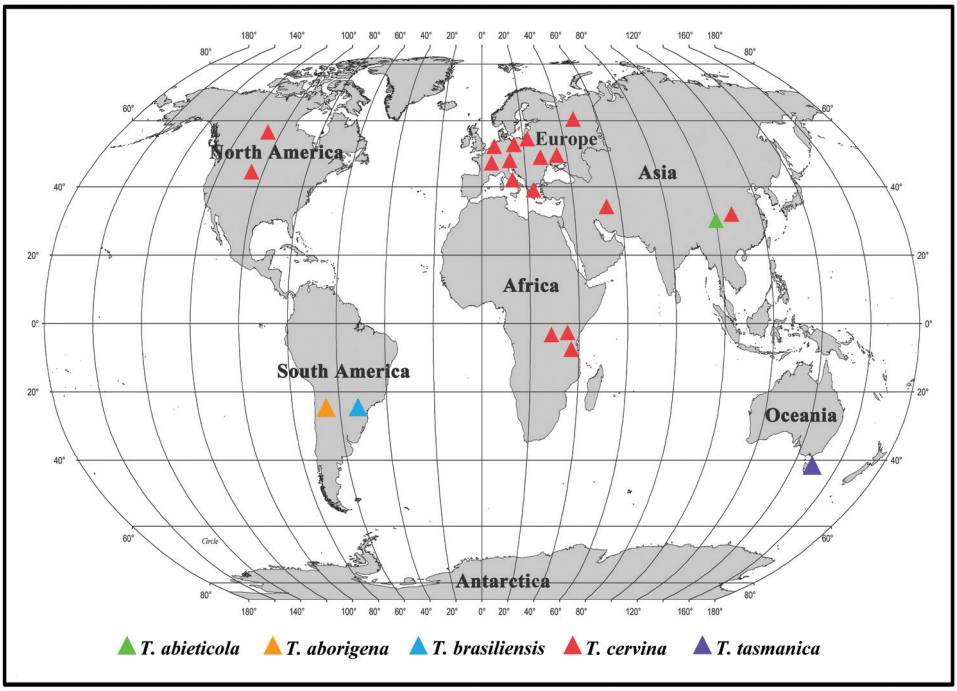

Figure 7. The geographical locations of the *Trametopsis* species distributed in the world.

(Gómez-Montoya et al. 2017); *T. brasiliensis* differs from *T. abieticola* in having smaller pores (1–2 per mm) and basidiospores (4.5–5.5 × 1.8–2.2 µm), and being distributed in neotropical regions of Brazil (Gómez-Montoya et al. 2017).

Trametopsis tasmanica is distributed in Tasmania, Australia and grows on *Eucalyptus* sp. Before that, there was no report of *Trametopsis* in Oceania. Morphologically, *T. tasmanica* and *T. cervina* share similar-sized pores, but *T. cervina* differs from *T. tasmanica* by its pileate to effused-reflexed basidiomata, larger basidiospores (6–9 × 2–3 µm; Tomšovský 2008). *Trametopsis aborigena*, *T. brasiliensis* and *T. tasmanica* are only distributed in the southern hemisphere and grow on angiosperm trees. However, *T. aborigena* differs from *T. tasmanica* by having pileate, effused-reflexed to occasionally resupinate basidiomata, larger basidia (19–22 × 5–6 µm) and basidiospores (5–7 × 1–2.5 µm), and being distributed in neotropical regions of Argentina (Gómez-Montoya et al. 2017); *T. brasiliensis* differs from *T. tasmanica* in having pileate basidiomata, larger pores (1–2 per mm) and distributed in neotropical regions of Brazil (Gómez-Montoya et al. 2017).

In summary, we performed a taxonomic and phylogenetic study of *Trametopsis*. The concepts and species number of the *Trametopsis* are updated. So far, five species are accepted in the *Trametopsis* around the world. Currently, *Trametopsis* is characterised by an annual growth habit, effused-reflexed to pileate or resupinate, solitary or imbricate basidiomata, pinkish buff to cinnamon or clay-buff, zonate or azonate, glabrous or

velutinate to strigose pileal surface, cream, pale yellow to greyish brown pore surface with round to angular, irregular, daedaleoid to irpicoid pores, a monomitic hyphal system in context, dimitic in trama, clamped generative hyphae, and allantoid to cylindrical basidiospores; it grows on different angiosperm and gymnosperm trees, causing white rot of wood (Tomšovský 2008; Gómez-Montoya et al. 2017).

Acknowledgements

We express our gratitude to Ms. Xing Ji (China) for help during field collections and molecular studies. Also to Drs. Genevieve Gates (Australia), Xiao-Lan He (China) and Hai-Xia Ma (China) for their assistance during field collections. The research is supported by the National Natural Science Foundation of China (Nos. 31870008, U2003211, 31900017), Beijing Forestry University Outstanding Young Talent Cultivation Project (No. 2019JQ03016).

References

Binder M, Justo A, Riley R, Salamov A, López-Giráldez F, Sjökvist E, Copeland A, Foster B, Sun H, Larsson E, Larsson KH, Townsend J, Grigoriev IV, Hibbett DS (2013) Phylogenetic and phylogenomic overview of the Polyporales. Mycologia 105(6): 1350–1373. https://doi.org/10.3852/13-003

Chen CC, Wu SH, Chen CY (2018) Four species of polyporoid fungi newly recorded from Taiwan. Mycotaxon 133(1): 45–54. https://doi.org/10.5248/133.45

Chen CC, Chen CY, Lim YW, Wu SH (2020) Phylogeny and taxonomy of *Ceriporia* and other related taxa and description of three new species. Mycologia 112(1): 64–82. https://doi.org/10.1080/00275514.2019.1664097

Chen CC, Chen CY, Wu SH (2021) Species diversity, taxonomy and multi-gene phylogeny of phlebioid clade (Phanerochaetaceae, Irpicaceae, Meruliaceae) of Polyporales. Fungal Diversity 6(1): 337–442. https://doi.org/10.1007/s13225-021-00490-w

Cui BK, Li HJ, Ji X, Zhou JL, Song J, Si J, Yang ZL, Dai YC (2019) Species diversity, taxonomy and phylogeny of Polyporaceae (Basidiomycota) in China. Fungal Diversity 97(1): 137–392. https://doi.org/10.1007/s13225-019-00427-4

El-Gharabawy HM, Leal-Dutra CA, Griffith GW (2021) *Crystallicutis* gen. nov. (Irpicaceae, Basidiomycota), including *C. damiettensis* sp. nov., found on *Phoenix dactylifera* (date palm) trunks in the Nile Delta of Egypt. Fungal Biology 125(6): 447–458. https://doi.org/10.1016/j.funbio.2021.01.004

Farris JS, Källersjö M, Kluge AG, Kluge AG, Bult C (1994) Testing significance of incongruence. Cladistics 10(3): 315–319. https://doi.org/10.1111/j.1096-0031.1994.tb00181.x

Felsenstein J (1985) Confidence intervals on phylogenies: An approach using the bootstrap. Evolution; International Journal of Organic Evolution 39(4): 783–791. https://doi.org/10.1111/j.1558-5646.1985.tb00420.x

Floudas D, Hibbett DS (2015) Revisiting the taxonomy of *Phanerochaete* (Polyporales, Basidiomycota) using a four gene dataset and extensive ITS sampling. Fungal Biology 119(8): 679–719. https://doi.org/10.1016/j.funbio.2015.04.003

Gómez-Montoya N, Drechsler-Santos ER, Ferreira-Lopes V, Tomšovský M, Urcelay C, Robledo GL (2017) New insights on *Trametopsis* Tomšovský (Polyporales Gäum.) based on phylogenetic evidences and morphological analyses of neotropical species. Phytotaxa 311(2): 155–166. https://doi.org/10.11646/phytotaxa.311.2.3

Hall TA (1999) Bioedit: A user-friendly biological sequence alignment editor and analysis program for Windows 95/98/NT. Nucleic Acids Symposium Series 41: 95–98.

Hillis DM, Bull JJ (1993) An empirical test of bootstrapping as a method for assessing confidence in phylogenetic analysis. Systematics and Biodiversity 42: 182–192. https://doi.org/10.1093/sysbio/42.2.182

Jang Y, Jang S, Lee J, Lee H, Lim YW, Kim C, Kim JJ (2016) Diversity of wood-inhabiting polyporoid and corticioid fungi in Odaesan National Park, Korea. Mycobiology 44(4): 217–236. https://doi.org/10.5941/MYCO.2016.44.4.217

Ji X, Zhou JL, Song CG, Xu TM, Wu DM, Cui BK (2022) Taxonomy, phylogeny and divergence times of *Polyporus* (Basidiomycota) and related genera. Mycosphere: Journal of Fungal Biology 13: 1–52. https://doi.org/10.5943/mycosphere/13/1/1

Jia BS, Zhou LW, Cui BK, Rivoire B, Dai YC (2014) Taxonomy and phylogeny of *Ceriporia* (Polyporales, Basidiomycota) with an emphasis of Chinese collections. Mycological Progress 13(1): 81–93. https://doi.org/10.1007/s11557-013-0895-5

Justo A, Hibbett DS (2011) Phylogenetic classification of *Trametes* (Basidiomycota, Polyporales) based on a five-marker dataset. Taxon 60(6): 1567–1583. https://doi.org/10.1002/tax.606003

Justo A, Miettinen O, Floudas D, Ortiz-Santana B, Sjökvist E, Lindner D, Nakason K, Niemelä T, Larsson K-H, Ryvarden L, Hibbett DS (2017) A revised family-level classification of the Polyporales (Basidiomycota). Fungal Biology 121(9): 798–824. https://doi.org/10.1016/j.funbio.2017.05.010

Lee JS, Kim C, Lim YW (2008) *Irpex hacksungii* sp. nov. (Polyporaceae) from Korea. Mycotaxon 106: 423–429.

Liu S, Han ML, Xu TM, Wang Y, Wu DM, Cui BK (2021a) Taxonomy and phylogeny of the *Fomitopsis pinicola* complex with descriptions of six new species from east Asia. Frontiers in Microbiology 12: e644979. https://doi.org/10.3389/fmicb.2021.644979

Liu S, Shen LL, Wang Y, Xu TM, Gates G, Cui BK (2021b) Species diversity and molecular phylogeny of *Cyanosporus* (Polyporales, Basidiomycota). Frontiers in Microbiology 12: 631166. https://doi.org/10.3389/fmicb.2021.631166

Liu S, Xu TM, Song CG, Zhao CL, Wu DM, Cui BK (2022) Species diversity, molecular phylogeny and ecological habits of *Cyanosporus* (Polyporales, Basidiomycota) with an emphasis on Chinese collections. MycoKeys 86: 19–46. https://doi.org/10.3897/mycokeys.86.78305

Matheny PB (2005) Improving phylogenetic inference of mushrooms with RPB1 and RPB2 nucleotide sequences (*Inocybe*, Agaricales). Molecular Phylogenetics and Evolution 35(1): 1–20. https://doi.org/10.1016/j.ympev.2004.11.014

Matheny PB, Liu YJ, Ammirati JF, Hall BD (2002) Using RPB1 sequences to improve phylogenetic inference among mushrooms (*Inocybe*, Agaricales). American Journal of Botany 89(4): 688–698. https://doi.org/10.3732/ajb.89.4.688

Miettinen O, Spirin V, Vlasák J, Rivoire B, Stenroos S, Hibbett D (2016) Polypores and genus concepts in Phanerochaetaceae (Polyporales, Basidiomycota). MycoKeys 17: 1–46. https://doi.org/10.3897/mycokeys.17.10153

Miettinena O, Larssonb E, Sjökvist E, Larssonc KH (2012) Comprehensive taxon sampling reveals unaccounted diversity and morphological plasticity in a group of dimitic polypores (Polyporales, Basidiomycota). Cladistics 28(3): 251–270. https://doi.org/10.1111/j.1096-0031.2011.00380.x

Nylander JAA (2008) MrModeltest2 v. 2.3. Evolutionary Biology Centre, Uppsala University, Program distributed by the author.

Posada D, Crandall KA (1998) Modeltest: Testing the model of DNA substitution. Bioinformatics (Oxford, England) 14(9): 817–818. https://doi.org/10.1093/bioinformatics/14.9.817

Psurtseva NV (2010) Conservation of medicinal mushrooms in the V. L. Komarov Botanical Institute Basidiomycetes Culture Collection (LE-BIN, Russia). International Journal of Medicinal Mushrooms 12(2): 193–199. https://doi.org/10.1615/IntJMedMushr.v12.i2.100

Rehner S (2001) Primers for Elongation Factor 1-a (EF1-a). http://ocid.nacse.org/research/deephyphae/EF1primer.pdf

Ronquist F, Huelsenbeck JP (2003) MRBAYES 3: Bayesian phylogenetic inference under mixed models. Bioinformatics (Oxford, England) 19(12): 1572–1574. https://doi.org/10.1093/bioinformatics/btg180

Ryvarden L, Meijer AAR (2002) Studies in neotropical polypores 14. New species from the state of Paraná, Brazil. Synopsis Fungorum 15: 34–69.

Sjökvist E, Larsson E, Eberhardt U, Ryvarden L, Larsson KH (2012) Stipitate stereoid basidiocarps have evolved multiple times. Mycologia 104(5): 1046–1055. https://doi.org/10.3852/11-174

Song CG, Ji X, Liu S, He XL, Cui BK (2021) Taxonomy and molecular phylogeny of *Phellodon* (Thelephorales) with descriptions of four new species from Southwest China. Forests 12(7): e932. https://doi.org/10.3390/f12070932

Spirin V, Vlasák J, Rivoire B, Kout J, Kotiranta H, Miettinen O (2016) Studies in the *Ceriporia purpurea* group (Polyporales, Basidiomycota), with notes on similar *Ceriporia* species. Cryptogamie. Mycologie 37(4): 421–435. https://doi.org/10.7872/crym/v37.iss4.2016.421

Stamatakis A (2014) RAxML Version 8: A tool for phylogenetic analyses and post analyses of large phylogenies. Bioinformatics (Oxford, England) 30(9): 1312–1313. https://doi.org/10.1093/bioinformatics/btu033

Sun YF, Costa-Rezende DH, Xing JH, Zhou JL, Zhang B, Gibertoni TB, Gates G, Glen M, Dai YC, Cui BK (2020) Multi-gene phylogeny and taxonomy of *Amauroderma* s. lat. (Ganodermataceae). Persoonia 44(1): 206–239. https://doi.org/10.3767/persoonia.2020.44.08

Sun YF, Xing JH, He XL, Wu DM, Song CG, Liu S, Vlasák J, Gates G, Gibertoni TB, Cui BK (2022) Species diversity, systematic revision and molecular phylogeny of Ganodermataceae

(Polyporales, Basidiomycota) with an emphasis on Chinese collections. Studies in Mycology 101: 287–415. https://doi.org/10.3767/10.3114/sim.2022.101.05

Swofford DL (2002) PAUP*: phylogenetic analysis using parsimony (*and other methods). Version 4.0b10. Sinauer Associates, Sunderland.

Thompson JD, Gibson TJ, Plewniak F, Jeanmougin F, Higgins DG (1997) The ClustalX windows interface: Fexible strategies for multiple sequence alignment aided by quality analysis tools. Nucleic Acids Research 25(24): 4876–4882. https://doi.org/10.1093/nar/25.24.4876

Tomšovský M (2008) Molecular phylogeny and taxonomic position of *Trametes cervina* and description of a new genus *Trametopsis*. Czech Mycology 60(1): 1–11. https://doi.org/10.33585/cmy.60101

Tomšovský M, Menkis A, Vasaitis R (2010) Phylogenetic relationships in European *Ceriporiopsis* species inferred from nuclear and mitochondrial ribosomal DNA sequences. Fungal Biology 114(4): 350–358. https://doi.org/10.1016/j.funbio.2010.02.004

Westphalen MC, Tomšovský M, Gugliotta AM, Rajchenberg M (2019) An overview of *Antrodiella* and related genera of Polyporales from the Neotropics. Mycologia 111(5): 813–831. https://doi.org/10.1080/00275514.2019.1633895

White TJ, Bruns T, Lee S, Taylor J (1990) Amplification and direct sequencing of fungal ribosomal RNA genes for phylogenetics. In: Innis MA, Gefand DH, Sninsky JJ, White JT (Eds) PCR Protocols: a guide to methods and applications. Academic Press, San Diego, 315–322. https://doi.org/10.1016/B978-0-12-372180-8.50042-1

Wu SH, Nilsson HR, Chen CT, Yu SY, Hallenberg N (2010) The white-rotting genus *Phanerochaete* is polyphyletic and distributed throughout the phleboid clade of the Polyporales (Basidiomycota). Fungal Diversity 42(1): 107–118. https://doi.org/10.1007/s13225-010-0031-7

Wu F, Chen JJ, Ji XH, Vlasák J, Dai YC (2017) Phylogeny and diversity of the morphologically similar polypore genera *Rigidoporus*, *Physisporinus*, *Oxyporus*, and *Leucophellinus*. Mycologia 109: 749–765. https://doi.org/10.1080/00275514.2017.1405215

MycoKeys 90: 53–69 (2022)
doi: 10.3897/mycokeys.90.83801
https://mycokeys.pensoft.net

RESEARCH ARTICLE

A peer-reviewed open-access journal
MycoKeys
Launched to accelerate biodiversity research

Morphological and molecular analyses reveal two new species of *Gibellula* (Cordycipitaceae, Hypocreales) from China

MingJun Chen[1], Ting Wang[1], Yan Lin[1], Bo Huang[1]

1 *Anhui Provincial Key Laboratory for Microbial Pest Control, Anhui Agricultural University, Hefei 230036, China*

Corresponding author: Bo Huang (bhuang@ahau.edu.cn)

Academic editor: S. Maharachchikumbura | Received 15 March 2022 | Accepted 13 May 2022 | Published 2 June 2022

Citation: Chen MJ, Wang T, Lin Y, Huang B (2022) Morphological and molecular analyses reveal two new species of *Gibellula* (Cordycipitaceae, Hypocreales) from China. MycoKeys 90: 53–69. https://doi.org/10.3897/mycokeys.90.83801

Abstract

Gibellula penicillioides **sp. nov.** and *G. longispora* **sp. nov.**, two new species parasitising spiders collected in China, are illustrated and described, based on morphological features and multiloci phylogenetic analysis. The *G. penicillioides* **sp. nov.** group is sister to the *G. scorpioides* group, but form long penicilloid conidiophore producing enlarged fusiform conidia ((7–) 7.5–9 (–10) × 2.5–3.5 µm). *G. longispora* **sp. nov.** is sister to *G. pigmentosinum*, but has slender long conidia (5–7 × 1–2 µm); teleomorph and Granulomanus-synanamorphic conidiogenous cells are absent in these two species. Type specimens of *G. penicillioides* **sp. nov.** and *G. longispora* **sp. nov.** were deposited in the Research Center for Entomogenous Fungi of Anhui Agricultural University (RCEF). In addition, a key to all known species of Gibellula is illustrated.

Keywords

Araneogenous fungi, Cordycipitaceae, spider, Taxonomy

Introduction

Spider–pathogenic fungi, also called araneogenous or araneopathogenic fungi, are the group that infect spiders (phylum Arthropoda, class Arachnida, order Araneae) and belong to the Hypocreales (Evans and Samson 1987). About 91 Hypocrealean spider- and harvestman-pathogenic fungi were recognised to accommodate the genera

Akanthomyces Lebert, *Beauveria* Vuill., *Clonostachys* Corda, *Cordyceps* Fr., *Engyodontium* de Hoog, *Gibellula* Cavara, *Hevansia* Luangsa-ard, Hywel-Jones & Spatafora, *Hirsutella* Pat., *Hymenostilbe* Petch, *Lecanicillium* W. Gams & Zare, *Ophiocordyceps* Petch, *Purpureocillium* Luangsa-ard, Hywel-Jones, Houbraken & Samson and *Torrubiella* Boud. (Shrestha et al. 2019). Of the above genera, only *Gibellula* and *Hevansia* are exclusively spider–pathogenic and present host specificity (Shrestha et al. 2019; Kuephadungphan et al. 2020). *Gibellula* species are amongst the most common spider pathogens in the world and are distributed from temperate to subtropical and tropical regions. Morphologically, the group can produce cylindrical synnemata from the outer loose hyphae covering spider cadavers with conidiophores abruptly narrowing to a short distinct neck and forming a subsphaeroidal vesical (Mains 1950; Samson and Evans 1992; Kuephadungphan et al. 2019).

In 1894, the genus *Gibellula* was proposed by Cavara (1894), based on *Gibellula pulchra* (Sacc.) Cavara (*Corethropsis pulchra* Sacc.). Since then, many new taxa of parasitic *Gibellula* (mostly on spiders) have been described. Petch (1932) and Mains (1949, 1950) treated a number of *Gibellula* species as synonyms of *G. pulchra* and recognised only four species in the genus *Gibellula*. Kobayasi and Shimizu (1976, 1982) revised some of the existing species of *Gibellula* and described two new taxa. In a phylogenetically-based nomenclature for Cordycipitaceae (Hypocreales), all *Gibellula* samples fell into a single clade in the Cordycipitaceae; therefore, the genus *Gibellula* was revised and recognised as spider pathogens that produce synnemata with swollen conidiophores reminiscent of *Aspergillus* (Kepler et al. 2017). Recently, current nomenclature, diversity and distributions of *Gibellula* were reviewed and seventeen *Gibellula* species were recognised (Shrestha et al. 2019). Since then, five new species were described (Kuephadungphan et al. 2020; Chen et al. 2021): *G. cebrennini* Tasan., Kuephadungphan & Luangsa-ard, *G. fusiformispora* Tasan., Kuephadungphan & Luangsa-ard, *G. pigmentosinum* Tasan., Kuephadungphan & Luangsa-ard, *G. scorpioides* Tasan., Khons., Kuephadungphan & Luangsa-ard and *G. flava* Ming J. Chen & B. Huang. In all, we consider the genus *Gibellula* to include 22 species.

We carried out a series of collection trips for insect and spider pathogenic fungi in the Guniujiang National Forest Park in Anhui Province, China beginning in 2020. A total of seven spider cadavers infected by *Gibellula* were collected. One was identified as *G. flava* and four were similar to *G. scorpioides* in having solitary whip-like synnemata arising from host abdomens and penicillately-arranged conidiogenous cells. However, the four differed from *G. scorpioides* in having much longer synnemata and conidiophores and, thus, are here described as a new species, *G. penicillioides*. Three specimens from Nanling Nature Reserve, Guangdong Province were also identified as this new species through combined morphological and sequence data. We also found two collections similar to *G. pigmentosinum*, but with long and thin fusiform conidia. Due to these differences, we also describe them as a new species, *G. longispora*. Two additional specimens from Shenzheng, Guangdong Province were recognised as *G. longispora*. Multi-gene phylogenetic trees from these sampled fungi confirm their taxonomic placements. Here, we describe these two new species, distinguish them morphologically and phylogenetically and compare them with closely-related species.

Materials and methods

Sample collection and morphology

We collected five *Gibellula* samples from Guniujiang National Forest Park, Anhui Province, two samples from Shenzhen City, Guangdong Province and three samples from Nanling National Nature Reserve, Guangdong Province. The collections were carefully deposited in plastic boxes and returned to the laboratory. Microscopic observations were made from squash mounts and sections made from fresh material. The fresh structures were mounted in water for measurements and lactophenol cotton blue solution for microphotography, following Kuephadungphan et al. (2020). We observed microscopic characteristics, such as size and shape of conidia, phialide, vesicles, metulae and conidiophores using a ZEISS Axiolab 5 microscope. All samples studied here were deposited in the Research Center for Enotomogenous Fungi of Anhui Agricultural University (**RCEF**).

DNA extraction, PCR amplification and sequencing

Total genomic DNA was extracted from fresh synnema with a modified CTAB method (Spatafora et al. 1998). Two gene portions from cell nuclei and three protein coding genes were used in this study: small subunit ribosomal RNA (SSU), large subunit ribosomal RNA (LSU), elongation factor-1a (TEF) and the largest and second largest subunits of RNA polymerase II (RPB1 and RPB2). SSU with NS1 and NS2 (White et al. 1990), LSU was amplified with primers LR0R and LR5 (Rehner and Samuels 1994), TEF-1 with TEF1–983F and TEF1–2218R (Rehner and Buckley 2005), RPB1 with CRPB1and RPB1–Cr (Castlebury et al. 2004) and RPB2 with fRPB2–7CR and fRPB2–5 (Liu et al. 1999). PCR amplification of the five nuclear loci was performed according to Kuephadungphan et al. (2019). PCR products were purified and sequenced by Sangon Company (Shanghai, China). The resulting sequences were checked manually before submission to GenBank.

Sequence alignment and phylogenetic analysis

We constructed a phylogenetic tree using the five loci (SSU, LSU, TEF, RPB1 and RPB2) from 50 taxa (Table 1) within the Cordycipitaceae (Hypocreales). Multiple sequence alignment was performed with Clustal X (version 2.0) (Larkin et al. 2007) and manual adjustments of sequences were done using BioEdit, adjusted to maximise homology. All loci were subsequently concatenated using PhyloSuite v1.2.1 (https://github.com/dongzhang0725/PhyloSuite). The alignment was deposited at TreeBase (No. S29496).

Phylogenetic inference was done according to Maximum Likelihood (ML) using RAxML 7.2.8 (Stamatakis 2006) and Bayesian Inference (BI) using MrBayes 3.3.7 (Ronquist and Huelsenbeck 2003). For the ML analysis, we used the GTRCAT model for all partitions, in accordance with recommendations in the RAxML manual against

the use of invariant sites and 1000 rapid bootstrap replicates. The GTR+I+G model was selected by MrModeltest 2.2 (Nylander 2004) as the best nucleotide substitution model for the Bayesian analysis. Four MCMC chains were executed simultaneously for 2000,000 generations, sampling every 100 generations. Finally, phylogenetic trees were visualised using the Interactive Tree of Life (iTOL) (https://itol.embl.de) online tool (Letunic and Bork 2016).

Table 1. Accession numbers, strain numbers, and origins of *Gibellula* and related taxa used in this study, new sequences were shown in bold.

Taxon	Specimen vouchera	GenBank accession nos				
		SSU	LSU	*TEF*	RPB1	RPB2
Akanthomyces aculeatus	TS772	EU369110	KC519370	–	–	–
A. aculeatus	HUA 186145T	MF416572	MF416520	MF416465	–	–
Beauveria bassiana	ARSEF 7518	–	–	HQ880975	HQ880834	HQ880906
B. bassiana	ARSEF 1564T	–	–	HQ880974	HQ880833	HQ880905
Cordyceps militaris	OSC 93623	AY184977	AY184966	DQ522332	DQ522377	AY545732
C. nidus	TS903C	KY360300	KY360293	–	KY360296	–
C. caloceroides	MCA 2249	MF416578	MF416578	MF416525	MF416470	MF416632
Blackwellomyces cardinalis	OSC 93609T	AY184973	AY184962	DQ522325	DQ522370	DQ522422
B. cardinalis	OSC 93610	AY184974	AY184963	EF469059	EF469088	EF469106
Engyodontium aranearum	CBS 309.85	AF339576	AF339526	DQ522341	DQ522387	DQ522439
E. aranearum	CBS 658.80	–	LC092916	–	–	–
Gibellula cebrennini	BCC 39705	–	MH394673	MH521895	MH521822	MH521859
G. cebrennini	BCC 53605T	–	MT477062	MT503328	MT503321	MT503336
G. clavulifera var. alba	ARSEF 1915T	DQ522562	DQ518777	DQ522360	DQ522408	DQ522467
G. flava	WFS09061701	–	GU827389	–	–	–
G. flava	WFS20190625-25	MW036749	MW084343	MW091325	MW384883	–
G. fusiformispora	BCC 56802T	–	MT477063	MT503329	MT503322	MT503337
G. fusiformispora	BCC 45076	–	–	–	MH521823	MH521860
G. gamsii	BCC 27968T	–	MH152539	MH152560	MH152547	–
G. gamsii	BCC 28797	–	MH152541	MH152562	MH152549	MH152557
G. leiopus	BCC 16025	MF416602	MF416548	MF416492	MF416649	–
G. longispora	NHJ 12014	EU369098	–	EU369017	EU369055	EU369075
G. longispora	**GNJ20200813–16**	**–**	**–**	**MW961414**	**MW980145**	**–**
G. longispora	**GNJ20210710-02**	**OL854201**	**OL854212**	**OL981628**	**–**	**OL981635**
G. longispora	**SZ20210904-02**	–	–	**OL981630**	–	–
G. longispora	**SZ20210915-01**	–	–	**OL981631**	–	–
G. pigmentosinum	NHJ 11679	–	–	EU369016	EU369054	–
G. pulchra	GNHJ 10808	EU369099	EU369035	EU369018	EU369056	EU369076
G. pigmentosinum	BCC 41203T	–	–	MT503330	MT503323	–
G. pigmentosinum	BCC 39707	–	MH394674	MH521894	MH521801	MH521856
G. scorpioides	BCC 47976T	–	MT477066	MT503335	MT503325	MT503339
G. scorpioides	BCC 47530	–	MT477065	MT503334	–	MT503338
G. scorpioides	BCC 47514	–	–	MT503333	–	–
G. scorpioides	BCC 43298	–	MH394677	MH521900	MH521816	MH521858
G. scorpioides	BCC 13020	–	MH394686	MH521901	MH521814	–
Gibellula sp.	NHJ 7859	EU369107	–	–	EU369064	EU369085

Taxon	Specimen vouchera	GenBank accession nos				
		SSU	LSU	*TEF*	RPB1	RPB2
Gibellula sp.	NHJ 10788	EU369101	EU369036	EU369019	EU369058	EU369078
Gibellula sp.	NHJ 5401	EU369102	–	–	EU369059	EU369079
G. penicillioides	**GNJ20200814–11**	**MW969669**	**MW969661**	**MW961415**	**MZ215998**	**–**
G. penicillioides	**GNJ20200814–14**	**MW969670**	**MW969662**	**MW961416**	**MZ215999**	**–**
G. penicillioides	**GNJ20200814–17**	**MW969671**	**MW969663**	**MW961417**	**–**	**–**
G. penicillioides	**GNJ20200812–05**	**MW969672**	**MW969664**	**MW961418**	**–**	**–**
G. penicillioides	**NL20210822-01**	**–**	**–**	**OL981632**	**–**	**–**
G. penicillioides	**NL20210822-09**	**–**	**–**	**OL981633**	**–**	**–**
G. penicillioides	**NL20210822-20**	**–**	**–**	**OL981634**	**–**	**–**
Hevansia cinerea	NHJ 3510	EU369091	–	EU369009	EU369048	EU369070
H. novoguineensis	CBS 610.80T	–	MH394646	MH521885	–	MH521844
H. novoguineensis	NHJ 11923	EU369095	EU369032	EU369013	EU369052	EU369072
H. novoguineensis	BCC 47881	–	MH394650	MH521886	MH521807	MH521845

References: (Sanjuan et al. 2014; Kepler et al. 2017; Rehner et al. 2011; Spatafora et al. 2007; Luangsa-ard et al. 2005; Helaly et al. 2019; Sung et al. 2007; Sung et al. 2001; Johnson et al. 2009; Kuephadungphan et al. 2020; Chirivi-Salomon et al. 2015; Kepler et al. 2012; Sung and Spatafora 2004; Tsang et al. 2016; Kuephadungphan et al. 2019; Helaly et al. 2017)

Results

Taxonomy

Gibellula penicillioides **Ming J. Chen & B. Huang, sp. nov.**
MycoBank No: 843174
Fig. 1

Etymology. Latin "*penicillioides*" referring to the fungus with penicillate conidiophores.

Type. China. Anhui Province: Shitai County, Guniujiang National Nature Reserve, on a spider, on unidentified leaf, 1 August 2020, Mingjun Chen & Bo Huang, holotype GNJ20200814-14. GenBank sequence data for GNJ20200814-14: SSU = MW969670; LSU = MW96966; TEF = MW961416; RPB1 = MZ215999.

Description. Mycelium covering the host, brownish–white cream–yellow to light–brown mycelial mat. Light greyish-brown to violaceous-brown when dried. Synnema solitary, white to yellowish, arising from the tip of the host's abdomen, slender, cylindrical, 6.8 mm long, 0.6 mm wide at base and 0.1 mm at tip. Conidiophores rising from mycelial mat and synnema, smooth, septate, cylindrical, mostly biverticillate, (40–) 52.5–92 (115) × (4–) 4.5–6 µm (Fig. 1d, e), vesicles rarely developed. Several metulae are borne on the apex of conidiophore. Metulae clavate (slightly broadening towards the base) to cylindrical, (11–) 13–17.5 (21.5) × 3.5–5 (–5.5) µm, with a number of phialides in whorls. Phialides broadly cylindrical, with the apex tapering abruptly to a short neck (10–) 12.5–15.5 (–17) × (2.5–) 3–4 (–5) µm. Conidia fusiform, (7–) 7.5–9 (–10) × 2.5–3.5 µm, in chains, borne on each phialide (Figs 1i–j). Teleomorph and granulomanus synanamorphs not observed.

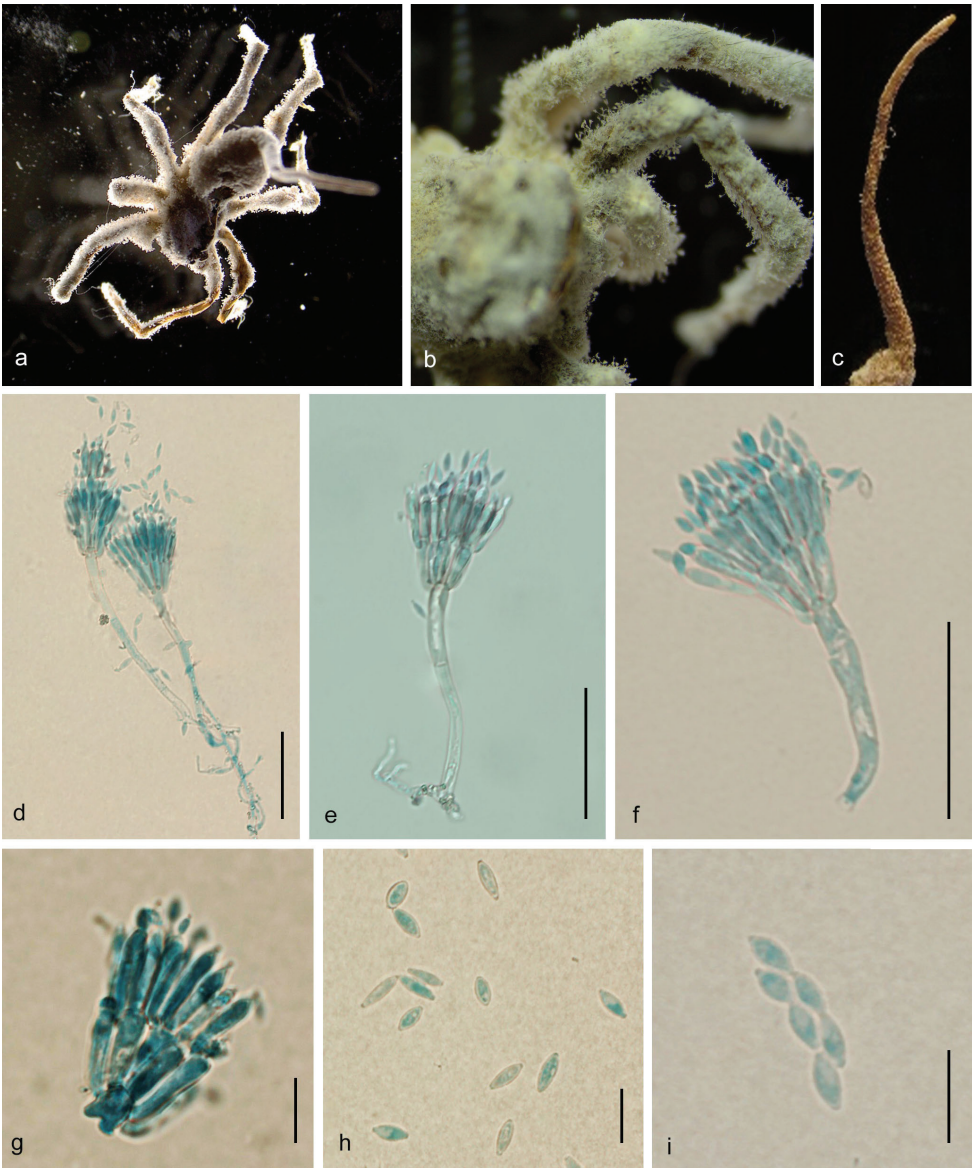

Figure 1. *Gibellula penicillioides* sp. nov. **a–b** fungus on spider **c** synnema solitary **d–f** Penicillate conidiophores **g** conidiophore head bearing conidia **h** conidia **i** conidia in chains. Scale bars: 50 μm (**d, e, f**); 10 μm (**g, h, i**).

Habitat. Occurring on spider attached to the underside of unidentified leaves nearby rivers.

Additional materials examined. China. Anhui Province: Shitai County, Guniujiang National Nature Reserve, on a spider, 1 August 2020, Mingjun Chen & Ting Wang, GNJ20200814–11, GNJ20200814–17 and GNJ20200812–05. China.

Guangdong Province: Nanling Nature Reserve, August 2021, on a spider, Qianle Lu, NL20210822-01, NL20210822-09, and NL20210822-20.

Notes. In its morphological characters, *G. penicillioides* resembles *G. scorpioides*, *G. dabieshanensis* B. Huang, M.Z. Fan & Z.Z. Li, G. *clavulifera* var. *clavulifera* (Petch) Samson & H.C. Evans, G. *clavulifera* var. *major* Tzean, L.S. Hsieh, J.Y. Liou & W.J. Wu and *G. clavulifera* var. *alba* Humber & Rombach by single synnema producing smooth penicillate conidiophores. Table 2 provides a comparative summary of the main characters of *G. penicillioides* and the other four species. Microscopically, *G. penicillioides* can be distinguished from *G. scorpioides*, *G. dabieshanensis* and *G. clavulifera* var. *clavulifera* by having longer conidiophores and slightly larger conidia. Furthermore, *G. penicillioides* differs from *G. clavulifera* var. *alba* by forming larger metulae, phialides and conidia, while *G. clavulifera* var. *major* produces the largest conidia and the longest conidiophore.

***Gibellula longispora* Ming J. Chen & B. Huang, sp. nov.**
MycoBank No: 843175
Fig. 2

Etymology. Latin "*longispora*" referring to the fungus with slender long conidia.

Type. China. Anhui Province: Shitai County, Guniujiang National Nature Reserve, on a spider, on unidentified leaf, 1 August 2020, Mingjun Chen & Bo Huang, holotype GNJ20200813–16. GenBank sequence data for GNJ20200813–16: TEF = MW961414; RPB1 = MW980145.

Description. Mycelium covering the host, white to cream fluffy, light greyish-brown to violaceous-brown when dried. Synnema multiple, cylindrical, growing from abdomen of host spider, cream to yellowish–white. Conidiophores, (19-) 60-153.5 (-170) × 8–10 µm (Fig. 2d), crowded, lately arising from hyphae loosely attached to the surface of the synnema, verrucose, multiseptate, suddenly narrowing to a tip, then forming a globose vesicle, (5.5–) 6–8.5 (–9.5) × (5–) 5.5–8µm (Fig. 2c, f). Spherical conidial heads consisting of vesicle, metulae and phialide, (25.5–) 38.5–49 (–50) × (24.5) 36–46.5 (–49) µm. A number of broadly obovate to oval metulae, 6.5–9.5 × (4.5–)5–7 µm (Fig. 2c), borne on vesicle, each metulae bearing several clavate phialides, (6.5–) 7–9.5 (–11) × (1.5–) 2–3 µm (Fig. 2c, f). Conidia, 5–7 × 1–2 µm (Fig. 2g), narrowly fusiform. Teleomorph and granulomanus synanamorphs not observed. (Fig. 2f).

Habitat. Occurring on spider attached to the underside of leaf nearby the river.

Additional materials examined. China. Anhui Province: Shitai County, Guniujiang National Nature Reserve, on a spider, 10 July 2020, Mingjun Chen & Ting Wang, GNJ20210710-02. China. Guangdong Province: Shenzhen, 10 October 2021, on spiders, Qianle Lu, SZ20210904-02, and SZ20210915-01.

Note. The new species *G. longispora* is similar to five *Gibellula* species in having multi-synnemum and aspergillate, distinctly roughened conidiophores (Table 3), namely *G. pigmentosinum*, *G. flava*, *G. pulchra*, *G. clavispora* Z.Q. Liang, Wan H.

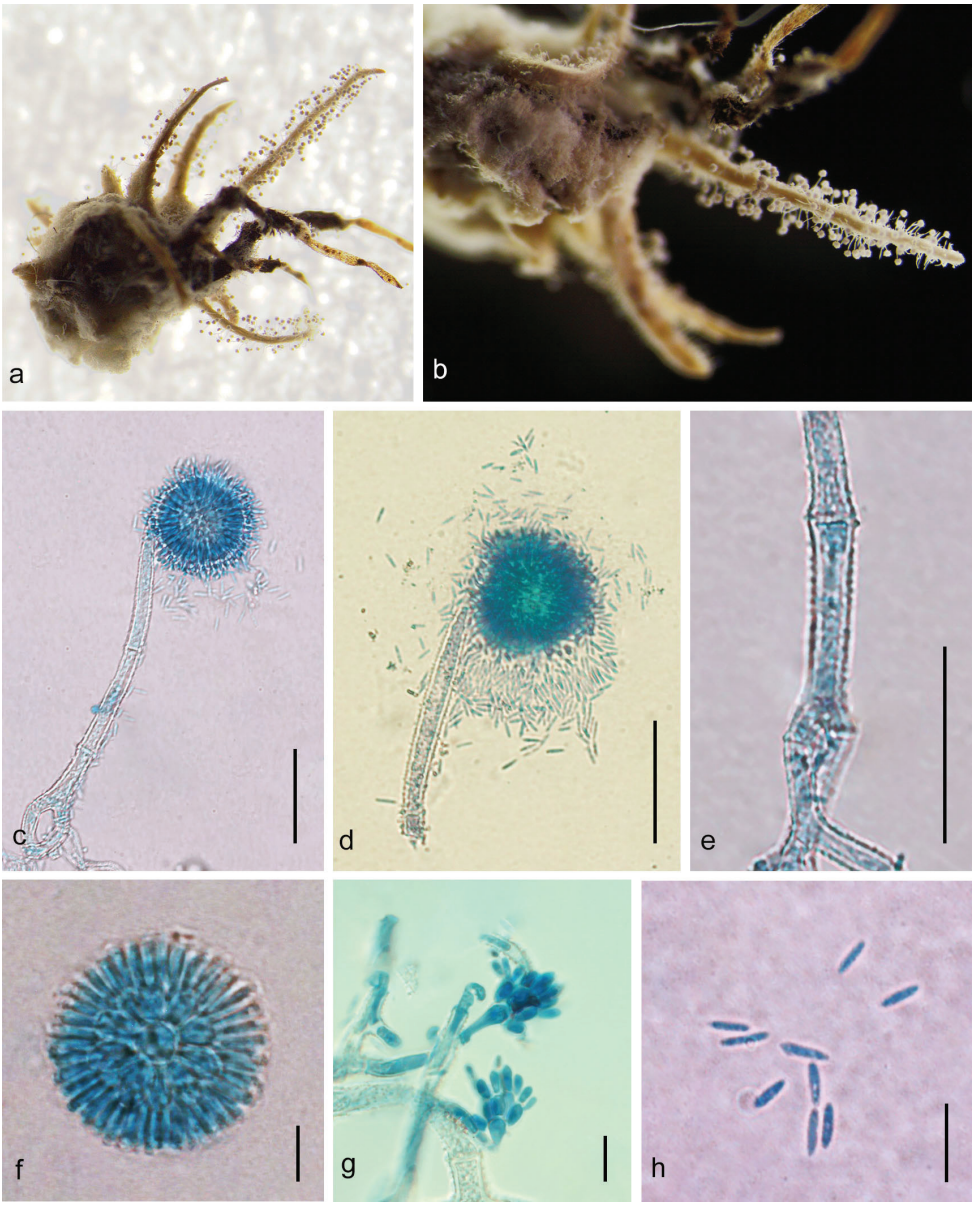

Figure 2. *Gibellula longispora* sp. nov. **a, b** fungus on a spider **c, d** conidiophores showing conidial head **e** part of conidiophore showing rough walls **f, g** conidial head **h** conidia. Scale bars: 50 µm (**c, d**); 20 µm (**e**), 10 µm (**f, g, h**).

Chen & Y.F. Han and *G. shennongjiaensis* X. Zou, Wan H. Chen, Y.F. Han & Z.Q. Liang. However, *G. longispora* differs from *G. pigmentosinum*, *G. flava* and *G. pulchra* by its longer, slender conidia. Furthermore, compared to *G. longispora*, the species *G. shennongjiaensis* has shorter conidiophores with smaller phialide and metulae and slightly smaller conidia, while *G. clavispora* bears clavate conidia.

Table 2. Comparison of *Gibellula clavulifera*, *G. dabieshanensis*, *G. scorpioides and G. penicillioides* sp. nov. with penicillate conidiophores.

Species	Conidiophore(μm)	metulae (μm)	Phialide (μm)	Conidia (μm)
***Gibellula penicillioides* sp. nov.**[1]	penicillate, smooth, mostly biverticillate or terverticillate, (40–) 52.5–92 (115) × (4–) 4.5–6	obovoid to cylindrical, (11–) 13–17.5 (21.5) × 3.5–5 (–5.5)	broadly cylindrical, (10–) 12.5–15.5 (–17) × (2.5–) 3–4 (–5)	(7–) 7.5–9 (–10) × 2.5–3.5
***Gibellula clavulifera* var. major**[2]	penicillate, Smooth-walled, mostly bi- or terverticillate, occasionally monoverticillate 140 × 4.8-7.1	clavate to cylindrical, 12.7-19.8 × 4.0-5.6	ampulliform to cylindrical, 12.7–19.8 × 3.6–4.8 (-5.3)	7.1–12.0 (–13.9) × 2.4–4.0 (–5.6)
Gibellula scorpioides[3]	penicillate, smooth, mostly biverticillate, 20–29 (–30) × 4	obovoid, slightly broadening toward the base, (7–) 9.5–12.5 (–15) × (2–) 3–5 (–7)	broadly cylindrical, (9–) 10–12.5 (–14) × (2–) 2.5–3.5 (–4)	5–7 (–9) × (1.5–) 2–3
Gibellula clavulifera* var. *clavulifera[4]	penicillate, Smooth-walled, 45–50	clavate	cylindrical, with short neck 15–17.3 × 3.2–4.3	5.4–7.6 × 2.1–3.2
Gibellula clavulifera* var. *alba[5]	penicillate, smooth, mono-or biverticillate, up to 100	cylindricrical, 9–15 × 3–4	cylindrical or slightly swollen near the middle 10–12.4 × 1.5–2.5	5–7.5 × 1.5–2
Gibellula dabieshanensis	penicillate with swollen vesicle, smooth 27–44	Obovoid to cylindricrical 8.6–11.5 × 5–6	cylindrical, 7.9-10.8 × 1.8-2.9	3.2-4.0 × 1.1-1.8

Note: [1]Current study, [2]Tzean et al. 1997, [3]Kuephadungphan et al. 2020, [4]Chen et al. 2014, [5]Humber and Rombach 1987, [6] Huang et al. 1998.

Phylogenetic analysis

We constructed phylogenetic trees of the five concatenated loci from 11 newly-collected samples and 39 closely-related taxa from GenBank (Table 1). Our sampling included seven genera belonging to Cordycipitaceae, including *Akanthomyces*, *Beauveria*, *Blackwellomyces*, *Cordyceps*, *Engyodontium*, *Gibellula* and *Hevansia*, with *Engyodontium aranearum* being used as the outgroup. The concatenated alignment was 4581 bases long, with 525 bases from SSU, 838 bases from LSU, 924 bases from TEF, 720 bases from RPB1 and 1056 bases from RPB2. The ML and BI phylogenic topologies were generally congruent (Fig. 3).

All *Gibellula* species, including the 11 new specimens, formed a monophyletic group with high support that was sister to *Hevansia*. Moreover, the seven samples (GNJ20200814–11, 20200814-14, 20200814–17, 20200812–05; NL20210822-01, 20210822-09, 20210822-20), newly described as *G. penicillioides*, formed a clade sister to *G. scorpioiodes*. The four *Gibellula* specimens, newly described as *G. longispora* (GNJ20200813–16, 20210710-02; SZ20210904-02, 20210915-01), formed a clade with two previous *Gibellula* collections (NHJ 12014, 7859) with posterior probability of 1% and 71% bootstrap support, respectively; this lineage was sister to *G. pigmentosinum*. Furthermore, a BLASTn search for homologues showed that the *Gibellula* GNJ20200813–16 TEF sequence had highest similarity to the corresponding sequence of *Gibellula* sp. (NHJ 12014) (99.33%), further supporting that all members of this lineage belong to *G. longispora*.

Table 3. Comparison of the morphological characters of *Gibellula longispora* sp. nov. and related species.

Species	Conidiophore (μm)	Metulae (μm)	Phialide (μm)	Conidia (μm)
***Gibellula longispora* sp. nov.**[1]	verrucose, (19–) 60–153.5 (–170) × 8–10	obovoid to cylindrical, 6.5–9.5 × (4.5–) 5–7	clavate to broadly cylindrical, (6.5–) 7–9.5 (–11) × (1.5–) 2–3	fusiform, 5–7 × 1–2
Gibellula pigmentosinum[2]	smooth to verrucose, (55–) 97.5–170 (–226) × (5–) 7–10 (–12.5)	broadly obovoid, (5.5–) 6–8 (–10) × (3–) 4–6 (–7.5)	obovoid to clavate, (5-) 5.5-8 (-9) × 2-3 (-4.5)	obovoid with an acute apex (2.5-) 3.5-5 (-5.5) × 1-2 (-3)
Gibellula flava[3]	verrucose, 33.5–123.5(–182.5) × (3–) 4–9.5 (–11.5)	obovoid to broadly obovoid, (4.5–) 5.5–7 × 3.5–5.5	narrowly obovate to clavate, 5.5–7 × 1.5–2.5	fusiform, (2.5–) 3–4 (–5.5) × 1–2(–3)
Gibellula pulchra[4]	verrucose, 155–170 × (6–) 7.5–10	cylindrical, 6.2–7.5 × 5	clavate, 7.5–8 × 1.5–2.5	fusiform to fusiform-ellipsoid, 3–5 × 1.5–2.5
Gibellula clavispora[5]	smooth or occasionally roughened 96–113 long	obovoid, 8.6–10.8 × 2.2	clavate 5.4–6.5 × 1.1–2.2	clavate, single, 5.4–6.5 × 1.1–2.2
Gibellula shennongjiaensis[6]	verrucose, 77–107 long	elliptical, 5.4–7.6 × 2.1–4.3	clavate,5.4–10.8 × 1.1–2.2	cylindrical or fusiform, 3.2–6.5 × 1.1–1.6

Note: [1]Current study, [2]Kuephadungphan et al. 2020, [3]Chen et al. 2021, [4] Chen et al. 2016, [5]Faruk et al. 2004, [6]Zou et al. 2016.

Discussion

Our combined morphological and multilocus phylogenetic analyses distinguish *Gibellula penicillioides* and *G. longispora* as new species, which we described and illustrated. We showed that *G. penicillioides* is sister to *G. scorpioides*, but forms long penicilloid conidiophores producing enlarged fusiform conidia ((7–) 7.5–9 (–10) × 2.5–3.5 μm) and that *G. longispora* is sister to *G. pigmentosinum*, but has slender long conidia (5–7 × 1–2 μm).

The fungal name *Gibellula longispora* for isolate NHJ12014 was first proposed, based on phylogenetic analysis with SSU, TEF, RPB1 and RPB2 sequences, but without morphological description (Johnson et al. 2009). In GenBank, sequences of isolate NHJ12014 were recorded as an unidentified *Gibellula* isolate. Furthermore, the name *G. longispora* has not been recorded in the global fungal databases Index Fungorum (www.indexfungorum.org) or MycoBank (www.mycobank.org) (Kuephadungphan et al. 2020). Therefore, due to the lack of formal description of isolate NHJ12014, the species name *G. longispora* was an invalid publication in 2009. Our molecular phylogeny showed that the five specimens from China (GNJ20200813–16, GNJ20210710-02, NL20210822-20, SZ20210904-02 and SZ20210915-01) formed a clade with isolates NHJ12014 and NHJ 7859. The close phylogenetic relationship of these specimens suggests that they are conspecific despite the lack of morphological data for isolates NHJ12014 and NHJ 7859. Here, we described and illustrated the type specimen GNJ20200813–16 as a new species under the name *Gibellula longispora.*

In China, spider-pathogenic fungi have been investigated for a long time, but until the 1980s, only one species (*G. pulchra*) was reported (Gao 1981). However, the first

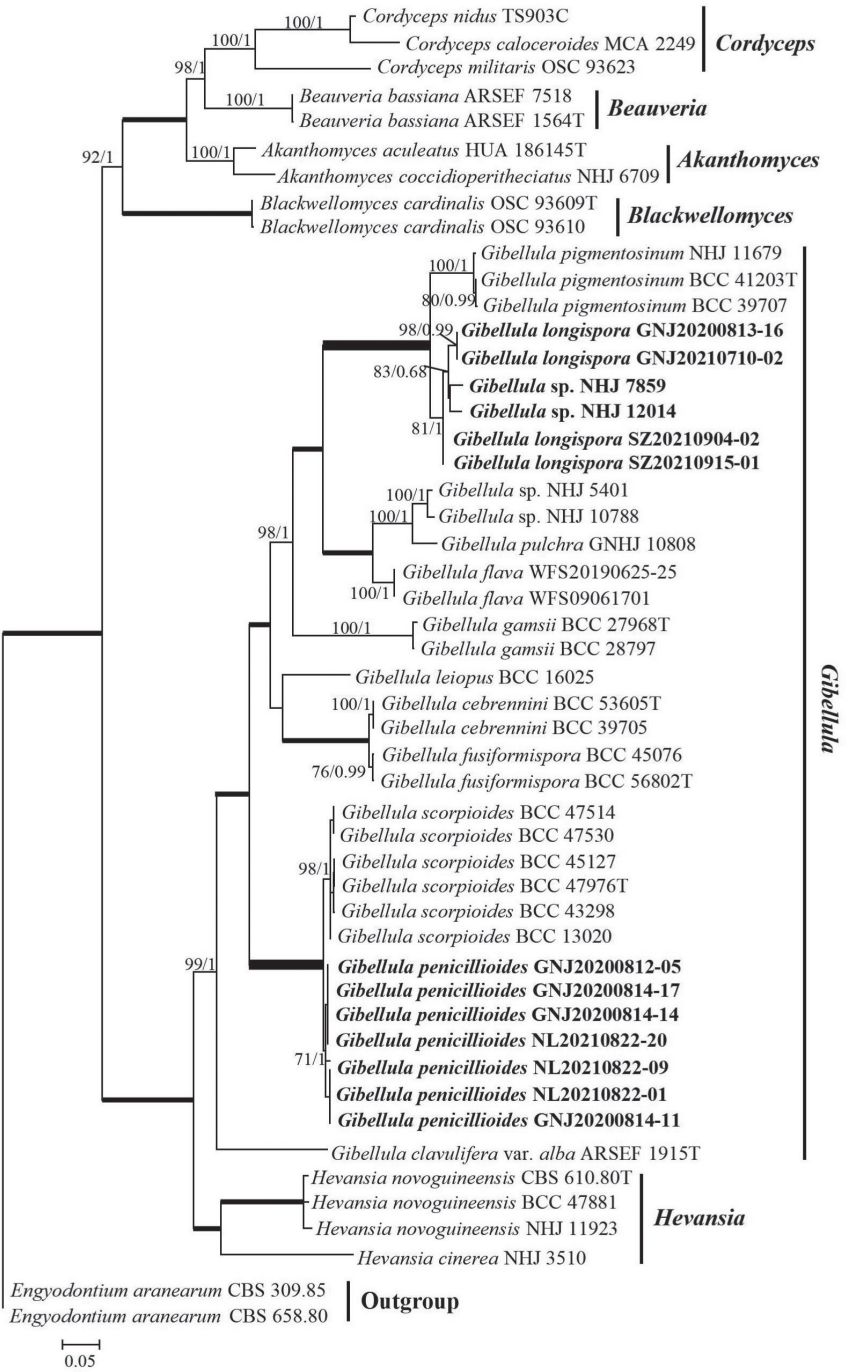

Figure 3. Phylogenetic relationships amongst *Gibellula* and related genera in Cordycipitaceae obtained from analyses of Maximum Likelihood (ML) analysis of five loci (SSU, LSU, TEF, RPB1 and RPB2). ML and BI topologies were generally congruent; therefore, we show only the ML analysis for brevity. At each node with support < 100%, we show ML bootstrap support / BI posterior probabilities; thick branches indicate 100% ML and BI support. The newly-proposed stains are highlighted in bold.

Gibellula species in China was misidentified and is actually *G. leiopus* (Vuill. ex Maubl.), mainly based on its very short conidiophore, which imparts a compact appearance. In the 1990s, three new *Gibellula* species and a new variety were described from Taiwan and Anhui Province. During the past decade, Zongqi Liang's research group have carried out a comprehensive study of the taxonomy of *Gibellula* in China and proposed three new species and two Chinese new records. Recently, we also found and published a new *Gibellula* species with Torrubiella-like sexual morph. Overall, ten species or varieties have been reported in China (Kuephadungphan et al. 2020; Chen et al. 2021): *G. clavispora*, *G. clavulifera*, *G. clavulifera* var. *major*, *G. curvispora* Y.F. Han, Wan H. Chen, X. Zou & Z.Q. Liang, *G. dabieshanensis*, *G. dimorpha* Tzean, L.S. Hsieh & W.J. Wu, *G. flava*, *G. leiopus*, *G. pulchra*, *G. shennongjiaensis* and *G. unica* L.S. Hsieh, Tzean & W.J. Wu. *G. pulchra* and *G. leiopus* are commonly distributed spider pathogenic fungi in southern China. The specimens used in this study were collected from Anhui and Guangdong Provinces, which suggests that the two new species may be widely distributed in southern China.

Kuephadungphan et al. (2020) indicated that host specificity can be used to assess the virulence and potential of biocontrol agents. Mycologists are increasingly interested in exploiting *Gibellula* fungi for bioactive compounds. For example, EPF083CE extracted from *G. pulchra* EPF083 was shown to be a new effective antimicrobial compound (Kuephadungphan et al. 2013). Pigmentosins A and B have been isolated from the spider–associated fungus *G. pigmentosinum* (Helaly et al. 2019) and two secondary metabolites, named gibellamines A and B, have been extracted from *G. gamsii* Kuephadungphan, Tasan. & Luangsa-ard (Kuephadungphan et al. 2019). Interestingly, pigmentosin B and gibellamines are specific to *G. pigmentosinum* and *G. gamsii*, respectively and these specialised compounds may be used as markers for the species' chemical taxonomy (Kuephadungphan et al. 2020).

Gibellula is characterised by its specialised growth requirements; it is very hard to establish in culture (Samson and Evans 1973). Fortunately, the new taxon *G. penicillioides* was successfully isolated from conidia on the standard medium of potato dextrose agar (PDA), although the isolates grew slowly. In the future, we may be able to take advantage of *Gibellula* culture to explore more useful bio-active secondary metabolites or chemotaxonomic markers.

Key to the species of *Gibellula*

1 Conidiophores smooth-walled, mononematous or synnematous **2**
– Conidiophores typically rough-walled, mostly synnematous **8**
2 Conidiophores strictly mononematous, with abruptly narrowing apex and vesicle ..... ***G. mainsii***
– Conidiophores mononematous or synnematous; typically penicillate **3**
3 Conidiophores mononematous or synnematous, teleomorph absent or present **4**
– Conidiophores strictly mononematous, hyaline; teleomorph *Torrubiella ratticaudata* ..... ***G. clavulifera* var. *alba***
4 Conidiophores > 90 µm long; conidia large **5**
– Conidiophores < 50 µm long; conidia small **6**

5 Granulomanus synanamorph present ..... ***G. clavulifera* var. *major***
– Granulomanus synanamorph absent ..... ***G. penicillioides***
6 Conidial heads purple, teleomorph absent ..... ***G. clavulifera* var. *clavulifera***
– Conidial heads colourless, teleomorph present **7**
7 Vesicle swollen; conidia 3.2–4.0 × 1.1–1.8 µm ..... ***G. dabieshanensis***
– Vesicles absent or hardly developed; conidia 5–7(–9) × (1.5–)2–3 µm ..... ***G. scorpioides***
8 Synnemata single or double **9**
– Synnemata multiple **16**
9 Synnemata terminating in a bulbous outgrowth from which a number of conidiophores and a typical wing-like structure arise ..... ***G. alata***
– Synnemata not terminating in a bulbous outgrowth with a wing-like structure, but cylindrical, clavate or bulb-shaped **10**
10 Synnemata typically club-shaped or clavate with a cylindrical sterile apical projection **11**
– Synnemata cylindrical without a sterile apical projection **13**
11 Synnemata typically club-shaped; conidiophores > 80 µm long ..... ***G. mirabilis***
– Synnemata clavate; conidiophores < 80 µm long **12**
12 Granulomanus synanamorph present ..... ***G. clavata***
– Granulomanus synanamorph absent ..... ***G. gamsii***
13 Granulomanus synanamorph present **14**
– Granulomanus synanamorph absent or occasionally present **15**
14 Granulomanus synanamorph with well-differentiated conidiophore and polyblastic conidiogenous cells ..... ***G. dimorpha***
– Granulomanus synanamorph with polyblastic conidiogenous cells .... ***G. cebrennini***
15 Conidiophore 97–170 µm long; conidia obovoid with an acute apex ..... ***G. pigmentosinum***
– Conidiophore 31–53 µm long; conidia fusiform to broadly fusiform ..... ***G. fusiformispora***
16 Synnemata with a stout yellowish-tan stipe, broadening into globose to pyriform fertile area and narrowed into a pale brown compact acuminate sterile tip .... ***G. brunnea***
– Synnemata cylindrical **17**
17 Granulomanus synanamorph present **18**
– Granulomanus synanamorph absent **19**
18 Granulomanus synanamorph with well-differentiated conidiophore and polyblastic conidiogenous cells ..... ***G. unica***
– Granulomanus synanamorph with polyblastic conidiogenous cells in culture ..... ***G. shennongjiaensis***
19 Conidia clavate or botuliform **20**
– Conidia fusiform **21**
20 Conidia 4.7–11 µm long, botuliform; Phialide globose in base ..... ***G. curvispora***
– Conidia 3.2–6.5 µm long, clavate; Phialide clavate ..... ***G. clavispora***
21 Conidia > 5 µm long ..... ***G. longispora***
– Conidia < 5 µm long **22**

22 Conidiophores long, with radiate and often loose conidial heads **23**
– Conidiophores short, with compact conidial heads .....***G. leiopus***
23 Conidiophores up to 600 μm; conidia 3–5 μm in size.....***G. pulchra***
– Conidiophores up to 120 μm; conidia 3–4 μm in size.....***G. flava***

Acknowledgements

The authors would like to thank to Deshui Yu and Cheng Zhao in our laboratory for their help during field investigations and Qianle Lu, a lover of arachnology in Shenzhen, for providing some specimens. We also thank Dr. Ian Gilman at Yale University for his assistance with English language and grammatical editing. This study was conducted under research projects (Nos. 32172473 and 31972332) of the National Natural Science Foundation of China.

References

Castlebury LA, Rossman AY, Sung GH, Hyten AS, Spatafora JW (2004) Multigene phylogeny reveals new lineage for *Stachybotrys chartarum*, the indoor air fungus. Mycological Research 108(8): 864–872. https://doi.org/10.1017/S0953756204000607

Cavara F (1894) Ulteriore contribuzione alla Micologia Lombarda. Atti dell'Ist Bot Univ e Lab Crittogamico Pavia 3: 313–350.

Chen WH, Han YF, Liang ZQ, Wang YR, Zou X (2014) Classification of *Gibellula* spp. by DELTA system. Microbiology China 41(2): 399–407.

Chen WH, Han YF, Liang ZQ, Zou X (2016) Morphological traits, DELTA system, and molecular analysis for *Gibellula clavispora* sp. nov. from China. Mycotaxon 131(1): 111–121. https://doi.org/10.5248/131.111

Chen MJ, Wang T, Lin YAN, Huang BO (2021) *Gibellula flava* sp. nov. (Cordycipitaceae, Hypocreales), a new pathogen of spider from China. Phytotaxa 527(2): 125–133. https://doi.org/10.11646/phytotaxa.527.2.5

Evans HC, Samson RA (1987) Fungal pathogens of spiders. Mycologists: 152–159. https://doi.org/10.1016/S0269-915X(87)80107-6

Faruk S, Elşad H, Muhammet G (2004) Occurrence of the araneogenous fungus *Gibellula pulchra* in Turkey. Mycologia Balcanica 1: 61–62.

Gao RX (1981) Description of a parasitic fungus *Gibellula suffulta* on spiders in Fujian. Acta Microbiologica Sinica 21: 308–310.

Helaly SE, Kuephadungphan W, Phongpaichit S, Luangsa-Ard JJ, Rukachaisirikul V, Stadler M (2017) Five unprecedented secondary metabolites from the spider parasitic fungus *Akanthomyces novoguineensis.* Molecules (Basel, Switzerland) 22(6): e991. https://doi.org/10.3390/molecules22060991

Helaly SE, Kuephadungphan W, Phainuphong P, Ibrahim MAA, Tasanathai K, Mongkolsamrit S, Luangsa-Ard JJ, Phongpaichit S, Rukachaisirikul V, Stadler M (2019) Pigmentosins from

Gibellula sp. as antibiofilm agents and a new glycosylated asperfuran from *Cordyceps javanica.* Beilstein Journal of Organic Chemistry 15: 2968–2981. https://doi.org/10.3762/bjoc.15.293

Huang B, Ding DG, Fan MZ, Li ZZ (1998) A new entomopathogenic fungus on spiders. Junwu Xuebao 17(2): 109–113.

Humber RA, Rombach MC (1987) *Torrubiella ratticaudata* sp. nov. (Pyrenomycetes: Clavicipitales) and other fungi from spiders on the Solomon Islands. Mycologia 79(3): 375–382. https://doi.org/10.1080/00275514.1987.12025393

Johnson D, Sung GH, Hywel-Jones NL, Luangsa-Ard JJ, Bischoff JF, Kepler RM, Spatafora JW (2009) Systematics and evolution of the genus *Torrubiella* (Hypocreales, Ascomycota). Mycological Research 113(Pt 3): 279–289. https://doi.org/10.1016/j.mycres.2008.09.008

Kepler RM, Sung GH, Ban S, Nakagiri A, Chen MJ, Huang B, Li Z, Spatafora JW (2012) New teleomorph combinations in the entomopathogenic genus *Metacordyceps.* Mycologia 104(1): 182–197. https://doi.org/10.3852/11-070

Kepler RM, Luangsa-Ard JJ, Hywel-Jones NL, Quandt CA, Sung GH, Rehner SA, Aime MC, Henkel TW, Sanjuan T, Zare R, Chen M, Li Z, Rossman AY, Spatafora JW, Shrestha B (2017) A phylogenetically-based nomenclature for Cordycipitaceae (Hypocreales). IMA Fungus 8(2): 335–353. https://doi.org/10.5598/imafungus.2017.08.02.08

Kobayasi Y, Shimizu D (1976) The genus *Cordyceps* and its allies from New Guinea. Bulletin of the National Science Museum, Tokyo 2: 133–152.

Kobayasi Y, Shimizu D (1982) Monograph of the genus *Torrubiella.* Bulletin of the National Science Museum, Tokyo 8: 43–78.

Kuephadungphan W, Phongpaichit S, Luangsa-ard JJ, Rukachaisirikul V (2013) Antimicrobial activity of invertebrate-pathogenic fungi in the genera *Akanthomyces* and *Gibellula.* Mycoscience 55(2): 127–133. https://doi.org/10.1016/j.myc.2013.06.007

Kuephadungphan W, Macabeo APG, Luangsa-ard JJ, Tasanathai K, Thanakitpipattana D, Phongpaichit S, Yuyama K, Stadler M (2019) Studies on the biologically active secondary metabolites of the new spider parasitic fungus *Gibellula gamsii.* Mycological Progress 18(1–2): 135–146. https://doi.org/10.1007/s11557-018-1431-4

Kuephadungphan W, Tasanathai K, Petcharad B, Khonsanit A, Stadler M, Luangsa-Ard JJ (2020) Phylogeny- and morphology-based recognition of new species in the spider-parasitic genus *Gibellula* (Hypocreales, Cordycipitaceae) from Thailand. MycoKeys 72: 17–42. https://doi.org/10.3897/mycokeys.72.55088

Larkin MA, Blackshields G, Brown NP, Chenna R, McGettigan PA, McWilliam H, Valentin F, Wallace IM, Wilm A, Lopez R, Thompson JD, Gibson TJ, Higgins DG (2007) Clustal W and Clustal X version 2.0. Bioinformatics (Oxford, England) 23(21): 2947–2948. https://doi.org/10.1093/bioinformatics/btm404

Letunic I, Bork P (2016) Interactive tree of life (iTOL) v3: An online tool for the display and annotation of phylogenetic and other trees. Nucleic Acids Research 44(W1): W242–W245. https://doi.org/10.1093/nar/gkw290

Liu YJ, Whelen S, Hall BD (1999) Phylogenetic relationships among ascomycetes: Evidence from an RNA polymerse II subunit. Molecular Biology and Evolution 16(12): 1799–1808. https://doi.org/10.1093/oxfordjournals.molbev.a026092

Mains EB (1949) New species of *Torrubiella*, *Hirsutella* and *Gibellula.* Mycologia 41(3): 303–310. https://doi.org/10.1080/00275514.1949.12017774

Mains EB (1950) The genus *Gibellula* on spiders in north America. Mycologia 42(2): 306–321. https://doi.org/10.1080/00275514.1950.12017836

Nylander JAA (2004) MrModeltest V2. Program Distributed by the Author. Evolutionary Biology Centre, Uppsala University.

Petch T (1932) Gibellula. Annales Mycologici 30: 386–393.

Rehner SA, Buckley E (2005) A *Beauveria* phylogeny inferred from nuclear ITS and EF1-α sequences: Evidence for cryptic diversification and links to *Cordyceps* teleomorphs. Mycologia 97(1): 84–98. https://doi.org/10.3852/mycologia.97.1.84

Rehner SA, Samuels GJ (1994) Taxonomy and phylogeny of *Gliocladium* analysed from nuclear large subunit ribosomal DNA sequences. Mycological Research 98(6): 625–634. https://doi.org/10.1016/S0953-7562(09)80409-7

Rehner SA, Minnis AM, Sung GH, Luangsa-ard JJ, Devotto L, Humber RA (2011) Phylogeny and systematics of the anamorphic, entomopathogenic genus *Beauveria.* Mycologia 103(5): 1055–1073. https://doi.org/10.3852/10-302

Ronquist F, Huelsenbeck JP (2003) MrBayes 3: Bayesian phylogenetic inference under mixed models. Bioinformatics (Oxford, England) 19(12): 1572–1574. https://doi.org/10.1093/bioinformatics/btg180

Samson RA, Evans HC (1973) NOTES on entomogenous fungi from Ghana I. The genera *Gibellula* and *Pseudogibellula.* Acta Botanica Neerlandica 22(5): 522–528. https://doi.org/10.1111/j.1438-8677.1973.tb00873.x

Samson RA, Evans HC (1992) New species of *Gibellula* on spiders (Araneida) from south America. Mycologia 84(3): 300–314. https://doi.org/10.1080/00275514.1992.12026143

Sanjuan T, Tabima J, Restrepo S, Læssøe T, Spatafora JW, Franco-Molano AE (2014) Entomopathogens of Amazonian stick insects and locusts are members of the *Beauveria* species complex (*Cordyceps* sensu stricto). Mycologia 106(2): 260–275. https://doi.org/10.3852/13-020

Shrestha B, Kubátová A, Tanaka E, Oh J, Yoon DH, Sung JM, Sung GH (2019) Spider-pathogenic fungi within Hypocreales (Ascomycota): Their current nomenclature, diversity, and distribution. Mycological Progress 18(8): 983–1003. https://doi.org/10.1007/s11557-019-01512-3

Spatafora JW, Volkmann-Kohlmeyer B, Kohlmeyer J (1998) Independent terrestrial origins of the Halosphaeriales (Marine Ascomycota). American Journal of Botany 85(11): 1569–1580. https://doi.org/10.2307/2446483

Spatafora JW, Sung GH, Sung JM, Hywel-Jones NL, White Jr JF (2007) Phylogenetic evidence for an animal pathogen origin of ergot and the grass endophytes. Molecular Ecology 16(8): 1701–1711. https://doi.org/10.1111/j.1365-294X.2007.03225.x

Stamatakis A (2006) RAxML-VI-HPC: Maximum likelihood-based phylogenetic analyses with thousands of taxa and mixed models. Bioinformatics (Oxford, England) 22(21): 2688–2690. https://doi.org/10.1093/bioinformatics/btl446

Tsang CC, Chan JFW, Pong WM, Chen JHK, Ngan AHY, Cheung M, Lai CKC, Tsang DNC, Lau SKP, Woo PCY (2016) Cutaneous hyalohyphomycosis due to *Parengyodontium album* gen. et comb. nov. Medical Mycology 54(7): 699–713. https://doi.org/10.1093/mmy/myw025

Tzean SS, Hsieh LS, Wu WJ (1997) The genus *Gibellula* on spiders from Taiwan. Mycologia 89(2): 309–318. https://doi.org/10.1080/00275514.1997.12026787

White TJ, Bruns TD, Lee S, Taylor JW (1990) Amplification and direct sequencing of fungal ribosomal RNA for phylogenetics. In: Innis MA, Gelfand DH, Sninsky JJ, White TJ (Eds) PCR protocols: a guide to methods and applications. Academic Press, San Diego, 315–322. https://doi.org/10.1016/B978-0-12-372180-8.50042-1

Zou X, Chen WH, Han YF, Liang ZQ (2016) A new species of the genus *Gibellula.* Junwu Xuebao 35(10): 1161–1168.

MycoKeys 90: 71–83 (2022)
doi: 10.3897/mycokeys.90.84767
https://mycokeys.pensoft.net

RESEARCH ARTICLE

A peer-reviewed open-access journal
MycoKeys
Launched to accelerate biodiversity research

Two new species of *Phylloporia* (Hymenochaetales) from the Neotropics

Meng Zhou[1], Fang Wu[1], Yu-Cheng Dai[1], Josef Vlasák[2]

1 *Institute of Microbiology, School of Ecology and Nature Conservation, Beijing Forestry University, Beijing 100083, China* **2** *Biology Centre of the Academy of Sciences of the Czech Republic, Branišovská 31, CZ-370 05 České Budějovice, Czech Republic*

Corresponding authors: Yu-Cheng Dai (yuchengdai@bjfu.edu.cn), Josef Vlasák (vlasak@umbr.cas.cz)

Academic editor: R. Henrik Nilsson | Received 2 April 2022 | Accepted 26 May 2022 | Published 7 June 2022

Citation: Zhou M, Wu F, Dai Y-C, Vlasák J (2022) Two new species of *Phylloporia* (Hymenochaetales) from the Neotropics. MycoKeys 90: 71–83. https://doi.org/10.3897/mycokeys.90.84767

Abstract

Two new species of *Phylloporia*, *P. crystallina* and *P. sumacoensis*, are described based on 28S ribosomal RNA phylogeny, morphology, host, and geographic distribution. *Phylloporia crystallina* is characterized by pileate, perennial basidiomata with a duplex context, small pores 9–10 per mm, a monomitic hyphal system, absence of cystidia and cystidioles, presence of large rhomboid crystals in tube trama, broadly ellipsoid to subglobose basidiospores measuring 2.8–3 × 2–2.3 µm, and growth on angiosperm stump. *Phylloporia sumacoensis* is characterized by pileate, perennial basidiomata with a duplex context, very small pores 10–12 per mm, a monomitic hyphal system, hyphae at dissepiment edges bearing fine crystals, presence of cystidioles, broadly ellipsoid to subglobose basidiospores measuring 3–3.7 × 2.1–2.8 µm, and growth on living liana.

Keywords

Hymenochaetaceae, n28S, phylogeny, taxonomy

Introduction

Phylloporia Murrill (Hymenochaetaceae, Hymenochaetales) was established with *P. parasitica* Murrill as the type (Murrill 1904). The genus is characterized by annual or perennial, effused-reflexed, pileate or stipitate, soft corky to hard corky basidiomata, tomentose to velutinate pileal surface, a context mostly duplex with a black line between upper tomentum and lower contextual layer, a monomitic hyphal system in

most species, generative hyphae with simple septa, absence of setal elements (with the exception of *Phylloporia mori* Wu et al.), and subglobose, ellipsoid or cylindric, hyaline to yellowish, fairly thick-walled basidiospores which are usually collapsed when mature and < 6 μm in the greatest dimension. *Phylloporia* species mostly grow parasitically on living angiosperm trees, causing a white rot. Phylogenetically, *Phylloporia* is related to *Flaviporellus* Murrill and *Fulvifomes* Murrill, but *Flaviporellus* and *Fulvifomes* have mostly homogeneous contexts (Wu et al. 2022).

Seventy-one species are currently recognized in *Phylloporia*, among them 17 and 37 species from the Neotropics and China, respectively (Wu et al. 2022). Because more tree species occur in Neotropics than in China (Anonymous 1997) and species diversity of *Phylloporia* is related to tree species diversity (Wu et al. 2019), it seems probable that many unknown species of *Phylloporia* exist in the Neotropics. During investigations of the neotropical polypores, specimens morphologically corresponding to *Phylloporia* were collected from Ecuador. Based on morphological, ecological, and phylogenetic evidence, we hereby propose two new species of *Phylloporia*.

Materials and methods

Studied specimens are deposited in herbaria of the Institute of Microbiology, Beijing Forestry University (BJFC) and the National Museum Prague of Czech Republic (PRM). The sections were prepared in 5% potassium hydroxide (KOH), Melzer's reagent (IKI), and Cotton Blue (CB). The following abbreviations are used: **KOH** = 5% potassium hydroxide, **IKI** = Melzer's reagent, **IKI–** = neither amyloid nor dextrinoid, **CB** = Cotton Blue, **CB–** = acyanophilous, **CB (+)** = cyanophilous after 12 hours stained with Cotton Blue, L = mean spore length (arithmetic average of spores), **W** = mean spore width (arithmetic average of spores), **Q** = variation in the ratios of L/W between specimens studied, and n = number of spores measured from given number of specimens. The microscopic procedure follows Dai (2010), and the special color terms follow Petersen (1996) and Anonymous (1969). Sections were studied at magnifications up to 1000× using a Nikon Eclipse 80i microscope with phase contrast illumination. Drawings were made with the aid of a drawing tube. Microscopic features, measurements, and illustrations were made from the slide preparations stained with Cotton Blue. Microscopic measurements were made from slide preparations stained with Cotton Blue.

The extraction of total genomic DNA from frozen specimens followed Góes-Neto et al. (2005) using the protocol of CTAB 2%. The CTAB rapid plant genome extraction kit-DN14 (Aidlab Biotechnologies Co., Ltd, Beijing) was used to obtain PCR products from dried specimens, following the manufacturer's instructions with some modifications (Chen et al. 2015, 2016). The primer pairs LR0R and LR7 (Vilgalys and Hester 1990) and LR0R and LR5 (White et al. 1990) were used for PCR amplification. The PCR procedure for 28S was as follows: initial denaturation at 94 °C for 1 min, followed by 35 cycles at 94 °C for 30 s, 50 °C for 1 min and 72 °C for 1.5 min,

and a final extension of 72 °C for 10 min. The PCR products were purified and directly sequenced at Beijing Genomics Institute. All newly generated sequences were deposited at GenBank (Sayers et al. 2022) and are shown in the tree (Fig 1).

In addition to the newly generated sequences, 28S sequences (Fig. 1) from Zhou (2016), Ren and Wu (2017), Qin et al. (2018), and Wu et al. (2019, 2022) were downloaded from GenBank and included in the dataset for phylogenetic analysis. *Inonotus hispidus* (Bull.) P. Karst. was selected as outgroup following Zhou (2016). The dataset was

Figure 1. Phylogeny of *Phylloporia* inferred from the 28S dataset. The topology is from the ML analysis, and the support values from ML (former) and BI (latter) analyses simultaneously greater than or equal to 50% and 0.90 are indicated at the nodes, respectively. The new species are in boldface.

aligned using MAFFT v. 7.0 with the Q-INS-i strategy with default parameters (Katoh et al. 2019), and then edited as necessary in BioEdit v. 7.0.5.3 (Hall 1999). Sequence alignments were deposited at TreeBase (submission ID: 29564). Maximum Likelihood (ML) and Bayesian Inference (BI) methods were used for the phylogenetic analysis. The GTR+I+ G model was estimated as the best-fit evolutionary model by MrModeltest v. 2.3 (Nylander 2004) using the Akaike information criterion (AIC). The ML analysis was carried out with raxmlGUI v. 1.2 (Stamatakis 2006; Silvestro and Michalak 2012), and the BI tree reconstruction was carried out with MrBayes v. 3.2.5 (Ronquist et al. 2012). Four Markov chains were run for two runs from random starting trees for 10 million generations, and trees were sampled every 100 generations. BI analysis stopped after effective sample sizes (ESSs) reached more than 200 and the potential scale reduction factors (PSRFs) were close to 1.000 for all parameters. Branches that received bootstrap support for ML (BS) and Bayesian Posterior Probability (BPP) methods greater than or equal to 75% (BS) and 0.95 (BPP) were considered as significantly supported, respectively.

Results

Phylogenetic results

Two 28S sequences were generated in this study and were deposited in GenBank. Their accession numbers are specified in the phylogenetic tree (Fig. 1). The final 28S dataset included 135 sequences and resulted in an alignment of 993 characters. The ML and BI analyses resulted in nearly identical topologies, and thus only the ML tree is presented with the BS and BPP when they were greater than or equal to 50% and 0.90, respectively (Fig. 1).

The phylogeny inferred from the 28S dataset (Fig. 1) shows that the specimen JV 2106/102 together with one specimen (MUCL 45062 from Cuba) form a distinct lineage and that the specimen JV2109/73 forms another independent *Phylloporia* lineage.

Taxonomy

Phylloporia crystallina **Y.C. Dai, F. Wu, Meng Zhou & Vlasák, sp. nov.**
MycoBank No: 843482
Figs 2, 3

Type. Ecuador, Mindo Valley, San Carlos, Cascadas; alt. 1400m; 0°4'S, 78°45'W; 20 Jun. 2021; Vlasák leg.; on angiosperm freshly dead stump in tropical cloud forest; JV2106/102 (holotype BJFC038563, isotype PRM957106). GenBank: ON129551 (ITS); ON006467 (LSU)

Etymology. — *Crystallina* (Lat.): refer to the species having abundant large rhomboid crystals in tube trama.

Diagnosis. *Phylloporia crystallina* is characterized by pileate, perennial basidiomata with a thin layer of context between individual tube layers, a duplex context

with a black line separating the upper tomentum and a lower compacted layer, small pores 9–10 per mm, a monomitic hyphal system, generative hyphae thin- to distinctly thick-walled with simple septa, the absence of cystidia and cystidioles, the presence of large rhomboid crystals in tube trama, broadly ellipsoid basidiospores measuring 2.8–3 × 2–2.3 µm, and growth on angiosperm stump in the Neotropics.

Basidiomata. Perennial, effused reflexed, imbricate, broadly attached to the substrate, hard corky when fresh, woody hard when dry. Pilei applanate to semi-circular, projecting up to 2 cm and 3 cm wide. Pileal surface curry yellow to cinnamon buff when fresh, become purplish chestnut when dry, concentrically sulcate with narrow zones, densely tomentum when juvenile, become velutinate to matted with age, the tomentum up to 1 mm thick, wearing off, leaving a dense trichoderm, sometime covered by mosses; margin sharp, entire. Pore surface pinkish buff to buff yellow and glancing when fresh, become honey yellow when dry; pores round, 9–10 per mm; dissepiments thin, entire. Context umber, up to 3 mm thick, duplex, with a black line separating the upper tomentum and a lower compacted layer, the upper tomentum soft corky, the lower layer hard corky. Tubes fulvous, paler than context, up to 5 mm long, distinctly stratified, usually filled a thin context among tube layers.

Hyphal structure. Hyphal system monomitic; generative hyphae simple septate; tissue darkening but otherwise unchanged in the shape of the hyphae in KOH.

Context. Hyphae in the lower context golden yellow, fairly thick-walled with a wide lumen, unbranched, frequently simple-septate, loosely interwoven, slightly CB+, 3–5 µm diam.; hyphae in the upper tomentum yellow, fairly thick-walled with a wide lumen, unbranched, frequently simple septate, straight, regularly arranged, 5–7 µm diam.

Tubes. Tramal hyphae hyaline to yellow, thin- to thick-walled with a narrow to medium lumen, rarely branched, frequently to occasionally simple septate, flexu-

Figure 2. Basidiomata of *Phylloporia crystallina* (holotype, JV2106/102). Scale bar: 1 cm.

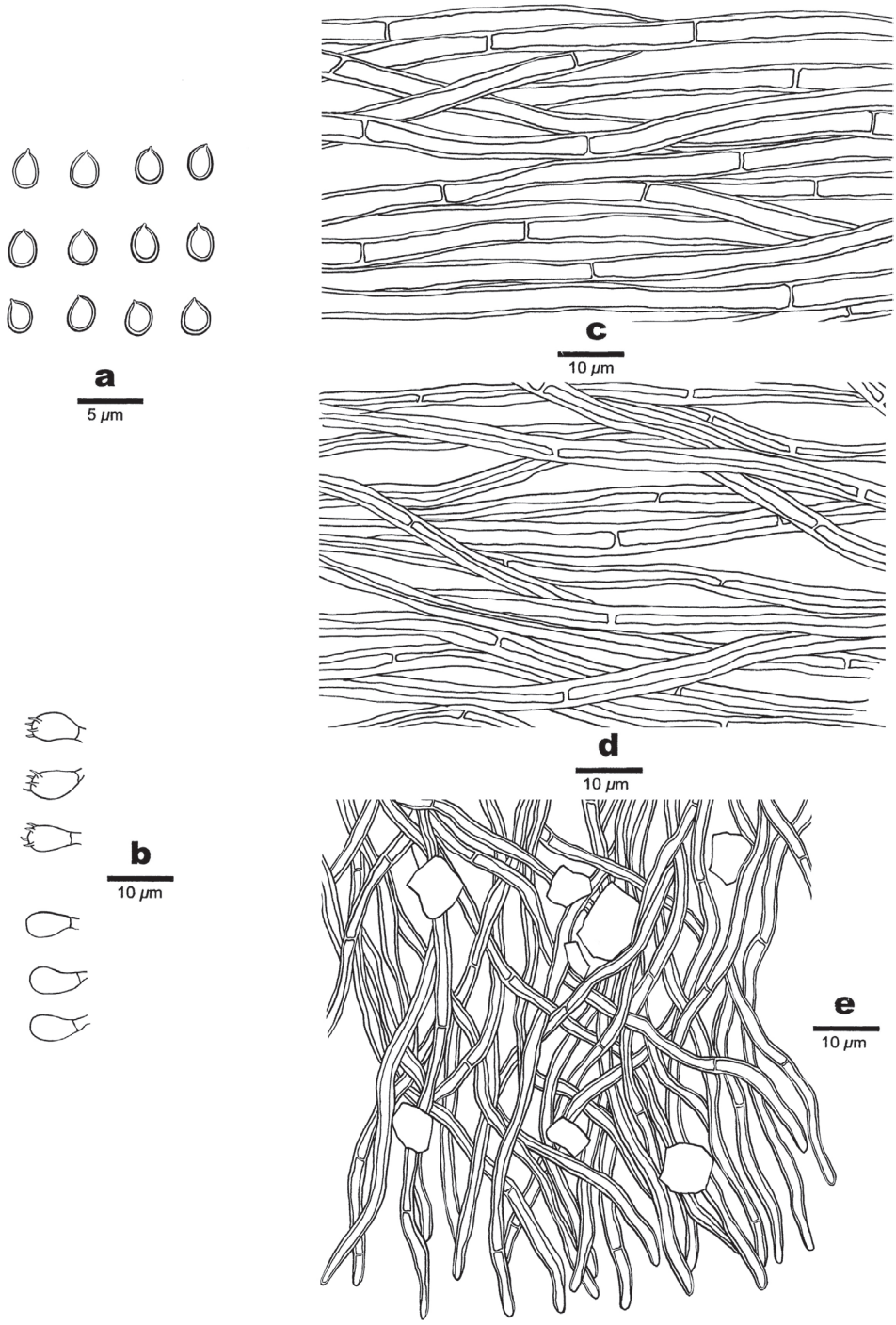

Figure 3. Microscopic structures of *Phylloporia crystallina* (drawn from the holotype, JV2106/102). **a** basidiospores **b** basidia and basidioles **c** hyphae from upper tomentum **d** hyphae from lower compacted context **e** hyphae from dissepiment edge.

ous, loosely interwoven, slightly CB+, 2–3.5 µm diam.; hyphae at dissepiment edges smooth; large rhomboid crystals abundant among tube trama.

Hymenium. Cystidia and cystidioles absent; basidia barrel-shaped with four sterigmata and a simple septum at the base, 5–7 × 3.5–4 µm. Basidioles similar to basidia in shape, but slightly smaller. Basidiospores broadly ellipsoid to subglobose, yellowish, thick-walled, smooth, not collapsed, IKI–, CB–, (2.7–) 2.8–3 (–3.1) × 2–2.3 (–2.4) µm, L = 2.9 µm, W = 2.1 µm, Q = 1.38 (n = 30/1).

Notes. Phylogenetically (Fig. 1), *Phylloporia crystallina* is related to *P. montana* Oliveira-Filho & Gibertoni (Wu et al. 2019). However, *P. montana* has wider pores (3–5 per mm vs. 9–10 per mm) and larger and cylindrical basidiospores (4–5 × 2–3 µm vs. 2.8–3 × 2–2.3 µm) (Wu et al. 2019). Morphologically, *P. crystallina* resembles *P. crataegi* L.W. Zhou & Y.C. Dai by sharing perennial and pileate basidiomata with duplex context, a monomitic hyphal system, interwoven tramal hyphae, the absence of cystidia and cystidioles, and broadly ellipsoid to subglobose basidiospores (Zhou and Dai 2012). However, the latter species differs from *P. crystallina* by the absence of rhomboid crystals, distinctly longer basidia (8–11 µm vs. 5–7 µm), and growth on living *Crataegus* in temperate China (Zhou and Dai 2012). In addition, *P. crystallina* and *P. crataegi* are phylogenetically distantly related (Fig. 1). *P. chrysites* (Berk.) Ryvarden is a Neotropical species. It has similar basidiospores as *P. crystallina*, but the former is readily distinguished from the latter by its annual habit and larger pores (9–10 per mm vs. pores 6–8 per mm, Wu et al. 2022).

Trametes lilliputiana Speg. and *Pyropolyporus subpectinatus* Murrill were originally described from Brazil and Cuba, respectively (Spegazzini 1889; Murrill 1908), and they were treated as synonyms of *Phylloporia pectinata* (Klotzsch) Ryvarden (Bresadola 1912; Ryvarden 1985; Rajchenberg and Wright 1987). However, these two taxa may be different from *Phylloporia pectinata* because its type locality is in India (Wu et al. 2022). The type of *T. lilliputiana* is sterile, but its pilei are confluent and thin, and its upper surface is smooth according to its original description (Spegazzini 1889). *P. subpectinatus* has globose basidiospores (Murrill 1908). So, these two taxa are closer or identical to *P. pectinata* which has a dimitic hyphal structure and globose basidiospores (Ryvarden 2004); while *P. crystallina* has a monomitic hyphal system and broadly ellipsoid basidiospores.

Phylloporia sumacoensis **Y.C. Dai, F. Wu, Meng Zhou & Vlasák, sp. nov.**
MycoBank No: 843484
Figs 4, 5

Type. Ecuador, Guamani, Wild Sumaco Lodge; alt. 1200m; 0°40'S, 77°36'W; 30. Sep. 2021; Vlasák leg.; on living liana in tropical cloud forest; JV2109/73 (holotype BJFC038576, isotype PRM957107). GenBank: ON129552 (ITS); ON006468 (LSU).

Etymology. — *Sumacoensis* (Lat.): refer to the species being found close to Sumaco Vulcan, Ecuador.

Diagnosis. *Phylloporia sumacoensis* is characterized by pileate, perennial basidiomata with a thin layer of context between individual tube layers, a duplex context with a black line separating the upper tomentum and a lower compacted layer, very small pores 10–12 per mm, a monomitic hyphal system, generative hyphae thin- to distinctly thick-walled with simple septa, the hyphae at dissepiment edges bearing fine crystals, presence of cystidioles, broadly ellipsoid to subglobose basidiospores as 3–3.7 × 2.1–2.8 µm, and growth on living liana at medium elevation in the Neotropical cloud forest.

Basidiomata. Perennial, pileate, solitary, broadly attached to the substrate, corky when fresh, hard corky when dry. Pilei applanate to semi-circular, projecting up to 4 cm, 5 cm wide and 15 mm thick at base. Pileal surface fuscous to vinaceous gray when fresh, become fulvous to date brown when dry, concentrically zonate and sulcate, densely tomentose, the tomentum up to 4 mm thick; margin obtuse, entire. Pore surface brownish gray to yellowish gray and glancing when fresh, become snuff brown when dry; pores round, 10–12 per mm; dissepiments thick, entire. Context fulvous, up to 8 mm thick, duplex, with a black line separating an upper soft corky tomentum, up to 4 mm thick and the lower compacted layer, hard corky, up to 4 mm thick. Tubes fawn, darker than context, up to 7 mm long, distinctly stratified, usually with a thin layer of context between individual tube layers.

Hyphal structure. Hyphal system monomitic; generative hyphae simple septate; tissue darkening but otherwise unchanged in the shape of the hyphae in KOH.

Context. Hyphae in the lower context golden yellow, thick-walled with a narrow to medium lumen, unbranched, occasionally simple septate, interwoven, 3–5 µm

Figure 4. A basidiomata of *Phylloporia sumacoensis* (holotype, JV2109/73). Scale bar: 1 cm.

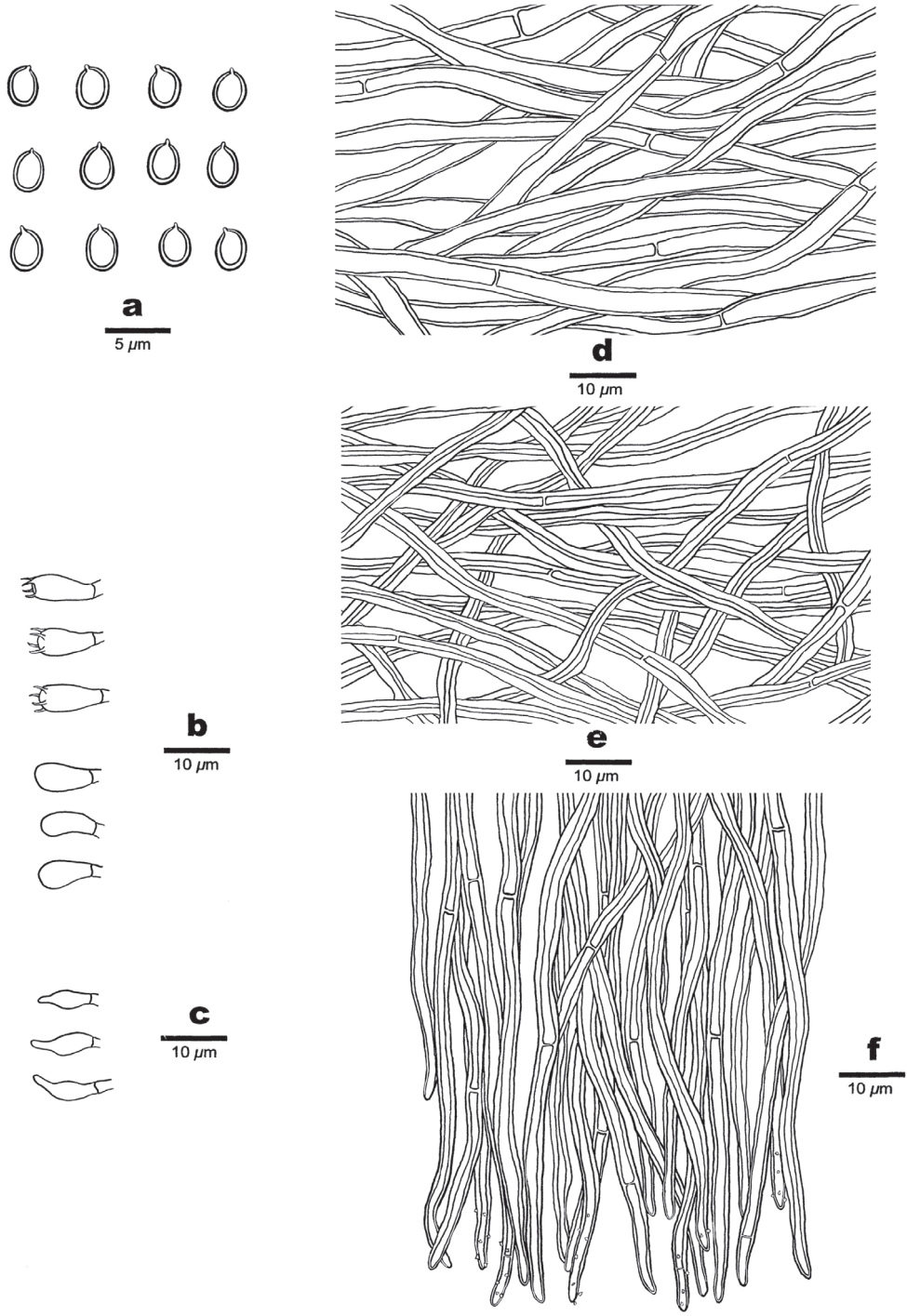

Figure 5. Microscopic structures of *Phylloporia sumacoensis* (drawn from the holotype, JV2109/73). **a** basidiospores **b** basidia and basidioles **c** cystidioles **d** hyphae from upper tomentum **e** hyphae from lower compacted context **f** hyphae from dissepiment edge.

diam.; hyphae in the tomentum brownish yellow, fairly thick-walled with a wide lumen, unbranched, frequently simple septate, some collapsed, loosely interwoven, 5–7 μm diam.

Tubes. Tramal hyphae hyaline to golden yellow, thin- to thick-walled with a narrow to medium lumen, rarely branched, frequently to occasionally simple septate, parallel or subparallel along the tubes, 2–4 μm diam.; hyphae at dissepiment edges bearing fine crystals.

Hymenium. Cystidia absent, fusoid cystidioles rarely present; basidia barrel-shaped with four sterigmata and a simple septum at the base, 10–12 × 4.5–5 μm. Basidioles similar to basidia in shape, but slightly smaller. Basidiospores broadly ellipsoid to subglobose, yellowish, thick-walled, smooth, some collapsed, IKI–, CB–, (2.9–)3–3.7(–3.9) × 2.1–2.8 μm, L = 3.18 μm, W = 2.48 μm, Q = 1.28 (n = 30/1).

Notes. Phylogenetically, *Phylloporia sumacoensis* is closely related to two other Neotropical species, *P. spathulata* (Hook.) Ryvarden sensu auctore and *P. ulloae* R. Valenz. et al. (Fig. 1). However, *P. spathulata* differs from *P. sumacoensis* in having stipitate basidiomata, wider pores (7–9 per mm vs. 10–12 per mm), and the absence of cystidioles (Ryvarden 2004). *Phylloporia ulloae* differs from *P. sumacoensis* in having wider pores (6–8 per mm vs. 10–12 per mm) and longer basidia (14.5–16 μm vs. 10–12 μm) (Valenzuela et al. 2011). Morphologically, *P. sumacoensis* is similar to *P. fontanesiae* L.W. Zhou & Y.C. Dai by sharing same pores size and broadly ellipsoid basidiospore (Zhou and Dai 2012), but the latter species has an annual habit, shorter basidia (6–7 × 3.5–4 μm vs. 10–12 × 4.5–5 μm), shorter basidiospores (2.5–3 μm vs. 3–3.7 μm), and growth on living *Fontanesia* in Asia (Zhou and Dai 2012). In addition, *P. sumacoensis* and *P. fontanesiae* are phylogenetically distantly related (Fig. 1).

Discussion

Most *Phylloporia* species grow parasitically on living hardwoods, and speciation in the genus seems to be driven by the process of colonizing and adapting to new hosts (Wu et al. 2019). The genus is taxonomically difficult, however, because of the similar morphology among species. Before the era of molecular phylogenetics, the diversity of *Phylloporia* was grossly underestimated. The genus has received considerable attention through LSU-based phylogenetic studies (Wagner and Ryvarden 2002). So far, 73 species in the genus are accepted, and most of them were described and confirmed by molecular data recently (Wu et al. 2019, 2022). In addition, the majority of the recently described species were from subtropical and tropical areas, pointing to a remarkable species richness of the genus in tropical regions. There can be little doubt that more undescribed taxa of *Phylloporia* are present in the Neotropics, and the more samples are collected the better our understanding of species diversity of the genus will be.

Unlike other wood-inhabiting fungal genera, very long and complex ITS sequences are present in most *Phylloporia* species. These are difficult to align confidently. Accordingly, most phylogenies were based on LSU sequences (Decock et al. 2015; Yombiyeni et al. 2015; Ferreira-Lopes et al. 2016; Zhou 2016; Rajchenberg et al. 2019;

Wu et al. 2019, 2022). Although *Phylloporia* is shown to be monophyletic based on LSU sequences, the genus is composed of a non-trivial number of subclades (Fig. 1). In addition, in some cases, phylogenetic estimates of *Phylloporia* look strikingly different depending on what exact taxa are included in the analyses. Phylogenetic inference based on multiple genetic markers is a better solution, but most described taxa are represented by only a very limited number of sequences and different genetic markers in GenBank. Sequences from multiple genetic markers from samples of *Phylloporia* are much needed, from fairly conserved genetic markers. Ideally, the next version of MAFFT and other multiple sequence alignment tools will furthermore be able to handle the ITS sequences of the genus *Phylloporia* in a better way.

Acknowledgements

The research was financed by National Natural Science Foundation of China (Project Nos. 32161143013 and 32011540380) and the Second Tibetan Plateau Scientific Expedition and Research Program (STEP, Grant No. 2019QZKK0503), and by the institutional support of the Academy of Sciences of the Czech Republic RVO: 60077344.

References

Anonymous (1969) Flora of British fungi. Colour identification chart. Her Majesty's Stationery Office, London, 3 pp.

Anonymous (1997) The forests in China 1. The Chinese Forest Press, Beijing, 584 pp.

Bresadola G (1912) Basidiomycetes Philippinenses 2. Hedwigia 53: 46–80.

Chen JJ, Cui BK, Zhou LW, Korhonen K, Dai YC (2015) Phylogeny, divergence time estimation, and biogeography of the genus *Heterobasidion* (Basidiomycota, Russulales). Fungal Diversity 71(1): 185–200. https://doi.org/10.1007/s13225-014-0317-2

Chen JJ, Cui BK, Dai YC (2016) Global diversity and molecular systematics of *Wrightoporia* s.l. (Russulales, Basidiomycota). Persoonia 37(1): 21–36. https://doi.org/10.3767/003158516X689666

Dai YC (2010) Hymenochaetaceae (Basidiomycota) in China. Fungal Diversity 45(1): 131–343. https://doi.org/10.1007/s13225-010-0066-9

Decock C, Yombiyeni P, Memiaghe H (2015) Hymenochaetaceae from the Guineo-Congolian Rainforest: *Phylloporia flabelliforma* sp. nov. and *Phylloporia gabonensis* sp. nov., two undescribed species from Gabon. Cryptogamie. Mycologie 36(4): 449–467. https://doi.org/10.7872/crym/v36.iss4.2015.449

Ferreira-Lopes V, Robledo GL, Reck MA, Góes-Neto A, Drechsler-Santos ER (2016) *Phylloporia spathulata* sensu stricto and two new South American stipitate species of *Phylloporia* (Hymenochaetaceae). Phytotaxa 257(2): 133–148. https://doi.org/10.11646/phytotaxa.257.2.3

Góes-Neto A, Loguercio-Leite C, Guerrero RT (2005) DNA Extraction from frozen field-collected and dehydrated herbarium fungal basidiomata: Performance of SDS and CTAB-based methods. Biotemas 18: 19–32.

Hall TA (1999) Bioedit: A user-friendly biological sequence alignment editor and analysis program for Windows 95/98/NT. Nucleic Acids Symposium Series 41: 95–98. https://doi.org/10.1021/bk-1999-0734.ch008

Katoh K, Rozewicki J, Yamada KD (2019) MAFFT online service: Multiple sequence alignment, interactive sequence choice and visualization. Briefings in Bioinformatics 20(4): 1160–1166. https://doi.org/10.1093/bib/bbx108

Murrill WA (1904) The Polyporaceae of North America 9. Bulletin of the Torrey Botanical Club 31: 593–610. https://doi.org/10.2307/2478612

Murrill WA (1908) Polyporaceae 2. North American Flora 9(2): 73–131.

Nylander JAA (2004) MrModeltest v2. Program distributed by the author. Evolutionary Biology Centre, Uppsala University, Uppsala.

Petersen JH (1996) Farvekort. The Danish Mycological Society's colour-chart. Foreningen til Svampekundskabens Fremme, Greve, 6 pp.

Qin WM, Wang XW, Sawahata T, Zhou LW (2018) *Phylloporia lonicerae* (Hymenochaetales, Basidiomycota), a new species on *Lonicera japonica* from Japan and an identification key to worldwide species of *Phylloporia.* MycoKeys 30: 17–30. https://doi.org/10.3897/mycokeys.30.23235

Rajchenberg M, Wright JE (1987) Type studies of Corticiaceae and Polyporaceae (Aphyllophorales) described by C. Spegazzini. Mycologia 79(2): 246–464. https://doi.org/10.1080/00275514.1987.12025704

Rajchenberg M, Pildain MB, Cajas Madriaga D, de Errasti A, Riquelme C, Becerra J (2019) New poroid Hymenochaetaceae (Basidiomycota, Hymenochaetales) from Chile. Mycological Progress 18(6): 865–877. https://doi.org/10.1007/s11557-019-01495-1

Ren GJ, Wu F (2017) *Phylloporia lespedezae* sp. nov. (Hymenochaetaceae, Basidiomycota) from China. Phytotaxa 299(2): 243–251. https://doi.org/10.11646/phytotaxa.299.2.8

Ronquist F, Teslenko M, van der Mark P, Avres DL, Darling A, Höhna S, Larget B, Liu L, Suchard MA, Huelsenbeck JP (2012) MrBayes3.2: Efficient Bayesian phylogenetic inference and model choice, across a large model space. Systematic Biology 61(3): 539–542. https://doi.org/10.1093/sysbio/sys029

Ryvarden L (1985) Type studies in the Polyporaceae 17. Species described by W.A. Murrill. Mycotaxon 23: 169–198.

Ryvarden L (2004) Neotropical polypores 1. Introduction, Hymenochaetaceae and Ganodermataceae. Synopsis Fungorum 19: 1–227.

Sayers EW, Cavanaugh M, Clark K, Pruitt KD, Schoch CL, Sherry ST, Karsch-Mizrachi I (2022) GenBank. Nucleic Acids Research 50(D1): 161–164. https://doi.org/10.1093/nar/gkab1135

Silvestro D, Michalak I (2012) raxmlGUI: A graphical front-end for RAxML. Organisms, Diversity & Evolution 12(4): 335–337. https://doi.org/10.1007/s13127-011-0056-0

Spegazzini C (1889) Fungi Puiggariani. Pugillus 1. Boletín de la Academia Nacional de Ciencias en Córdoba 11: 381–622. https://doi.org/10.5962/bhl.title.3624

Stamatakis A (2006) RAxML-VI-HPC: Maximum likelihood-based phylogenetic analyses with thousands of taxa and mixed models. Bioinformatics (Oxford, England) 22(21): 2688–2690. https://doi.org/10.1093/bioinformatics/btl446

Valenzuela R, Raymundo T, Cifuentes J, Castillo G, Amalfi M, Decock C (2011) Two undescribed species of *Phylloporia* are evidenced in Mexico based on morphological, phylogenetic, and ecological data. Mycological Progress 10: 341–349. https://doi.org/10.1007/s11557-010-0707-0

Vilgalys R, Hester M (1990) Rapid genetic identification and mapping of enzymatically amplified ribosomal DNA from several *Cryptococcus* species. Journal of Bacteriology 172(8): 4238–4246. https://doi.org/10.1128/jb.172.8.4238-4246.1990

Wagner T, Ryvarden L (2002) Phylogeny and taxonomy of the genus *Phylloporia* (Hymenochaetales). Mycological Progress 1(1): 105–106. https://doi.org/10.1007/s11557-006-0009-8

White TJ, Bruns T, Lee S, Taylor JW (1990) Amplification and direct sequencing of ribosomal RNA genes for phylogenetics. In: Innis MA, Gelfand DH, Sninsky JJ, White TJ (Eds) PCR Protocols, a Guide to Methods and Applications. Academic Press, New York, 315–322. https://doi.org/10.1016/B978-0-12-372180-8.50042-1

Wu F, Ren GJ, Wang L, Oliveira-Filho JRC, Gibertoni TB, Dai YC (2019) An updated phylogeny and diversity of Phylloporia (Hymenochaetales): Eight new species and keys to species of the genus. Mycological Progress 18(5): 615–639. https://doi.org/10.1007/s11557-019-01476-4

Wu F, Zhou LW, Vlasák J, Dai YC (2022) Global diversity and systematics of Hymenochaetaceae with poroid hymenophore. Fungal Diversity 113(1): 1–192. https://doi.org/10.1007/s13225-021-00496-4

Yombiyeni P, Balezi A, Amalfi M, Decock C (2015) Hymenochaetaceae from the Guineo-Congolian rainforest: Three new species of *Phylloporia* based on morphological, DNA sequences and ecological data. Mycologia 107(5): 996–1011. https://doi.org/10.3852/14-298

Zhou LW (2016) *Phylloporia minutipora* and *P. radiata* spp. nov. (Hymenochaetales, Basidiomycota) from China and a key to worldwide species of *Phylloporia.* Mycological Progress 15(6): e57. https://doi.org/10.1007/s11557-016-1200-1

Zhou LW, Dai YC (2012) Phylogeny and taxonomy of *Phylloporia* (Hymenochaetales): New species and a worldwide key to the genus. Mycologia 104(1): 211–222. https://doi.org/10.3852/11-093

Supplementary material 1

The sequence alignments and tree

Authors: Meng Zhou, Fang Wu, Yu-Cheng Dai, Josef Vlasák

Data type: NEX file

Explanation note: The NEX file includes Phylloporia phylogenetic sequence alignments inferred from the 28S dataset and the topology of the ML analysis.

Link: https://doi.org/10.3897/mycokeys.90.84767.suppl1

MycoKeys 90: 85–118 (2022)
doi: 10.3897/mycokeys.90.82871
https://mycokeys.pensoft.net

RESEARCH ARTICLE

A peer-reviewed open-access journal
MycoKeys
Launched to accelerate biodiversity research

New polyketides from the liquid culture of *Diaporthe breyniae* sp. nov. (Diaporthales, Diaporthaceae)

Blondelle Matio Kemkuignou[1,2], Lena Schweizer[1], Christopher Lambert[1,2], Elodie Gisèle M. Anoumedem[3], Simeon F. Kouam[3], Marc Stadler[1,2], Yasmina Marin-Felix[1,2]

1 *Department of Microbial Drugs, Helmholtz Centre for Infection Research (HZI) and German Centre for Infection Research (DZIF), Partner Site Hannover/Braunschweig, Inhoffenstrasse 7, 38124 Braunschweig, Germany* **2** *Institute of Microbiology, Technische Universität Braunschweig, Spielmannstraße 7, 38106 Braunschweig, Germany* **3** *Department of Chemistry, Higher Teacher Training College, University of Yaoundé I, Yaoundé P.O. Box 47, Cameroon*

Corresponding author: Yasmina Marin Felix (Yasmina.marinfelix@helmholtz-hzi.de)

Academic editor: Thorsten Lumbsch | Received 9 March 2022 | Accepted 2 May 2022 | Published 14 June 2022

Citation: Matio Kemkuignou B, Schweizer L, Lambert C, Anoumedem EGM, Kouam SF, Stadler M, Marin-Felix Y (2022) New polyketides from the liquid culture of *Diaporthe breyniae* sp. nov. (Diaporthales, Diaporthaceae). MycoKeys 90: 85–118. https://doi.org/10.3897/mycokeys.90.82871

Abstract

During the course of a study on the biodiversity of endophytes from Cameroon, a fungal strain was isolated. A multigene phylogenetic inference using five DNA loci revealed that this strain represents an undescribed species of *Diaporthe*, which is introduced here as *D. breyniae*. Investigation into the chemistry of this fungus led to the isolation of two previously undescribed secondary metabolites for which the trivial names fusaristatins G (**7**) and H (**8**) are proposed, together with eleven known compounds. The structures of all of the metabolites were established by using one-dimensional (1D) and two-dimensional (2D) Nuclear Magnetic Resonance (NMR) spectroscopic data in combination with High-Resolution Electro-Spray Ionization Mass Spectrometry (HR-ESIMS) data. The absolute configuration of phomopchalasin N (**4**), which was reported for the first time concurrently to the present publication, was determined by analysis of its Rotating frame Overhauser Effect SpectroscopY (ROESY) spectrum and by comparison of its Electronic Circular Dichroism (ECD) spectrum with that of related compounds. A selection of the isolated secondary metabolites were tested for antimicrobial and cytotoxic activities, and compounds **4** and **7** showed weak antifungal and antibacterial activity. On the other hand, compound **4** showed moderate cytotoxic activity against all tested cancer cell lines with IC_{50} values in the range of 5.8–45.9 µM. The latter was found to be less toxic than the other isolated cytochalasins (**1**–**3**) and gave hints in regards to the structure-activity relationship (SAR) of the studied cytochalasins. Fusaristatin H (**8**) also exhibited weak cytotoxicity against KB3.1 cell lines with an IC_{50} value of 30.3 µM.

Graphical abstract

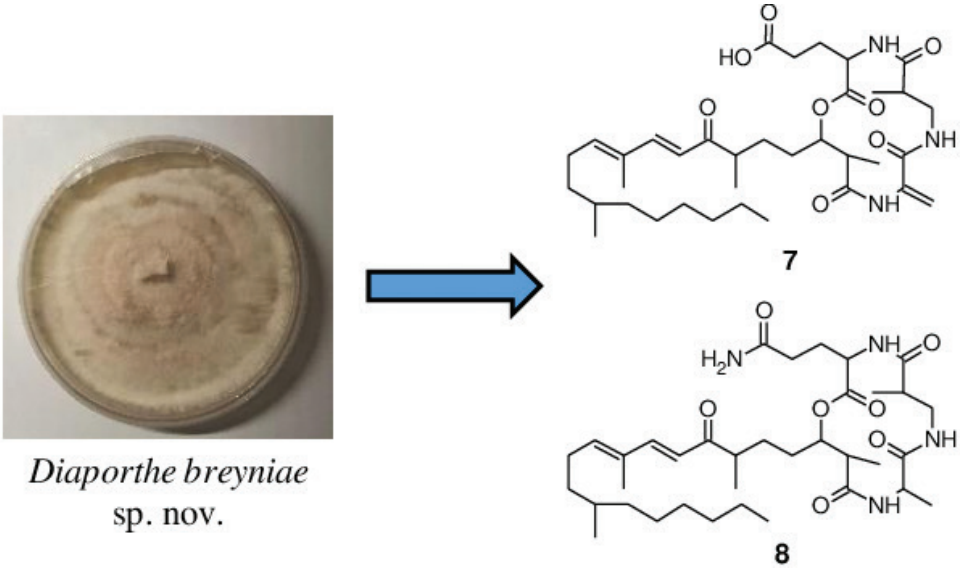

Keywords
Antimicrobial, cytotoxicity, *Diaporthe*, endophytic fungi, one new species, secondary metabolites

Introduction

The genus *Diaporthe* (including their asexual states, which were previously referred to as *Phomopsis* spp.) comprises several hundred species mostly attributed to plant pathogens, non-pathogenic endophytes, or saprobes in terrestrial host plants (Chepkirui and Stadler 2017; Xu et al. 2021). The term "endophytic fungi" herein refers to a group of microorganisms that inhabit the internal parts of a plant, but typically cause no apparent symptoms of disease in the host plant (Stone et al. 2000). Fungal endophytes belonging to the genus *Diaporthe* have been widely investigated by natural product chemists and have proven to be a rich source of novel organic compounds with interesting biological activities and a high level of chemical diversity (Chepkirui and Stadler 2017). They have been shown to predominantly produce polyketides, but PKS/NRPS-derived hybrids like cytochalasins have also been frequently reported from *Diaporthe* (Jouda et al. 2016; Chepkirui and Stadler 2017). Initially, cytochalasins have been discovered for their potent cytotoxic effects, which are due to their interference with the actin cytoskeleton (Yahara et al. 1982) and have been targeted primarily as anticancer agents. However, not all cytochalasins are equally active on actin (Kretz et al. 2019), and they were even found to significantly inhibit biofilm formation of an important human pathogenic bacterium (Yuyama et al. 2018). The current paper supports the activities of an interdisciplinary consortium that aims at exploring the

chemical space of the cytochalasins, in order to establish structure-activity relationships (SAR) and systematically explore their utility for application in various medical applications. Owing to the structural complexity of cytochalasins, their total synthesis remains tedious and requires several reaction steps with relatively low final yields (Zaghouani et al. 2016; Long et al. 2018). Moreover, most of the compounds that were reported previously have not been studied thoroughly for their biological effects; hence, it is worth obtaining them from the fungal producer organisms by *de novo* isolation and characterization.

We have recently isolated and studied a new endophytic species of *Diaporthe* from the twigs of *Breynia oblongifolia*. We noted prominent antimicrobial effects in the extracts derived from this strain and decided to study its secondary metabolites. The current paper includes the description of the new species *D. breyniae* sp. nov., and reports details on the isolation and structure elucidation of its secondary metabolites, as well as an account of their biological properties.

Materials and methods

Fungal isolation

The fungus was isolated from fresh twigs of an apparently healthy plant belonging to *Breynia oblongifolia* in Kala Mountain (Yaoundé, Cameroon). Fresh twigs (5 × 5 cm length) of *Breynia oblongifolia* were thoroughly washed with running tap water, then disinfected in 75% ethanol for 1 min, in 3% sodium hypochlorite (NaClO) for 10 min, and finally in 75% ethanol for 30 s. These twigs were then rinsed three times in sterile distilled water and dried on sterile tissue paper under a laminar flow hood. Small segments of the twigs were transferred to Petri dishes containing potato dextrose agar (PDA, HiMedia, Mumbai, India) supplemented with 100 mg/mL penicillin and 100 µg/mL streptomycin sulphate and incubated at 28 °C. After 10 days, fungal colonies were examined and hyphal tips were transferred to PDA using a sterile needle and incubated at 28 °C.

Herbarium type material and the ex-type strain of the new species are maintained at the collection of the Westerdijk Fungal Biodiversity Institute (CBS), Utrecht, the Netherlands.

Phenotypic study

For cultural characterization, the isolate was grown for 15 days on malt extract agar (MEA; HiMedia, Mumbai, India), oatmeal agar (OA; Sigma-Aldrich, St. Louis, Missouri, USA), and PDA at 21 °C in darkness (Guarnaccia et al. 2018). Color notations in parentheses are taken from the color chart of The Royal Horticultural Society London (1966). The fungus was grown in 2% tap water agar supplemented with sterile pine needles (PNA; Smith et al. 1996) to induce sporulation.

Molecular study

DNA of the fungus was extracted and purified directly from colony growing in yeast malt agar (YM agar; malt extract 10 g/L, yeast extract 4 g/L, D-glucose 4 g/L, agar 20 g/L, pH 6.3 before autoclaving), following the Fungal gDNA Miniprep Kit EZ-10 Spin Column protocol (NBS Biologicals, Cambridgeshire, UK). The amplification of the ITS, *cal*, *his3*, *tef1* and *tub2* loci were performed according to White et al. (1990) (ITS), Carbone and Kohn (1999) (*cal* and *tef1*), Glass and Donaldson (1995) (*his3* and *tub2*) and Crous et al. (2004) (*his3*). PCR products were purified and sequenced using Sanger Cycle Sequencing method at Microsynth Seqlab GmbH (Göttingen, Germany), and the consensus sequences obtained employing the de-novo assembly feature of the Geneious 7.1.9 (http://www.geneious.com, Kearse et al. 2012) program package using a forward and reverse read.

In order to restrict the phylogenetic inference to the relevant species to compare with, a first phylogenetic analysis was carried out based on the combination of the five loci sequences (ITS, *cal*, *his3*, *tef1*, *tub2*) of our isolate and a selection of sequence data derived from type material or reference strains from all *Diaporthe* spp. available in NCBI. Each locus was aligned separately using MAFFT v. 7.017 (algorithm G-INS-I, gap open penalty set to 1.53, offset value 0.123 with options set for automatically determining sequence direction automatically and more accurately) as available as a Geneious 7.1.9 plugin (Katoh and Standley 2013) and manually adjusted in MEGA v. 10.2.4 (Kumar et al. 2018). Alignment errors were minimized by using gblocks (Talavera and Castresana 2007); with options set for allowed block positions 'with half', minimum length of a block set to 5 and a maximum of 10 contiguous nonconserved positions) and concatenated by employing the phylosuite v 1.2.2 program package (Zhang et al. 2020). Maximum-Likelihood tree inference followed using IQTree V2.1.3 (Minh et al. 2020) preceded by calculation and automatic selection of the appropriate nucleotide exchange model using ModelFinder (Chernomor et al. 2016; Kalyaanamoorthy et al. 2017) based on Bayesian inference criterion. Bootstrap support was calculated by parallelizing 10 independent maximum-likelihood (ML) tree searches with 100 bootstrap replicates each to minimize computational burden. The total 1000 bootstrap replicates were consequently mapped onto the ML tree with the best (highest) ML score. After selection of the core group related to the sequences derived from *D. breyniae* sp. nov., a second phylogenetic analysis was performed including all five sequenced loci, using *D. amygdali* CBS 126679^{T} and *D. eres* CBS 138594^{T} as outgroups. Sequence alignment and curation steps were identical, with exemption of a manual curation instead of employing automatic filtering for misaligned alignment sections using gblocks. ML trees using the supermatrix and single loci, respectively, were inferred using IQTree 2.1.3 with ModelFinder to determine optimal substitution models for each loci and partition, using 1000 bootstrap replicates to assign statistical support. The clade in which the sequences of the novel strain clustered, was checked visually for congruence among the single locus trees. Concurrently, a second tree was

inferred following a Bayesian approach using MrBayes 3.2.7a (Ronquist et al. 2012) with nucleotide substitution models previously determined using PartitionFinder2 (Lanfear et al. 2016, options set for unlinked partitions, BIC, restricting models for Bayesian inference) and concatenated in Phylosuite V.1.2.2. Bayesian inference was done in Mr. Bayes v. 3.2.7 (Ronquist et al. 2012), using Markov Chain Monte Carlo (MCMC) with four incrementally heated chains (temperature parameter set to 0.15), starting from a random tree topology. Generations were set to 100.000.000 with convergence controlled by average standard deviation of split frequencies arriving below 0.01. Trees were sampled every 1000 generations with the first 25% of saved trees treated as "burn-in" phase. Posterior probabilities were mapped using the remaining trees. Bootstrap support (bs) ≥ 70 and posterior probability values (pp) ≥ 0.95 were considered significant (Alfaro et al. 2003). The sequences generated in this study are deposited in GenBank (Table 1) and the alignments used in the phylogenetic analysis are included in Supplementary material. Sequences retrieved from GenBank are indicated in Table 1 and Suppl. material 1: S4.

Chromatography and spectral methods

Electrospray ionization mass (ESIMS) spectra were recorded with an UltiMate 3000 Series uHPLC (Thermo Fischer Scientific, Waltman, MA, USA) utilizing a C18 Acquity UPLC BEH column (2.1 × 50 mm, 1.7 µm; Waters, Milford, USA) connected to an amaZon speed ESI-Iontrap-MS (Bruker, Billerica, MA, USA). HPLC parameters were set as follows: solvent A: H_2O + 0.1% formic acid, solvent B: acetonitrile (ACN) + 0.1% formic acid, gradient: 5% B for 0.5 min increasing to 100% B in 19.5 min, then isocratic condition at 100% B for 5 min, a flow rate of 0.6 mL/min, and Diode-Array Detection (DAD) of 210 nm and 190–600 nm.

High-resolution electrospray ionization mass spectrometry (HR-ESIMS) spectra were recorded with an Agilent 1200 Infinity Series HPLC-UV system (Agilent Technologies, Santa Clara, USA; column 2.1 × 50 mm, 1.7 µm, C18 Acquity UPLC BEH (waters), solvent A: H_2O +0.1% formic acid; solvent B: ACN + 0.1% formic acid, gradient: 5% B for 0.5 min increasing to 100% B in 19.5 min and then maintaining 100% B for 5 min, flow rate 0.6 mL/min, UV/Vis detection 200–640 nm) connected to a MaXis ESI-TOF mass spectrometer (Bruker) (scan range 100–2500 *m/z*, capillary voltage 4500 V, dry temperature 200 °C).

Optical rotations were recorded in methanol (Uvasol, Merck, Darmstadt, Germany) by using an Anton Paar MCP-150 polarimeter (Seelze, Germany) at 20 °C. UV/Vis spectra were recorded using methanol (Uvasol, Merck, Darmstadt, Germany) with a Shimadzu UV/Vis 2450 spectrophotometer (Kyoto, Japan). ECD spectra were obtained on a J-815 spectropolarimeter (JASCO, Pfungstadt, Germany). Nuclear magnetic resonance (NMR) spectra were recorded at a temperature of 298 K with an Avance III 500 spectrometer (Bruker, Billerica, MA/USA, ^{1}H-NMR: 500 MHz and ^{13}C-NMR: 125 MHz) and an Ascend 700 spectrometer with 5 mm TCI cryoprobe (Bruker, Billerica, MA/USA, ^{1}H-NMR: 700 MHz and ^{13}C-NMR: 175 MHz).

Table 1. Isolated and reference strains of *Diaporthe* included in this study. # GenBank accession numbers in **bold** were newly generated in this study. The taxonomic novelty is indicated in ***bold italic***.

Species	Isolates[1]	GenBank accession numbers[2]					References
		ITS	*tub2*	*his3*	*tef1*	*cal*	
Diaporthe acaciarum	CBS 138862^T	KP004460	KP004509	KP004504	-	-	Crous et al. (2014)
D. acericola	MFLUCC 17-0956^T	KY964224	KY964074	-	KY964180	KY964137	Dissanayake et al. (2017)
D. alangii	CFCC 52556^T	MH121491	MH121573	MH121451	MH121533	MH121415	Yang et al. (2018)
D. ambigua	CBS 114015^T	KC343010	KC343978	KC343494	KC343736	KC343252	Gomes et al. (2013)
D. amygdali	CBS 126679^T	KC343022	KC343990	KC343506	KC343748	KC343264	Gomes et al. (2013)
D. angelicae	CBS 111592^T	KC343026	KC343994	KC343511	KC343752	KC343268	Gomes et al. (2013)
D. arctii	CBS 136.25	KC343031	KC343999	KC343515	KC343757	KC343273	Gomes et al. (2013)
D. arezzoensis	MFLU 19-2880^T	MT185503	MT454055	-	-	-	Li et al. (2020)
D. batatas	CBS 122.21	KC343040	KC344008	KC343524	KC343766	KC343282	Gomes et al. (2013)
D. beilharziae	BRIP 54792^T	JX862529	KF170921	-	JX862535	-	Thompson et al. (2015)
D. biguttulata	ICMP 20657^T	KJ490582	KJ490403	KJ490524	KJ490461	-	Huang et al. (2015)
D. breyniae	CBS 148910^T	**ON400846**	**ON409186**	**ON409187**	**ON409188**	**ON409189**	Present study
D. camporesii	JZB 320143^T	MN533805	MN561316	-	-	-	Hyde et al. (2020)
D. caryae	CFCC 52563^T	MH121498	MH121580	MH121458	MH121540	MH121422	Yang et al. (2018)
D. celtidis	NCYU 19-0357^T	MW114346	MW148266	-	MW192209	-	Tennakoon et al. (2021)
D. cerradensis	CMRP 4331^T	MN173198	MW751671	MW751663	MT311685	MW751655	Iantas et al. (2021)
D. chimonanthi	SCHM 3614^T	AY622993					Chang et al. (2005)
D. chinensis	MFLUCC 19-0101^T	MW187324	MW245013	-	MW205017	MW294199	de Silva et al. (2021)
D. chromolaenae	MFLUCC 17-1422^T	MH094275	-	-	-	-	Mapook et al. (2020)
D. cichorii	MFLUCC 17-1023^T	KY964220	KY964104	-	KY964176	KY964133	Dissanayake et al. (2017)
D. cinnamomi	CFCC 52569^T	MH121504	MH121586	MH121464	MH121546	-	Yang et al. (2018)
D. citriasiana	CBS 134240^T	JQ954645	KC357459	MF418282	JQ954663	KC357491	Huang et al. (2013)
D. compacta	LC3083^T	KP267854	KP293434	KP293508	KP267928	-	Gao et al. (2016)
D. convolvuli	CBS 124654	KC343054	KC344022	KC343538	KC343780	KC343296	Gomes et al. (2013)
D. cucurbitae	DAOM 42078^T	KM453210	KP118848	KM453212	KM453211	-	Udayanga et al. (2015)
D. cuppatea	CBS 117499^T	AY339322	JX275420	KC343541	AY339354	JX197414	Van Rensburg et al. (2006)
D. discoidispora	ICMP 20662^T	KJ490624	KJ490445	KJ490566	KJ490503	-	Huang et al. (2015)
D. durionigena	VTCC 930005^T	MN453530	MT276159	-	MT276157	-	Crous et al. (2020)
D. endophytica	CBS 133811^T	KC343065	KC344033	KC343549	KC343791	KC343307	Gomes et al. (2013)
D. eres	CBS 138594^T	KJ210529	KJ420799	KJ420850	KJ210550	KJ434999	Udayanga et al. (2014)
D. fici-septicae	MFLU 18-2588^T	MW114348	MW148268	-	MW192211	-	Tennakoon et al. (2021)
D. fructicola	MAFF 246408^T	LC342734	LC342736	LC342737	LC342735	LC342738	Crous et al. (2019)
D. ganjae	CBS 180.91^T	KC343112	KC344080	KC343596	KC343838	KC343354	Gomes et al. (2013)
D. glabrae	SCHM 3622^T	AY601918	-	-	-	-	Chang et al. (2005)
D. goulteri	BRIP 55657a^T	KJ197290	KJ197270	-	KJ197252	-	Thompson et al. (2015)

Species	Isolates[1]	GenBank accession numbers[2]					References
		ITS	*tub2*	*his3*	*tef1*	*cal*	
D. guangdongensis	ZHKUCC20-0014[T]	MT355684	MT409292	-	MT409338	MT409314	Dong et al. (2021)
D. gulyae	BRIP 54025[T]	JF431299	KJ197271	-	JN645803	-	Thompson et al. (2015)
D. guttulata	CGMCC 3.20100[T]	MT385950	MT424705	MW022491	MT424685	MW022470	Dissanayake et al. (2020)
D. helianthi	CBS 592.81[T]	KC343115	KC344083	KC343599	KC343841	JX197454	Gomes et al. (2013)
D. heterostemmatis	SAUCC 194.85[T]	MT822613	MT855810	MT855581	MT855925	MT855692	Sun et al. (2021)
D. hordei	CBS 481.92	KC343120	KC344088	KC343604	KC343846	KC343362	Gomes et al. (2013)
D. hubeiensis	JZB 320123[T]	MK335809	MK500148	-	MK523570	MK500235	Manawasinghe et al. 2019
D. infecunda	CBS 133812[T]	KC343126	KC344094	KC343610	KC343852	KC343368	Gomes et al. (2013)
D. infertilis	CBS 230.52[T]	KC343052	KC344020	KC343536	KC343778	KC343294	Guarnaccia and Crous (2017)
D. kochmanii	BRIP 54033[T]	JF431295	-	-	JN645809	-	Thompson et al. (2011)
D. kongii	BRIP 54031[T]	JF431301	KJ197272	-	JN645797	-	Thompson et al. (2011)
D. leucospermi	CBS 111980[T]	JN712460	KY435673	KY435653	KY435632	KY435663	Crous et al. (2011c)
D. longicolla	FAU 599[T]	KJ590728	KJ610883	KJ659188	KJ590767	KJ612124	Udayanga et al. (2015)
D. longispora	CBS 194.36[T]	KC343135	KC344103	KC343619	KC343861	KC343377	Gomes et al. (2013)
D. lusitanicae	CBS 123212[T]	KC343136	KC344104	KC343620	KC343862	KC343378	Gomes et al. (2013)
D. machili	SAUCC 194.111[T]	MT822639	MT855836	MT855606	MT855951	MT855718	Huang et al. (2021)
D. manihotia	CBS 505.76	KC343138	KC344106	KC343622	KC343864	KC343380	Gomes et al. (2013)
D. masirevicii	BRIP 57892a[T]	KJ197277	KJ197257	-	KJ197239	-	Thompson et al. (2015)
D. mayteni	CBS 133185[T]	KC343139	KC344107	KC343623	KC343865	KC343381	Gomes et al. (2013)
D. megalospora	CBS 143.27	KC343140	KC344108	KC343624	KC343866	KC343382	Gomes et al. (2013)
D. melonis	CBS 507.78[T]	KC343142	KC344110	KC343626	KC343868	KC343384	Gomes et al. (2013)
D. micheliae	SCHM 3603	AY620820	-	-	-	-	Chang et al. (2005)
D. middletonii	BRIP 54884e[T]	KJ197286	KJ197266	-	KJ197248	-	Thompson et al. (2015)
D. myracrodruonis	URM 7972[T]	MK205289	MK205291	-	MK213408	MK205290	da Silva et al. (2019)
D. neoarctii	CBS 109490	KC343145	KC344113	KC343629	KC343871	KC343387	Gomes et al. (2013)
D. neoraonikayaporum	MFLUCC 14-1136[T]	KU712449	KU743988	-	KU749369	KU749356	Doilom et al. (2017)
D. novem	CBS 127271[T]	KC343157	KC344125	KC343641	KC343883	KC343399	Gomes et al. (2013)
D. ovalispora	ICMP 20659[T]	KJ490628	KJ490449	KJ490570	KJ490507	-	Huang et al. (2015)
D. pachirae	COAD 2074[T]	MG559537	MG559541	-	MG559539	MG559535	Milagres et al. (2018)
D. passifloricola	CBS 141329[T]	KX228292	KX228387	KX228367	-	-	Crous et al. (2016)
D. phaseolorum	CBS 113425	KC343174	KC344142	KC343658	KC343900	KC343416	Gomes et al. (2013)
D. pseudolongicolla	CBS 117165[T]	DQ286285	-	-	DQ286259	-	Petrović et al. (2018)
D. pyracanthae	CBS142384[T]	KY435635	KY435666	KY435645	KY435625	KY435656	Santos et al. (2017)
D. racemosae	CBS 143770[T]	MG600223	MG600227	MG600221	MG600225	MG600219	Marin-Felix et al. (2019)
D. raonikayaporum	CBS 133182[T]	KC343188	KC344156	KC343672	KC343914	KC343430	Gomes et al. (2013)
D. rosae	MFLUCC 17-2658[T]	MG828894	MG843878	-	-	MG829273	Wanasinghe et al. (2018)
D. rosiphthora	COAD 2913[T]	MT311196	-	-	MT313692	MT313690	Pereira et al. (2021)
D. rossmaniae	CAA 762[T]	MK792290	MK837914	MK871432	MK828063	MK883822	Hilário et al. (2020)
D. sackstonii	BRIP 54669b[T]	KJ197287	KJ197267	-	KJ197249	-	Thompson et al. (2015)
D. sambucusii	CFCC 51986[T]	KY852495	KY852511	KY852503	KY852507	KY852499	Yang et al. (2018)

Species	Isolates[1]	GenBank accession numbers[2]					References
		ITS	*tub2*	*his3*	*tef1*	*cal*	
D. schini	CBS 133181[T]	KC343191	KC344159	KC343675	KC343917	KC343433	Gomes et al. (2013)
D. schoeni	MFLU 15-1279[T]	KY964226	KY964109	-	KY964182	KY964139	Dissanayake et al. (2017a)
D. sclerotioides	CBS 296.67[T]	KC343193	KC344161	KC343677	KC343919	KC343435	Gomes et al. (2013)
D. serafiniae	BRIP 55665a[T]	KJ197274	KJ197254	-	KJ197236	-	Thompson et al. (2015)
D. siamensis	MFLUCC 10-0573a	JQ619879	JX275429	-	JX275393	-	Udayanga et al. (2012)
D. sinensis	CGMCC 3.19521[T]	MK637451	MK660447	-	MK660449	-	Feng et al. (2019)
D. sojae	CBS 139282[T]	KJ590719	KJ610875	KJ659208	KJ590762	KJ612116	Udayanga et al. (2015)
D. stewartii	CBS 193.36	FJ889448	-	-	GQ250324	-	Santos et al. (2010)
D. subellipicola	KUMCC 17-0153[T]	MG746632	MG746634	-	MG746633	-	Hyde et al. (2018)
D. subordinaria	CBS 101711	KC343213	KC344181	KC343697	KC343939	KC343455	Gomes et al. (2013)
D. tecomae	CBS 100547	KC343215	KC344183	KC343699	KC343941	KC343457	Gomes et al.(2013)
D. tectonae	MFLUCC 12-0777[T]	KU712430	KU743977	-	KU749359	KU749345	Doilom et al. (2017)
D. tectonendophytica	MFLUCC 13-0471[T]	KU712439	KU743986	-	KU749367	KU749354	Doilom et al. (2017)
D. terebinthifolii	CBS 133180[T]	KC343216	KC344184	KC343700	KC343942	KC343458	Gomes et al. (2013)
D. thunbergiicola	MFLUCC 12-0033[T]	KP715097	-	-	KP715098	-	Liu et al. (2015)
D. tulliensis	BRIP 62248a	KR936130	KR936132	-	KR936133	-	Crous et al. (2015)
D. ueckeri	FAU 656	KJ590726	KJ610881	KJ659215	KJ590747	KJ612122	Huang et al. (2015)
	BRIP 54736j (type of *D. miriciae*)	KJ197283	KJ197263	-	KJ197245	-	Thompson et al. (2015)
D. unshiuensis	CGMCC 3.17569[T]	KJ490587	KJ490408	KJ490529	KJ490466	-	Huang et al. (2015)
D. vexans	CBS 127.14	KC343229	KC344197	KC343713	KC343955	KC343471	Gomes et al.(2013)
D. vitimegaspora	STE-U 2675	AF230749	-	-	-	-	Mostert et al. (2001)
D. vochysiae	LGMF 1583[T]	MG976391	MK007527	MK033323	MK007526	MK007528	Noriler et al. (2019)
D. yunnanensis	CGMCC 3.18289[T]	KX986796	KX999228	KX999267	KX999188	KX999290	Gao et al. (2017)

[1]BRIP: Queensland Plant Pathology Herbarium, Brisbane, Australia; CBS: Westerdijk Fungal Biodiversity Institute, Utrecht, the Netherlands; CGMCC: Chinese General Microbiological Culture Collection Center, Beijing, China; COAD: Culture Collection of Octávio de Almeida Drumond. Universidade Federal de Viçosa, Viçosa, Brasil; FAU: Isolates in culture collection of Systematic Mycology and Microbiology Laboratory; ICMP: International Collection of Micro-organisms from Plants, Auckland, New Zealand; KUMCC: Kumming Institute of Botany, Kumming, China; LGMF, Laboratório de Genética de Microrganismos (LabGeM) culture collection, at the Federal University of Paraná, Brazil; MAFF: Ministry of Agriculture, Forestry and Fisheries, Tokyo, Japan; MFLUCC: Mae Fah Luang University Culture Collection, Chiang Rai, Thailand; SAUCC: Shandong Agricultural University Culture Collection, Shandong, China; STE-U: Department of Plant Pathology, Stellenbosch University, Stellenbosch, South Africa; URM: Culture Collection at the Universidade Federal de Pernambuco, Recife, Brazil; VTCC: Vietnam Type Culture Collection, Center of Biotechnology, Vietnam National University, Hanoi, Vietnam; ZHKUCC: Culture Collection of Zhongkai University of Agriculture and Engineering, Guangzhou, China. [T] indicates type material.

[2]ITS: internal transcribed spacers and intervening 5.8S nrDNA; *tub2*: partial β-tubulin gene; *his3*: partial histone H3 gene; *tef1*: partial elongation factor 1-alpha gene; *cal*: partial calmodulin gene.

Small-scale fermentation and extraction

The fungus was cultivated in three different liquid media (YM 6.3 medium: 10g/mL malt extract, 4g/mL, yeast extract, 4g/mL, D-glucose and pH = 6.3, Q6 ½ medium: 10 g/mL glycerin, 2.5 g/mL D-glucose, 5 g/mL cotton seed flour and pH = 7.2; ZM ½ medium: 5 g/mL molasses, 5 g/mL oatmeal, 1.5 g/mL D-glucose, 4 g/mL saccharose, 4 g/mL mannitol, 0.5 g/mL edamin, ammonium sulphate 0.5 g/mL, 1.5 g/mL calcium carbonate and pH = 7.2) (Chepkirui et al. 2016). A well-grown 14-day-old mycelial culture grown on YM agar was cut into small pieces using a cork borer (7mm), and five pieces used for inoculation of 500 mL Erlenmeyer flasks containing 200 mL of media. The cultures were incubated at 23 °C on a rotary shaker at 140 rpm. The growth of the fungus was monitored by checking the amount of free glucose daily using Medi-Test glucose strips (Macherey Nagel, Düren, Germany). The fermentation was terminated three days after glucose depletion and the biomasses and supernatants were separated via vacuum filtration. Afterwards, the supernatants were extracted with equal amount of ethyl acetate (200 mL) and filtered through anhydrous sodium sulphate. The resulting ethyl acetate extracts were evaporated to dryness *in vacuo* (Rotary Evaporator: Heidolph Instruments GmbH & Co. KG, Schwabach, Germany; pump: Vacuubrand GmbH & Co. KG, Wertheim am Main, Germany) at 40 °C. The mycelia were extracted with 200 mL of acetone in an ultrasonic bath (Sonorex Digital 10 P, Bandelin Electronic GmH & Co. KG, Berlin, Germany) at 40 °C for 30 min, filtered and the organic phase evaporated. The volume of the remaining aqueous phase was adjusted with an equal amount of distilled water and subjected to the same procedure as described for the supernatants.

The small-scale cultivation of *Diaporthe breyniae* was also carried out on YM agar medium and rice solid medium (BRFT, brown rice 28 g as well as 0.1 L of base liquid (yeast extract 1 g/L, di-sodium tartrate di-hydrate 0.5 g/L, KH_2PO_4 0.5 g/L) (Becker et al. 2020a). Briefly, the fungus was grown on a YM agar plate and the mycelia was extracted with 200 mL of ethyl acetate in an ultrasonic water bath at 40 °C for 30 min, filtered and the filtrate evaporated to dryness *in vacuo* at 40 °C. For BFRT medium, three small pieces of the mycelial culture grown on a YM agar plate were inoculated into a 250 ml Erlenmeyer flask containing 100 mL of YM 6.3 medium. The seed culture was incubated at 23 °C under shake condition at 140 rpm. After 5 days, 10 mL of this seed culture were transferred to a 500 mL Erlenmeyer flask containing BRFT medium and incubated for 28 days at 23 °C. Afterwards, extraction of the culture was performed following the same procedure as above mentioned for the mycelia obtained from the liquid cultures.

Scale-up fermentation in shake flask batches and extraction

Preliminary results obtained from small-scale screening suggested that the fungus grew and produced best in ZM ½ medium (Suppl. material 1: Figs S1, S2). Moreover, the extracts obtained from the fungal culture in ZM ½ were active against *Bacillus subtilis*

and *Mucor plumbeus*. Therefore, this medium was selected for scale-up fermentation. Three well-grown 14-day-old YM agar plate of the mycelial culture were cut into small pieces using a 7 mm cork borer and 5 pieces inoculated in 10 × 500 mL Erlenmeyer flasks containing 200 mL of ZM ½ medium. The culture was incubated at 23 °C on a rotary shaker at 140 rpm for 11 days. Fermentation was aborted 3 days after the depletion of free glucose. The mycelia and supernatant from the batch fermentation were separated *via* vacuum filtration. The mycelia were extracted with 3 × 500 mL of acetone in an ultrasonic water bath at 40 °C for 30 min. The extracts were combined and the solvent evaporated *in vacuo* (40 °C). The remaining water phase was subjected to the same procedure as previously described for the mycelial fraction in small-scale extraction, repeating the extraction step 3 times, yielding 955 mg dark brown solid-like extract. The supernatant (2 L) was extracted with equal amount of ethyl acetate and filtered through anhydrous sodium sulphate. The resulting ethyl acetate extract was evaporated to dryness *in vacuo* to afford 251 mg of extract.

Isolation of secondary metabolites

The mycelial and the supernatant extracts from shake flask batch fermentation dissolved in methanol were centrifuged by means of a centrifuge (Hettich Rotofix 32 A, Tuttlingen, Germany) for 10 min at 4000 rpm. Afterwards, the mycelia and supernatant extracts were fractionated separately using preparative reverse phase HPLC (Büchi, Pure C-850, 2020, Switzerland). VP Nucleodur 100-5 C18ec column (150 × 40 mm, 7 µm: Machery-Nagel, Düren, Germany) was used as stationary phase. Deionized water (Milli-Q, Millipore, Schwalbach, Germany) supplemented with 0.1% formic acid (FA) (solvent A) and acetonitrile (ACN) with 0.1% FA (solvent B) were used as the mobile phase. The elution gradient used for fractionation was 5–35% solvent B for 20 min, 35–80% B for 30 min, 80–100% B for 10 min and thereafter isocratic condition at 100% solvent B for 15 min. The flow rate was set to 30 mL/min and UV detection was carried out at 210, 320 and 350 nm. For the supernatant extract, 13 fractions (F1-F13) were selected according to the observed peaks, and further analysis of the fractions using HPLC-MS revealed that four of the obtained fractions constituted pure compounds. Using the same elution conditions as mentioned, the mycelia extract afforded 17 fractions (F1–F17) selected from the observed peaks. HPLC-MS analysis of the obtained fractions revealed that seven fractions constituted pure compounds. The compounds obtained from mycelial and supernatant extracts were combined according to their respective HPLC-ESIMS retention time and molecular weight. Compound **1** (55.2 mg, t_R = 7.80 min) was obtained from both the mycelium and supernatant extracts as well as compounds **2** (10.9 mg, t_R = 6.27 min), **3** (2.6 mg, t_R = 11.42 min) and **4** (5.6 mg, t_R = 9.49 min). Compounds **5** (3.6 mg, t_R = 13.46 min), **11** (0.7 mg, t_R = 12.11 min) and **12** (2.0 mg, t_R = 3.83 min) were only isolated from the mycelial extract. Fractions F4 from both the mycelium and supernatant extracts were combined and purified using an Agilent Technologies 1200 Infinity Series semi-

preparative HPLC instrument (Waldbronn, Germany). The elution gradient used was 20–30% solvent B for 5 min followed by isocratic condition at 30% B for 25 min and thereafter increased gradient from 30–100% B for 5 min. VP Nucleodur 100-5 C18ec column (250 × 10 mm, 5 µm: Machery-Nagel, Düren, Germany) was used as stationary phase and the flow rate was 3 mL/min. These fractions afforded compound **13** (2.34 mg, t_R = 5.13 min). Fractions F13 and F14 from the mycelial extract were combined with F12 from the supernatant as they contained the same compounds. The pooled fractions were purified by preparative reverse phase HPLC (Büchi, Pure C-850, 2020, Switzerland). VP Nucleodur 100-5 C18ec column (250 × 21 mm, 5 µm: Machery-Nagel, Düren, Germany) was used as stationary phase with a flow rate of 15 mL/min and an elution gradient of 5–70% solvent B for 5 min, followed by isocratic conditions at 70% B for 25min, and thereafter increased gradient from 70–100% B for 5 min. These fractions afforded compound **9** (10.5 mg, t_R = 13.02 min) and sub-fraction G1. Sub-fraction G1 was further purified using an Agilent Technologies 1200 Infinity Series semi-preparative HPLC with the elution gradient starting from 65–70% B for 5 min followed by isocratic condition at 70% B for 25 min and thereafter increased gradient from 70–100% B for 5 min to afford compounds **7** (1.4 mg, t_R = 13.91 min) and **8** (0.52 mg, t_R = 13.56 min). Fraction F15 from the mycelium were also purified using the same instrument and same elution conditions as described for sub-fraction G1. This fraction afforded compounds **6** (1.1 mg, t_R = 14.02 min) and **10** (1.7 mg, t_R = 13.58 min).

Note: The given retention times were obtained from HPLC-ESIMS following the HPLC parameters as described in the general experimental procedures.

Antimicrobial assay

The antifungal and antibacterial activities (Minimum Inhibition Concentration, MIC) of all extracts obtained from small-scale fermentation were determined in serial dilution assays as described previously (Chepkirui et al. 2016; Becker et al. 2020b) against *Bacillus subtilis*, *Candida tenuis*, *Escherichia coli and Mucor plumbeus*. The assays were carried out in 96-well microtiter plates in YM 6.3 medium for filamentous fungi and yeast and MHB medium (Müller-Hinton Broth: SN X927.1, Carl Roth GmbH, Karlsruhe, Germany) for bacteria. Starting concentration for all extracts were 300 µg/mL. In addition, the antimicrobial activity of the isolated pure compounds was also assessed as previously described (Matio Kemkuignou et al. 2020) against a panel of bacteria and fungi including *Pichia anomala* DSM 6766, *Schizosaccharomyces pombe* DSM 70572, *Mucor hiemalis* DSM 2656, *Candida albicans* DSM 1665, and *Rhodotorula glutinis* DSM 10134 for fungal microorganisms, *Bacillus subtilis* DSM 10, *Staphyloccocus aureus* DSM 346 and *Mycobacterium smegmatis* ATCC 700084 for Gram-positive bacteria, *Acinetobacter baumannii* DSM 30008, *Chromobacterium violaceum* DSM 30191, *Escherichia coli* DSM 1116 and *Pseudomonas aeruginosa* for Gram-negative bacteria. Starting concentration for tested compounds was adjusted to 66.7 µg/mL.

Cytotoxicity assay

The *in vitro* cytotoxicity (IC_{50}) of the isolated metabolites against several mammalian cell lines (human endocervical adenocarcinoma KB 3.1, mouse fibroblasts L929, squamous cancer A431, breast cancer MCF-7, lung cancer A549, ovary cancer SK-OV-3 and prostate cancer PC-3) was determined by colorimetric tetrazolium dye MTT assay using epothilone B as a positive control in accordance to our previously reported experimental procedure (Becker et al. 2020b).

Results and discussion

Phylogenetic study

The lengths of the fragments of the first phylogenetic inference using the five previously mentioned loci used in the combined dataset for the tree including all *Diaporthe* spp. were 454 bp (ITS), 318 bp (*cal*), 296 bp (*his3*), 153 bp (*tef1*) and 487 bp (*tub2*), comprising in total 341 taxa. The length of the final alignment was 1708 bp. The inferred phylogeny with the best maximum likelihood score with bootstrap support (bs) values mapped onto branch bipartitions is shown in Suppl. material 1: Fig. S100. The here studied strain was located in a clade with 92% bs including 341 taxa, including species belonging to the *D. sojae* complex. A second molecular phylogeny was inferred including sequences of the same loci, but restricted to the aforementioned clade, including 98 taxa. The lengths of the fragments used in the combined dataset were 572 bp (ITS), 449 bp (*cal*), 373 bp (*his3*), 452 bp (*tef1*) and 862 bp (*tub2*), totaling 2708 bp for the final alignment. Fig. 1 shows the consensus ML tree, including bs and Bayesian posterior probability (pp) values at the nodes. Our strain was located in an independent branch distant from other species of *Diaporthe*, demonstrating that this represented a new species, which is introduced here as *D. breyniae*. Unfortunately, the new species lacked sporulation in all media tested in the present study. Therefore, the introduction of it is based only on molecular data.

Taxonomy

Diaporthe breyniae **Y. Marín & C. Lamb., sp. nov.**
MycoBank No: 843243

Etymology. Name refers to the host genus that this fungus was isolated from, *Breynia*.

Description. Not sporulated. *Diaporthe breyniae* differs from its closest phylogenetic neighbour, *D. durionigena* by unique fixed alleles in three loci based on alignments of the separate loci included in the supplementary material: ITS positions 93 (indel), 159 (G), 436 (T), 437 (C), 451 (G), 453 (A), 485 (C); *tef1* positions 46 (A), 62 (G), 80 (T), 100 (G), 146 (T), 274 (indel), 304 (A), 310 (G), 313 (C), 339 (T), 343 (A), 385 (G); *tub2* positions 393 (A), 402 (indel), 426 (A), 565 (C), 675 (T), 713 (G), 770 (T).

Figure 1. ML (lnL = -28100.2019) phylogram obtained from the combined ITS, *cal*, *his3*, *tef1* and *tub2* sequences of our strain and related *Diaporthe* spp. *Diaporthe amygdali* CBS 126679^{T} and *D. eres* CBS 138594^{T} were used as an outgroup. Bootstrap support values ≥ 70/Bayesian posterior probability scores ≥ 0.95 are indicated along branches. Branch lengths are proportional to distance. New taxon is indicated in bold. Type material of the different species is indicated with ^{T}.

Culture characters. Colonies on PDA reaching 55–70 mm in 2 weeks, greyed yellow (161A) with a white ring and transparent margins, lobate, cottony, raised, margins filamentous to fimbriate; reverse greyed yellow (161A–D) with transparent margins. Colonies on MEA covering the surface of the Petri dish in 2 weeks, white with greyed yellow center (161A), velvety to cottony, flat to raised in some zones, margins filamentous to fimbriate; reverse greyed yellow (162A–B). Colonies on OA covering the surface of the Petri dish in 2 weeks, white with greyed yellow ring (161D), velvety, flat, margins filamentous to fimbriate; reverse grey brown (199D).

Specimen examined. Cameroon, Kala mountain, on leaves of *Breynia oblongifolia*, 02 Jan. 2019, *S.C.N. Wouamba* (holotype: CBS H-24920, culture ex-type CBS 148910 = STMA 18284).

Notes. *Diaporthe breyniae* is introduced based only on molecular data since sporulation could not be induced in any media used. This species is located in a well-supported clade (97% bs / 1 pp) together with *D. durionigena*, *D. passifloricola*, *D. rosae*, *D. thunbergiicola*, *D. ueckeri* and *D. vochysiae*. The latter species has only been reported from Brazil occurring on different hosts, i.e. *Stryphnodendron adstringens* (Fabaceae, Fabales) and *Vochysia divergens* (Vochysiaceae, Myrtales) (Noriler et al. 2019). *Diaporthe durionigena* has been only isolated from *Durio zibethinus* (Malvaceae, Malvales) in Vietnam (Crous et al. 2020, 2021). *Diaporthe passifloricola* has been found on *Passiflora foetida* (Passifloraceae, Malpighiales) and *Citrus* spp. (Rutaceae, Sapindales) in China and Malaysia (Crous et al. 2016; Chaisiri et al. 2021; Dong et al. 2021), while *D. rosae* has been isolated from *Rosa* sp. (Rosaceae, Rosales), *Magnolia champaca* (Magnoliaceae, Magnoliales) and *Senna siamea* (Fabaceae, Fabales) in Thailand (Perera et al. 2018; Wanasinghe et al. 2018). *Diaporthe ueckeri* (syn. *D. miriciae*, Gao et al. 2016) has been reported in Australia, Colombia and the USA, on *Cucumis melo* (Cucurbitaceae, Cucurbitales), *Glycine max* (Fabaceae, Fabales) and *Helianthus annuus* (Asteraceae, Asterales) (Thompson et al. 2015; Udayanga et al. 2015; López-Cardona et al. 2021). *Diaporthe thunbergiicola* has been only isolated from *Thunbergia laurifolia* (Acanthaceae, Lamiales) in Thailand (Liu et al. 2015). The new species *D. breyniae* is the only of these species reported on *Breynia* (Phyllanthaceae, Malpighiales) in Africa. In fact, to the best of our knowledge, this is the first species of *Diaporthe* reported in Cameroon and occurring in this host.

Structure elucidation of compounds 1–13

Cultivation trials carried out on *Diaporthe breyniae* in different culture media including YM 6.3, Q6 ½, ZM ½, rice solid and YM agar highlighted its potential for producing secondary metabolites. During antimicrobial screening of the extracts, the fungus revealed significant antifungal and antibacterial activity against *Mucor hiemalis* and *Bacillus subtilis* respectively, especially when cultured in ZM ½ medium, encouraging more detailed examination. Investigation into the chemistry of *Diaporthe breyniae* led to the isolation of two new secondary metabolites (**7**, **8**) together with eleven known compounds (**1**–**4**, **5**, **6**, **9**–**13**) from the EtOAc extracts of a 2 L scale-up ZM ½ liquid

medium of the fungus (Fig. 2). The structure elucidation of **1–13** was determined by detailed spectroscopic analysis of their 1D and 2D NMR data in combination with their HR-ESIMS data.

HR-ESI(+)MS and NMR spectroscopic analysis identified compounds **1–3** as cytochalasin H (**1**) (Suppl. material 1: Figs S3–S10) (Beno et al. 1977; Shang et al. 2017), deacetylcytochalasin H or cytochalasin J (**2**) (Suppl. material 1: Figs S11–S17) (Cole et al. 1981; Shang et al. 2017) and cytochalasin RKS-1778 (**3**) (Suppl. material 1: Figs S18–S24) (Kakeya et al. 1997) respectively. The absolute configuration of cytochalasins H (**1**) and J (**2**) was confirmed by comparing their optical rotation values ($[\alpha]^{20}_{D}$ +55.7 (c 0.158, MeOH) for 1 and $[\alpha]^{20}_{D}$ +35.3 (c 0.394, MeOH) for **2**) and ECD spectrum (Fig. 3) with those reported in the literature (Shang et al. 2017; Ma et al. 2021). The literature reports only the relative configuration of compound **3** (*rel-* (3*S*, 4*R*, 5*S*, 8*S*, 9*S*, 13*E*, 16*S*, 18*R*, 19*E*, 21*R*)) (Kakeya et al. 1997), therefore, its absolute configuration was investigated by comparison of its ECD spectrum with that of cytochalasins H (**1**) and J (**2**) (Fig. 3). The ECD spectrum of **3** showed negative (~ 200 nm) cotton effect, the shape of which matched with that of compounds **1** and **2**. Thus, the hitherto unestablished absolute configuration of cytochalasin RKS-1778 (**3**) was confirmed to be 3*S*, 4*R*, 5*S*, 8*R*, 9*R*, 13*E*, 16*S*, 18*R*, 19*E*, 21*R*.

HR-ESI (+) MS analysis of **4** isolated as a yellowish oil afforded pseudo-molecular ion peaks $[M+H]^+$ at *m/z* 436.2852 and $[M+Na]^+$ at *m/z* 458.2665 attributed to the molecular formula $C_{28}H_{37}NO_3$ (11 degrees of unsaturation). Comparison of the 1D and 2D NMR spectroscopic data for 4 (DMSO-d_6) with those for **3** (Table 2) revealed that both compounds are closely related, with compound **4** being the deacetylated derivative of **3**. This was confirmed on the ^{1}H NMR spectrum of compound **4** by the absence of the methyl group H_3-25 and on its ^{13}C NMR spectrum by the absence of both C-24 carbonyl group and C-25 methyl group as visible on the NMR data recorded for compound **3** (Table 2). The relative configuration of compound **4** was determined by analysis of the coupling constants and NOESY correlations. The E-geometry of the $\Delta^{13,14}$ and $\Delta^{19,20}$ double bonds in the macrocyclic ring was determined based on the large coupling constants J = 15.3 and 16.7 Hz observed between H-13 and H-14 and between H-19 and H-20 respectively. The small coupling constant J = 4.4 Hz observed between H-4 and H-5 confirmed their *cis* relationship (Kakeya et al. 1997). The NOESY spectrum arbitrarily suggested *α*-orientation of H-3, H-11, H-21 and H-23 based on the observed correlations between H-3/H-11, H-20/H-21 and H-20/H-23,while the *β*-orientation of H-4, H-5, H-8, H-16, 18-OH and 21-OH were apparent from a network NOESY correlations between H-4/H-5, H-5/H-8, H-8/21-OH, 21-OH/H-19, H-19/H-16 and H-16/18-OH (Fig. 4). These correlations allowed the assignment of the relative configuration of compound **4** as either *rel-* (3*S*, 4*R*, 5*S*, 8*S*, 9*S*, 13*E*, 16*S*, 18*R*, 19*E*, 21*R*) or *rel-* (3*R*, 4*S*, 5*R*, 8*R*, 9*R*, 13*E*, 16*R*, 18*S*, 19*E*, 21*S*). In addition, the optical rotation value of **4** ($[\alpha]^{20}_{D}$ -17.6 (c 0.278, MeOH)) approximating that reported in the literature for **3** ($[\alpha]^{20}_{D}$ -20 (c 0.05, MeOH, Kakeya et al. 1997) revealed that both compounds are levorotatory, and this suggested the stereochemistry of **4** to be identical to that of **3**. The latter assumption was confirmed

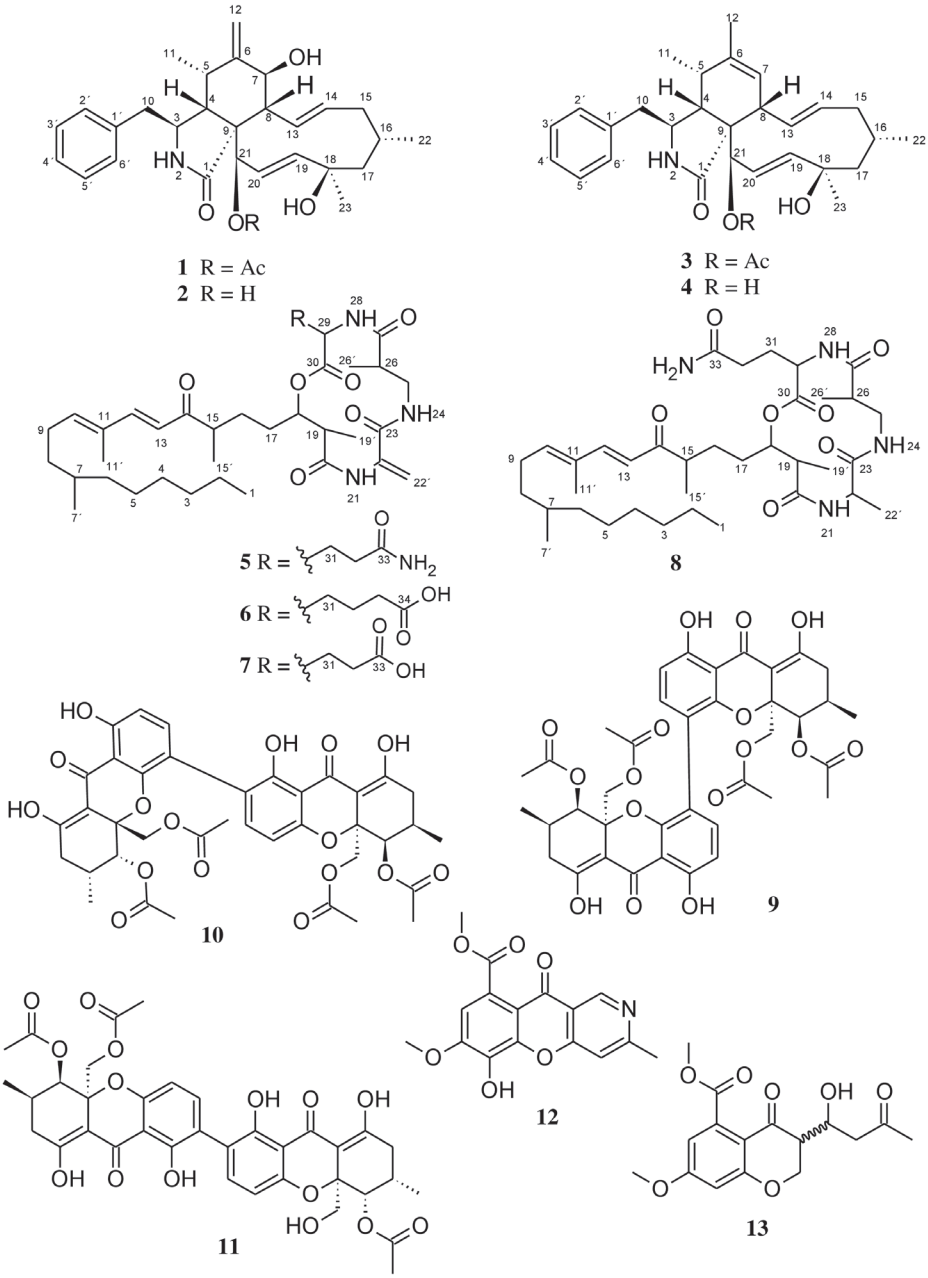

Figure 2. Chemical structures of compounds **1**–**13** isolated from *Diaporthe breyniae*.

by comparing the ECD spectrum of **4** with those of compounds **1**, **2** and **3**. The same negative Cotton effect (~200 nm) observed for all those compounds unambiguously certified the absolute configuration of compound **4** established as 3*S*, 4*R*, 5*S*, 8*S*, 9*S*,

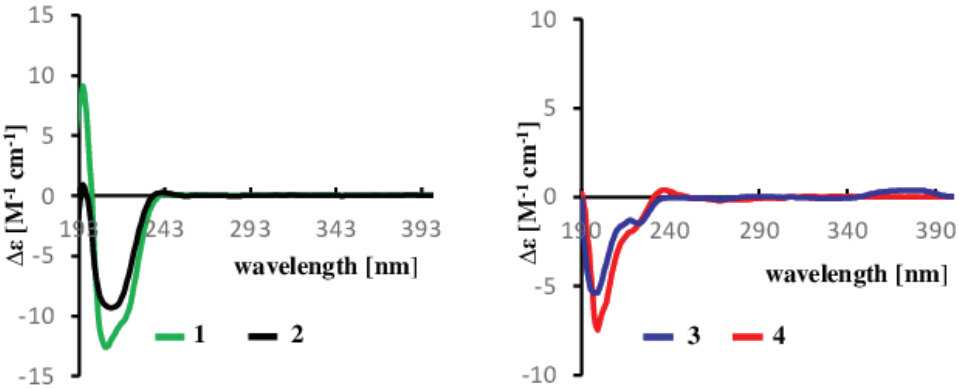

Figure 3. ECD spectra of compounds **1**–**4** in MeOH.

13*E*, 16*S*, 18*R*, 19*E*, 21*R*. Thus, the structure of **4** was determined. This compound was regarded new while the current study has been under review, but concurrently it was published as phomopchalasin N by Chen et al. (2022). Interestingly, the authors also isolated it from a member of the genus *Diaporthe*, but inadvertently referred to their producer organism under the outdated name "*Phomopsis*". We have decided to leave our complete data on the structure elucidation in the manuscript, so they can be compared with those of Chen et al. (2022) by other scientists, but the compounds are indeed identical.

Compounds **5** and **6** were readily identified as the known fusaristatins A and B respectively, after careful analysis of their HR-ESI (+) MS and NMR spectroscopic data (Suppl. material 1: Figs S34–S47). Fusaristatins A (**5**) and B (**6**) were first reported in 2007 from an endophytic *Fusarium* sp. (Shiono et al. 2007) and so far, only fusaristatin A (**5**) has been isolated from *D. phaeseolorum* and *D. longicolla* (syn: *Phomopsis longicolla*) (Santos et al. 2011; Choi et al. 2013; Cui et al. 2017). Therefore, this is the first report for the isolation of fusaristatin B (**6**) from the genus *Diaporthe*. In addition, two new derivatives of fusaristatin A (**7**, **8**) were isolated from *Diaporthe breyniae* and their structures were established by intensive analysis of their 1D and 2D NMR spectroscopic data in combination with HR-ESIMS data and by comparison with the data reported in the literature for fusaristatins A (**5**) and B (**6**) (Shiono et al. 2007).

The molecular formula of compound **7,** isolated as a colorless oil, was determined to be $C_{36}H_{57}N_3O_8$ from the HR-ESIMS (positive mode) which showed pseudo-molecular ion peaks $[M+H]^+$ at *m/z* 660.4219 and $[M+Na]^+$ at *m/z* 682.4024, indicating 10 degrees of unsaturation. Inspection of the molecular formula of **7** ($C_{36}H_{57}N_3O_8$) in comparison to that of **5** ($C_{36}H_{58}N_4O_7$) suggested that an amino group ($-NH_2$) in compound **5** could probably have been replaced by a hydroxyl group (-OH) in compound **7**. Intensive analysis of 1D and 2D NMR spectroscopic data (C_5D_5N) of compound **7** in comparison to that of **5** indicated that most signals in **7** were the same as those for **5** (Table 3), implying that **7** and **5** are closely related. The only difference was observed on the ^{1}H NMR spectrum where the signal corresponding to the amino

Table 2. ^{13}C (125 MHz) and ^{1}H-NMR (500 MHz) spectroscopic data (DMSO-d_6, δ in ppm) of compounds **3**, **4**.

	3		**4**	
No.	δ_C, type	δ_H (J in Hz)	δ_C, type	δ_H (J in Hz)
1	174.3, C	-	175.9, C	-
2-NH	-	7.89, s	-	7.57, s
3	53.9, CH	3.16, m	53.8, CH	3.14, q (4.9)
4	50.5, CH	2.02, t (4.1)	50.9, CH	2.47, t (4.4)
5	34.1, CH	2.18, m*	34.3, CH	2.3, m
6	137.3, C	-	137.1, C	-
7	126.8, CH	5.21*	127.4, CH	5.17, br s
8	42.3, CH	3.06 br d (9.9)	40.9, CH	3.04, br d (9.8)
9	55.5, C	-	57.2, C	-
10	44.0, CH_2	2.59, dd (13.2, 7.4) 2.74, dd (13.1, 5.3)	43.6, CH_2	2.65, dd (13.6, 5.2) 2.70, dd (13.6, 5.2)
11	12.8, CH_3	0.64, d (7.2)	13.0, CH_3	0.84, d (7.3)
12	19.2, CH_3	1.62, s	19.3, CH_3	1.63, s
13	129.2, CH	5.73, dd (15.7, 10.1)	129.7, CH	5.66, dd (15.3, 10.1)
14	133.5, CH	5.08, ddd (15.3, 10.9, 4.5)	132.8, CH	5.02, ddd (15.3, 11.0, 4.4)
15	42.1, CH_2	1.57, m* 1.89, br dd (12.4, 4.3)	42.3, CH_2	1.52, q (12.5) 1.84, br dd (12.5, 4.2)
16	27.6, CH	1.69, m	27.7, CH	1.69, m
17	53.1, CH	1.37, br dd (13.6, 3.2) 1.59, m*	53.1, CH_2	1.34, br dd (13.4, 3.3) 1.60, dd (13.6, 3.3)
18	72.1, C	-	72.2, C	-
19	137.3, CH	5.36, dd (16.6, 2.3)	136.2, CH	5.61, dd (16.7, 2.4)
20	125.1, CH	5.71, dd (16.9, 2.4)	130.7, CH	5.76, dd (16.7, 2.4)
21	75.7, CH	5.23*	73.7, CH	3.63, br s
22	25.8, CH_3	0.94, d (7.3)	25.9, CH_3	0.93, d (7.1)
23	31.0, CH_3	1.13, s	31.5, CH_3	1.12, s
24	169.3, C	-	-	-
25	20.2, CH_3	2.18, s	-	-
1′	136.8, C	-	136.9, C	-
2′/6′	129.6, CH (x2)	7.12, d (7.0)	129.8, CH (x2)	7.21*
3′/5′	127.9, CH (x2)	7.29, t (7.5)	127.7, CH (x2)	7.29, t (7.7)
4′	126.0, CH	7.21, t (7.5)	126.0, CH	7.21*
18-OH	-	4.36, s	-	4.17, s
21-OH	-	-	-	4.88, br d (5.6)

*overlapping signals, assignments were supported by HSQC and HMBC

group 34-NH_2 (δ_H 8.34) in compound **5** was absent in compound **7** (Table 3). Moreover, in the HMBC spectrum of **7**, correlations from H-31 to C-30, H-31/H-32 to C-33 suggested the presence of a glutamic acid residue instead of a glutamine residue as observed in **5**. Based on ^{1}H-^{1}H COSY, ^{1}H-^{13}C HSQC and ^{1}H-^{13}C HMBC experiments (Fig. 5), the signals of all protons and carbons in the molecule were unambiguously assigned and compound **7** was identified as a new derivative of fusaristatin A named fusaristatin G.

Compound **8** was obtained as a white amorphous solid. The molecular formula was established as $C_{36}H_{60}N_4O_7$ on the basis of the pseudo-molecular ion peaks $[M+H]^+$ at *m/z* 661.4542 and $[M+Na]^+$ at *m/z* 683.4354 observed in the HR-ESI(+)MS, indicating 9 double bond equivalents. The molecular formula of **8** ($C_{36}H_{60}N_4O_7$) compared to that of **5** ($C_{36}H_{58}N_4O_7$) showed an increase of 2 Da suggesting that a reduction occurred in compound **5** to afford compound **8**. This assumption was confirmed on

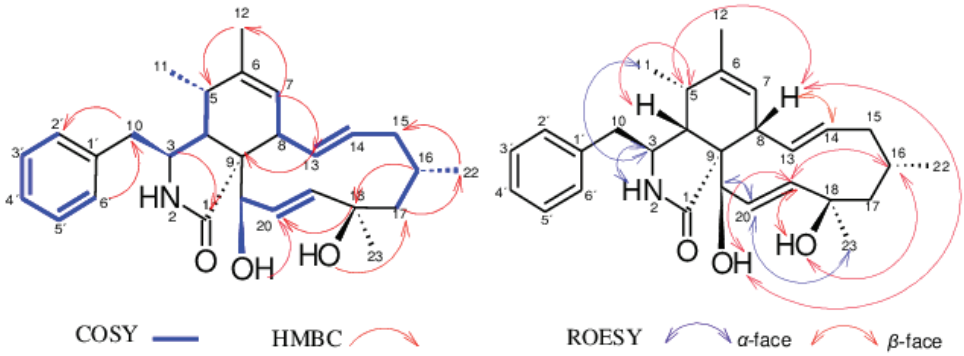

Figure 4. Selected ^{1}H–^{1}H COSY, NOESY and HMBC correlations of 4.

the ^{1}H NMR spectrum of **8** where the signals in the downfield region corresponding to H_a-22′ (δ_H 5.60) and H_b-22′ (δ_H 6.24) as observed in **5** were missing, but instead the signal in the upfield region corresponding to a methyl group H_3-22′ at δ_H 1.65 was recorded (Table 3). Moreover, an additional signal observed on the ^{1}H NMR of **8** attributable to the methine H-22 (δ_H 4.89) further confirmed this assumption, indicating that the reduction of **5** occurred on the $\Delta^{22\text{-}22'}$ double bond to afford **8**. The reduction of the double bond $\Delta^{22\text{-}22'}$ further justified the upfield shift of the nitrogen-bearing proton 21-NH, which resonated at δ_H 8.15 in compound 8 instead of δ_H 10.43 as in compound 5. In the HMBC spectrum, the correlations observed between H-22′ and C-22/C-23, H-22 and C-22′/C-23 confirmed the presence of an alanine residue instead of dehydroalanine residue as previously reported for **5** (Shiono et al. 2007). Finally, the unambiguous assignment of all proton and carbon signals in metabolite **8** was achieved based on ^{1}H-^{13}C HSQC and ^{1}H-^{13}C HMBC experiments, thus identifying compound **8** as a new derivative of fusaristatin A, for which the trivial name fusaristatin H was assigned.

Compounds **9**–**13** were respectively identified as phomoxanthones A (**9**) and B (**10**) (Isaka et al. 2001), dicerandrol B (**11**) (Wagenaar and Clardy 2001), phomochromenone C (**12**) (Ding et al. 2017; Wei et al. 2021), and diaporchromanone C (**13**) (Wei et al. 2021) by comparison of their HR-ESIMS and 1D and 2 D NMR spectroscopic data (Suppl. material 1: Figs S65–S99) with those reported in the literature.

Physico-chemical characteristic of compounds 4, 7 and 8

Phomopchalasin N (**4**): Yellowish oil. $[\alpha]^{20}_{D}$ -17.6 (c 0.278, MeOH), UV (MeOH, c = 0.013 mg/mL) λ_{max} (log ε) 202 (4.32) nm. CD (c = 2.83 × 10^{-3} M, MeOH) λ_{max} (Δε) 200 (-7.66) nm. HR-ESIMS *m/z* 458.2665 $[M + Na]^+$, *m/z* 893.5440 $[2M + Na]^+$, *m/z* 871.5621 $[2M + H]^+$, *m/z* 418.2746 $[M + H - H_2O]^+$, *m/z* 436.2852 $[M + H]^+$ (Calcd for $C_{28}H_{38}NO_3^+$ 436.2846), t_R = 10.47 min. For NMR data (^{1}H: 500 MHz, ^{13}C: 125 MHz, DMSO-d_6), see Table 2.

Fusaristatin G (**7**): colorless oil. $[\alpha]^{20}_{D}$ -8 (*c* 0.1, MeOH), UV (MeOH, c = 0.02 mg/mL) λ_{max} (log ε) 201 (4.21), 283 (3.96) nm. HR-ESIMS *m/z* 682.4024 [M + Na]$^+$, *m/z* 1341.8157 [2M + Na]$^+$, *m/z* 1319.8354 [2M + H]$^+$, *m/z* 642.4102 [M + H

Table 3. ^{13}C and ^{1}H-NMR spectroscopic data (pyridine-d_5, δ in ppm) of compounds **5**, **7**, **8**.

	5[a]		**7**[b]		**8**[b]	
No.	δ_C, type	δ_H (*J* in Hz)	δ_C, type	δ_H (*J* in Hz)	δ_C, type	δ_H (*J* in Hz)
1	14.7, CH_3	0.88*	14.7, CH_3	0.87*	14.5, CH_3	0.87, t (6.9)*
2	23.4, CH_2	1.20~1.31, m*	23.4, CH_2	1.20~1.31, m*	23.1, CH_2	1.20~1.31, m*
3	32.6, CH_2	1.20~1.31, m*	32.6, CH_2	1.20~1.31, m*	32.3, CH_2	1.20~1.31, m*
4	27.7, CH_2	1.20~1.31, m*	27.7, CH_2	1.20~1.31, m*	27.4, CH_2	1.20~1.31, m*
5	30.3, CH_2	1.20~1.31, m*	30.3, CH_2	1.20~1.31, m*	30.1, CH_2	1.20~1.31, m*
6	37.5, CH_2	1.09, m* 1.20-1.31, m*	37.5, CH_2	1.09, m* 1.20~1.31, m*	37.3, CH_2	1.09, m* 1.20~1.31, m*
7	33.2, CH	1.39, m*	33.2, CH	1.40, m*	32.9, CH	1.38, m*
7′	20.0, CH_3	0.88*	20.0, CH_3	0.88*	19.8, CH_3	0.87, d (6.9)*
8	36.8, CH_2	1.20~1.31* 1.40, m*	36.9, CH_2	1.20~1.31, m* 1.40, m*	36.6, CH_2	1.20~1.31, m* 1.40, m*
9	27.2, CH_2	2.19, m*	27.2, CH_2	2.18, m	27.0, CH_2	2.21, m*
10	144.5, CH	6.03, br t (7.4)	144.5, CH	6.03, br t (7.2)	144.3, CH	6.01, t (7.4)
11	133.9, C	-	140.0, C	-	133.9, C	-
11′	12.6, CH_3	1.83, s	12.7, CH_3	1.83, s	12.5, CH_3	1.85, s
12	148.4, CH	7.54, d (15.7)	148.3, CH	7.56, d (15.7)	148.2, CH	7.55, d (15.7)
13	123.7, CH	6.40, d (15.7)	123.8, CH	6.40, d (15.7)	123.6, CH	6.45, d (15.7)
14	203.8, C	-	203.6, C	-	204.1, C	-
15	44.5, CH	2.84, m	44.6, CH	2.80~2.88, m*	44.6, CH	2.88, m
15′	17.7, CH_3	1.10, d (6.9)	17.6, CH_3	1.10, d (6.9)	17.1, CH_3	1.13, d (6.9)
16	28.5, CH_2	1.57, m 1.93~2.00, m*	28.3, CH_2	1.54, m 1.93~2.00, m*	29.1, CH_2	1.66, m 2.04, m*
17	30.3, CH_2	1.87, m 1.93~2.00, m*	30.2, CH_2	1.84, m 1.93~2.00, m*	31.3, CH_2	1.97, m 2.04, m*
18	77.3, CH	5.44, m	77.2, CH	5.48, m	77.6, CH	5.45, m
19	44.6, CH	3.03, quin (7.0)	44.5, CH	3.05, quin (7,0)	45.6, CH	2.95, m
19′	15.8, CH_3	1.30, d (7.0)*	15.9, CH_3	1.33, d (7.3)*	14.9, CH_3	1.35, d (7.3)
20	173.9, C	-	174.0, C	-	173.5, C	-
21-NH	-	10.43, s	-	10.55, s	-	8.15, br s
22	139.6, C	-	139.8, C	-	50.9, CH	4.89, m
22′	114.6, CH_2	5.60, s 6.24, s	114.3, CH_2	5.59, s 6.22, s	17.3, CH_3	1.65, d (7.1)
23	165.2, C	-	165.3, C		173.9, C	-
24-NH	-	7.81, br s	-	7.88, br t (6.1)	-	7.96, br s
25	43.0, CH_2	3.81, dt (13.5, 6.9) 3.92, dt (13.3, 4.9)	43.0, CH_2	3.78, dt (13.5, 6.7) 3.94, m	42.1, CH_2	3.49, dt (13.6, 3.8) 4.04, dt (13.5, 7.9)
26	42.7, CH	2.87, m	42.7, CH	2.92, m	42.8, CH	2.85, m
26′	15.5, CH_3	1.30, d (7.0)*	15.8, CH_3	1.33, d (7.3)*	14.9, CH_3	1.22, d (7.3)
27	175.0, C	-	175.1, C	-	175.4, C	-
28-NH	-	9.06, br d (7.5)	-	9.11, br d (7.7)	-	8.90, br d (7.7)
29	53.6, CH	5.13, dd (14.3, 7.6)	53.4, CH	5.18, m*	53.6, CH	5.06, dd (12.9, 6.2)
30	172.3, C	-	172.4, C	-	172.5, C	-
31	27.6, CH_2	2.63, dt (13.7, 7.0) 2.69~2.77, m*	27.5, CH_2	2.62, dt (13.8, 6.9) 2.71, tt (13.8, 6.9)	27.3, CH_2	2.51, m 2.68~2.74, m*
32	32.8, CH_2	2.69~2.77, m*	32.1, CH_2	2.80~2.88, m*	32.7, CH_2	2.68~2.74, m*
33	175.7, C	-	176.1, C	-	176.7, C	-
34-NH_2	-	8.34, s	-	-	-	8.32, br s

*overlapping signals: assignments were supported by HSQC and HMBC, [a] ^{1}H 500 MH_Z, ^{13}C 125 MHz; [b] ^{1}H 700 MH_Z, ^{13}C 175 MH_Z.

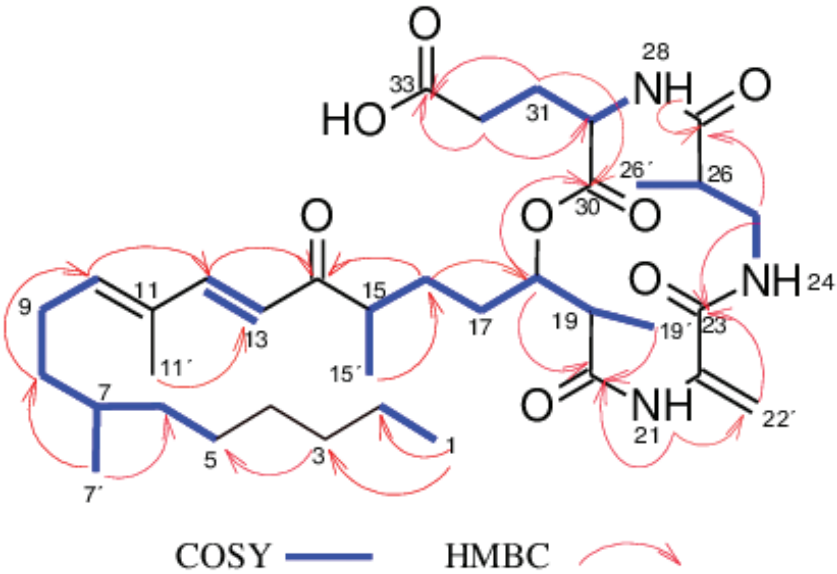

Figure 5. Selected ^{1}H–^{1}H COSY and HMBC correlations of **7**.

- $H_2O]^+$, *m/z* 660.4219 $[M + H]^+$ (Calcd for $C_{36}H_{58}N_3O_8^+$ 660.4218), t_R = 14.80 min. For NMR data (^{1}H: 700 MHz, ^{13}C: 175 MHz, C_5H_5N-d_5), see Table 3.

Fusaristatin H (**8**): White amorphous solid. $[\alpha]^{20}_{D}$ +14 (*c* 0.03, MeOH), UV (MeOH, c = 0.02 mg/mL) λ_{max} (log ε) 201 (4.24), 283 (4.20) nm. HR-ESIMS *m/z* 683.4354 $[M + Na]^+$, *m/z* 1343.8820 $[2M + Na]^+$, *m/z* 1321.9000 $[2M + H]^+$, *m/z* 661.4542 $[M + H]^+$ (Calcd for $C_{36}H_{61}N_4O_7^+$ 661.4535), t_R = 14.46 min. For NMR data (^{1}H: 700 MHz, ^{13}C: 175 MHz, C_5H_5N-d_5), see Table 3.

Biological activity

The extracts obtained from the fungal culture in ZM ½ exhibited activities against *Bacillus subtilis* with MIC values of 75 µg/mL for the supernatant´s extract and 2.3 µg/mL for the mycelial extract. These extracts were also active against *Mucor plumbeus* with respective MIC values of 150 and 37.5 µg/mL. Moreover, the purified compounds **1**–**7**, **9**, **10**, **12**, and **13** were subjected to antimicrobial assays against a panel of bacteria and fungi. The minimum inhibitory concentration (MIC) values showed that all compounds were active against at least one of the tested micro-organisms at concentration of 66.7 µg/mL (Table 4). Overall, the majority of the tested compounds exhibited weak to moderate activity. However, significant activity was noted for phomoxanthones A (**9**) and B (**10**) against *Bacillus subtilis*. Both compounds inhibited the growth of the latter bacterium with a MIC value of 1.7 µg/mL, which turned out to be 5 times stronger than that of oxytetracyclin used as positive control. In addition, their MIC value of 4.2 µg/mL against the Gram-positive bacterium *S. aureus* was

quite considerable in comparison to that of the other tested compounds. This finding concurs well with previously published data which reported the antimicrobial activity of xanthone derivatives isolated from *Diaporthe* spp. (Wagenaar and Clardy 2001; Elsässer et al. 2005; Lim et al. 2010). The antimicrobial activity of dicerandrol B (**11**), a closely related congener of phomoxanthones A (**9**) and B (**10**) was not investigated in the present work due to the low amount of available sample, however, its activity against *B. subtilis* and *S. aureus* has previously been reported (Wagenaar and Clardy 2001). The antimicrobial activity of compound 8 was not assessed due to the paucity of the sample.

The cytotoxicity of all the isolated compounds except **11** was evaluated against a panel of mammalian cell lines. Eight compounds, **1**–**5** and **8**–**10** showed activity in this assay whereas the other isolated metabolites were inactive under test conditions (Table 5). The very significant activity exhibited by compounds **1**–**4** against all tested cancer cell lines were in agreement with previous studies which have reported cytochalasins as potent cytotoxins (Shang et al. 2017). However, when comparing the activity of the cytochalasin **4**, which is the deacetylated derivative of **3**, it was quite interesting to notice that **4** is significantly less toxic than **3** leading to the hypothesis that the presence of the acetyl group in **3** is an important structural element in the biological activity of the studied cytochalasins. The aforementioned assumption, was also observed when comparing the cytotoxicity of compound **1** and **2**. In effect, **2** is the deacetylated derivative of **1**, and the latter was also found to be less toxic than **1**. These results therefore give some hints in regards to the structure activity relationship (SAR) of the isolated cytochalasins, which will be tested further for their inhibitory effect on actin. In the same assay, compound **5** and **8** were found to be active against KB3.1 cell line with IC_{50} value of 10.63 and 30.3 µM respectively whereas compound **6** and **7** bearing the same core skeleton did not show any activity. These results indicated that the cytotoxicity of this class of compounds might possibly be enhanced by the presence of an amide group (C-33) as

Table 4. Minimum Inhibitory Concentrations (MIC) of compounds **1**–**7**, **9**–**10**, **12**–**13** against tested microorganisms.

	MIC (µg/mL)											
Test organisms	**1**	**2**	**3**	**4**	**5**	**6**	**7**	**9**	**10**	**12**	**13**	**References**
Acinetobacter baumanii	-	-	-	-	-	-	-	-	-	-	-	0.26[c]
Bacillus subtilis	-	-	16.7	66.7	16.7		16.7	1.7	1.7	66.7		8.3[o]
Candida albicans	-	-	-	-	-	-		66.7	-	-	-	16.6[n]
Chromobacterium violaceum	-	-	-	-	-	-	-	-	-	-	-	0.83[o]
Escherichia coli	-	-	-	-	-	-	-	-	-	-		1.7[o]
Mucor hiemalis	66.7	-	66.7	66.7	66.7	66.7	66.7	16.7	66.7	66.7	66.7	8.3[n]
Mycobacterium smegmatis	-	-	-	-	-	-	-	66.7	-	-	-	1.7[k]
Pichia anomala	-	-	-	-	-	-	-	-	-	-	-	8.3[n]
Pseudomonas aeruginosa	-	-	-	-	-	-	-	-	-	-	-	0.21[g]
Rhodoturula glutinis	66.7	-	-	-	-	-	-	-	-	-	-	4.2[n]
Schizosaccharomyces pombe	16.7	66.7	66.7	66.7	-	-	-	-	66.7	-	-	8.3[n]
Staphylococcus aureus	-	-	66.7	66.7	66.7		66.7	4.2	4.2	66.7	-	0.83[o]

(-): No inhibition, [c]Ciprobay 2.54 mg/mL, [g]Gentamycin 1 mg/mL, [k]Kanamycin 1 mg/mL, [n]Nystatin 1 mg/mL, [o]Oxytetracyclin 1 mg/mL. Starting concentration for antimicrobial assay were 66.7 µg/mL.

Table 5. Cytotoxic activity of compounds **1–10**, **12–13**.

	IC_{50} (μM)												
Cell lines	**1**	**2**	**3**	**4**	**5**	**6**	**7**	**8**	**9**	**10**	**12**	**13**	**Epothilone B**
KB3.1	0.064	0.33	1.7	5.8	10.6	-	-	30.3	0.36	0.91	-	-	6.5×10^{-5}
L929	0.19	1.5	1.3	10.8	>30.4	-	-	-	1.06	5.6	-	-	6.5×10^{-4}
A431	0.085	0.33	14.3	11.0	12.0	n.t	n.t	n.t	0.04	0.17	n.t	n.t	1.2×10^{-4}
MCF-7	0.14	3.1	7.3	19.3	7.44	n.t	n.t	n.t	0.02	0.36	n.t	n.t	8.2×10^{-5}
A549	0.16	0.73	3.1	10.3	19.7	n.t	n.t	n.t	0.43	1.0	n.t	n.t	6.1×10^{-5}
SKOV-3	0.073	0.33	13.6	45.9	13.9	n.t	n.t	n.t	0.15	0.65	n.t	n.t	2.9×10^{-4}
PC-3	0.14	0.29	4.2	9.4	7.3	n.t	n.t	n.t	1.1	9.7	n.t	n.t	9.5×10^{-4}

n.t: not tested, (-): no activity. Starting concentration for cytotoxicity assay was 37 μg/mL

shown in **5** and **8** instead of a carboxylic acid as observed in **6** (C-34) and 7 (C-33). In addition, phomoxanthones A (**9**) and B (**10**), exhibited strong cytotoxic activities with half-maximal inhibitory concentrations (IC_{50}) in the range 0.02 – 9.7 μM. These results were in accordance with previous published cytotoxicity of dimeric tetrahydroxanthone derivatives against human epidermoid carcinoma (KB), human breast cancer (BC-1), mouse lymphoma (L5178Y), human ovarian carcinoma (A2780), and African monkey kidney fibroblast (Vero) cell lines among others (Isaka et al. 2001; Rönsberg et al. 2013).

Conclusion

The genus *Diaporthe* has been regarded for decades as a potential source for the production of diverse bioactive secondary metabolites. In the present study, we suggest the introduction of the new species *D. breyniae* isolated from the twigs of *Breynia oblongifolia* in Cameroon. From the liquid culture of this fungus, two previously undescribed polyketides were isolated together with eleven known compounds. The isolated compounds showed weak to strong antimicrobial activities as well as moderate cytotoxic activities overall. These results demonstrated that it should certainly be worthwhile to explore untapped geographic area like the African tropics in general and Cameroon in particular for the discovery of new fungi and the isolation of novel secondary metabolites produced by these with significant biological activities.

Acknowledgments

We are grateful to W. Collisi for conducting the cytotoxicity assays, C. Kakoschke for recording NMR data and E. Surges for recording HPLC-MS data. The authors wish to thank V. Nana (National Herbarium of Cameroon) for the botanical identifications and S.C.N. Wouamba for the isolation of the strain CBS 148910. Financial support by a personal PhD stipend from the German Academic exchange service (DAAD) to B.M.K. is gratefully acknowledged (programme ID- 57440921). Y.M.F. is grateful for the postdoctoral stipendium received from Alexander-von-Humboldt Foundation,

Germany. We are also grateful to The World Academy of Sciences (TWAS) (grant 18-178 RG/CHE/AF/AC_G-FR 3240303654), and the Alexander von Humboldt Foundation (AvH) through the equipment subsidies (Ref 3.4 - 8151/20 002), the Research Group Linkage (grant IP-CMR-1121341) and the hub project CECANO-PROF (3.4-CMR-Hub). Furthermore, we are grateful to the Deutsche Forschungsgemeinschaft for a Research Unit grant "Cytolabs" (DFG-FOR-5170).

References

Alfaro ME, Zoller S, Lutzoni F (2003) Bayes or bootstrap. A simulation study comparing the performance of Bayesian Markov chain Monte Carlo sampling and bootstrapping in assessing phylogenetic confidence. Molecular Biology and Evolution 20(2): 255–266. https://doi.org/10.1093/molbev/msg028

Becker K, Wongkanoun S, Wessel AC, Bills GF, Stadler M, Luangsa-Ard JJ (2020a) Phylogenetic and chemotaxonomic studies confirm the affinities of *Stromatoneurospora phoenix* to the coprophilous Xylariaceae. Journal of Fungi (Basel, Switzerland) 6(3): 1–21. https://doi.org/10.3390/jof6030144

Becker K, Wessel AC, Luangsa-Ard JJ, Stadler M (2020b) Viridistratins A–C, antimicrobial and cytotoxic benzo[*j*]fluoranthenes from stromata of *Annulohypoxylon viridistratum* (Hypoxylaceae, Ascomycota). Biomolecules 10(5): 805. https://doi.org/10.3390/biom10050805

Beno MA, Christoph GG, Cox RH, Wells JM, Cole RJ, Kirksey JW (1977) Structure of a New [1 l]Cytochalasin, Cytochalasin H or Kodo-cytochalasin-1. Journal of the American Chemical Society 99(12): 4123–4130. https://doi.org/10.1021/ja00454a035

Carbone I, Kohn LM (1999) A method for designing primer sets for the speciation studies in filamentous ascomycetes. Mycologia 91(3): 553–556. https://doi.org/10.1080/00275514.1999.12061051

Chaisiri C, Liu X-Y, Yin W-X, Luo C-X, Lin Y (2021) Morphology characterization, molecular phylogeny, and pathogenicity of *Diaporthe passifloricola* on *Citrus reticulata* cv. Nanfengmiju in Jiangxi Province, China. Plants 10(2): e218. https://doi.org/10.3390/plants10020218

Chang CQ, Cheng YH, Xiang MM, Jiang ZD (2005) New species of *Phomopsis* on woody plants in Fujian Province. Junwu Xuebao 24: 6–11.

Chen Y, Yang W, Zou G, Wang G, Kang W, Yuan J, She Z (2022) Cytotoxic bromine- and iodine-containing cytochalasins produced by the mangrove endophytic fungus *Phomopsis* sp. QYM-13 using the OSMAC approach. Journal of Natural Products. https://doi.org/10.1021/acs.jnatprod.1c01115

Chepkirui C, Stadler M (2017) The genus *Diaporthe*: A rich source of diverse and bioactive metabolites. Mycological Progress 16(5): 477–494. https://doi.org/10.1007/s11557-017-1288-y

Chepkirui C, Richter C, Matasyoh JC, Stadler M (2016) Monochlorinated calocerins A-D and 9-oxostrobilurin derivatives from the basidiomycete *Favolaschia calocera*. Phytochemistry 132: 95–101. https://doi.org/10.1016/j.phytochem.2016.10.001

Chernomor O, von Haeseler A, Monh BQ (2016) Terrace aware data structure for Phylogenomic Inference from Supermatrices. Systematic Biology 65(6):997-1008. https://doi.org/10.1093/sysbio/syw037

Choi JN, Kim J, Ponnusamy K, Lim C, Kim JG, Muthaiya MJ, Lee CH (2013) Metabolic Changes of *Phomopsis longicolla* Fermentation and Its Effect on Antimicrobial Activity Against *Xanthomonas oryzae*. Journal of Microbiology and Biotechnology 23(2): 177–183. https://doi.org/10.4014/jmb.1210.10020

Cole RJ, Wells JM, Cox RH, Cutler HG (1981) Isolation and biological properties of deacetylcytochalasin H from *Phomopsis* sp. Journal of Agricultural and Food Chemistry 29(1): 205–206. https://doi.org/10.1021/jf00103a057

Crous PW, Groenewald JZ, Risede JM, Simoneau P, Hyde KD (2004) *Calonectria* species and their *Cylindrocladium* anamorphs: Species with sphaeropedunculate vesicles. Studies in Mycology 50: 415–430. https://doi.org/10.3114/sim.55.1.213

Crous PW, Summerell BA, Shivas RG, Romberg M, Mel'nik VA, Verkley GJM, Groenewald JZ (2011) Fungal Planet description sheets: 92–106. Persoonia 27(1): 130–162. https://doi.org/10.3767/003158511X617561

Crous PW, Wingfield MJ, Schumacher RK, Summerell BA, Giraldo A, Gené J, Guarro J, Wanasinghe DN, Hyde KD, Camporesi E, Garethjones EB, Thambugala KM, Malysheva EF, Malysheva VF, Acharya K, Álvarez J, Alvarado P, Assefa A, Barnes CW, Bartlett JS, Blanchette RA, Burgess TI, Carlavilla JR, Coetzee MPA, Damm U, Decock CA, Denbreeÿen A, Devries B, Dutta AK, Holdom DG, Rooney-Latham S, Manjón JL, Marincowitz S, Mirabolfathy M, Moreno G, Nakashima C, Papizadeh M, Shahzadehfazeli SA, Amoozegar MA, Romberg MK, Shivas RG, Stalpers JA, Stielow B, Stukely MJC, Swart WJ, Tan YP, Vanderbank M, Wood AR, Zhang Y, Groenewald JZ (2014) Fungal Planet description sheets: 281–319. Persoonia 33(1): 212–289. https://doi.org/10.3767/003158514X685680

Crous PW, Wingfield MJ, Le Roux JJ, Richardson DM, Strasberg D, Shivas RG, Alvarado P, Edwards J, Moreno G, Sharma R, Sonawane MS, Tan YP, Altés A, Barasubiye T, Barnes CW, Blanchette RA, Boertmann D, Bogo A, Carlavilla JR, Cheewangkoon R, Daniel R, de Beer ZW, Yáñez-Morales M de Jesús, Duong TA, Fernández-Vicente J, Geering ADW, Guest DI, Held BW, Heykoop M, Hubka V, Ismail AM, Kajale SC, Khemmuk W, Kolařík M, Kurli R, Lebeuf R, Lévesque CA, Lombard L, Magista D, Manjón JL, Marincowitz S, Mohedano JM, Nováková A, Oberlies NH, Otto EC, Paguigan ND, Pascoe IG, Pérez-Butrón JL, Perrone G, Rahi P, Raja HA, Rintoul T, Sanhueza RMV, Scarlett K, Shouche YS, Shuttleworth LA, Taylor PWJ, Thorn RG, Vawdrey LL, Solano-Vidal R, Voitk A, Wong PTW, Wood AR, Zamora JC, Groenewald JZ (2015) Fungal Planet description sheets: 371–399. Persoonia 35(1): 264–327. https://doi.org/10.3767/003158515X690269

Crous PW, Wingfield MJ, Richardson DM, Leroux JJ, Strasberg D, Edwards J, Roets F, Hubka V, Taylor PWJ, Heykoop M, Martín MP, Moreno G, Sutton DA, Wiederhold NP, Barnes CW, Carlavilla JR, Gené J, Giraldo A, Guarnaccia V, Guarro J, Hernández-Restrepo M, Kolařík M, Manjón JL, Pascoe IG, Popov ES, Sandoval-Denis M, Woudenberg JHC, Acharya K, Alexandrova AV, Alvarado P, Barbosa RN, Baseia IG, Blanchette RA, Boekhout T, Burgess TI, Cano-Lira JF, Čmoková A, Dimitrov RA, Dyakov MY, Dueñas M, Dutta AK, Esteve-Raventós F, Fedosova AG, Fournier J, Gamboa P, Gouliamova DE, Grebenc T, Groenewald M, Hanse B, Hardy GESTJ, Held BW, Jurjević Ž, Kaewgrajang T, Latha KPD, Lombard L, Luangsaard JJ, Lysková P, Mallátová N, Manimohan P, Miller AN, Mirabolfathy M, Morozova OV, Obodai M, Oliveira NT, Ordóñez ME, Otto EC, Paloi S, Peterson SW, Phosri C, Roux J, Salazar WA, Sánchez A, Sarria GA, Shin H-D, Silva BDB, Silva GA, Smith MTH, Souza-

Motta CM, Stchigel AM, Stoilova-Disheva MM, Sulzbacher MA, Telleria MT, Toapanta C, Traba JM, Valenzuela-Lopez N, Watling R, Groenewald JZ (2016) Fungal Planet description sheets: 400–468. Persoonia 36(1): 316–458. https://doi.org/10.3767/003158516X692185

Crous PW, Carnegie AJ, Wingfield MJ, Sharma R, Mughini G, Noordeloos ME, Santini A, Shouche YS, Bezerra JDP, Dima B, Guarnaccia V, Imrefi I, Jurjević Ž, Knapp DG, Kovács GM, Magistà D, Perrone G, Rämä T, Rebriev YA, Shivas RG, Singh SM, Souza-Motta CM, Thangavel R, Adhapure NN, Alexandrova AV, Alfenas AC, Alfenas RF, Alvarado P, Alves AL, Andrade DA, Andrade JP, Barbosa RN, Barili A, Barnes CW, Baseia IG, Bellanger J-M, Berlanas C, Bessette AE, Bessette AR, Biketova AYu, Bomfim FS, Brandrud TE, Bransgrove K, Brito ACQ, Cano-Lira JF, Cantillo T, Cavalcanti AD, Cheewangkoon R, Chikowski RS, Conforto C, Cordeiro TRL, Craine JD, Cruz R, Damm U, de Oliveira RJV, de Souza JT, de Souza HG, Dearnaley JDW, Dimitrov RA, Dovana F, Erhard A, Esteve-Raventós F, Félix CR, Ferisin G, Fernandes RA, Ferreira RJ, Ferro LO, Figueiredo CN, Frank JL, Freire KTLS, García D, Gené J, Gęsiorska A, Gibertoni TB, Gondra RAG, Gouliamova DE, Gramaje D, Guard F, Gusmão LFP, Haitook S, Hirooka Y, Houbraken J, Hubka V, Inamdar A, Iturriaga T, Iturrieta-González I, Jadan M, Jiang N, Justo A, Kachalkin AV, Kapitonov VI, Karadelev M, Karakehian J, Kasuya T, Kautmanová I, Kruse J, Kušan I, Kuznetsova TA, Landell MF, Larsson K-H, Lee HB, Lima DX, Lira CRS, Machado AR, Madrid H, Magalhães OMC, Majerova H, Malysheva EF, Mapperson RR, Marbach PAS, Martín MP, Martín-Sanz A, Matočec N, McTaggart AR, Mello JF, Melo RFR, Mešič A, Michereff SJ, Miller AN, Minoshima A, Molinero-Ruiz L, Morozova OV, Mosoh D, Nabe M, Naik R, Nara K, Nascimento SS, Neves RP, Olariaga I, Oliveira RL, Oliveira TGL, Ono T, Ordoñez ME, de M Ottoni A, Paiva LM, Pancorbo F, Pant B, Pawłowska J, Peterson SW, Raudabaugh DB, Rodríguez-Andrade E, Rubio E, Rusevska K, Santiago ALCMA, Santos ACS, Santos C, Sazanova NA, Shah S, Sharma J, Silva BDB, Siquier JL, Sonawane MS, Stchigel AM, Svetasheva T, Tamakeaw N, Telleria MT, Tiago PV, Tian CM, Tkalčec Z, Tomashevskaya MA, Truong HH, Vecherskii MV, Visagie CM, Vizzini A, Yilmaz N, Zmitrovich IV, Zvyagina EA, Boekhout T, Kehlet T, Læssøe T, Groenewald JZ (2019) Fungal Planet description sheets: 868–950. Persoonia 42: 291–473. https://doi.org/10.3767/persoonia.2019.42.11

Crous PW, Wingfield MJ, Chooi Y-H, Gilchrist CLM, Lacey E, Pitt JI, Roets F, Swart WJ, Cano-Lira JF, Valenzuela-Lopez N, Hubka V, Shivas RG, Stchigel AM, Holdom DG, Jurjević Ž, Kachalkin AV, Lebel T, Lock C, Martín MP, Tan YP, Tomashevskaya MA, Vitelli JS, Baseia IG, Bhatt VK, Brandrud TE, De Souza JT, Dima B, Lacey HJ, Lombard L, Johnston PR, Morte A, Papp V, Rodríguez A, Rodríguez-Andrade E, Semwal KC, Tegart L, Abad ZG, Akulov A, Alvarado P, Alves A, Andrade JP, Arenas F, Asenjo C, Ballarà J, Barrett MD, Berná LM, Berraf-Tebbal A, Bianchinotti MV, Bransgrove K, Burgess TI, Carmo FS, Chávez R, Čmoková A, Dearnaley JDW, Santiago ALCMA, Freitas-Neto JF, Denman S, Douglas B, Dovana F, Eichmeier A, Esteve-Raventós F, Farid A, Fedosova AG, Ferisin G, Ferreira RJ, Ferrer A, Figueiredo CN, Figueiredo YF, Reinoso-Fuentealba CG, Garrido-Benavent I, Cañete-Gibas CF, Gil-Durán C, Glushakova AM, Gonçalves MFM, González M, Gorczak M, Gorton C, Guard FE, Guarnizo AL, Guarro J, Gutiérrez M, Hamal P, Hien LT, Hocking AD, Houbraken J, Hunter GC, Inácio CA, Jourdan M, Kapitonov VI, Kelly L, Khanh TN, Kisło K, Kiss L, Kiyashko A, Kolařík M, Kruse J, Kubátová A, Kučera V, Kučerová I, Kušan I, Lee HB, Levicán G, Lewis A, Liem NV, Liimatainen K, Lim HJ, Lyons MN, Maciá-Vicente JG, Magaña-Dueñas V, Mahiques R, Malysheva EF, Marbach

PAS, Marinho P, Matočec N, McTaggart AR, Mešić A, Morin L, Muñoz-Mohedano JM, Navarro-Ródenas A, Nicolli CP, Oliveira RL, Otsing E, Ovrebo CL, Pankratov TA, Paños A, Paz-Conde A, Pérez-Sierra A, Phosri C, Pintos Á, Pošta A, Prencipe S, Rubio E, Saitta A, Sales LS, Sanhueza L, Shuttleworth LA, Smith J, Smith ME, Spadaro D, Spetik M, Sochor M, Sochorová Z, Sousa JO, Suwannasai N, Tedersoo L, Thanh HM, Thao LD, Tkalčec Z, Vaghefi N, Venzhik AS, Verbeken A, Vizzini A, Voyron S, Wainhouse M, Whalley AJS, Wrzosek M, Zapata M, Zeil-Rolfe I, Groenewald JZ (2020) Fungal Planet description sheets: 1042–1111. Persoonia 44(1): 301–459. https://doi.org/10.3767/persoonia.2020.44.11

Crous PW, Hernández-Restrepo M, Schumacher RK, Cowan DA, Maggs-Kölling G, Marais E, Wingfield MJ, Yilmaz N, Adan OCG, Akulov A, Duarte E Álvarez, Berraf-Tebbal A, Bulgakov TS, Carnegie AJ, de Beer ZW, Decock C, Dijksterhuis J, Duong TA, Eichmeier A, Hien LT, Houbraken JAMP, Khanh TN, Liem NV, Lombard L, Lutzoni FM, Miadlikowska JM, Nel WJ, Pascoe IG, Roets F, Roux J, Samson RA, Shen M, Spetik M, Thangavel R, Thanh HM, Thao LD, van Nieuwenhuijzen EJ, Zhang JQ, Zhang Y, Zhao LL, Groenewald JZ (2021) New and Interesting Fungi. 4. Fungal Systematics and Evolution 7: 255–343. https://doi.org/10.3114/fuse.2021.07.13

Cui H, Yu J, Chen S, Ding M, Huang X, Yuan J, She Z (2017) Alkaloids from the mangrove endophytic fungus *Diaporthe phaseolorum* SKS019. Bioorganic & Medicinal Chemistry Letters 27(4): 803–807. https://doi.org/10.1016/j.bmcl.2017.01.029

da Silva RMF, Soares AM, Pádua APSL, Firmino AL, Souza-Motta CM, da Silva GA, Plautz Jr HL, Bezerra JDP, Paiva LM, Ryvarden L, Oliani LC, de Mélo MAC, Magalhães OMC, Pereira OL, Oliveira RJV, Gibertoni TB, Oliveira TGS, Svedese VM, Fan XL (2019) Mycological Diversity Description II. Acta Botanica Brasílica 33(1): 163–173. https://doi.org/10.1590/0102-33062018abb0411

de Silva NI, Maharachchikumbura SSN, Thambugala KM, Bhat DJ, Karunarathna SC, Tennakoon DS, Phookamsak R, Jayawardena RS, Lumyong S, Hyde KD (2021) Morphomolecular taxonomic studies reveal a high number of endophytic fungi from *Magnolia candolli* and *M. garrettii* in China and Thailand. Mycosphere: Journal of Fungal Biology 11(1): 163–237. https://doi.org/10.5943/mycosphere/12/1/3

Ding B, Wang Z, Xia G, Huang X, Xu F, Chen W, She Z (2017) Three new chromone derivatives produced by *Phomopsis* sp. HNY29-2B from *Acanthus ilicifolius* Linn. Wiley Online Library 35(12): 1889–1893. https://doi.org/10.1002/cjoc.201700375

Dissanayake AJ, Camporesi E, Hyde KD, Zhang W, Yan JY, Li XH (2017) Molecular phylogenetic analysis reveals seven new *Diaporthe* species from Italy. Mycosphere: Journal of Fungal Biology 8(5): 853–877. https://doi.org/10.5943/mycosphere/8/5/4

Dissanayake AJ, Chen Y-Y, Liu J-K (2020) Unravelling *Diaporthe* species associated with woody hosts from karst formations (Guizhou) in China. Journal of Fungi 6: e251. https://doi.org/10.3390/jof6040251

Doilom M, Dissanayake AJ, Wanasinghe DN, Boonmee S, Liu J-K, Bhat DJ, Taylor JE, Bahkali AH, McKenzie EHC, Hyde KD (2017) Microfungi on *Tectona grandis* (teak) in Northern Thailand. Fungal Diversity 82: 107–182.

Dong Z, Manawasinghe IS, Huang Y, Shu Y, Phillips AJL, Dissanayake AJ, Hyde KD, Xiang M, Luo M (2021) Endophytic *Diaporthe* associated with *Citrus grandis* cv. *tomentosa* in China. Frontiers in Microbiology 11: e3621. https://doi.org/10.3389/fmicb.2020.609387

Elsässer B, Krohn K, Flörke U, Root N, Aust HJ, Draeger S, Schulz B, Antus S, Kurtán T (2005) X-ray structure determination, absolute configuration and biological activity of Phomoxanthone A. European Journal of Organic Chemistry 2005(21): 4563–4570. https://doi.org/10.1002/ejoc.200500265

Feng X-X, Chen J-J, Wang G-R, Cao T-T, Zheng Y-L, Zhang C-L (2019) *Diaporthe sinensis*, a new fungus from *Amaranthus* sp. in China. Phytotaxa 425(5): 259–268. https://doi.org/10.11646/phytotaxa.425.5.1

Gao Y, Liu F, Cai L (2016) Unravelling *Diaporthe* species associated with *Camellia*. Systematics and Biodiversity 14(1): 102–117. https://doi.org/10.1080/14772000.2015.1101027

Gao YH, Liu F, Duan W, Crous PW, Cai L (2017) *Diaporthe* is paraphyletic. IMA Fungus 8(1): 153–187. https://doi.org/10.5598/imafungus.2017.08.01.11

Glass NL, Donaldson GC (1995) Development of primer sets designed for use with the PCR to amplify conserved genes from filamentous ascomycetes. Applied and Environmental Microbiology 61(4): 1323–1330. https://doi.org/10.1128/aem.61.4.1323-1330.1995

Gomes RR, Glienke C, Videira SIR, Lombard L, Groenewald JZ, Crous PW (2013) *Diaporthe*: A genus of endophytic, saprobic and plant pathogenic fungi. Persoonia 31(1): 1–41. https://doi.org/10.3767/003158513X666844

Guarnaccia V, Crous PW (2017) Emerging citrus diseases in Europe caused by *Diaporthe* spp. IMA Fungus 8(2): 317–334. https://doi.org/10.5598/imafungus.2017.08.02.07

Guarnaccia V, Groenewald JZ, Woodhall J, Armengol J, Cinelli T, Eichmeier A, Ezra D, Fontaine F, Gramaje D, Gutierrez-Aguirregabiria A, Kaliterna J, Kiss L, Larignon P, Luque J, Mugnai L, Naor V, Raposo R, Sándor E, Váczy KZ, Crous PW (2018) *Diaporthe* diversity and pathogenicity revealed from a broad survey of grapevine diseases in Europe. Persoonia 40(1): 135–153. https://doi.org/10.3767/persoonia.2018.40.06

Hilário S, Amaral IA, Gonçalves MFM, Lopes A, Santos L, Alves A (2020) *Diaporthe* species associated with twig blight and dieback of *Vaccinium corymbosum* in Portugal, with description of four new species. Mycologia 112(2): 293–308. https://doi.org/10.1080/00275514.2019.1698926

Huang F, Hou X, Dewdney MM, Fu Y, Chen G, Hyde KD, Li H (2013) *Diaporthe* species occurring on citrus in China. Fungal Diversity 61(1): 237–250. https://doi.org/10.1007/s13225-013-0245-6

Huang F, Udayanga D, Wang X, Hou X, Mei X, Fu Y, Hyde KD, Li H (2015) Endophytic *Diaporthe* associated with Citrus, a phylogenetic reassessment with seven new species from China. Fungal Biology 119(5): 331–347. https://doi.org/10.1016/j.funbio.2015.02.006

Huang S, Xia J, Zhang X, Sun W (2021) Morphological and phylogenetic analyses reveal three new species of *Diaporthe* from Yunnan, China. MycoKeys 78: 49–77. https://doi.org/10.3897/mycokeys.78.60878

Hyde KD, Chaiwan N, Norphanphoun C, Boonmee S, Camporesi E, Chethana KWT, Dayarathne MC, de Silva NI, Dissanayake AJ, Ekanayaka AH, Hongsanan S, Huang SK, Jayasiri SC, Jayawardena RS, Jiang HB, Karunarathna A, Lin CG, Liu JK, Liu NG, Lu YZ, Luo ZL, Maharachchimbura SSN, Manawasinghe IS, Pem D, Perera RH, Phukhamsakda C, Samarakoon MC, Senwanna C, Shang QJ, Tennakoon DS, Thambugala KM, Tibpromma, S, Wanasinghe DN, Xiao YP, Yang J, Zeng XY, Zhang JF, Zhang SN, Bulgakov TS, Bhat DJ, Cheewangkoon R, Goh TK, Jones EBG, Kang JC, Jeewon R, Liu ZY, Lumyong S, Kuo CH,

McKenzie EHC, Wen TC, Yan JY, Zhao Q (2018) Mycosphere notes 169–224. Mycosphere: Journal of Fungal Biology 9(2): 271–430. https://doi.org/10.5943/mycosphere/9/2/8

Hyde KD, Dong Y, Phookamsak R, Jeewon R, Bhat DJ, Jones EBG, Liu N-G, Abeywickrama PD, Mapook A, Wei D, Perera RH, Manawasinghe IS, Pem D, Bundhun D, Karunarathna A, Ekanayaka AH, Bao D-F, Li J, Samarakoon MC, Chaiwan N, Lin C-G, Phutthacharoen K, Zhang S-N, Senanayake IC, Goonasekara ID, Thambugala KM, Phukhamsakda C, Tennakoon DS, Jiang H-B, Yang J, Zeng M, Huanraluek N, Liu J-KJ, Wijesinghe SN, Tian Q, Tibpromma S, Brahmanage RS, Boonmee S, Huang S-K, Thiyagaraja V, Lu Y-Z, Jayawardena RS, Dong W, Yang E-F, Singh SK, Singh SM, Rana S, Lad SS, Anand G, Devadatha B, Niranjan M, Sarma VV, Liimatainen K, Aguirre-Hudson B, Niskanen T, Overall A, Alvarenga RLM, Gibertoni TB, Pfliegler WP, Horváth E, Imre A, Alves AL, da Silva Santos AC, Tiago PV, Bulgakov TS, Wanasinghe DN, Bahkali AH, Doilom M, Elgorban AM, Maharachchikumbura SSN, Rajeshkumar KC, Haelewaters D, Mortimer PE, Zhao Q, Lumyong S, Xu J, Sheng J (2020) Fungal diversity notes 1151–1276: Taxonomic and phylogenetic contributions on genera and species of fungal taxa. Fungal Diversity 100(1): 5–277. https://doi.org/10.1007/s13225-020-00439-5

Iantas J, Savi DC, Schibelbein Rd S, Noriler SA, Assad BM, Dilarri G, Ferreira H, Rohr J, Thorson JS, Shaaban KA, Glienke C (2021) Endophytes of Brazilian medicinal plants with activity against phytopathogens. Frontiers in Microbiology 12: e714750. https://doi.org/10.3389/fmicb.2021.714750

Isaka M, Jaturapat A, Rukseree K, Danwisetkanjana K, Tanticharoen M, Thebtaranonth Y (2001) Phomoxanthones A and B, novel xanthone dimers from the endophytic fungus *Phomopsis* species. Journal of Natural Products 64(8): 1015–1018. https://doi.org/10.1021/np010006h

Jouda JB, Tamokou J de D, Mbazoa CD, Douala-Meli C, Sarkar P, Bag PK, Wandji J (2016) Antibacterial and cytotoxic cytochalasins from the endophytic fungus *Phomopsis* sp. harbored in *Garcinia kola* (Heckel) nut. BMC Complementary and Alternative Medicine 16(1): 1–9. https://doi.org/10.1186/s12906-016-1454-9

Kakeya H, Morishita M, Onozawa C, Usami R, Horikoshi K, Kimura KI, Yoshihama M, Osada H (1997) RKS-1778, a new mammalian cell-cycle inhibitor and a key intermediate of the [11]cytochalasin group. Journal of Natural Products 60(7): 669–672. https://doi.org/10.1021/np970151o

Kalyaanamoorthy S, Minh BQ, Wong TKF, von Haeseler A, Jermiin LS (2017) ModelFinder: Fast model selection for accurate phylogenetic estimates. Nature Methods 14(6): 587–589. https://doi.org/10.1038/nmeth.4285

Katoh K, Standley DM (2013) MAFFT multiple sequence alignment software v. 7: Improvements in performance and usability. Molecular Biology and Evolution 30(4): 772–780. https://doi.org/10.1093/molbev/mst010

Kearse M, Moir R, Wilson A, Stones-Havas S, Cheung M, Sturrock S, Buxton S, Cooper A, Markowitz S, Duran C, Thierer T, Ashton B, Mentjies P, Drummond A (2012) Geneious basic: An integrated and extendable desktop software platform for the organization and analysis of sequence data. Bioinformatics (Oxford, England) 28(12): 1647–1649. https://doi.org/10.1093/bioinformatics/bts199

Kretz R, Wendt L, Wongkanoun S, Luangsa-Ard JJ, Surup F, Helaly SE, Noumeur SR, Stadler M, Stradal TEB (2019) The effect of cytochalasans on the actin cytoskeleton of eukaryotic

cells and preliminary structure-activity relationships. Biomolecules 9(2): e73. https://doi.org/10.3390/biom9020073

Kumar S, Stecher G, Li M, Knyaz C, Tamura K (2018) MEGA X: Molecular evolutionary Genetics analysis across computing platforms. Molecular Biology and Evolution 35(6): 1547–1549. https://doi.org/10.1093/molbev/msy096

Lanfear R, Frandsen PB, Wright AM, Senfeld T, Calcott B (2016) PartitionFinder 2: new methods for selecting partitioned models of evolution for molecular and morphological phylogenetic analyses. Molecular Biology and Evolution 34: 772–773. https://doi.org/10.1093/molbev/msw260

Li WJ, McKenzie EHC, Liu JK, Bhat DJ, Dai D-Q, Camporesi E, Tian Q, Maharachchikumbura SSN, Luo Z-L, Shang Q-J, Zhang J-F, Tangthirasunun N, Karunarathna SC, Xu J-C, Hyde KD (2020) Taxonomy and phylogeny of hyaline-spored coelomycetes. Fungal Diversity 100(1): 279–801. https://doi.org/10.1007/s13225-020-00440-y

Lim C, Kim J, Choi JN, Ponnusamy K, Jeon Y, Kim SU, Kim JG, Lee CH (2010) Identification, fermentation, and bioactivity against *Xanthomonas oryzae* of antimicrobial metabolites isolated from *Phomopsis longicolla* S1B4. Journal of Microbiology and Biotechnology 20: 494–500. https://doi.org/10.4014/JMB.0909.09026

Liu JK, Hyde KD, Jones EBG, Ariyawansa HA, Bhat DJ, Boonmee S, Maharachchikumbura SSN, McKenzie EHC, Phookamsak R, Phukhamsakda C, Shenoy BD, Abdel-Wahab MA, Buyck B, Chen J, Chethana KWT, Singtripop C, Dai DQ, Dai YC, Daranagama DA, Dissanayake AJ, Doilom M, D'souza MJ, Fan XL, Goonasekara ID, Hirayama K, Hongsanan S, Jayasiri SC, Jayawardena RS, Karunarathna SC, Li WJ, Mapook A, Norphanphoun C, Pang KL, Perera RH, Peršoh D, Pinruan U, Senanayake IC, Somrithipol S, Suetrong S, Tanaka K, Thambugala KM, Tian Q, Tibpromma S, Udayanga D, Wijayawardene NN, Wanasinghe D, Wisitrassameewong K, Zeng XY, Abdel-Aziz FA, Adamčík S, Bahkali AH, Boonyuen N, Bulgakov T, Callac P, Chomnunti P, Greiner K, Hashimoto A, Hofstetter V, Kang JC, Lewis D, Li XH, Liu XZ, Liu ZY, Matsumura M, Mortimer PE, Rambold G, Randrianjohany E, Sato G, Sri-Indrasutdhi V, Tian CM, Verbeken A, von Brackel W, Wang Y, Wen TC, Xu JC, Yan JY, Zhao RL, Camporesi E (2015) Fungal diversity notes 1–110: Taxonomic and phylogenetic contributions to fungal species. Fungal Diversity 72(1): 1–197. https://doi.org/10.1007/s13225-015-0324-y

Long X, Ding Y, Deng J (2018) Total synthesis of asperchalasines A, D, E, and H. Angewandte Chemie International Edition 130(43): 14417–14420. https://doi.org/10.1002/ange.201808481

López-Cardona N, Guevara-Castro A, Gañán-Betancur L, Amaya-Gómez CV (2021) First report of *Diaporthe ueckerae* causing stem canker on soybean (*Glycine max*) in Colombia. Disease Note. https://doi.org/10.1094/PDIS-04-21-0718-PDN

Ma K-L, Dong S-H, Li H-Y, Wei W-J, Tu Y-Q, Gao K (2021) Cytochalasins from *Xylaria* sp. CFL5, an endophytic fungus of *Cephalotaxus fortunei*. 11: 87–98. https://doi.org/10.1007/s13659-020-00279-5

Manawasinghe IS, Dissanayake AJ, Li X, Liu M, Wanasinghe DN, Xu J, Zhao W, Zhang W, Zhou Y, Hyde KD, Brooks S, Yan J (2019) High genetic diversity and species complexity of *Diaporthe* associated with grapevine dieback in China. Frontiers in Microbiology 10: e1936. https://doi.org/10.3389/fmicb.2019.01936

Mapook A, Hyde KD, McKenzie EHC, Jones EBG, Bhat DJ, Jeewon R, Stadler M, Samarakoon MC, Malaithong M, Tanunchai B, Buscot F, Wubet T, Purahong W (2020) Taxonomic and phylogenetic contributions to fungi associated with the invasive weed *Chromolaena odorata* (Siam weed). Fungal Diversity 101(1): 1–175. https://doi.org/10.1007/s13225-020-00444-8

Marin-Felix Y, Hernandez-Restrepo M, Wingfield MJ, Akulov A, Carnegie AJ, Cheewangkoon R, Gramaje D, Groenewald JZ, Guarnaccia V, Halleen F, Lombard L, Luangsa-ard J, Marincowitz S, Moslemi A, Mostert L, Quaedvlieg W, Schumacher RK, Spies CFJ, Thangavel R, Taylor PWJ, Wilson AM, Wingfield BD, Wood AR, Crous PW (2019) Genera of phytopathogenic fungi: GOPHY 2. Studies in Mycology 92(1): 47–133. https://doi.org/10.1016/j.simyco.2018.04.002

Matio Kemkuignou B, Treiber L, Zeng H, Schrey H, Schobert R, Stadler M (2020) Macrooxazoles A-D, new 2,5-disubstituted oxazole-4-carboxylic acid derivatives from the plant pathogenic fungus *Phoma macrostoma*. Molecules (Basel, Switzerland) 25(23): 1–18. https://doi.org/10.3390/molecules25235497

Milagres CA, Belisário R, Silva MA, Lisboa DO, Pinho DB, Furtado GQ (2018) A novel species of *Diaporthe* causing leaf spot in *Pachira glabra*. Tropical Plant Pathology 43(5): 460–467. https://doi.org/10.1007/s40858-018-0242-0

Minh BQ, Schmidt HA, Chernomor O, Schrempf D, Woodhams MD, von Haeseler A, Lanfear R (2020) IQ-TREE 2: New models and efficient methods for phylogenetic inference in the genomic era. Molecular Biology and Evolution 6–10(5): 1530–1534. https://doi.org/10.1093/molbev/msaa015

Mostert L, Crous PW, Kang J-C, Phillips AJL (2001) Species of *Phomopsis* and a *Libertella* sp. occurring on grapevines with specific reference to South Africa: Morphological, cultural, molecular and pathological characterization. Mycologia 93(1): 146–167. https://doi.org/10.1080/00275514.2001.12061286

Noriler SA, Savi DC, Ponomareva L, Rodrigues R, Rohr J, Thorson JS, Glienke C, Shaaban KA (2019) Vochysiamides A and B: Two new bioactive carboxamides produced by the new species *Diaporthe vochysiae*. Fitoterapia 138: 104–273. https://doi.org/10.1016/j.fitote.2019.104273

Pereira C, Ferreira B, Aucique-Perez C, Barreto R (2021) *Diaporthe rosiphthora* sp. nov.: Yet another rose dieback fungus. Crop Protection (Guildford, Surrey) 139: e105365. https://doi.org/10.1016/j.cropro.2020.105365

Perera RH, Hyde KD, Peršoh D, Jones EBG, Liu JK, Liu ZY (2018) Additions to wild seed and fruit fungi 1: The sexual morph of *Diaporthe rosae* on *Magnolia champaca* and *Senna siamea* fruits in Thailand. Mycosphere : Journal of Fungal Biology 9(2): 256–270. https://doi.org/10.5943/mycosphere/9/2/7

Petrović K, Riccioni L, Dordević V, Tubic SB, Miladinović J, Ceran M, Rajković D (2018) *Diaporthe pseudolongicolla* - the new pathogen on soybean seed in Serbia. Ratarstvo i Povrtarstvo 55(2): 103–109. https://doi.org/10.5937/ratpov55-18582

Ronquist F, Teslenko M, van der Mark P, Ayres DL, Darling A, Höhna S, Larget B, Liu L, Suchard MA, Huelsenbeck JP (2012) MrBayes 3.2: Efficient Bayesian Phylogenetic Inference and Model Choice Across a Large Model Space. Systematic Biology 61(3): 539–542. https://doi.org/10.1093/sysbio/sys029

Rönsberg D, Debbab A, Mándi A, Vasylyeva V, Böhler P, Stork B, Engelke L, Hamacher A, Sawadogo R, Diederich M, Wray V, Lin W, Kassack MU, Janiak C, Scheu S, Wesselborg S,

Kurtán T, Aly AH, Proksch P (2013) Pro-apoptotic and immunostimulatory tetrahydroxanthone dimers from the endophytic fungus *Phomopsis longicolla*. The Journal of Organic Chemistry 78(24): 12409–12425. https://doi.org/10.1021/jo402066b

Santos JM, Correia VG, Phillips AJL (2010) Primers for mating-type diagnosis in *Diaporthe* and *Phomopsis*, their use in teleomorph induction in vitro and biological species definition. Fungal Biology 114(2–3): 255–270. https://doi.org/10.1016/j.funbio.2010.01.007

Santos JM, Vrandečić K, Ćosić J, Duvnjak T, Phillips AJL (2011) Resolving the *Diaporthe* species occurring on soybean in Croatia. Persoonia 27(1): 9–19. https://doi.org/10.3767/003158511X603719

Santos L, Phillips AJL, Crous PW (2017) *Diaporthe* species on Rosaceae with descriptions of *D. pyracanthae* sp. nov. and *D. malorum* sp. nov. Mycosphere : Journal of Fungal Biology 8(5): 485–511. https://doi.org/10.5943/mycosphere/8/5/1

Shang Z, Raju R, Salim AA, Khalil ZG, Capon RJ (2017) Cytochalasins from an Australian Marine Sediment-Derived *Phomopsis* sp. (CMB-M0042F): Acid-Mediated Intramolecular Cycloadditions Enhance Chemical Diversity. The Journal of Organic Chemistry 82(18): 9704–9709. https://doi.org/10.1021/acs.joc.7b01793

Shiono Y, Tsuchinari M, Shimanuki K, Miyajima T, Murayama T, Koseki T, Laatsch H, Funakoshi T, Takanami K, Suzuki K (2007) Fusaristatins A and B, two new cyclic lipopeptides from an endophytic *Fusarium* sp. The Journal of Antibiotics 60(5): 309–316. https://doi.org/10.1038/ja.2007.39

Smith H, Wingfield MJ, Crous PW, Coutinho TA (1996) *Sphaeropsis sapinea* and *Botryosphaeria dothidea* endophytic in *Pinus* spp. and *Eucalyptus* spp. in South Africa. South African Journal of Botany 62(2): 86–88. https://doi.org/10.1016/S0254-6299(15)30596-2

Stone KJ, Bacon WC, White FJ (2000) An overview of endophytic microbes: endophytism defined. Microbial Endophytes: 17–44. https://doi.org/10.1201/9781482277302-1

Sun W, Huang S, Xia J, Zhang X, Li Z (2021) Morphological and molecular identification of *Diaporthe* species in south-western China, with description of eight new species. MycoKeys 77: 65–95. https://doi.org/10.3897/mycokeys.77.59852

Talavera G, Castresana J (2007) Improvement of phylogenies after removing divergent and ambiguously aligned blocks from protein sequence alignments. Systematic Biology 56(4): 564–577. https://doi.org/10.1080/10635150701472164

Tennakoon DS, Kuo CH, Maharachchikumbura SSN, Thambugala KM, Gentekaki E, Phillips AJL, Bhat DJ, Wanasinghe DN, de Silva NI, Promputtha I, Hyde KD (2021) Taxonomic and phylogenetic contributions to *Celtis formosana*, *Ficus ampelas*, *F. septica*, *Macaranga tanarius* and *Morus australis* leaf litter inhabiting microfungi. Fungal Diversity 108(1): 1–215. https://doi.org/10.1007/s13225-021-00474-w

The Royal Horticultural Society London (1966) R.H.S. Colour Chart. London, UK.

Thompson SM, Tan YP, Young AJ, Neate SM, Aitken EAB, Shivas RG (2011) Stem cankers on sunflower (*Helianthus annuus*) in Australia reveal a complex of pathogenic *Diaporthe* (*Phomopsis*) species. Persoonia 27(1): 80–89. https://doi.org/10.3767/003158511X617110

Thompson SM, Tan YP, Shivas RG, Neate SM, Morin L, Bissett A, Aitken EAB (2015) Green and brown bridges between weeds and crops reveal novel *Diaporthe* species in Australia. Persoonia 35(1): 39–49. https://doi.org/10.3767/003158515X687506

Udayanga D, Liu XZ, Mckenzie EHC, Chukeatirote E, Hyde KD (2012) Multi-locus phylogeny reveals three new species of *Diaporthe* from Thailand. Cryptogamie. Mycologie 33(3): 295–309. https://doi.org/10.7872/crym.v33.iss3.2012.295

Udayanga D, Castlebury LA, Rossman AY, Chukeatirote E, Hyde KD (2014) Insights into the genus *Diaporthe*: Phylogenetic species delimitation in the *D. eres* species complex. Fungal Diversity 67(1): 203–229. https://doi.org/10.1007/s13225-014-0297-2

Udayanga D, Castlebury LA, Rossman AY, Chukeatirote E, Hyde KD (2015) The *Diaporthe sojae* species complex, phylogenetic re-assessment of pathogens associated with soybean, cucurbits and other field crops. Fungal Biology 119(5): 383–407. https://doi.org/10.1016/j.funbio.2014.10.009

Van Rensburg JCJ, Lamprecht SC, Groenewald JZ, Castlebury LA, Crous PW (2006) Characterization of *Phomopsis* spp. associated with die-back of rooibos (*Aspalathus linearis*) in South Africa. Studies in Mycology 55: 65–74. https://doi.org/10.3114/sim.55.1.65

Wagenaar MM, Clardy J (2001) Dicerandrols, new antibiotic and cytotoxic dimers produced by the fungus *Phomopsis longicolla* isolated from an endangered mint. Journal of Natural Products 64(8): 1006–1009. https://doi.org/10.1021/np010020u

Wanasinghe DN, Phukhamsakda C, Hyde KD, Jeewon R, Lee HB, Gareth Jones EB, Tibpromma S, Tennakoon DS, Dissanayake AJ, Jayasiri SC, Gafforov Y, Camporesi E, Bulgakov TS, Ekanayake AH, Perera RH, Samarakoon MC, Goonasekara ID, Mapook A, Li W-J, Senanayake IC, Li J, Norphanphoun C, Doilom M, Bahkali AH, Xu J, Mortimer PE, Tibell L, Tibell S, Karunarathna SC (2018) Fungal diversity notes 709–839: Taxonomic and phylogenetic contributions to fungal taxa with an emphasis on fungi on Rosaceae. Fungal Diversity 89(1): 1–236. https://doi.org/10.1007/s13225-018-0395-7

Wei C, Sun C, Feng Z, Zhang X, Xu J (2021) Four new chromones from the endophytic fungus *Phomopsis asparagi* DHS-48 isolated from the chinese mangrove plant *Rhizophora mangle*. Marine Drugs 19(6): e348. https://doi.org/10.3390/md19060348

White TJ, Bruns T, Lee S, Taylor J (1990) Amplification and direct sequencing of fungal ribosomal genes for phylogenetics. In: Gelfand M, Sninsky JI, White TJ (Eds) PCR protocols: a guide to methods and applications. Academic Press, New York, 315–322. https://doi.org/10.1016/B978-0-12-372180-8.50042-1

Xu TC, Lu YH, Wang JF, Song ZQ, Hou YG, Liu SS, Liu CS, Wu SH (2021) Bioactive secondary metabolites of the genus *diaporthe* and anamorph *phomopsis* from terrestrial and marine habitats and endophytes: 2010–2019. Microorganisms 9(2): 1–49. https://doi.org/10.3390/microorganisms9020217

Yahara I, Harada F, Sekita S, Yoshihira K, Natori S (1982) Correlation between effects of 24 different cytochalasins on cellular structures and cellular events and those on actin in vitro. The Journal of Cell Biology 92(1): 69–78. https://doi.org/10.1083/jcb.92.1.69

Yang Q, Fan X-L, Guarnaccia V, Tian C-M (2018) High diversity of *Diaporthe* species associated with dieback diseases in China, with twelve new species described. MycoKeys 39: 97–149. https://doi.org/10.3897/mycokeys.39.26914

Yuyama KT, Wendt L, Surup F, Kretz R, Chepkirui C, Wittstein K, Boonlarppradab C, Wongkanoun S, Luangsa-ard J, Stadler M, Abraham W-R (2018) Cytochalasans act as inhibitors of biofilm formation of *Staphylococcus* aureus. Biomolecules 8(4): e129. https://doi.org/10.3390/biom8040129

Zaghouani M, Kunz C, Guédon L, Blanchard F, Nay B (2016) First total synthesis, structure revision, and natural history of the smallest cytochalasin: (+)-periconiasin G. Chemistry (Weinheim an der Bergstrasse, Germany) 22(43): 15257–15260. https://doi.org/10.1002/chem.201603734

Zhang D, Gao F, Jakovlić I, Zou H, Zhang J, Li WX, Wang GT (2020) PhyloSuite: An integrated and scalable desktop platform for streamlined molecular sequence data management and evolutionary phylogenetics studies. Molecular Ecology Resources 20(1): 348–355. https://doi.org/10.1111/1755-0998.13096

Supplementary material 1

Figures S1–S100, Tables S1–S5

Authors: Blondelle Matio Kemkuignou, Lena Schweizer, Christopher Lambert, Elodie Gisèle M. Anoumedem, Simeon F. Kouam, Marc Stadler, Yasmina Marin-Felix

Data type: Docx file.

Explanation note: The following are available online: 1D, 2D NMR, ESIMS and HR-ESIMS spectra of compounds **1**–**13**; Fig S100, ML phylogram including our strain and type and reference strains of *Diaporthe* spp.; Table S1–S4, Information of the phylogenetic study; Alignment of the ITS, *cal*, *his3*, *tef1*, *tub2* sequences used in the second phylogenetic study.

Link: https://doi.org/10.3897/mycokeys.90.82871.suppl1

MycoKeys 90: 119–145 (2022)
doi: 10.3897/mycokeys.90.78880
https://mycokeys.pensoft.net

RESEARCH ARTICLE

A peer-reviewed open-access journal
MycoKeys
Launched to accelerate biodiversity research

Taxonomic studies of bluish *Mycena* (Mycenaceae, Agaricales) with two new species from northern China

Qin Na[1], Zewei Liu[1], Hui Zeng[2,3], Binrong Ke[2,3], Zhizhong Song[1], Xianhao Cheng[1], Yupeng Ge[1]

1 *Shandong Key Laboratory of Edible Mushroom Technology, School of Agriculture, Ludong University, Yantai 264025, China* **2** *Institute of Edible Mushroom, Fujian Academy of Agricultural Sciences, Fuzhou 350011, China* **3** *National and Local Joint Engineering Research Center for Breeding and Cultivation of Featured Edible Mushroom, Fuzhou 350011, China*

Corresponding author: Yupeng Ge (gaiyupeng@126.com)

Academic editor: Thorsten Lumbsch | Received 5 December 2021 | Accepted 2 June 2022 | Published 17 June 2022

Citation: Na Q, Liu Z, Zeng H, Ke B, Song Z, Cheng X, Ge Y (2022) Taxonomic studies of bluish *Mycena* (Mycenaceae, Agaricales) with two new species from northern China. MycoKeys 90: 119–145. https://doi.org/10.3897/mycokeys.90.78880

Abstract

Bluish *Mycena* are rare, but constitute a taxonomically complex group. A total of eight bluish species in four sections have previously been reported from North America, Europe, Oceania and Asia. Two species with a blue pileus, collected in China during our taxonomic study of *Mycena* s.l., are described here as new to science: *Mycena caeruleogrisea* **sp. nov.** and *M. caeruleomarginata* **sp. nov.** Detailed descriptions, line drawings and a morphological comparison with closely-related species, especially herbarium specimens of *M. subcaerulea* from the USA, are provided. The results of Bayesian Inference and Maximum Likelihood phylogenetic analyses of a dataset of 96 nuclear rDNA ITS and 20 nLSU sequences of 43 *Mycena* species are also presented. The morphological data and the results of the phylogenetic analyses support the introduction of *M. caeruleogrisea* and *M. caeruleomarginata* as new species. A taxonomic key to bluish *Mycena* species of sections *Amictae*, *Cyanocephalae*, *Sacchariferae* and *Viscipelles* is provided.

Keywords

Mycenoid fungi, phylogeny, taxonomy, two new taxa

Introduction

Mycena (Pers.) Roussel, with almost 600 species distributed worldwide, is one of the largest genera in Agaricales (He et al. 2019). Maas Geesteranus (1980, 1992a, 1992b) proposed an infrageneric classification of *Mycena*, based on a combination of macroscopic and microscopic features. In this classification, the species are defined macroscopically based on basidiomata colour (pileus, stipe and lamellae face and edge). Within *Mycena*, species of sect. *Adonideae* (Fr.) Quél., now treated as *Atheniella* Redhead, Moncalvo, Vilgalys, Desjardin & B.A. Perry, sect. *Aciculae* Kühner ex Singer and sect. *Oregonenses* Maas Geest., are well characterised by their bright colours, such as pink, red, white or yellow (Maas Geesteranus 1980). Members of sect. *Calodontes* (Fr. ex Berk.) Quél. are prominently violet and dark colours can also be observed in sect. *Rubromarginatae* Singer ex Maas Geest. (Robich 2003, 2016; Aravindakshan and Manimohan 2015; Aronsen and Læssøe 2016). In addition, the microscopic characters are also considered to be very important in the infrageneric division of *Mycena*, containing basidiospores, cheilocystidia, pileipellis and stipitipellis (Maas Geesteranus 1992a, 1992b; Robich 2003, 2016; Aravindakshan and Manimohan 2015; Aronsen and Læssøe 2016). No current published framework exists for the genus as a whole, however and the morphologically based classification of Maas Geesteranus (1992a, 1992b) has not been fully tested and validated. Some recent studies indicate that several *Mycena* sections, for example, sects. *Amparoina* T. Bau & Q. Na, *Calodontes* (Fr. Ex Berk.) Quél and *Sacchariferae* Kühner ex Singer, are apparently monophyletic, whereas others are not (Harder et al. 2010; Na and Bau 2019b). Several taxa, traditionally assigned to *Mycena*, such as the *Atheniella* group, have been removed from the genus and others may need to be incorporated into genera, such as *Cruentomycena* R.H. Petersen, Kovalenko & O.V. Morozova, *Favolaschia* (Pat.) Pat., *Hemimycena* Singer, *Panellus* P. Karst., *Resinomycena* Redhead & Singer and *Roridomyces* Rexer (Redhead and Singer 1981; Rexer 1994; Antonín and Noordeloos 2004; Petersen et al. 2008; Redhead et al. 2012).

Eight bluish *Mycena* in four sections have been documented so far. Amongst these species, five have been reported from the Northern Hemisphere: *M. subcaerulea* Sacc. in North America, *M. amicta* (Fries) Quél. and *M. cyanorhiza* Quél. in Europe, *M. indigotica* Wei & Kirschner and *M. lazulina* Har. Takah., Taneyama and Terashima & Oba in Asia (Smith 1947; Maas Geesteranus 1980, 1992a, 1992b; Perry 2002; Robich 2003; Aronsen and Læssøe 2016; Terashima et al. 2016; Wei and Kirschner 2019; Perry et al. 2020). A bluish tint is often present on the pileus or stipe of these five species, four of them being classified into three sections: sect. *Amictae* Alexander H. Smith ex Maas Geesteranus, sect. *Sacchariferae* and sect. *Viscipelles* Kühner, but *M. indigotica* has tubes confused with members of *Favolaschia* (Pat.) Pat. and not assigned any section (Smith 1947; Maas Geesteranus 1980, 1992a, 1992b; Perry 2002; Robich 2003; Aronsen and Læssøe 2016; Terashima et al. 2016; Wei and Kirschner 2019; Perry et al. 2020). The three known bluish *Mycena* species from the Southern

Hemisphere are *M. caesiocana* Singer, *M. cyanosyringea* Singer and *M. interrupta* (Berkeley) Sacc. (Singer 1969; Singer and Gomez 1982; Grgurinovic 2003). These species are distributed in Oceania and South America, Australia, Chile, Costa Rica, New Caledonia and New Zealand, where they usually grow on dead woods, decaying logs or tree stumps in deciduous forests of trees, such as *Eucalyptus robusta* Smith and *Persea lingue* (Ruiz & Pav.) Nees and develop basidiomata under high temperatures (Singer 1969; Singer and Gomez 1982; Grgurinovic 2003). The three allied species can be easily recognised: *M. caesiocana* and *M. cyanosyringea* are well characterised by the presence of a storm-grey pileus and extremely small basidiomata (pileus diameter and stipe length all less than 3 mm) and *M. interrupta* has a blue stipe base (Singer 1969; Singer and Gomez 1982; Grgurinovic 2003). In addition, *M. cyanocephala* Singer described from Chile, is considered to be synonymous with *M. interrupta* (Grgurinovic 2003). Although *M. cyanorhiza*, from the Northern Hemisphere, also has a blue stipe base similar to *M. interrupta*, but differs in pale brown to pale grey pileus and smaller basidiospores and cheilocystidia (Robich 2003; Aronsen and Læssøe 2016; Perry et al. 2020).

To date, fewer than 100 species of *Mycena* have been documented from China; amongst them, 14 new species have been described in recent years (He and Fang 1994; Guo et al. 1999; Shih et al. 2014; Li et al. 2015; Na and Bau 2018, 2019a, 2019b; Liu et al. 2021). During our investigations of mycenoid fungi in north-western China, we discovered two putative new taxa possessing a blue pileus with a greyish or brownish tint and a gelatinous pileipellis, clearly distinct from other species of *Mycena*, in the Liupan and Changbai Mountains. The results of our morphological observations and phylogenetic analyses support the introduction of these two new taxa.

Materials and methods

Morphology

Macromorphological observations were made on fresh specimens in the field and from photographs, with colour terms and notation following Kornerup and Wanscher (1978). Specimen pieces were mounted in 5% potassium hydroxide (KOH) and stained with Congo red when necessary. The prepared specimens were observed under a Lab A1 microscope (Carl Zeiss AG, Jena, Germany) and photographed and recorded using the supplied ZEN 2.3 (blue edition) software (Carl Zeiss AG). Melzer's Reagent was used to test whether spores and tissues were amyloid and dextrinoid (Horak 2005). The dimensions of basidiospores were recorded according to Ge et al. (2021), Liu et al. (2021) and Na et al. (2021, 2022). The examined collections have been deposited in the Fungarium of the Fujian Academy of Agricultural Sciences (FFAAS), China. In the subsequent taxonomic description, author abbreviations follow Index Fungorum (http://www.indexfungorum.org).

Phylogenetic analysis

Genomic DNAs of the putative new species were extracted from dried materials using a NuClean PlantGen DNA kit (Kangwei Century Biotechnology, Beijing, China). The internal transcribed spacer (ITS) region and the nuclear large subunit (nLSU) of nuclear ribosomal DNA were amplified using the PCR cycling protocol detailed in Ge et al. (2021) with primers ITS1/ITS4 and LR0R/LR7, respectively (White et al. 1990; Hopple and Vilgalys 1999). In addition, no sequence information has been published for *M. subcaerulea* and only a few ITS sequences of *M. cyanorhiza* and *M. amicta*, which were found to be phylogenetically closely related to the new species, are available in GenBank. For three *M. subcaerulea* specimens, we tried to obtain our target sequences by using next-generation sequencing (NGS) technology and whole-genome sequencing of the specimens was performed on the Illumina sequencing platform (HiSeq PE150) with standard procedures. The 150 bp paired-end libraries were prepared to generate approximately 3G raw data. ITS (GenBank accessions KT900146, NR_154169) and nLSU (GenBank accessions MK629349 and NG_070530) were randomly selected for using as custom seed and custom label databases according to the instructions (https://github.com/Kinggerm/GetOrganelle/wiki/FAQ: How to assemble custom loci?) of the software programme GetOrganelle (Jin et al. 2020). Finally, two ITS sequences (GenBank accessions OL711671 and OL711672) and three nLSU sequences (OL711666, OL711667 and OL711668) were captured from next-generation sequencing data of three specimens (TENN-F-051121, TENN-F-057919 and CUP-A-015335) of *M. subcaerulea* and used for subsequent analysis. Thirteen sequences (six ITS and seven nLSU) newly generated in this study were deposited in GenBank. Additionally, a total of 103 ITS and nLSU sequences (including *Xeromphalina campanella* [Batsch] Kühner & Maire, which is often chosen as an outgroup for *Mycena*) were retrieved from GenBank for use in the phylogenetic analysis. Information on all analysed sequences (116) is given in Table 1. Generated sequences and those retrieved from GenBank were aligned and manually checked using BioEdit 7.0.4.1 and Clustal X 1.81 (Thompson et al. 1997; Hall 1999), with gaps in the alignment treated as missing data. The ITS and nLSU datasets were aligned separately. After estimating the optimal model of nucleotide evolution for the two partitions independently using Modeltest 3.7 (Posada and Crandall 1998), the two datasets were concatenated. The combined aligned dataset, which was deposited in TreeBase (submission ID 29069; study accession URL: http://purl.org/phylo/treebase/phylows/study/TB2:S29069), was subjected to Bayesian Inference (BI) and Maximum Likelihood (ML) phylogenetic analyses. The BI analysis was performed in MrBayes 3.2.6 (Ronquist and Huelsenbeck 2003). For the BI analysis, Markov Chain Monte Carlo chains were run for two million generations, with sampling carried out every 100th generation until the critical value for the topological convergence diagnostic was less than 0.01 (Ronquist and Huelsenbeck 2003). The ML analysis, with a rapid bootstrapping algorithm involving 1,000 replicates, was performed in raxmlGUI 1.5b1 (Stamatakis et al. 2005).

Table 1. Specimens along with GenBank accession numbers used in the phylogenetic analysis. Sequences newly generated in this study are indicated in bold.

No.	Species	Voucher	Origin	ITS ID	LSU ID	References
1.	*Mycena abramsii*	231a	Venice	JF908400	—	Unpublished
2.	*M. abramsii*	HMJAU 43282	China	MH396626	MK629348	Unpublished
3.	*M. abramsii*	HMJAU 43468	China	MH396627	—	Unpublished
4.	*M. abramsii*	KA12-0434	Korea	KR673481	—	Kim et al. (2015)
5.	*M. adscendens*	Aronsen120803	Norway	KT900140	—	Aronsen and Larsson (2015)
6.	*M. adscendens*	Orstadius329-05	Norway	KT900141	—	Aronsen and Larsson (2015)
7.	*M. adscendens*	Aronsen061119	Norway	KT900142	—	Aronsen and Larsson (2015)
8.	*M. adscendens*	Aronsen120826	Norway	KT900143	—	Aronsen and Larsson (2015)
9.	*M. albiceps*	MGW1504	USA	KY744173	MF797661	Unpublished
10.	*M. albiceps*	SAT1518708	USA	KY777372	MF797659	Unpublished
11.	*M. alnetorum*	CM14-RG2	USA	KU295552	—	Unpublished
12.	*M. amicta*	189f	Italy	JF908394	—	Osmundson et al. (2013)
13.	*M. amicta*	4745-HRL 1312	Canada	KJ705188	—	Unpublished
14.	*M. amicta*	CBS 352.50	France	MH856655	—	Vu et al. (2019)
15.	*M. amicta*	CBS 254.53	France	MH857183	—	Vu et al. (2019)
16.	*M. amicta*	CBS 257.53	France	MH857184	MH868722	Vu et al. (2019)
17.	*M. amicta*	H6036851	Finland	MW540687	—	Unpublished
18.	*M. arcangeliana*	252b	Italy	JF908401	—	Osmundson et al. (2013)
19.	*M. arcangeliana*	252f	Italy	JF908402	—	Osmundson et al. (2013)
20.	***M. caeruleogrisea***	**FFAAS 0001 Holotype**	**China**	**MW051896**	**OL711662**	**This study**
21.	***M. caeruleogrisea***	**FFAAS 0002**	**China**	**MW051897**	**OL711663**	**This study**
22.	***M. caeruleomarginata***	**FFAAS 0357 Holotype**	**China**	**OL711669**	**OL711664**	**This study**
23.	***M. caeruleomarginata***	**FFAAS 0358**	**China**	**OL711670**	**OL711665**	**This study**
24.	*M. chlorophos*	ACL257	Malaysia	KJ206983	—	Chew et al. (2015)
25.	*M. chlorophos*	ACL271	Malaysia	KJ206986	—	Chew et al. (2015)
26.	*M. cinerella*	Aronsen051014	Norway	KT900146	—	Aronsen and Larsson (2015)
27.	*M. cinerella*	173	Russia	MF926553	—	Malysheva et al. (2017)
28.	*M. citrinomargina*ta	317h	Italy	JF908416	—	Osmundson et al. (2013)
29.	*M. citrinomargina*ta	AD4TN	Tunisia	KU973883	—	Unpublished
30.	*M. clavicular*is	615i	Italy	JF908466	—	Osmundson et al. (2013)
31.	*M. clavicularis*	615b	Italy	JF908467	—	Osmundson et al. (2013)
32.	*M. cyanorhiza*	120b	Italy	JF908385	—	Osmundson et al. (2013)
33.	*M. deeptha*	DM334g	India	JX481737	—	Aravindakshan et al. (2012)
34.	*M. diosma*	KA13-1230	Korea	KR673698	—	Kim et al. (2015)
35.	*M. diosm*a	320f	Italy	JF908417	—	Osmundson et al. (2013)
36.	*M. entolomoides*	HMJAU 43048	China	MG654736	—	Na and Bau (2018)
37.	*M. entolomoides*	HMJAU 43052	China	MG654737	MK722348	Na and Bau (2018)
38.	*M. entolomoides*	HMJAU 43126	China	MG654738	MK722349	Na and Bau (2018)
39.	*M. filopes*	3782	Canada	KJ705175	—	Unpublished
40.	*M. filopes*	KA12-1699	Korea	KR673631	—	Kim et al. (2015)
41.	*M. filopes*	287f	Italy	JF908410	—	Osmundson et al. (2013)
42.	*M. galericulata*	DM136-40516	USA	OM212953	—	Unpublished
43.	*M. galericulata*	LXL71	China	MZ669083	—	Unpublished
44.	*M. galericulata*	F26441	USA	MZ317346	—	Unpublished
45.	*M. galericulata*	EP.19-A1625	Greece	MT458520	—	Unpublished
46.	*M. galericulata*	50	Norway	MW576935	—	Unpublished
47.	*M. galericulata*	TFB14649	USA	MN088382	—	Unpublished
48.	*M. illuminans*	ACL161	Malaysia	KJ206975	—	Chew et al. (2015)
49.	*M. illuminans*	ACL175	Malaysia	KJ206976	—	Chew et al. (2015)
50.	*M. illuminans*	ACL212	Malaysia	KJ206980	—	Chew et al. (2015)
51.	*M. leaiana*	1028	Italy	JF908376	—	Osmundson et al. (2013)
52.	*M. leaiana*	CNH03 (TENN)	USA	MF686520	—	Unpublished
53.	*M. meliige*na	39	Italy	JF908423	—	Osmundson et al. (2013)
54.	*M. meliigena*	39d	Italy	JF908429	—	Osmundson et al. (2013)
55.	*M. metata*	313b	Italy	JF908412	—	Osmundson et al. (2013)
56.	*M. olivaceomarginata*	GG436-86	Svalbard	GU234119	—	Geml et al. (2015)
57.	*M. olivaceomarginata*	CBS 228.47	France	MH856228	MH867756	Vu et al. (2019)

No.	Species	Voucher	Origin	ITS ID	LSU ID	References
58.	*M. olivaceomarginata*	CBS 229.47	France	MH856229	MH867757	Vu et al. (2019)
59.	*M. olivaceomarginata*	HK47-15	Norway	MT153141	—	Thoen et al. (2020)
60.	*M. pachyderma*	979a	Italy	JF908491	—	Osmundson et al. (2013)
61.	*M. pearsoni*ana	FCME25817	USA	JN182198	—	Harder et al. (2012)
62.	*M. pearsoniana*	TENN61544	USA	JN182199	—	Harder et al. (2012)
63.	*M. pearsoniana*	TENN61384	USA	JN182200	—	Harder et al. (2012)
64.	*M. pelianthina*	CBH164	Denmark	FN394548	—	Unpublished
65.	*M. pelianthi*na	108b	Italy	JF908379	—	Osmundson et al. (2013)
66.	*M. pelianthina*	108f	Italy	JF908380	—	Osmundson et al. (2013)
67.	*M. plumbea*	JN198391	China	JN198391	—	Wu et al. (2013)
68.	*M. plumbea*	420526MF0010	China	MG719769	—	Unpublished
69.	*M. polygramma*	439b	Italy	JF908433	—	Osmundson et al. (2013)
70.	*M. polygramma*	439f	Italy	JF908434	—	Osmundson et al. (2013)
71.	*M. pu*ra	TENN65043	USA	JN182202	—	Harder et al. (2012)
72.	*M. pura f. a*lba	CBH410	USA	FN394595	—	Unpublished
73.	*M. purpureofus*ca	SL09-06	Canada	HQ604766	—	Unpublished
74.	*M. purpureofusca*	G. Alfredsen	Norway	JQ358809	—	Unpublished
75.	*M. ros*ea	938a	Italy	JF908488	—	Osmundson et al. (2013)
76.	*M. ros*ea	Champ-21	Spain	KX449424	—	Pérez-Izquierdo et al. (2017)
77.	*M. rubromarginata*	407q	Italy	JF908430	—	Osmundson et al. (2013)
78.	*M. rubromarginata*	TL-12780	USA	KX513845	KX513849	Perry and Desjardin (2016)
79.	*M. seminau*	ACL136	Malaysia	KF537250	KJ206952	Chew et al. (2015)
80.	*M. seminau*	ACL308	Malaysia	KF537252	KJ206964	Chew et al. (2015)
81.	*M. seynesii*	71l	Italy	JF908469	—	Osmundson et al. (2013)
82.	*M. seynesii*	71h	Italy	JF908470	—	Osmundson et al. (2013)
83.	*M. silvae-nigrae*	515	Italy	JF908452	—	Osmundson et al. (2013)
84.	*M. silvae-nigrae*	CC 13-12	USA	KF359604	—	Baird et al. (2014)
85.	*M. stylobates*	455	Italy	JF908439	—	Osmundson et al. (2013)
86.	***M. subcaerul***ea	**TENN-F-051121**	**USA**	**OL711671**	**OL711666**	**This study**
87.	***M. subcaerulea***	**TENN-F-057919**	**USA**	**OL711672**	**OL711667**	**This study**
88.	***M. subcaerulea***	**CUP-A-015335**	**USA**	**—**	**OL711668**	**This study**
89.	*M. supina*	128a	Italy	JF908388	—	Osmundson et al. (2013)
90.	*M. tenax*	p187i	USA	EU669224	—	Unpublished
91.	*M. tenax*	OSC 113746	USA	EU846251	—	Unpublished
92.	*M. viridimarginata*	104h	Italy	JF908378	—	Osmundson et al. (2013)
93.	*M. vulgaris*	447h	Italy	JF908435	—	Osmundson et al. (2013)
94.	*M. vulgaris*	3781	Canada	KJ705177	—	Unpublished
95.	*M. zephirus*	KA13-1265	Korea	KR673722	—	Kim et al. (2015)
96.	*Xeromphalina campanella*	TFB14487	USA	KP835678	KM011910	Aldrovandi et al. (2015)
97.	*X. campanella*	TFB7283A	USA	KM024575	KM024671	Aldrovandi et al. (2015)

Results

Phylogenetic analysis

BI and ML reconstructions, based on the optimal evolutionary model selected for the ITS and nLSU partitions (GTR + I + G), recovered similar topologies. The BI tree was selected as a representative phylogeny (Fig. 1).

In the tree shown in Fig. 1, which is based on 116 concatenated ITS+nLSU sequences of 43 *Mycena* species and the new taxa, the two samples of *M. caeruleogrisea* and the two samples of *M. caeruleomarginata* each form monophyletic lineages with high statistical support (*M. caeruleogrisea*, ML bootstrap support [BS] = 100, Bayesian posterior probability [BPP] = 1.00; *M. caeruleomarginata*, BS = 100, BPP = 1.00). According to the tree topology, *M. subcaerulea* is the species most closely related to *M. caeruleogrisea* and *M. caeruleomarginata*, consistent with morphology and clusters

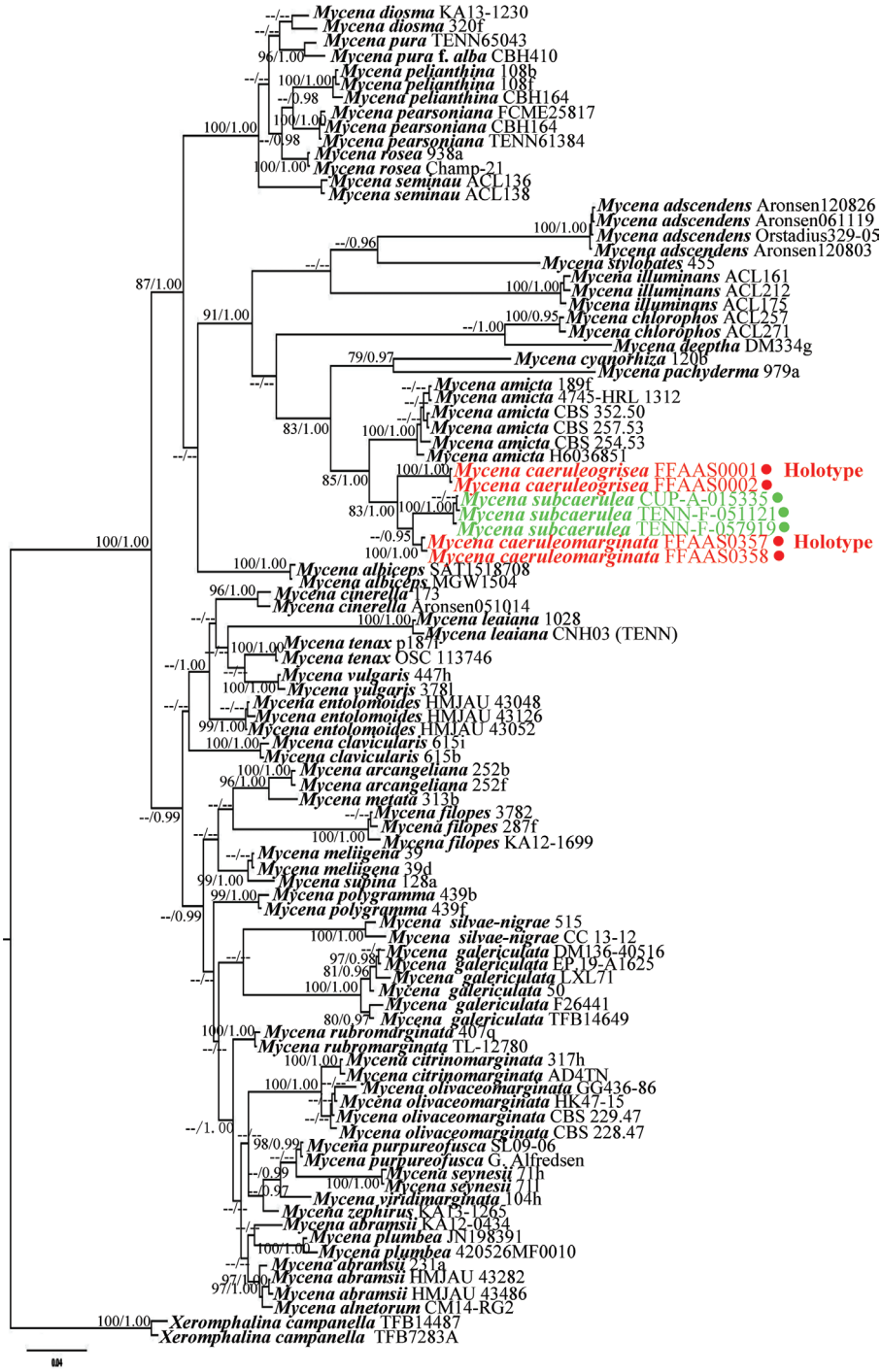

Figure 1. Phylogenetic tree inferred from partial ITS+nLSU sequence data by Bayesian inference and maximum likelihood. The tree is rooted with *Xeromphalina campanella*. Maximum likelihood support values (BS) ≥ 75 and Bayesian posterior probabilities (BPP) ≥ 0.95 are indicated above or below branches (BS/BPP). Red dots indicate two new species, while green dots indicate *Mycena subcaerulea* specimens from TENN and CUP.

with the latter two species with high statistical support (BS = 100, BPP = 1.00). The *M. subcaerulea* clade comprises three samples: CUP-A-015335 (originally identified as *M. cyanothrix* G.F. Atk.), TENN-F-051121 and TENN-F-057919 (BS = 100, BPP = 1.00). By its morphological features and phylogenetic placement, sample CUP-A-015335 should be re-assigned to *M. subcaerulea*. The clade comprising *M. subcaerulea* and the two new taxa are sister to *M. amicta*, with the clade constituted by these four species in turn sister to *M. cyanorhiza*. Despite the close relationships, the two new species are strongly supported as distinct from *M. amicta* and *M. cyanorhiza* (Fig. 1).

It is noteworthy that the six samples of *M. amicta* from Europe and North America cluster together with strong support (BS = 100, BPP = 1.00), but the Canadian material (voucher no. 189f) seems to be closer to the Italian sample (voucher no. 4745-HRL 1312) than to the specimens from France and Finland. In addition, *M. pachyderma* Kühner, a non-bluish species in sect. *Viscipelles*, is a sister taxon (BS = 79, BPP = 0.97) to *M. cyanorhiza* in the same section.

Taxonomy

In addition to morphological studies of the new taxa collected in China, morphological observations were made on 17 bluish specimens of *Mycena* loaned from fungal herbaria in the USA, namely, four specimens from the University of Tennessee (TENN) and 13 specimens from University of Cornell (CUP).

Our morphological observations using a light microscope confirmed the identity of 12 specimens as *M. subcaerulea*: TENN-F-014183, TENN-F-051121, TENN-F-052683, TENN-F-057919, CUP-A-002382, CUP-A-009686, CUP-A-014679, CUP-A-015138, CUP-A-015335, CUP-A-022677, CUP-A-023037 and CUP-A-023304. Another specimen, CUP-A-021234, previously identified as *M. iris*, was well characterised as *M. amicta*, based on its elongated ellipsoid basidiospores and clavate cheilocystidia with a rounded apex. As already noted by Smith (1947), the basidiomata of CUP-A-018443, CUP-A-022667, CUP-A-051322 and CUP-A-051323 were too small to be examined.

Mycena caeruleogrisea **Q. Na, Y.P. Ge & H. Zeng, sp. nov.**
MycoBank No: MB837656
Figs 2, 3, 4

Diagnosis. This species is characterised by blue pileus, turning bluish-grey with age, pileus covered by a separable, gelatinous pellicle, stipe pruinose and with a blue base and stipe basal disc and acanathocysts of pileipellis absent. *Mycena subcaerulea* differs from *M. caeruleogrisea* by a greenish-blue to greyish-brown pileus that turns yellow and remains blue at the centre and margin with age, a greenish-blue to brownish-blue stipe and smaller, globose to subglobose basidiospores.

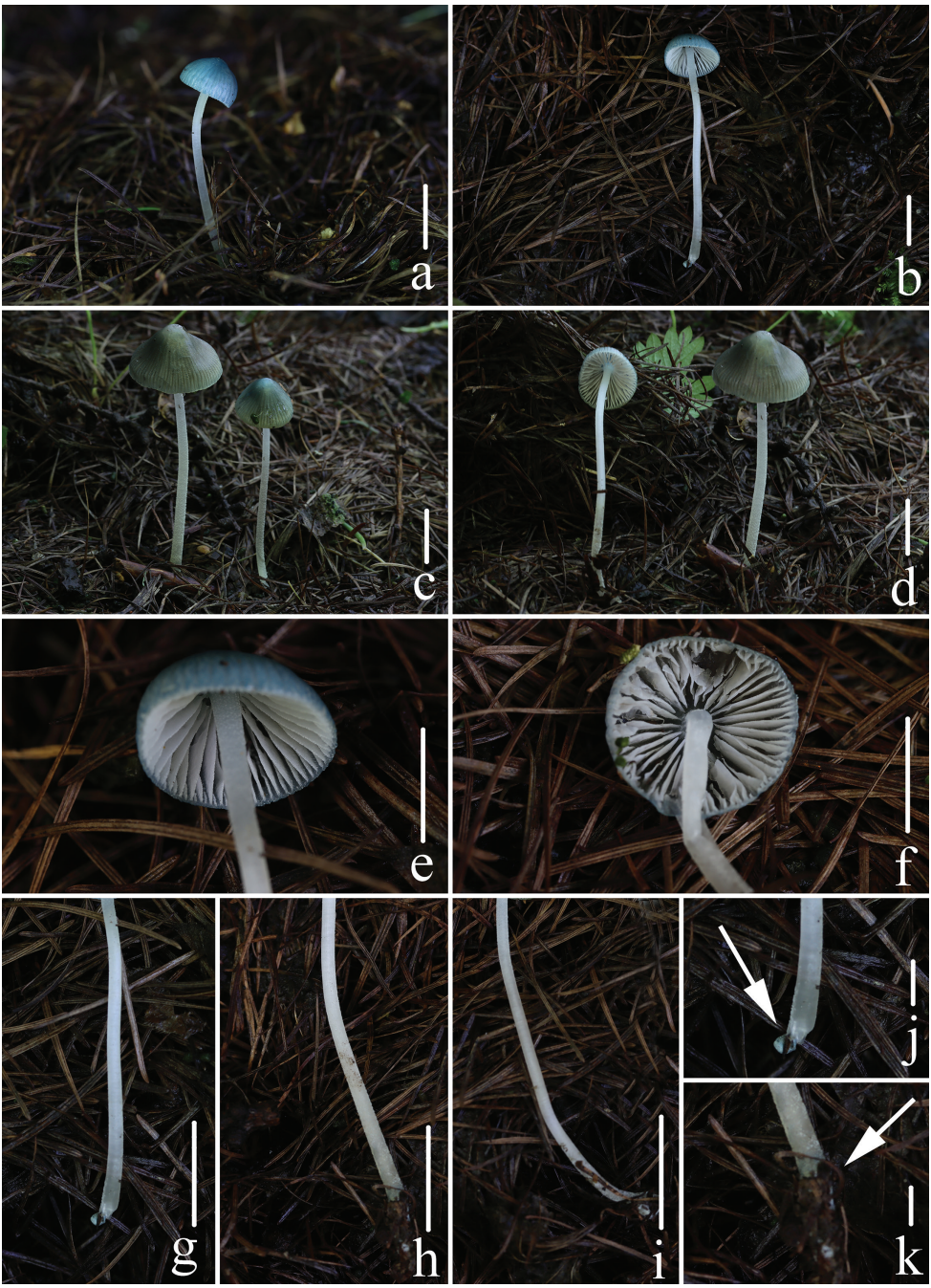

Figure 2. Fresh basidiomata of *Mycena caeruleogrisea* **a–d** *M. caeruleogrisea* (*FFAAS 0001*, holotype) **e, f** *M. caeruleogrisea* (*FFAAS 0002*) **g–i** entirely pruinose stipe **j, k** bluish base. Scale bars: 10 mm (**a–i**); 2 mm (**j–k**). Photographs by Yupeng Ge (**a, b**) and Qin Na (**c–k**).

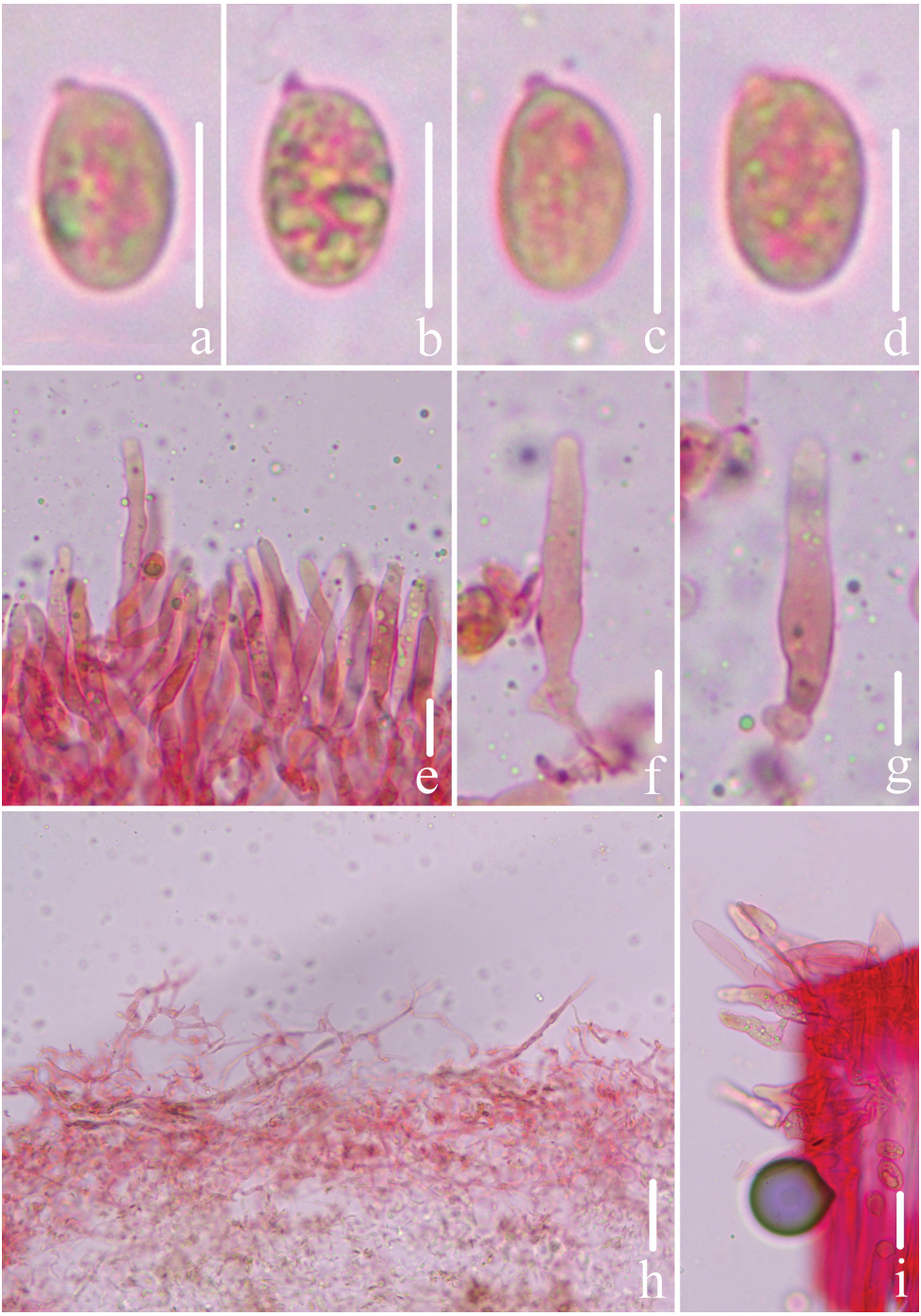

Figure 3. Microscopic features of *Mycena caeruleogrisea* (*FFAAS 0001*, holotype) **a–d** basidiospores **e–g** cheilocystidia **h** pileipellis **i** stipitipellis and caulocystidia. Scale bars: 10 μm (**a–i**). Structures were stained with Congo Red medium before photographing.

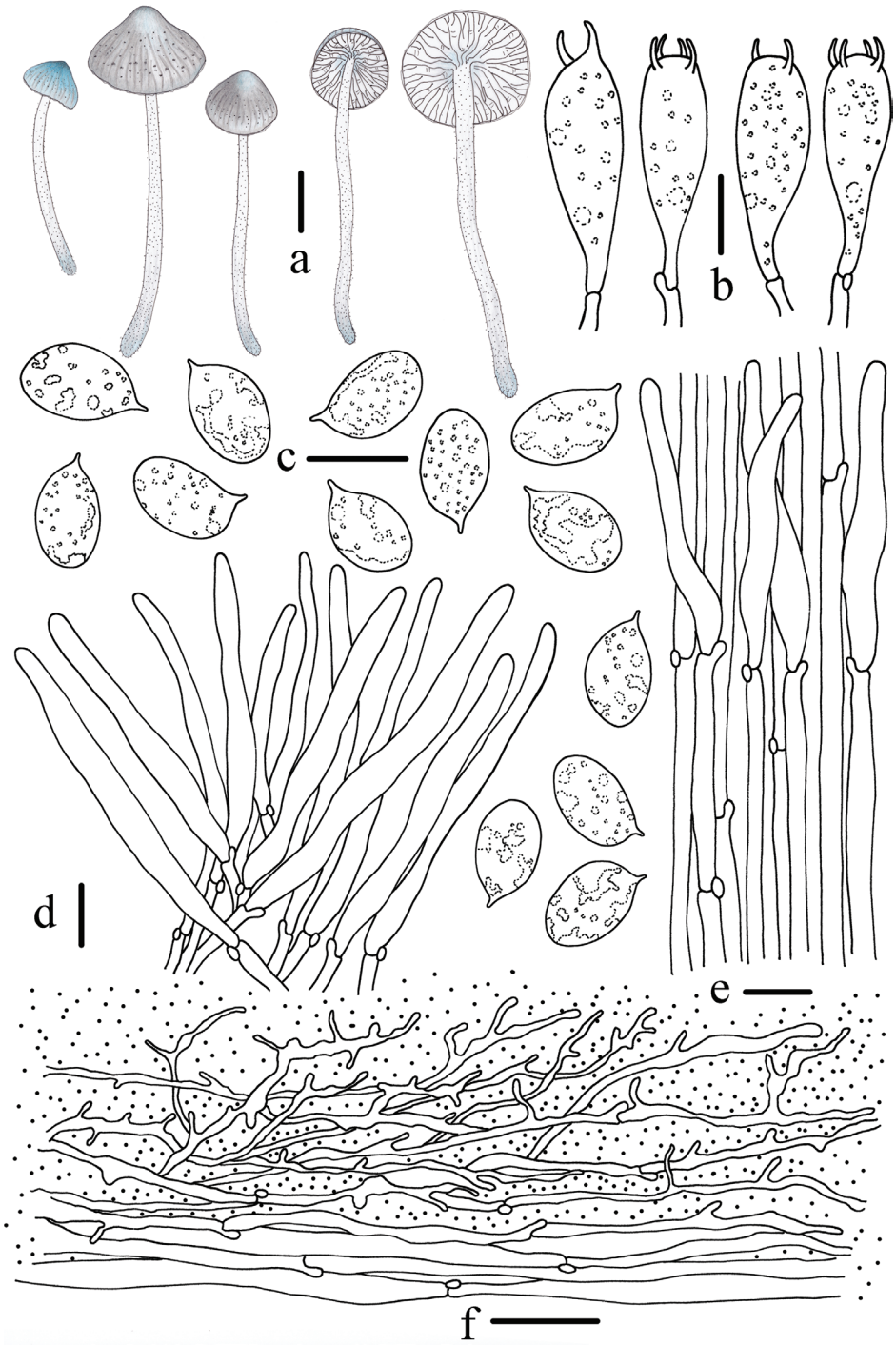

Figure 4. Morphological features of *Mycena caeruleogrisea* (*FFAAS 0001*, holotype) **a** basidiomata **b** basidia **c** basidiospores **d** cheilocystidia **e** stipitipellis and caulocystidia **f** pileipellis. Scale bars: 10 mm (**a**); 10 µm (**b–f**). Drawings by Qin Na and Yupeng Ge.

Holotype. China. Ningxia Hui Autonomous Region: Liangdianxia, Liupan Mountains National Forest Park, Jingyuan County, Guyuan City, 35°21'74"N, 106°18'37"E, 19 July 2020, Qin Na, Yupeng Ge, Hui Zeng, Junqing Yan and Zewei Liu, *FFAAS 0001* (collection number MY0164).

Etymology. Refers to the pileus colour: blue when young, becoming bluish-grey with age.

Description. Pileus 12–25 mm in diameter, hemispherical when young, conical, obtusely conical, campanulate with age, shallowly sulcate, translucently striate, almost smooth when young, becoming slightly brownish scaly at the centre, pruinose, with a glabrescent margin, dull blue (23D5) at the centre, margin pallescent to pastel blue (23A4), turning bluish-grey (23D2–23D3), a bit sticky, covered by a separable, gelatinous pellicle. Context white, thin, fragile. Lamellae 16–28 reaching the stem, adnate to slightly adnexed with a short tooth, narrowly spaced, white, with intervenose veins, edges concolorous with the face. Stipe 48–76 × 1.5–2.0 mm, equal or slightly broadened below, hollow, fragile, entirely pruinose (Fig. 2g–i), white, base greyish-blue (23B5) (Fig. 2j, k), covered with white fibrils, a basal disc absent. Odour and taste indistinctive.

Basidiospores [60/3/2] (8.8) 9.3–**10.4**–11.3 (11.8) × (5.5) 5.7–**6.5**–6.9 (7.3) µm [Q = 1.57–1.68, **Q** = ***1.60*** ± 0.072] [holotype [40/2/1] (9.1) 9.4–**10.3**–11.3 (11.6) × (5.6) 6.0–**6.5**–6.9 (7.2) µm, Q = 1.55–1.63, **Q** = ***1.59*** ± 0.049], ellipsoid, hyaline in 5% KOH, smooth, guttulate, thin-walled, amyloid. Basidia 22–29 × 7–9 µm, 4- or 2-spored, clavate. Cheilocystidia 40–62 × 4–6 µm, clustered, abundant, elongated clavate or cylindrical, apically broadly rounded, thin-walled, hyaline, forming a sterile lamellae edge. Pleurocystidia absent. Pileipellis an ixocutis with 1–4 µm wide hyphae, smooth or sparsely coated with simple cylindrical excrescences or inflated cells, 3–11 × 1–2 µm, embedded in gelatinous matter; acanathocysts absent. Hypodermium undifferentiated. Hyphae of the stipitipellis 3–8 µm in diameter, smooth, hyaline; caulocystidia 38–69 × 6–8 µm, long cylindrical, smooth, transparent. All tissues dextrinoid. Clamps present in all tissues.

Habit and habitat. Scattered on humus and fallen leaves in mixed forests of *Acer*, *Populus*, *Pinus* and *Quercus*.

Known distribution. Ningxia Hui Autonomous Region, China.

Additional material examined. Ningxia Hui Autonomous Region: Xiaonanchuan, Jingyuan County, Guyuan City, 20 July 2020, Qin Na, Yupeng Ge, Hui Zeng, Junqing Yan and Zewei Liu, *FFAAS 0002* (collection number MY0169).

Remarks. The original description of *M. subcaerulea* Sacc. was as follows: "*Pileo tenuissimo, campanulato v. convexo, striato, glabro, pallide cæruleo-viridi; stipite tenui, æquali, roseo-albo, subtiliter pruinoso; lamellis angustis, confertis, antice attenuatis, candidis; sporis subglobosis. 4 µ. d. Hab. In trunco fagineo in montibus Adirondack Amer. bor. – Cæspitosa, 5 cm. alta; pileus 8–13 mm. latus. Discus margine saturatius coloratus atque pileus cuticula secernibili obtectus.*" (Saccardo 1887). This North American species, which also has bluish basidiomata, is the taxon most closely resembling *M. caeruleogrisea* in both macro- and microscopic features; however, *M. subcaerulea* differs by a greenish-blue to greyish-brown pileus that turns yellow and remains blue at the centre and margin with age, a greenish-

blue to brownish-blue stipe and smaller, globose to subglobose, basidiospores [6–8 × 6–7(8) µm] (Saccardo 1887; Smith 1947). In addition, *M. subcaerulea* was found solitary, scattered or gregarious on debris, decaying wood or bark around the bases of living trees, especially of oak, but also occurring quite frequently on decaying wood of basswood, elm, beech and other hardwoods (Smith 1947). The following microscopic characteristics of *M. subcaerulea* were also observed on the 11 CUP-A and TENN-F specimens in our study: basidiospores 5.6–8.3 × 5.3–7.9 µm, globose to subglobose; basidia 19–24 × 6–8 µm, clavate, 4-spored; cheilocystidia 36–55 × 3–6 µm; pileipellis hyphae 2–4 µm wide, coated with cylindrical excrescences or inflated cells, 1.1–14.9 × 0.7–1.4 µm, embedded in gelatinous matter; hyphae of the stipitipellis 4–10 µm in diameter; caulocystidia 42–70 × 4–10 µm, fusiform or cylindrical, smooth; clamps present (Figs 5, 6). In *M. cyanorhiza*, the base of the stipe can be strikingly sky blue, but it has a pale brown, grey to almost white pileus, a stipe base arising from a patch of fine fibrils, clavate to obpyriform cheilocystidia with finger-like excrescences and basidiospores that are elongated ellipsoid (Q = 1.6–2.2); these features all contrast with those of the new species (Aronsen and Læssøe 2016; Perry et al. 2020) (Table 2). In addition, *M. amicta* can be easily mistaken for *M. caeruleogrisea*, as it sometimes also has a bluish pileus when mature and similarly-shaped basidiospores, cheilocystidia and caulocystidia, but *M. amicta* can be distinguished from the latter species in having a pileus generally more brownish with a bluish tinge more or less present, an indistinct to raphanoid odour, a greyish-brown stipe that has a blue to blue-green base and is covered with a dense, fairly coarse, white pubescence and smaller cheilocystidia (16–45 × 3.5–7 µm); in addition, *M. amicta* is restricted to growth on wood and woody debris (Robich 2003; Aronsen and Læssøe 2016) (Table 2). *Mycena interrupta*, which is well characterised by its acid blue to dull blue pileus and translucent stipe, is easily distinguished from *M. caeruleogrisea* by having smaller basidiomata, free lamellae, a white hirsute basal disc with blue margins on the stipe, broadly ellipsoid to subglobose spores and cheilocystidia covered with coarse excrescences (Grgurinovic 2003) (Table 2). *Mycena lazulina*, a new taxon reported from south-western Japan, possesses a blue stipe and cheilocystidia with numerous excrescences, which can be used to differentiate it from *M. caeruleogrisea* (Terashima et al. 2016). Another recently-described species of *Mycena* from Taiwan, *M. indigotica*, has blue basidiomata; however, the cap has tubes similar to *Boletus* and possesses globose basidiospores (Wei and Kirschner 2019).

Mycena caeruleomarginata **Q. Na & Y.P. Ge, sp. nov.**
MycoBank No: MB842100
Figs 7, 8, 9

Diagnosis. This species is characterised by dark brown pileus with a blue margin and the stipe densely pruinose, entirely covered with puberulous hairs and stipe basal disc and acanathocysts of pileipellis absent. *Mycena subcaerulea* differs from *M. caeruleogrisea* in having a pileus that is distinctly greyish-brown with a blue centre and margin, turning yellow with age, a stipe tinged greenish-blue and globose to subglobose basidiospores.

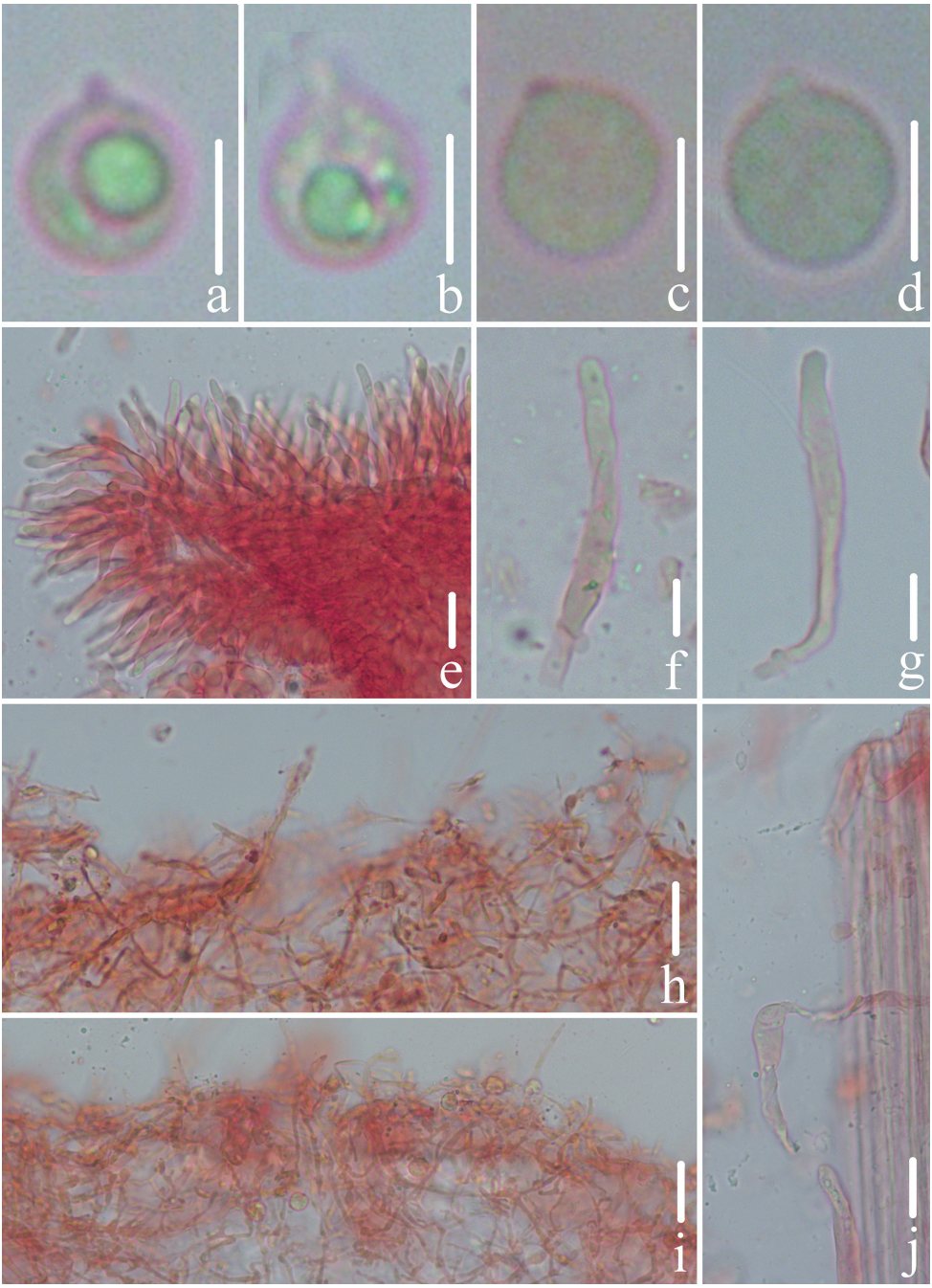

Figure 5. Microscopic features of *Mycena subcaerulea* **a, b** basidiospores (TENN-F-057919) **c** basidiospores (CUP-A-002382) **d** basidiospores (CUP-A-015138) **e–g** cheilocystidia (TENN-F-057919) **h, i** pileipellis (TENN-F-057919) **j** stipitipellis and caulocystidia (TENN-F-057919). Scale bars: 5 µm (**a–d**); 10 µm (**e–j**). Structures were stained with Congo Red medium before photographing.

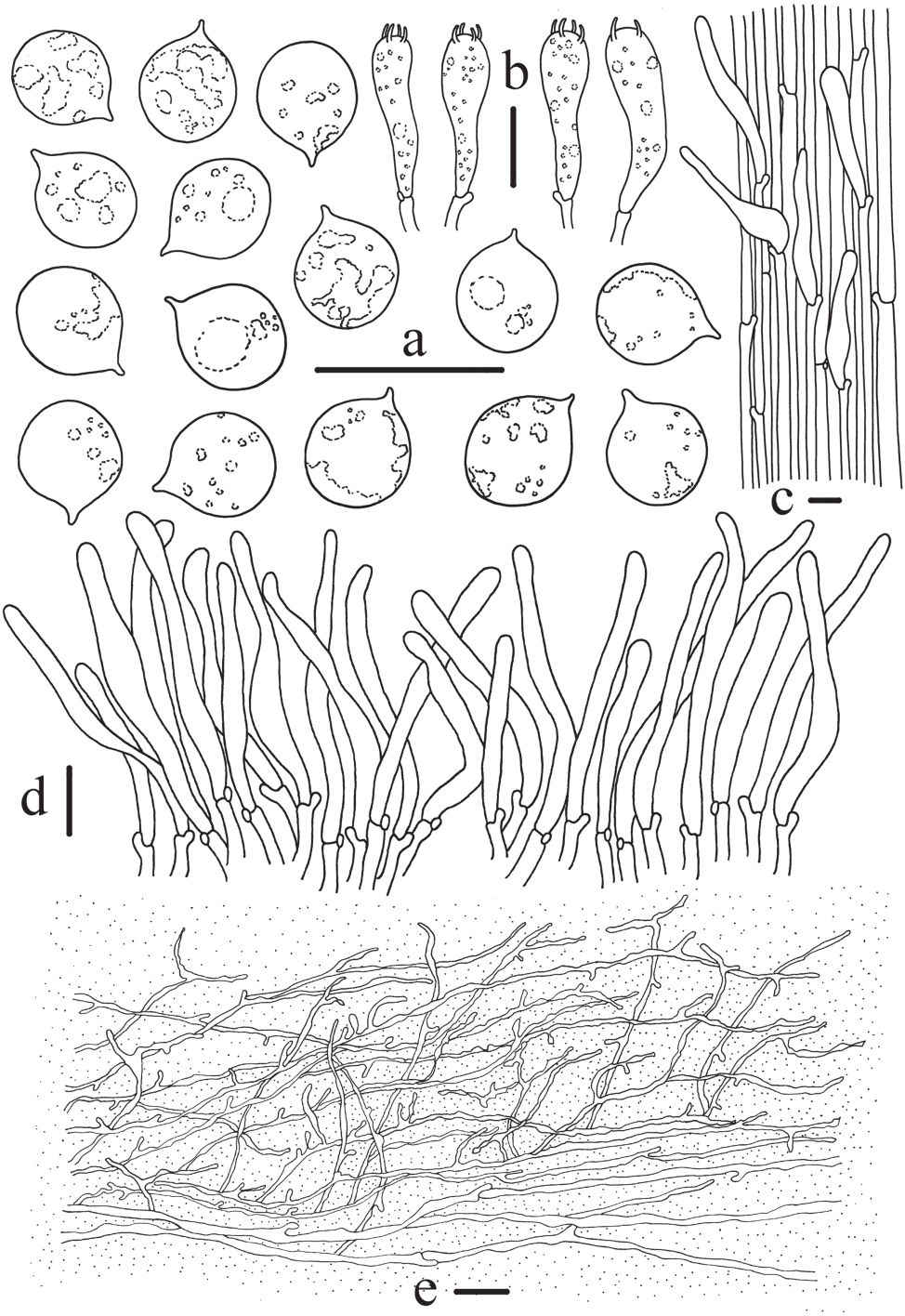

Figure 6. Morphological features of *Mycena subcaerulea* **a** basidiospores **b** basidia **c** stipitipellis and caulocystidia **d** cheilocystidia **e** pileipellis. Scale bars: 10 μm (**a–e**). Drawings by Qin Na and Yupeng Ge.

Holotype. China. Jilin Province: Chixi Protection Station, Erdaobaihe Town, Antu County, Yanbian Korean Autonomous Prefecture, 42°46'35"N, 128°15'04"E, 3 July 2021, Qin Na, Yupeng Ge, Binrong Ke and Chi Yang, *FFAAS 0357* (collection number MY0337).

Etymology. Refers to the pileus, which is blue at the margin.

Description. Pileus 3.5–13 mm in diameter, parabolic, obtusely conical when young, hemispherical, campanulate with age, with an umbo at the centre, shallowly sulcate, translucently striate, smooth, slightly gelatinous, the margin infrequently out of flatness, dark brown (6F5–6F7), disc brown (6E6–6E7), becoming greyish-blue (23B5) to blue (23B7) towards the margin (Fig. 7c, d, i), margin grey (23B1) (Fig. 7c, d, i), covered by a separable, viscid pellicle. Context white, fragile, thin. Lamellae 14–25 reaching the stem, adnate to slightly adnexed with a short tooth, white, inconspicuously intervenose, edges concolorous with the face. Stipe 32–46 × 1.0–2.0 mm, equal, base sometimes slightly broadened, fragile, hollow, pruinose, entirely puberulous when young (Fig. 7h), becoming sparingly so, especially in the middle part, when old (Fig. 7e), greyish-brown (5E3) to brown (5E4), base with an greyish-blue (23B5) tinge (Fig. 7a, f), sparsely covered with white fibrils, a basal disc absent. Odour and taste indistinctive.

Basidiospores [60/3/2] (6.2) 6.4–**7.1**–7.7 (7.9) × (4.4) 4.7–**5.2**–5.8 (6.0) µm [Q = 1.23–1.54, **Q** = ***1.36*** ± 0.071] [holotype [40/2/1] (6.4) 6.6–**7.2**–7.7 (7.8) × (4.7) 4.9–**5.2**–5.3 (5.7) µm, Q = 1.26–1.53, **Q** = ***1.39*** ± 0.070], broadly ellipsoid to ellipsoid, hyaline in 5% KOH, guttulate, smooth, thin-walled, amyloid. Basidia 26–35 × 6–12 µm, 4- or 2-spored, clavate. Cheilocystidia 32–48 × 4–6 µm, abundant, clustered, cylindrical or elongated clavate, apically broadly rounded, thin-walled, hyaline, forming a sterile lamellae edge. Pleurocystidia absent. Pileipellis an ixocutis with 2–4 µm wide hyphae, simple, cylindrical excrescences, 2–6 × 1–2 µm, embedded in gelatinous matter; acanathocysts absent. Hypodermium undifferentiated. Hyphae of the stipitipellis 3–6 µm in diameter, smooth, hyaline; caulocystidia smooth, transparent, of two shapes: (1) fusiform or cylindrical, 19–40 × 4–8 µm; (2) extremely long cylindrical, sometimes with a narrow apex, 115–178 × 5–9 µm. All tissues dextrinoid. Clamps present in all tissues.

Habit and habitat. Scattered on rotten wood in *Picea*, *Pinus*, *Quercus*, *Robinia* and *Tilia* mixed forests.

Known distribution. Jilin Province, China.

Additional material examined. Jilin Province: Hancongling, Erdaobaihe Town, Antu County, Yanbian Korean Autonomous Prefecture, 42°46'36"N, 128°15'04"E, 4 July 2021, Qin Na, Yupeng Ge, Binrong Ke and Chi Yang, *FFAAS 0358* (collection number MY0343).

Remarks. The diagnostic features of *M. caeruleomarginata* can be used to distinguish this new taxon from the closely-related bluish species *M. subcaerulea*, *M. cyanorhiza*, *M. amicta* and *M. interrupta* (Table 2). *Mycena subcaerulea*, the species most similar to *M. caeruleomarginata*, differs in having a pileus that is distinctly greyish-brown with a blue centre and margin, turning yellow with age, a stipe tinged greenish-blue and globose to subglobose basidiospores (Q = 1.01–1.14) according to the original description

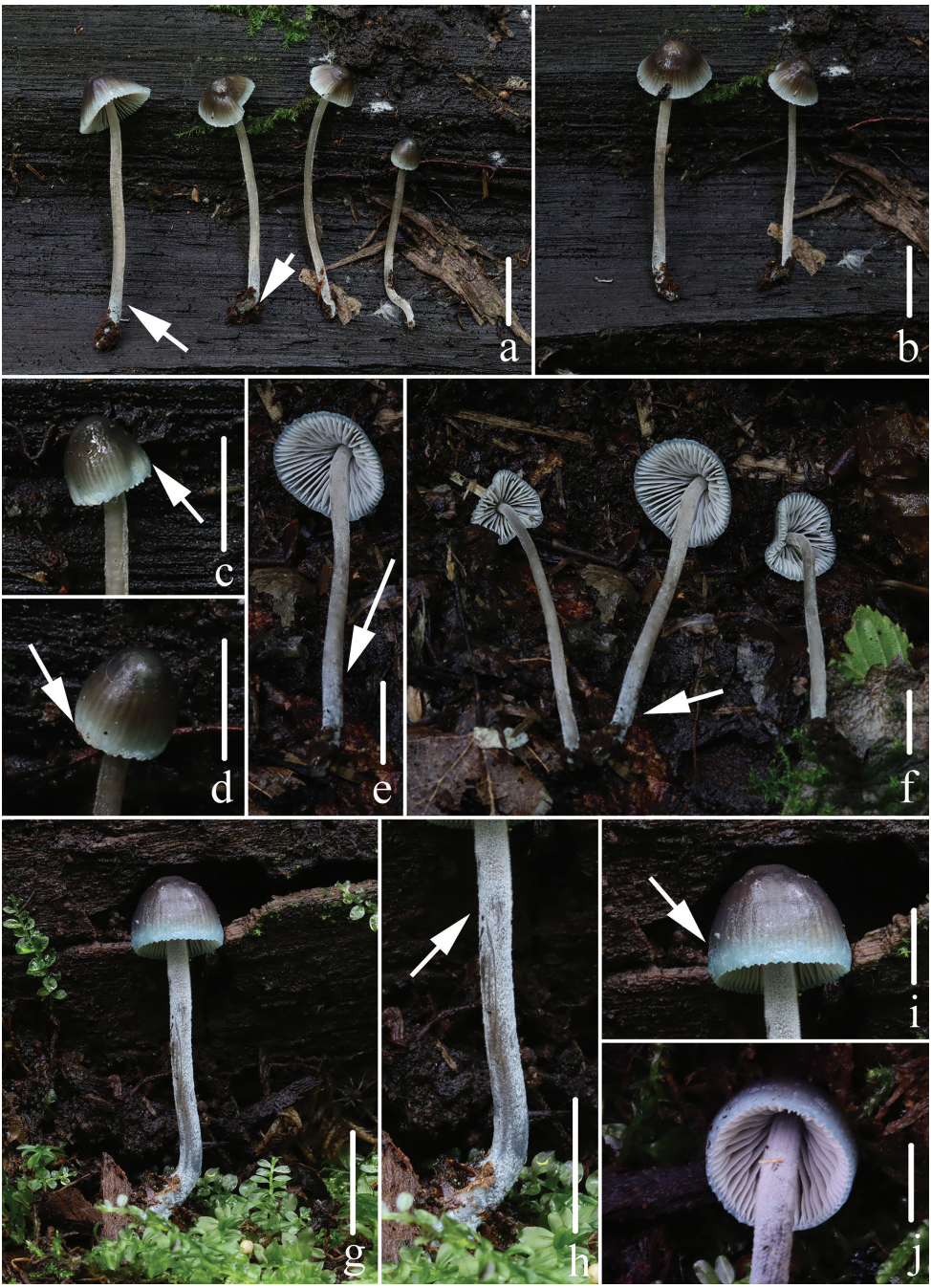

Figure 7. Fresh basidiomata of *Mycena caeruleomarginata* **a–f** *M. caeruleomarginata* (*FFAAS 0357*, holotype) **g–j** *M. caeruleomarginata* (*FFAAS 0358*) **a, f** stipe with a bluish base **c, d, i** pileus with blue margin **e, h** densely white, pruinose to pubescent stipe. Scale bars: 10 mm (**a, b, e, f, g, h**); 5 mm (**c, d**); 2 mm (**i, j**). Photographs by Qin Na (**a–f**) and Yupeng Ge (**g–j**).

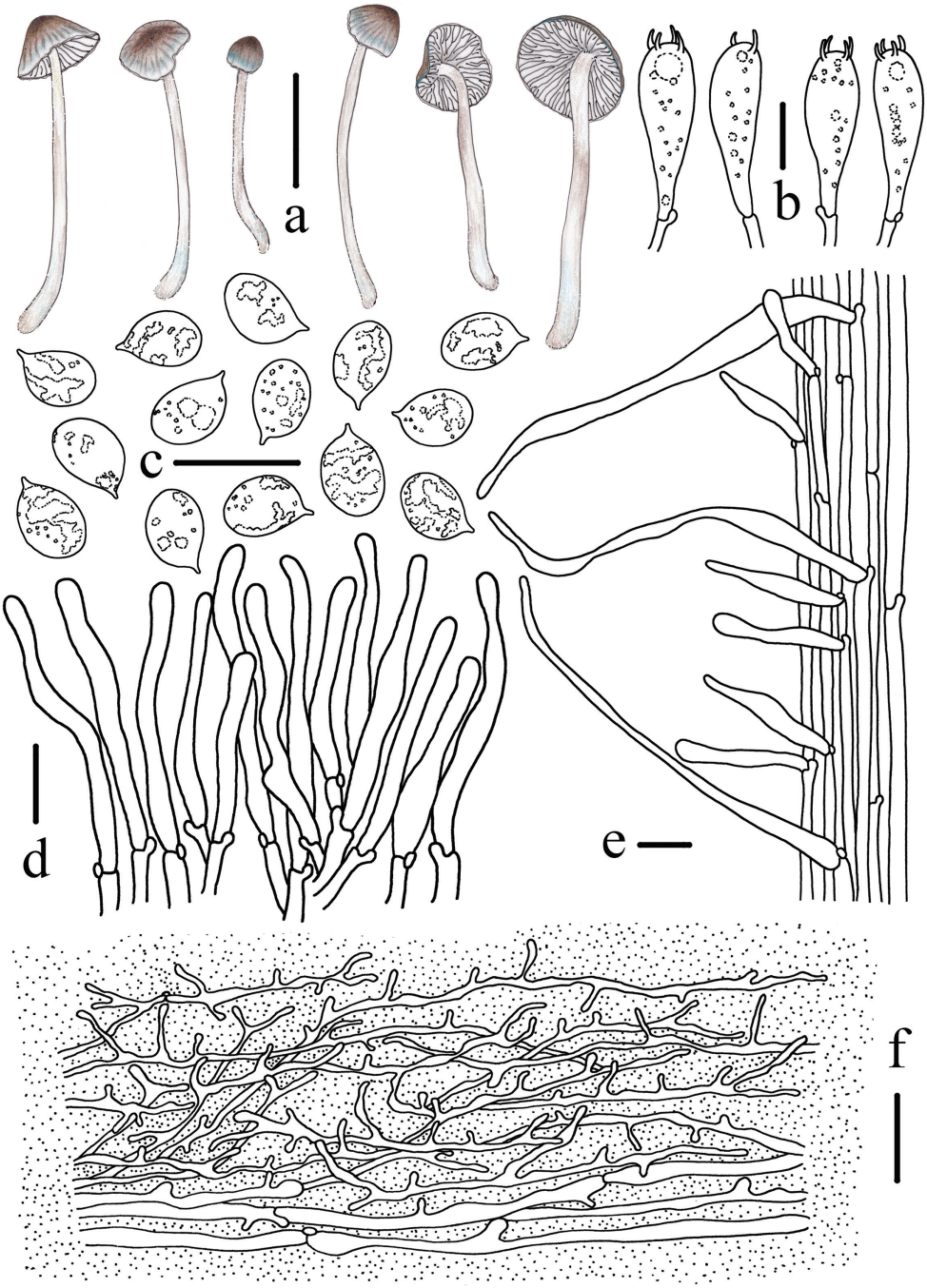

Figure 8. Morphological features of *Mycena caeruleomarginata* (*FFAAS 0357*, holotype) **a** basidiomata **b** basidia **c** basidiospores **d** cheilocystidia **e** stipitipellis and caulocystidia **f** pileipellis. Scale bars: 10 mm (**a**); 10 μm (**b–f**). Drawings by Qin Na and Yupeng Ge.

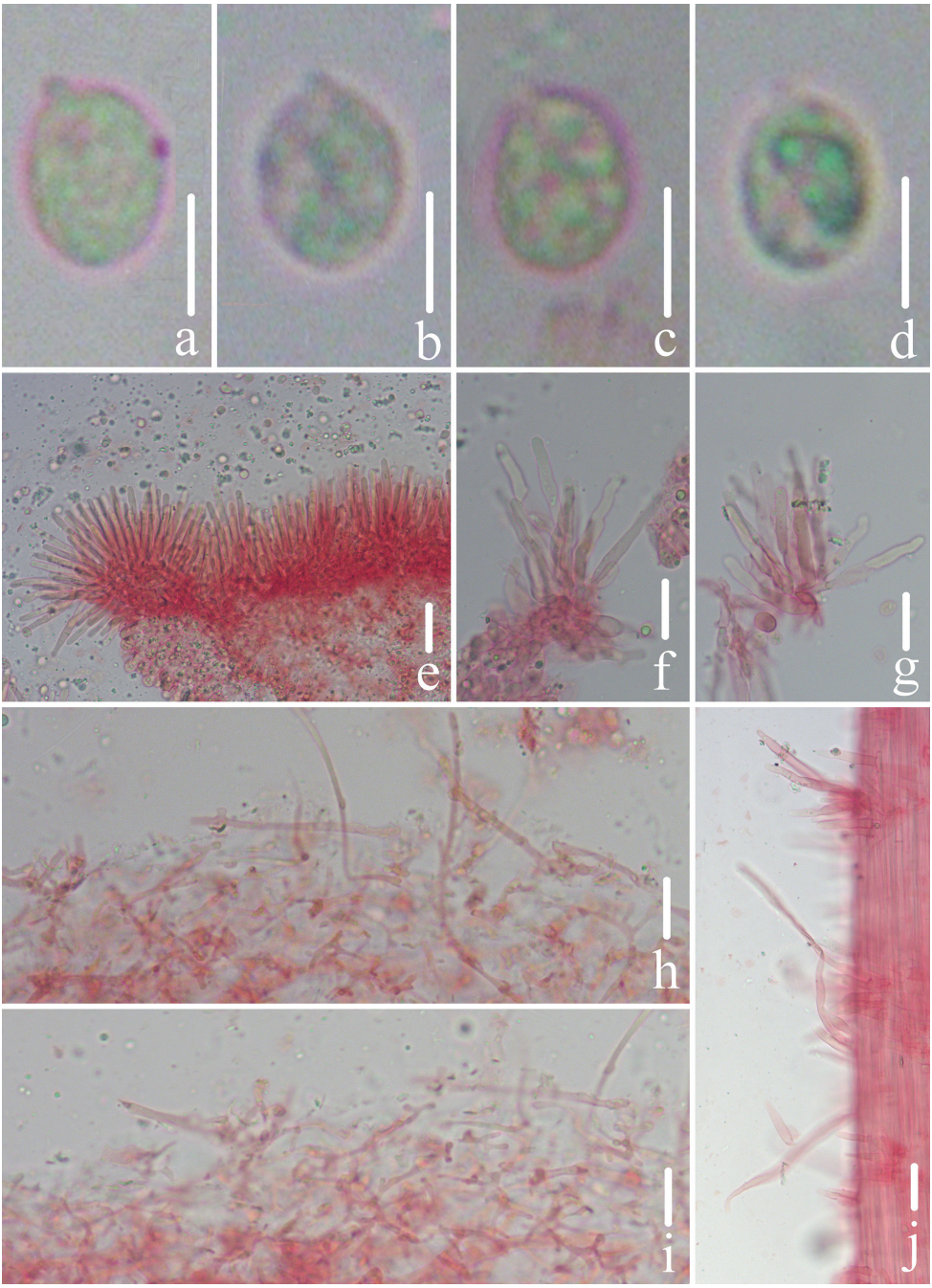

Figure 9. Microscopic features of *Mycena caeruleomarginata* (*FFAAS 0357*, holotype) **a–d** basidiospores **e–g** cheilocystidia **h–j** pileipellis **j** stipitipellis and caulocystidia. Scale bars: 5 µm (**a–d**); 10 µm (**e–j**). Structures were stained with Congo Red medium before photographing.

Table 2. Morphological comparison of *Mycena caeruleogrisea*, *M. caeruleomarginata*, and related species.

Taxa	*M. caeruleogrisea*	*M. caeruleomarginata*	*M. subcaerulea*	*M. amicta*	*M. cyanorhiza*	*M. interrupta*
Pileus	12–25 mm diam., hemispherical when young, conical, obtusely conical, campanulate with age, smooth when young, becoming slightly brownish scaly at the center, pruinose, acid blue to dull blue at the center and margin pallescent, turning bluish gray, covered by a separable, gelatinous pellicle.	3.5–13 mm in diam., parabolic, obtusely conical when young, hemispherical, campanulate with age, with an umbo at the center, shallowly sulcate, translucent-striate, smooth, gelatinous slightly, the margin infrequently out of flatness, brown to dark brown, becoming acid blue to dull blue towards the margin, with a greyish white margin, covered by a separable, sticky pellicle.	(3)5–15(25) mm broad, more or less ovoid with an appressed or slightly incurved margin, becoming obtusely conic to campanulate, surface lubricous subviscid, glabrous or appearing somewhat granulose near the margin, translucent-striate, pellicle tenacious and completely separable, pale blue or greenish blue, soon tinged with brown and assuming various degrees of bluish, greenish, or grayish brown with a pallid margin, often sordid yellowish in age, bluish tints often lingering on the margin.	5–15 mm wide, conical to campanulate, ± sulcate, translucent-striate, finely puberulous, covered with a separable gelatinous pellicle, pale grey-brown or pale sepia brown, sometimes with an olivaceous, greenish or bluish green shade, margin often bluish green, or more rarely dingy citrine to ochraceous yellow.	2–5(–10) mm wide, covered with a (separable), gelatinous pellicle, at first ± globose, then hemispherical to parabolic, becoming convex or somewhat depressed, but also with a small papilla, sulcate, translucent-striate, pruinose, glabrescent, somewhat lubricous, initially pale brown, then pale grey with darked centre, becoming almost white with age.	16 mm in diam., up to 4 mm high, at first subglobose to ovoid-conical, with age becoming convex to shallowly so, slightly depressed at apex, shiny, gelatinous, minutely radially rugulose, ± pruinose in places, at first dull blue at apex, below apex, becoming dull blue towards margin; margin decurved, entire, sulcate, striate, faintly translucent-striate.
Context	White, thin, fragile.	White, fragile, thin.	Thin, pallid, pliant.	–	–	Very thin to moderately thick at apex, translucent white or translucent greyish white.
Lamellae	16–28 reaching the stem, adnate to slightly adnexed with a short tooth, narrowly spaced, white, with intervenose veins.	14–25 reaching the stem, adnate to slightly adnexed with a short tooth, white, with unconspicuous intervenose veins, edges concolorous with the face.	Close to crowded, 18–25 reach the stipe, two or three tiers of lamellulae, ascending-adnate, sometimes narrowly adnate or practically free, narrow to moderately broad, white or tinged grayish, edges slightly fimbriate.	17–25 reaching the stem, ascending, adnexed, greyish to greyish brown; edge whitish, at times yellowish, greenish or bluish near the cap margin.	9–14 reaching the stem, ascending, adnexed to fairly broadly adnate or almost free, sometimes with a pseudocollarium, whitish or pale grey; edge whitish and separable as an elastic-tough thread.	Free from stipe or adnately attached to obvious circular descent of pileal flesh, moderately close to distant, five to seven per quadrant, subventricose, moderately broad to broad; edge marginate, blue; sides minutely pruinose, white; with one or two series of lamellulae.
Stipe	48–76 × 1.5–2.0 mm, equal or slightly broadened below, hollow, fragile, pruinose, white, base acid blue in the whole age, covered with white fibrils.	32–46 × 1.0–2.0 mm, equal, base sometimes slightly broaden, fragile, hollow, pruinose, puberulous entirely when young, becoming sparely especially in the middle part when old, yellowish brown to light brown, base with acid blue tinge, covered with a bit white fibrils.	3–8 cm long, 1–2 (2.5) mm. thick, equal, terete, flexuous or strict, tubular, cartilaginous, elastic, at first densely pruinose or minutely pubescent over all form a dense coating of caulocystidia, somewhat glabrescent, base mycelioid, the mycelium blue at first but soon fading to white, bluish to greenish blue above at first, soon fading to grayish or finally sordid brownish.	40–70 × 0.5–2 mm, cylindrical, entirely covered with a dense and fairly coarse, white pubescence, greyish brown, usually somewhat paler at the apex, occasionally with a slight lilaceous or violaceous tint; base at times somewhat rooting, concolorous or with some blue-green stains or entirely blue, even the substrate may be stained blue.	5–30 (–70) × 0.5–1 mm, cylindrical, entirely puberulous, glabrescent in the middle part, pale grey to hyaline-white; base hirsute, sky blue (also in the flesh), springing from a patch of fine, radiating, white fibrils.	Up to 22 mm long, cylindrical, moist to dry, often pruinose especially towards base, translucent white, attached to substratum via white pruinose disc borne on a flattened dull blue base.
Odor & taste	Indistinctive	Indistinctive	Mild	Indistinct to raphanoid.	Smell none or reported as faintly nitrous; taste not recorded.	Odour not distinctive.
Spores	(9.0) 9.3–11.6 (11.8) × (6.0) 6.2–7.3 (7.7) µm, Q = 1.5–1.7, ellipsoid, amyloid.	(6.2) 6.4–7.7 (7.9) × (4.4) 4.7–5.8 (6.0) µm, Q = 1.23–1.54, broadly ellipsoid to ellipsoid, amyloid.	6–8 × 6–7 (8) µm, globose or subglobose, amyloid.	7.5–10.7 × 4.5–6 µm, Q = 1.5–1.9, Qav ≈ 1.6, pip-shaped, amyloid.	6.5–9 × 4–5 µm, Q = 1.6–2.2, Qav ≈ 1.8, pip-shaped, amyloid.	(54/3), 8.4–11.6 ($\bar{x}$ = 9.9, SD = ± 0.7) × 5.7–8.8 ($\bar{x}$ = 7.0, SD = ± 0.6) µm, Q = 1.4, broadly ellipsoidal rarely subglobose, with prominent short, oblique apiculus, amyloid.

Taxa	*M. caeruleogrisea*	*M. caeruleomarginata*	*M. subcaerulea*	*M. amicta*	*M. cyanorhiza*	*M. interrupta*
Basidia	22–29 × 7–9 µm, 4- or 2-spored.	26–35 × 6–12 µm, 4- or 2-spored.	4-spored	30–40 × 6–7 µm, clavate, 4-spored.	18–25 × 6.5–11 µm, clavate, 4-spored.	(27/2), 21.6–39.8 ($\bar{x}$ = 29.0, SD = ± 5.2) × 8.3–16.0 ($\bar{x}$ = 11.6, SD = ± 2.6) µm, 4-spored, rarely 2-spored, sterigmata to 8.8 µm long.
Cheilocystidia	40–62 × 4–6 µm, clustered, abundant, long clavate or cylindrical, apically broadly rounded, thin-walled, hyaline, forming a sterile lamellae edge.	32–48 × 4–6 µm, abundant, clustered, cylindrical or long clavate, apically broadly rounded, thin-walled, hyaline, forming a sterile lamellae edge.	Abundant, 32–60 × 5–8 µm, subfusoid with obtuse apices but becoming more or less cylindric, sometimes flexuous, smooth, hyaline.	16–45 × 3.5–7 µm, clavate, subfusiform or more often cylindrical.	9–20 × 5.5–7 µm, embedded in gelatinous matter, clavate to obpyriform, with few, simple to branched excrescences, 3–14 × 1–1.5 µm.	Abundant, (30/1), 16.8–44.8 ($\bar{x}$ = 25.5, SD = ± 6.55) × 5.6–13.6 ($\bar{x}$ = 8.4, SD = ± 1.8) µm, filamentous, cylindrical, clavate to ovoid, sometimes ventricose at base, with nodulose excrescences.
Pleurocystidia	Absent	Absent	Not differentiated	Absent	Absent	Absent
Pileipellis	Hyphae 1–4 µm wide, sparse, smooth or sparsely coated with simple, cylindrical excrescences or inflated cells, 3.1–11.2 × 0.8–1.7 µm, embedded in gelatinous matter.	Hyphae 2–4 µm wide, with simple, cylindrical excrescences, 2.0–6.4 × 0.6–1.8 µm, embedded in gelatinous matter.	A thick gelatinous pellicle (blue color located along the surface of the pellicle in incompletely gelatinized hyphae).	Hyphae 2–4.5 µm wide, branched, anastomosing, smooth with scattered, cylindrical excrescences, embedded in a layer of gelatinous matter.	Hyphae 1.5–3.5 µm wide, embedded in gelatinous matter, very branched, covered with scattered, simple to branched excrescences, protruding through the gelatinous layer.	Hyphae (28/1), 2.8–8.0 ($\bar{x}$ = 5.4, SD = ± 1.4) µm in diam., nodulose-diverticulate with dense nodulose to cylindrical excrescences, gelatinized.
Stipitipellis	Hyphae 3–8 µm in diameter, smooth, hyaline.	Hyphae 3–6 µm in diameter, smooth, hyaline.	–	Hyphae 2–3.5 µm wide, smooth	Hyphae 1–3 µm wide, smooth.	Hyphae (26/1), 1.6–3.2 ($\bar{x}$ = 2.4, SD = ± 0.4) µm in diam., not gelatinized.
Caulocystidia	38–69 × 6–8 µm, long cylindrical, smooth, transparent.	19–40 × 4–8 µm, smooth, transparent, two shapes: fusiform or cylindrical.	Covered with numerous cystidia, elongated and flexuous.	50–145 × 8–11.5 µm, fusiform to subcylindrical.	Up to 60 × 7 µm, simple to furcate or somewhat branched.	Often fasciculate, (25/1), 50.6–128.0 ($\bar{x}$ = 75.0, SD = ± 19.8) × 5.0–8.8 ($\bar{x}$ = 6.3, SD = ± 1.1) µm, filamentous to slightly ventricose especially towards base, rarely bifurcate.
Clamps	Present	Present	Present	Present	Present	Present
Habitat	Scattered, on humus and fallen leaves in *Acer*, *Populus*, *Pinus*, and *Quercus* mixed forests.	Scattered, on rotten wood in *Picea*, *Pinus*, *Quercus*, *Robinia*, and *Tilia* mixed forests.	Single, scattered or gregarious on debris, decaying wood, or on the bark around the bases of live trees of oak in particular, but also occurring quite frequently on decaying wood of basswood, elm, beech, and other hardwoods.	On wood and woody debris, mostly from conifers but also deciduous trees, also among leaves and needles.	On conifers (*Picea*, *Pinus* and *Larix*) bark and twigs, often on small bark fragments deep in grass.	Generally gregarious, often abundant, rarely solitary or scattered, on fallen decayed logs or stumps of *Eucalyptus*, *Nothofagus*, *Bedfordia*, *Pinus*, etc. forest.
Distribution	China	China	North America (Alabama, Carolina, New York, Tennessee, Pennsylvania, Michigan); Canada (Nova Scotia, Ontario, Manitoba)	Europe (Scandinavia, Netherlands, Italy)	Europe (UK, Denmark, Italy)	Australia and New Zealand
Occurrence time	Summer to autumn.	Late summer to early autumn.	Spring to fall, more abundant locally in the spring.	Late summer to late autumn, rarely in spring.	Summer to autumn.	March to July.
References	This study	This study	Saccardo 1887; Smith 1947	Robich 2003; Aronsen and Læssøe 2016	Robich 2003; Aronsen and Læssøe 2016; Perry 2020	Grgurinovic 2003

and our observations (Saccardo 1887; Smith 1947) (Figs 5, 6; Table 2). Similar to *M. caeruleomarginata*, *M. cyanorhiza* has an entirely puberulous, pruinose stipe with a sky blue base and possesses a gelatinous pileus; however, the pileus of *M. cyanorhiza* is pale brown, grey to almost white, without a bluish tinge and this species has elongated ellipsoid basidiospores (Q > 1.6) and lacks smooth cheilocystidia and caulocystidia (Aronsen and Læssøe 2016; Perry et al. 2020). In addition, *M. amicta* resembles *M. caeruleomarginata* in its bluish pileus, pruinose stipe and pileipellis embedded in a layer of gelatinous matter, but the former differs in having a pale grey-brown pileus that is sometimes ochraceous yellow and greenish when young and bluish when old, a raphanoid odour and elongated ellipsoid basidiospores (7.5–10.7 × 4.5–6.0 µm) (Robich 2003; Aronsen and Læssøe 2016). The Southern Hemisphere species *M. interrupta* is well characterised by its blue pileus at maturity, a translucent stipe with a basal disc and cheilocystidia with excrescences (Grgurinovic 2003). Furthermore, two new species with bluish basidiomata reported from East Asia, *M. lazulina* and *M. indigotica*, can be easily distinguished from the new species in their whitish pileus or tubes similar to *Boletus*; *M. lazulina* having cheilocystidia with numerous excrescences and *M. indigotica* possesses globose basidiospores (Terashima et al. 2016; Wei and Kirschner 2019). *Mycena caeruleogrisea* and *M. caeruleomarginata* share the same bluish pileus and stipe base, smooth and cylindrical cheilocystidia and pileipellis embedded in a layer of gelatinous matter. *Mycena caeruleomarginata* can be readily distinguished, however, based on the dark brown colour of the pileus with a blue margin, yellowish-brown to light brown stipe, broadly ellipsoid to ellipsoid spores and caulocystidia of two shapes.

Key to seven bluish *Mycena* species of sections *Amictae*, *Cyanocephalae*, *Sacchariferae*, and *Viscipelles*

1 Cheilocystidia non-smooth **2**
– Cheilocystidia smooth (sect. *Amictae*) **4**
2 Acanthocysts present (sect. *Sacchariferae*) ..... ***M. lazulina***
– Acanthocysts absent **3**
3 Stipe with basal disc (sect. *Cyanocephalae*) ..... ***M. interrupta***
– Stipe without basal disc (sect. *Viscipelles*) ..... ***M. cyanorhiza***
4 Basidiospores subglobose ..... ***M. subcaerulea***
– Basidiospores broadly ellipsoid to ellipsoid **5**
5 Caulocystidia of two types: (1) fusiform or cylindrical, 19–40 × 4–8 µm; (2) extremely long, cylindrical (length > 100 µm) ..... ***M. caeruleomarginata***
– Caulocystidia of one type, fusiform, subcylindrical to cylindrical (length < 100 µm) **6**
6 Pileus pale grey-brown or pale sepia brown, sometimes with an olivaceous, greenish or bluish-green shade; margin often bluish-green or rarely dingy citrine to ochraceous yellow ..... ***M. amicta***
– Pileus sky blue, greyish-blue with age; margin blue when young, turning bluish-grey when old ..... ***M. caeruleogrisea***

Discussion

With their blue pileus and gelatinous pileipellis, the new taxa *M. caeruleogrisea* and *M. caeruleomarginata* are unique in China. Similar species described from North America and Europe, namely, *M. subcaerulea*, *M. cyanorhiza* and *M. amicta*, have bluish basidiomata as well, but with age, these species often change colours—to green, brown or yellow and the sizes and shapes of their basidiospores and cheilocystidia are also different (Saccardo 1887; Smith 1947; Maas Geesteranus 1980, 1992a, 1992b; Grgurinovic 2003; Robich 2003; Aronsen and Læssøe 2016) (Table 2). *Mycena interrupta*, described from the Southern Hemisphere, can be distinguished from the two newly-described species, based on both habitat and morphology (Grgurinovic 2003). *Mycena lazulina* (sect. *Sacchariferae*), which has a white pileus, blue stipe base, acanthocysts and a non-gelatinised pileipellis, seems to be the most distinct bluish species and is not included in Table 2 (Terashima et al. 2016). According to taxonomic research based on morphology and phylogeny, our newly-described species are more similar to *M. subcaerulea* and *M. amicta* and should, thus, be classified into sect. *Amictae*.

Although pileus colour has been used as a basis for sectional division in *Mycena*, this character does not seem to be satisfactory for species identification, especially within the same section (Smith 1947; Maas Geesteranus 1980, 1992a, 1992b; Grgurinovic 2003; Robich 2003; Aronsen and Læssøe 2016). In sect. *Viscipelles*, for example, *M. cyanorhiza* can be distinctly characterised by the presence of a sky blue stipe, but *M. ulmi* B.A. Perry & H.W. Keller, *M. pachyderma* and *M. pseudocyanorrhiza* Robich do not exhibit any bluish tint (Robich 2003; Aronsen and Læssøe 2016; Perry et al. 2020). A combination of macroscopic and microscopic features, such as the colour of basidiomata and the shapes and sizes of spores, cheilocystidia, pileipellis, caulocystidia and dextrinoid tissues, is, thus, generally regarded as more important for the identification of *Mycena* taxa.

Acknowledgements

This study was supported by the Natural Science Foundation of Shandong Province (grant No. ZR2020QC001), the National Natural Science Foundation of China (grant No. 3190012), the Natural Science Foundation of Shandong Province (grant No. ZR-2019PC028) and the Innovation Team of Shandong Agricultural Industry Technology System (grant No. 26, SDAIT-07-03). We are extremely grateful for the assistance of the Herbaria of Cornell University and the University of Tennessee and especially appreciate the kind help of Collections Manager Margaret Oliver, Dr P. Brandon Matheny and Curator Teresa Iturriaga with specimen loan requests. We sincerely thank Dr Jianwei Liu for help with phylogenetic analyses and Dr Xiaojuan Deng, Mr Bai Wang, Mr Chi Yang and colleagues of the Guyuan Branch Institute of Ningxia Academy of Agriculture and Forestry Sciences for help with fieldwork. We also thank the editors and reviewers for their corrections and suggestions to improve our work.

References

Aldrovandi MS, Johnson JF, O'Meara BC, Petersen RH, Hughes KW (2015) The *Xeromphalina campanella*/*kauffmanii* complex: Species delineation and biogeographical patterns of speciation. Mycologia 107(6): 1270–1284. https://doi.org/10.3852/15-087

Antonín V, Noordeloos ME (2004) A monograph of the genera *Hemimycena*, *Delicatula*, *Fayodia*, *Gamundia*, *Myxomphalia*, *Resinomycena*, *Rickenella*, and *Xeromphalina* (Tribus Mycenae sensu Singer, *Mycena* excluded) in Europe. IHW-Verlag, 280 pp.

Aravindakshan DM, Manimohan P (2015) Mycenas of Kerala. SporePrint Books, Calicut, India, 213 pp.

Aravindakshan DM, Kumar TK, Manimohan P (2012) A new bioluminescent species of *Mycena* sect. *Exornatae* from Kerala State, India. Mycosphere: Journal of Fungal Biology 3(5): 556–561. https://doi.org/10.5943/mycosphere/3/5/4

Aronsen A, Læssøe T (2016) The Genus *Mycena* s.l. Fungi of Northern Europe Vol. 5. Narayana Press, Gylling, Denmark, 373 pp.

Aronsen A, Larsson E (2015) Studier i slaktet *Mycena* (hattor). Svensk Mykologisk Tidskrift 36(3): 23–29.

Baird R, Stokes CE, Wood-Jones A, Watson C, Alexander M, Taylor G, Johnson K, Threadgill P, Diehl S (2014) A molecular clone and culture inventory of the root fungal community associated with Eastern Hemlock in Great Smoky Mountains National Park. Southeastern Naturalist (Steuben, ME) 13(6): 219–237. https://doi.org/10.1656/058.013.s601

Chew A, Desjardin DE, Tan YS, Musa MY, Sabaratnam V (2015) Bioluminescent fungi from peninsular Malaysia—A taxonomic and phylogenetic overview. Fungal Diversity 70(1): 149–187. https://doi.org/10.1007/s13225-014-0302-9

Ge YP, Liu ZW, Zeng H, Cheng XH, Na Q (2021) Updated description of *Atheniella* (Mycenaceae, Agaricales), including three new species with brightly coloured pilei from Yunnan Province, southwest China. MycoKeys 81: 139–164. https://doi.org/10.3897/mycokeys.81.67773

Geml J, Timling I, Robinson CH, Lennon N, Nusbaum HC, Brochmann C, Noordeloos MC, Taylor DL (2015) An arctic community of symbiotic fungi assembled by long-distance dispersers: Phylogenetic diversity of ectomycorrhizal basidiomycetes in Svalbard based on soil and sporocarp DNA. Journal of Biogeography 39(1): 74–88. https://doi.org/10.1111/j.1365-2699.2011.02588.x

Grgurinovic CA (2003) The genus *Mycena* in south-eastern Australia. Fungal Diversity Press, 329 pp.

Guo SX, Fan L, Cao WQ, Chen XM (1999) *Mycena dendrobii*, a new mycorrhizal fungus. Junwu Xuebao 18: 141–144. https://doi.org/10.13346/j.mycosystema.1999.02.007 [in Chinese]

Hall TA (1999) BioEdit: A user-friendly biological sequence alignment editor and analysis program for Windows 95/98/NT. Nucleic Acids Symposium Series 41: 95–98. https://doi.org/10.1021/bk-1999-0734.ch008

Harder CB, Læssøe T, Kjøller R, Frøslev TG (2010) A comparison between ITS phylogenetic relationships and morphological species recognition within *Mycena* sect. *Calodontes* in Northern Europe. Mycological Progress 9(3): 395–405. https://doi.org/10.1007/s11557-009-0648-7

Harder CB, Lodge DJ, Petersen RH, Hughes KW, Blanco JC, Frøslev TG, Læssøe T (2012) Amyloidity is not diagnostic for species in the *Mycena pearsoniana* complex (*Mycena* section *Calodontes*). Mycological Progress 2012(11): 725–732. https://doi.org/10.1007/s11557-011-0782-x

He X, Fang X (1994) Three new species of the genus *Mycena*. Junwu Xuebao 13(2): 92–98. https://doi.org/10.13346/j.mycosystema.1994.02.003 [in Chinese]

He MQ, Zhao RL, Hyde KD, Begerow D, Kemler M, Yurkov A, McKenzie EHC, Raspé O, Kakishima M, Sánchez-Ramírez S, Vellinga EC, Halling R, Papp V, Zmitrovich IV, Buyck B, Ertz D, Wijayawardene NN, Cui B-K, Schoutteten N, Liu X-Z, Li T-H, Yao Y-J, Zhu X-Y, Liu A-Q, Li G-J, Zhang M-Z, Ling Z-L, Cao B, Antonín V, Boekhout T, da Silva BDB, De Crop E, Decock C, Dima B, Dutta AK, Fell JW, Geml J, Ghobad-Nejhad M, Giachini AJ, Gibertoni TB, Gorjón SP, Haelewaters D, He S-H, Hodkinson BP, Horak E, Hoshino T, Justo A, Lim YW, Menolli Jr N, Mešić A, Moncalvo J-M, Mueller GM, Nagy LG, Nilsson RH, Noordeloos M, Nuytinck J, Orihara T, Ratchadawan C, Rajchenberg M, Silva-Filho AGS, Sulzbacher MA, Tkalčec Z, Valenzuela R, Verbeken A, Vizzini A, Wartchow F, Wei T-Z, Weiß M, Zhao C-L, Kirk PM (2019) Notes, outline and divergence times of Basidiomycota. Fungal Diversity 99(1): 105–367. https://doi.org/10.1007/s13225-019-00435-4

Hopple Jr JS, Vilgalys R (1999) Phylogenetic relationships in the mushroom genus *Coprinus* and dark-spored allies based on sequence data from the nuclear gene coding for the large ribosomal subunit RNA: Divergent domains, outgroups, and monophyly. Molecular Phylogenetics and Evolution 13(1): 1–19. https://doi.org/10.1006/mpev.1999.0634

Horak E (2005) Röhrlinge und Blätterpilze in Europa. Elsevier, Spektrum Akad. Verlag, 555 pp.

Jin JJ, Yu WB, Yang JB, Song Y, dePamphilis CW, Yi T-S, Li D-Z (2020) GetOrganelle: A fast and versatile toolkit for accurate de novo assembly of organelle genomes. Genome Biology 21(1): e241. https://doi.org/10.1186/s13059-020-02154-5

Kim CS, Jo JW, Kwag YN, Sung GH, Lee SG, Kim SY, Shin CH, Han SK (2015) Mushroom Flora of Ulleung-gun and a Newly Recorded *Bovista* Species in the Republic of Korea. Mycobiology 43(3): 239–257. https://doi.org/10.5941/MYCO.2015.43.3.239

Kornerup A, Wanscher JH (1978) Methuen handbook of colour. Eyre Methuen, London.

Li Y, Li TH, Yang ZL, Bau T, Dai YC (2015) Atlas of Chinese macrofungal resources. Central Chinese Farmer Press, Zhengzhou, China, 1351 pp.

Liu ZW, Na Q, Cheng XH, Wu XM, Ge YP (2021) *Mycena yuezhuoi* sp. nov. (Mycenaceae, Agaricales), a purple species from the peninsula areas of China. Phytotaxa 511(2): 148–162. https://doi.org/10.11646/phytotaxa.511.2.3

Maas Geesteranus RA (1980) Studies in Mycenas-15, A tentative subdivision of the genus *Mycena* in the Northern Hemisphere. Persoonia 11: 93–120.

Maas Geesteranus RA (1992a) Mycenas of the Northern Hemisphere I. Studies in Mycenas and other papers. Koninklijke Nederlandse Akademie van Wetenschappen, Amsterdam.

Maas Geesteranus RA (1992b) Mycenas of the Northern Hemisphere II. Conspectus of the Mycenas of the Northern Hemisphere. Koninklijke Nederlandse Akademie van Wetenschappen, Amsterdam.

Malysheva V, Malysheva E, Voronina EY, Fedosova A, Bibikov N, Kiseleva DS (2017) Mycorrhiza of Pyroloids (*Pyrola rotundifolia*, *P. media* and *Orthilia secunda*): Species composition of symbionts and trophic status of plants. Mikologiâ i Fitopatologiâ 51(6): 350–364. [in Russian]

Na Q, Bau T (2018) New species of *Mycena* (Mycenaceae, Agaricales) with colored lamellae and three new species records from China. Phytotaxa 361(3): 266–278. https://doi.org/10.11646/phytotaxa.361.3.2

Na Q, Bau T (2019a) *Mycena* section *Sacchariferae*: Three new species with basal discs from China. Mycological Progress 18(3): 483–493. https://doi.org/10.1007/s11557-018-1456-8

Na QC, Bau T (2019b) Recognition of *Mycena* sect. *Amparoina* sect. nov. (Mycenaceae, Agaricales), including four new species and revision of the limits of sect. *Sacchariferae.* MycoKeys 52: 103–124. https://doi.org/10.3897/mycokeys.52.34647

Na Q, Hu YP, Liu ZW, Zeng H, Qi LL, Ding H, Cheng XH, Ge YP (2021) The first reported occurrence of *Leucoinocybe* (Porotheleaceae, Agaricales) in China: *Leucoinocybe lishuiensis* sp. nov. from Zhejiang Province. Nova Hedwigia 113(3–4): 453–469. https://doi.org/10.1127/nova_hedwigia/2021/0661

Na Q, Hu YP, Zeng H, Song ZZ, Ding H, Cheng XH, Ge YP (2022) Updated taxonomy on *Gerronema* (Porotheleaceae, Agaricales) with three new taxa and one new record from China. MycoKeys 89: 87–120. https://doi.org/10.3897/mycokeys.89.79864

Osmundson TW, Robert VA, Schoch CL, Baker LJ, Smith A, Robich G, Mizzan L, Garbelotto MM (2013) Filling Gaps in Biodiversity Knowledge for Macrofungi: Contributions and Assessment of an Herbarium Collection DNA Barcode Sequencing Project. PLoS ONE 8(4): e62419. https://doi.org/10.1371/journal.pone.0062419

Pérez-Izquierdo L, Morin E, Maurice JP, Martin F, Rincón A, Buée M (2017) A new promising phylogenetic marker to study the diversity of fungal communities: The *Glycoside Hydrolase* 63 gene. Molecular Ecology Resources 2017(6): 1–17. https://doi.org/10.1111/1755-0998.12678

Perry BA (2002) A taxonomic investigation of *Mycena* in California. Doctoral dissertation, San Francisco State University, San Francisco, the United States.

Perry BA, Desjardin DE (2016) New species of *Mycena* (Basidiomycota, Agaricales) from California. Phytotaxa 269(1): 33–40. https://doi.org/10.11646/phytotaxa.269.1.4

Perry BA, Keller HW, Forrester ED, Stone BG (2020) A new corticolous species of *Mycena* sect. *Viscipelles* (Basidiomycota: Agaricales) from the bark of a Living American elm tree in Texas, U.S.A. Journal of the Botanical Research Institute of Texas 14(2): 167–185. https://doi.org/10.17348/jbrit.v14.i2.1000

Petersen RH, Hughes KW, Lickey EB, Kovalenko AE, Psurtseva V (2008) A new genus, *Cruentomycena*, with *Mycena viscidocruenta* as type species. Mycotaxon 105(4): 119–136.

Posada D, Crandall KA (1998) Modeltest: Testing the model of DNA substitution. Bioinformatics (Oxford, England) 14(9): 817–818. https://doi.org/10.1093/bioinformatics/14.9.817

Redhead SA, Singer R (1981) *Resinomycena* gen. nov. (Agaricales), an ally of *Hydropus*, *Mycena* and *Baeospora*. Mycotaxon 8(1): 150–170. [Fungi]

Redhead SA, Moncalvo JM, Vilgalys R, Desjardin DE, Perry BA (2012) Index Fungorum: Published Numbers 14: 1–1.

Rexer KH (1994) Die Gattung *Mycena* s.l., Studien zu ihrer Anatomie, Morphologie und Systematik. Eberhard-Karls-Universität Tübingen, Tübingen, Germany, 132 pp.

Robich G (2003) *Mycena* d'Europa. Associazione Micologica Bresadola, Trento, 728 pp.

Robich G (2016) *Mycena* d'Europa Volume 2. Associazione Micologica Bresadola, Trento, 796 pp.

Ronquist F, Huelsenbeck JP (2003) MrBayes 3: Bayesian phylogenetic inference under mixed models. Bioinformatics (Oxford, England) 19(12): 1572–1574. https://doi.org/10.1093/bioinformatics/btg180

Saccardo PA (1887) Sylloge Hymenomycetum, Vol. I. Agaricineae (in Latin). Sylloge Fungorum, Berlin, 1146 pp.

Shih YS, Chen CY, Lin WW, Kao HW (2014) *Mycena kentingensis*, a new species of luminous mushroom in Taiwan, with reference to its culture method. Mycological Progress 13(2): 429–435. https://doi.org/10.1007/s11557-013-0939-x

Singer R (1969) Mycoflora Australis. Beihefte zur Nova Hedwigia 29: 110.

Singer R, Gomez LD (1982) Basidiomycetes of Costa Rica. Brenesia 19–20: 31–47.

Smith AH (1947) North American species of *Mycena*. University of Michigan Press, Ann Arbor, Michigan, 521 pp.

Stamatakis A, Ludwig T, Meier H (2005) RAxML-III: A fast program for maximum likelihood-based inference of large phylogenetic trees. Bioinformatics maximum likelihood-based inference of large phylogenetic trees. Bioinformatics (Oxford, England) 21(4): 456–463. https://doi.org/10.1093/bioinformatics/bti191

Terashima Y, Takahashi H, Taneyama Y (2016) The fungal flora in southwestern Japan, Agarics and boletes. Tokai University Press, Kanagawa, Tokyo, 349 pp.

Thoen E, Harder CB, Kauserud H, Botnen SS, Vik U, Taylor AF, Menkis A, Skrede I (2020) In vitro evidence of root colonization suggests ecological versatility in the genus *Mycena*. The New Phytologist 227(2): 601–612. https://doi.org/10.1111/nph.16545

Thompson JD, Gibson TJ, Plewniak F, Jeanmougin F, Higgins DG (1997) The Clustal-X windows interface: Flexible strategies for multiple sequence alignment aided by quality analysis tools. Nucleic Acids Research 63: 215–228. https://doi.org/10.1093/nar/25.24.4876

Vu D, Groenewald M, de Vries M, Gehrmann T, Stielow B, Eberhardt U, AlHatmi A, Groenewald JZ, Cardinali G, Houbraken J, Boekhout T, Crous PW, Robert V, Verkley GJM (2019) Large-scale generation and analysis of filamentous fungal DNA barcodes boosts coverage for kingdom Fungi and reveals thresholds for fungal species and higher taxon delimitation. Studies in Mycology 92(1): 135–154. https://doi.org/10.1016/j.simyco.2018.05.001

Wei CL, Kirschner R (2019) A new *Mycena* species with blue basidiomata and porioid hymenophore from Taiwan. Mycoscience 60(1): 10–13. https://doi.org/10.1016/j.myc.2018.06.001

White TJ, Bruns T, Lee S, Taylor J (1990) Amplification and direct sequencing of fungal ribosomal RNA genes for phylogenetics. In: Innis, Seliger H, Gelfand DH, Sinsky JJ, White TJ (Eds) PCR Protocols: a Guide to Methods and Applications, 315–322. https://doi.org/10.1016/B978-0-12-372180-8.50042-1

Wu LS, Han T, Li WC, Jia M, Xue LM, Rahman K, Qin LP (2013) Geographic and tissue influences on endophytic fungal communities of *Taxus chinensis* var. *mairei* in China. Current Microbiology 66(1): 40–48. https://doi.org/10.1007/s00284-012-0235-z

MycoKeys 90: 147–162 (2022)
doi: 10.3897/mycokeys.90.85690
https://mycokeys.pensoft.net

RESEARCH ARTICLE

A peer-reviewed open-access journal
MycoKeys
Launched to accelerate biodiversity research

Iugisporipsathyra reticulopilea gen. et sp. nov. (Agaricales, Psathyrellaceae) from tropical China produces unique ridge-ornamented spores with an obvious suprahilar plage

Sheng-Nan Wang[1,2,3], Yu-Guang Fan[4,5], Jun-Qing Yan[1,2,3]

1 *Jiangxi Key Laboratory for Conservation and Utilization of Fungal Resources, Jiangxi Agricultural University, Nanchang, Jiangxi 330045, China* **2** *Key Laboratory of State Forestry Administration on Forest Ecosystem Protection and Restoration of Poyang Lake Watershed, Jiangxi Agricultural University, Nanchang, Jiangxi 330045, China* **3** *Institute of Edible Mushrooms, Fujian Academy of Agricultural Sciences; National and Local Joint Engineering Research Center for Breeding & Cultivation of Features Edible Mushrooms, Fuzhou 350011, China* **4** *Key Laboratory of Tropical Translational Medicine of Ministry of Education, Hainan Medical University, Haikou 571199, China* **5** *Hainan Provincial Key Laboratory for Research and Development of Tropical Herbs, School of Pharmacy, Hainan Medical University, Haikou 571199, China*

Corresponding author: Jun-Qing Yan (yanjunqing1990@126.com)

Academic editor: Kentaro Hosaka | Received 22 April 2022 | Accepted 13 June 2022 | Published 22 June 2022

Citation: Wang S-N, Fan Y-G, Yan J-Q (2022) *Iugisporipsathyra reticulopilea* gen. et sp. nov. (Agaricales, Psathyrellaceae) from tropical China produces unique ridge-ornamented spores with an obvious suprahilar plage. MycoKeys 90: 147–162. https://doi.org/10.3897/mycokeys.90.85690

Abstract

Iugisporipsathyra, a new psathyrelloid genus from tropical red soil of China, is established with *I. reticulopilea* as the type species. The new genus is characterised by basidiomata psathyrelloid, pileus rugose to appearing reticulate ridged, covered by persistent, but inconspicuous villus, pleurocystidia absent and ridge-ornamented spores with an obvious suprahilar plage. The genus is unique amongst Psathyrellaceae in producing ridge-ornamented spores with an obvious suprahilar plage and forms a distinct lineage within Psathyrellaceae, based on the Maximum Likelihood and Bayesian Inference analyses of a combined three-gene sequence dataset (ITS, LSU and β-*tub*). Full descriptions and photographs of the new genus and species are presented.

Keywords

Basidiomycete, fungal phylogeny, taxonomy

Introduction

The Psathyrellaceae Vilgalys, Moncalvo & Redhead was established in 2001, based on the type genus *Psathyrella* (Fr.) Quél. by Vilgalys and Redhead (Redhead et al. 2001). More than 1300 names within the family, including synonyms and subspecies, are listed in Index Fungorum (http://www.indexfungorum.org). Species of Psathyrellaceae are cosmopolitan and often grow on decaying logs, woody debris, humus or soil, in woodlands, lawns or bogs and can have either broad or specific substrate relationships (Kirk et al. 2008).

Traditionally, the family included two types of species: psathyrelloid species and coprinoid species. During the classic period of morphological research, Fries (1838) classified the psathyrelloid species to *Agaricus* L. trib. *Psathyrella* Fr. Quélet (1872) promoted this group to the rank of genus. *Psathyrella* was finally accepted after the transfer of *Drosophila* Quél. species and emendations by Singer (1951,1975). Subsequently, Kits van Waveren (1985) removed the species with warty spores from *Psathyrella* and treated these as the genus *Lacrymaria* Pat. Although the boundaries of the genus were disputed, most researchers agreed that the psathyrelloid species should be classified in Coprinaceae R.Heim ex Pouzar subfamily Psathyrelloideae (Kuhner) Singer (Hawksworth et al. 1983; Kirk et al. 2001). During this same period, the coprinoid species were classified in *Coprinus* Pers. (Coprinaceae subfamily Coprinoideae Henn.) (Hawksworth et al. 1995; Kirk et al. 2001). *Coprinus* was circumscribed by Persoon (1797). However, Fries (1821) did not recognise the genus in his monograph *Systema Mycologicum* and classified the species in *Agaricus*. However, in his subsequent monograph *Epierisis systematis Mycologici*, Fries discarded his previous classification and again placed the coprinoid species in the independent genus *Coprinus* (Fries, 1838).

Although morphological studies provide abundant support for recognition of Psathyrellaceae, morphological data are inadequate to conclusively resolve the systematic relationships amongst the constituent genera and species. When the works of Hopple and Vilgalys (1999) and Redhead et al. (2001) were published, it became apparent that molecular biology techniques would profoundly alter the classical systematics of psathyrelloid species and coprinoid species. Based on these studies, *Coprinus* was split into four genera (*Coprinellus* P.Karst., *Coprinopsis* P.Karst., *Coprinus* and *Parasola* Redhead, Vilgalys & Hopple) (Redhead et al. 2001), restraining the generic name *Coprinus* to a small group centred on the type species *Coprinu comatus* (O.F.Müll.) Pers., which is now classified in the Agaricaceae Chevall. The other three genera, together with *Psathyrella* and *Lacrymaria*, were incorporated into the newly-established Psathyrellaceae. In 2015, *Psathyrella*, as a paraphyletic group, was also split, with the establishment of the segregate genera *Cystoagaricus* Singer emend. Örstadius & E.Larss., *Homophron* (Britzelm.) Örstadius & E.Larss., *Kauffmania* Örstadius & E.Larss. and *Typhrasa* Örstadius & E.Larss. (Örstadius et al. 2015). In 2020, *Candolleomyces* D.Wächt. & A.Melzer, *Britzelmayria* D.Wächt. & A.Melzer and *Olotia* D.Wächt. & A.Melzer were separated from *Psathyrella*, *Punjabia* D.Wächt. &

A.Melzer and *Tulosesus* D.Wächt. & A.Melzer were separated from *Coprinellus*, *Narcissea* D.Wächt. & A.Melzer was segregated from *Coprinopsis* and *Hausknechtia* D.Wächt. & A.Melzer was erected for *Galerella floriformis* Hauskn. (Wächter and Melzer 2020). *Heteropsathyrella* T.Bau & J.Q.Yan was established in 2021, based on the new species *He. macrocystidia* T.Bau & J.Q.Yan (Bau and Yan 2021a). Thus, the main systematic framework of Psathyrellaceae has been confirmed. In addition, *Ozonium* Link and *Hormographiella* Guarro & Gené, formerly members of the Psathyrellaceae, were established to accommodate the conidial anamorphs of certain species, now classified in *Coprinellus* (Nagy et al. 2013). *Gasteroagaricoides* D.A.Reid and *Macrometrula* Donk & Singer, two genera that, to date, have not been included in phylogenetic analyses, are retained in the Psathyrellaceae. There were 19 genera, in total, in the Psathyrellaceae before the new taxon we discovered was added.

From 2015, we initiated a study of Chinese psathyrelloid species and described 15 new taxa (Yan and Bau 2017, 2018a,b; Yan et al. 2019; Bau and Yan 2021a,b; Wang et al. 2021). By chance, we collected a psathyrelloid species with a reticulate-ridged pileus, that was reminiscent of *Pluteus thomsonii* (Berk. & Broome) Dennis, on the roadside in tropical China. After examining the micromorphology of the specimens, we observed that it produced ridge-ornamented spores with an obvious suprahilar plage. Surprisingly, phylogenetic analysis of molecular data revealed that it belonged to the Psathyrellaceae. Although abundant genera and species are recognised in the Psathyrellaceae, the majority of species have smooth spores. Verrucous spores have been observed only in *Lacrymaria.* Rough spores have been observed in *Coprinopsis*, *Coprinellus* and *Psathyrella*, but are extremely rare. Thus, the specimens are unique amongst Psathyrellaceae in producing ridge-ornamented spores with an obvious suprahilar plage. On the basis of our morphological and phylogenetic analyses, the specimens are described herein as a new species and a new genus is erected to accommodate the new species.

Materials and methods

Morphological studies

Macroscopic descriptions and habitat details were based on detailed field notes of fresh basidiomata and photos. The location of the collection point is marked on the map (Fig 1). Colour codes follow the Methuen Handbook of Colour (Kornerup and Wanscher 1978). Microscopic structures were observed and measured from dried specimens mounted in water, 5% potassium hydroxide (KOH), 10% ammonium hydroxide (NH_4OH) or Melzer's Reagent. Congo red was used as a stain when necessary (Horak 2005). A minimum of 100 basidiospores, basidia and cystidia from seven basidiomata (three collections) were randomly measured using an Olympus BX53 microscope. Detailed observations of spores were made by SEM. The measurements and Q values are recorded as (a)b–c(d), in which "a" is the lowest value, "b–c" covers a

Figure 1. Map showing the location of the collection site of the specimens (red triangle).

minimum of 90% of the values and "d" is the highest value. "Q" stands for the ratio of length and width of a spore (Bas 1969; Yu et al. 2020). Specimens were deposited in the Herbarium of Fungi, Jiangxi Agricultural University (HFJAU).

DNA extraction and sequencing

DNA was extracted from dried specimens with the NuClean Plant Genomic DNA kit (CWBIO, China) (Ge et al. 2021; Na et al. 2022). Three regions (ITS, LSU and β-*tub*) were selected for the study and were amplified using the primer pairs by ITS1/ITS4 (White et al. 1990), LR0R/LR7 (Hopple and Vilgalys 1999) and B36f/B12r (Nagy et al. 2011), respectively. PCR was performed using a touchdown programme for all regions: 5 min at 95 °C; 1 min at 95 °C; 30 s at 65 °C (add -1 °C per cycle); 1 min at 72 °C; cycle 15 times; 1 min at 95 °C; 30 s at 50 °C; 1 min at 72 °C; cycle 20 times; 10 min at 72 °C (Bau and Yan 2021a). The sequencing was performed by Qing Ke Biotechnology Co. Ltd. (Wuhan City, China).

Data analyses

A total of 221 nucleotide DNA (ITS, LSU and β-*tub*) sequences representing 93 taxa were used in subsequent analyses. Details are presented in Table 1. Some species of Agaricaceae, Mythicomycetaceae Vizzini, Consiglio & M. Marchetti

Table 1. Sequences used in this study.

Taxon	Voucher	ITS	LSU	β-*tub*
Britzelmayria multipedata	LÖ237-04	KC992888	KC992888	KJ664867
B. supernula	LÖ250-04	KC992867	KC992867	KJ664849
Candolleomyces eurysporus	GLM-F126263 Type	MT651560	MT651560	MW369460
C. subcacao	HMJAU37807 Type	MW301064	MW301092	MW314063
C. subminutisporus	HMJAU37801 Type	MW301066	MW301094	MW314065
C. subsingeri	HMJAU37913 Type	MG734725	MW301098	MW314068
Coprinellus andreorum	CS1247 Type	MW621497	MW621007	–
C. aureogranulatus	CBS973.95	GQ249274	GQ249283	GQ249258
C. aureogranulatus	CBS753.96 Isotype	MH862611	–	–
C. curtus	NL-2339	FM878016	FM876273	FN396281
C. deminutus	NL-0761	JN159572	JN159592	JN159636
C. disseminatus	NL-2337	FM878017	FM876274	FN396282
C. domesticus	NL-1292	FN396102	HQ847132	FN396330
C. silvaticus	LÖ172-08	KC992943	KC992943	KJ664911
Coprinopsis babosiae	NL-4139 Type	FN396128	FN396177	FN396352
C. calospora	CBS612.91 Type	GQ249275	GQ249284	GQ249259
C. cortinatus	NL-1621	FN396121	FN396171	FN396346
C. musae	JV06-179 Type	KC992965	KC992965	KJ664920
C. musae	JV06-180	KC992966	KC992966	KJ664921
C. semitalis	CBS291.77 Type	GQ249278	GQ249287	GQ249262
C. udicola	AM1240 Type	KC992967	KC992967	KJ664922
C. villosa	NL-1758 Type	JN943128	JQ045877	HQ847173
Cystoagaricus hirtosquamulosa	Ramsholm800927	KC992945	KC992945	–
C. olivaceogrisea	WK8/15/63-5 Type	KC992948	KC992948	–
C. silvestris	LÖ191-92	KC992949	KC992949	–
C. squarrosiceps	Laessoe44835	KC992950	–	–
C. strobilomyces	E.Nagasawa9740	AY176347	AY176348	–
Hausknechtia floriformis	WU22833 Type	JX968254	JX968371	–
Heteropsathyrellamacrocystidia	HMJAU37803	MW405101	MW413358	–
H. macrocystidia	HMJAU37802 Type	MW405102	MW413359	MW410997
Homophron camptopodum	1997/956	KC992956	KC992956	–
H. cernuum	LÖ134-98	DQ389726	DQ389726	KJ664915
H. crenulata	W-K8/10/64-5 Type	KC992957	–	–
H. spadiceum	Enderle Epitype	DQ389729	DQ389729	–
Iugisporipsathyra reticulopilea	HFJAU1352 Type	ON207138	ON207137	ON210974
I. reticulopilea	HFJAU3181	ON207139	–	ON210975
I. reticulopilea	HFJAU3182	ON207140	–	ON210976
Kauffmania larga	LÖ223-90	DQ389694	DQ389694	KJ664912
K. larga	LAS97-054	DQ389695	DQ389695	–
Lacrymaria glareosa	LAS06-019	KC992954	KC992954	KJ664914
L. hypertropicalis	Guzman29585 Type	KC992958	KC992958	KJ664916
L. lacrymabunda	EL70-03	DQ389724	DQ389724	–
L. pyrotricha	CBS573	GQ249280	GQ249289	GQ249264
L. rigidipes	LAS00-081	KC992953	KC992953	KJ664913
L. subcinnamomea	Smith16957 Type	KC992951	KC992951	–
Narcissea cordispora	SFSUDEH2073	AY461827	–	–
N. cordispora	LÖ41-01	DQ389723	–	KJ664910
N. patouillardi	NL-1687	FM878009	FM876265	FN396257
Olotia codinae	GLM-F112430 Type	MG696611	MG674714	–
Parasola auricoma	NL-0087	JN943107	JQ045871	FN396252
P. conopilea	LÖ186-02 Neotype	DQ389725	DQ389725	–
P. kuehneri	Ulje31-V-1987 Type	KY928608	KY928633	–

Taxon	Voucher	ITS	LSU	β-*tub*
P. lactea	NL-0466	FM163192	FM160717	FN396254
P. misera	NL-0280 Neotype	FM163210	FM160699	–
P. ochracea	NL-3621 Type	JN943134	JQ045875	–
P. parvula	CAL1667 Type	NR_160509	NG064556	–
P. plicatilis	NL-0295	FM163216	FM160693	FN396253
P. plicatilis	NL-0075a Epitype	NR_171786	NG075167	–
P. psathyrelloides	CAL1753 Type	MK682756	MK682754	–
Psathyrella amygdalinospora	HMJAU37952 Type	MW405104	MW413361	MW410991
P.amygdalinospora	HMJAU57044	MW405105	–	–
P.fagetophila	LÖ210-85 (M) Type	KC992902	KC992902	KJ664879
P.fennoscandica	HMJAU37918	MG734723	MW413365	MW410993
P.fennoscandica	LÖ484-05 Type	KC992903	KC992903	KJ664881
P.noli-tangere	LÖ83-03 Neotype	DQ389713	DQ389713	KJ664890
P.seminuda	Smith34091 (MICH) Type	KC992907	KC992907	–
P.warrenensis	Smith70162 (MICH) Type	KC992906	KC992906	–
Punjabia pakistanica	MEL2382843	KP012718	KP012718	–
P. pakistanica	LAH35323 Type	MH366736	–	–
Tulosesus canistri	Walleyn877 Isotype	HQ846985	–	HQ847142
T. cinereopallidus	NL-0177 Type	HQ847001	HQ847090	HQ847149
T. fuscocystidiatus	NL-2720 Type	HQ846977	HQ847064	HQ847152
T. hiascens	NL-2536	FM878018	FM876275	FN396284
T. pseudoamphithallus	Ulje1288 Type	HQ846973	HQ847059	–
T. radicellus	NL-3168 Type	GU227719	HQ847077	GU227737
T. sassii	NL-1495	FN396101	FN396155	FN396329
Typhrasa gossypina	Schumacher024	KC992946	KC992946	–
T. nanispora	Barta980706 Type	KC992947	KC992947	–
T. polycystis	HFJAU1454 Type	MW466538	MW466544	–
T. rugocephala	HFJAU1467 Type	MW466541	MW466546	–
Outgroup				
Coprinus comatus	AFTOL_ID_626	AY854066	AY635772	–
Crucibulum laeve	REGCrul1/DSH96-02	DQ486696	AF336246	–
Cyathus striatus	DSH96-028/Cyst1/DSH96-001	DQ486697	AF336247	–
Lepiota cristata	ZRL20151133	LT716026	KY418841	–
Leucocoprinus fragilissimus	ZRL20151466	LT716029	KY418844	–
Lycoperdon ericaeum	ZRL20151498	LT716030	KY418845	–
Macrolepiota dolichaula	xml2013058	LT716021	KY418836	–
Mycocalia denudata	AFTOL2018/CBS494.85	DQ911596	DQ911597	–
Mythicomyces corneipes	AFTOL-ID972	DQ404393	AY745707	–
M. corneipes	KB51	KY648897	–	–
Nidula niveotomentosa	AFTOL1945/CBS250.84	DQ917654	DQ986295	–
Stagnicola perplexa	AH25260 Holotype	MK351609	MK353793	–
S. perplexa	AH25282 Paratype	MK351610	MK353794	–

and Nidulariaceae Dumort. were chosen as outgroup taxa according to the results of Zhao et al. (2017) and Vizzini et al. (2019). ITS, LSU and β-*tub* sequence datasets were separately aligned on the MAFFT online server (Katoh et al. 2019). Bayesian Inference (BI) and Maximum Likelihood (ML) phylogenetic analyses of the aligned concatenated dataset were respectively carried out in MrBayes v.3.2.7a and IQTREE v.2.1.2 (Nguyen et al. 2014) via the CIPRES web portal. For the BI analyses, optimal evolutionary models were selected using PartitionFinder2 (Lanfear

et al. 2017) with the greedy algorithm and the AICc criterion. Four Monte Carlo Markov chains were run for 2 million generations, sampling every 100th generation, with the first 25% of trees discarded as burn-in (Ronquist et al. 2012). For the ML analysis, models of sequence evolution were assessed in IQ-Tree prior to the analysis. The ML analysis was conducted using the ultrafast bootstrap option with 1,000 replicates and allowing partitions to have different seeds (--p). A nexus file contains alignment sequence and original tree of ML and Bayes is deposited in Suppl. material 1.

Results

Phylogenetic analysis

Based on the BLAST results, the new species were found sharing less than 90.82% (ITS), 97.66% (LSU) and 87.03% (β-*tub*) similarity with the known species. The aligned concatenated dataset comprised 2,591 characters (ITS 835 bp, LSU 1338 bp and β-*tub* 418 bp), of which 983 sites were variable and 757 were parsimony informative. The best-fit evolutionary models used for the phylogenetic analyses were as follows: for the BI analysis, GTR + I + G for ITS and LSU and TIM + I + G for β-*tub*; and for the ML analysis, TIM2 + F + I + G4 for ITS, GTR + F + R4 for LSU and HKY + F + I + G4 for β-*tub*. The log-likelihood of the ML consensus tree was –27426.323 and the average standard deviation of split frequencies was less than 0.01 after 1,115,000 generations in the BI analysis. In the resulting trees, clades with a Bayesian posterior probability (BI-PP) ≥ 0.95 and ML bootstrap support (ML-BP) ≥ 75% were considered to be well supported.

As shown in the BI tree in Fig. 2, all taxa of Psathyrellaceae formed a well-supported monophyletic lineage (BI-PP = 1; ML-BP = 100%). Within Psathyrellaceae, 18 major supported clades with a high statistical support value (BI-PP ≥ 0.95, ML-BP ≥ 75%) represented a total of 17 (out of 19) known genera and a new genus. *Iugisporipsathyra* formed a distinct lineage (BI-PP = 1; ML-BP = 100%) clearly separated from currently recognised genera.

Taxonomy

***Iugisporipsathyra* J.Q. Yan, Y.G. Fan & S.N. Wang, gen. nov.**
MycoBank No: 843734

Etymology. Iugi-, iugis (Latin), ridge; -spori-, sporis (Latin), spores; Iugispori-, refers to its spore ornamentation; -psathyra, one of the synonyms of *Psathyrella*, refers to its similarity to *Psathyrella*.

Description. Basidiomata psathyrelloid, fragile, non-deliquescent. Pileus hygrophanous, rugose to appearing reticulate ridged, covered by persistent and

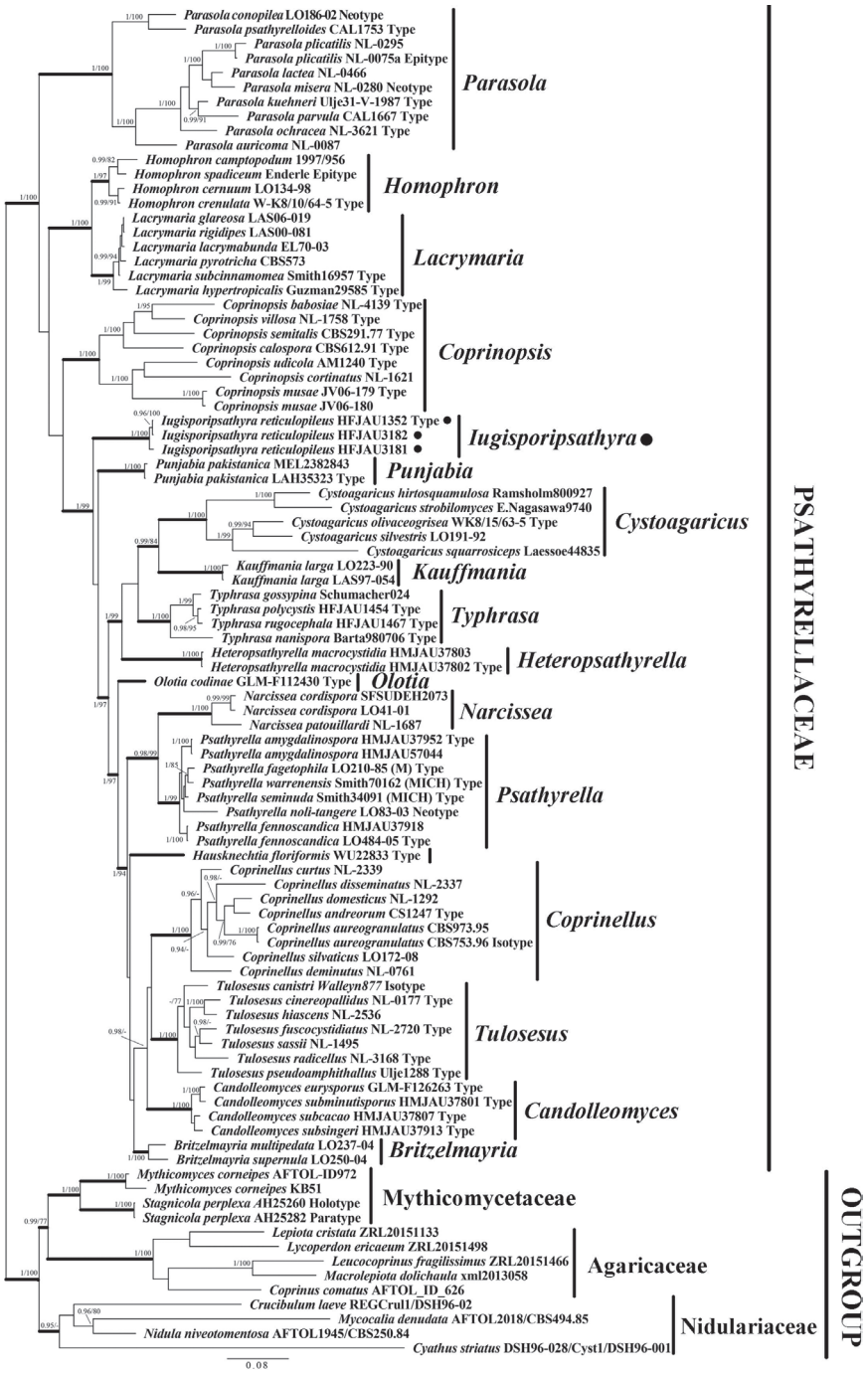

Figure 2. Phylogeny generated by Bayesian Inference, based on a concatenated sequence dataset for three nuclear DNA regions (ITS, LSU and β-*tub*). The tree was rooted with Agaricaceae spp., Mythicomycetaceae spp. and Nidulariaceae spp. Bayesian Inference posterior probabilities (BI-PP) ≥ 0.95 and Maximum Likelihood bootstrap percentages (ML-BP) ≥ 75% are shown as PP/BP at relevant nodes. (black circle) indicates newly-described taxa.

inconspicuous villus. Lamellae adnexed, brown. Stipe white, central, hollow. Spores amygdaliform in profile view, ovoid to elongate in face view, inamyloid, brown, fades in concentrated sulphuric acid, ridged and rarely verrucose ornamentation, suprahilar plage obvious. Basidia monomorphic. Pseudoparaphyses abundant. Pleurocystidia absent. Cheilocystidia present. Pileipellis hymeniderm, pyriform cell mixed with simple hairs.

Type species. *Iugisporipsathyra reticulopilea* J.Q. Yan, Y.G. Fan & S.N. Wang

Notes. The combination of veil absent, pleurocystidia absent and spores ornamented with ridges or rarely verrucose, with an obvious suprahilar plage is unique in Psathyrellaceae.

***Iugisporipsathyra reticulopilea* J.Q. Yan, Y.G. Fan & S.N. Wang, sp. nov.**
MycoBank No: 843801
Fig. 3

Etymology. reticulo-, reticular; reticulopilea, referring to the surface characteristic of the pileus.

Description. Pileus 30–90 mm broad, oblate when young, expanding to plane, surface dry, rugose to appearing reticulate ridged, hygrophanous, pale yellow to greyish-yellow (4A3–4B2), becoming yellowish-white (4A2) as pileus dries, centre and ridged area darker, brown to dark brown (7D6–7F6), becoming greyish-yellow (4B2) as pileus dries. Pileus surface covered by inconspicuous villus. Villus very short, white (4A2), persistent. Veil absent. Context 3.0–4.0 mm broad, fragile, dirty white (7A1–7B2). Lamellae 3.5–10 mm broad, crowded, adnexed, 2–3 tiers of lamellulae, dirty white (7A1–7B2), becoming brown (7E6–7E8) as spores mature, edge white (7A1–7B1) and saw-toothed under 20× magnification. Stipe 50–80 mm long, 3.0–10 mm thick, fragile to fibrous, white to dirty white (7A1–7B1), cylindrical, hollow, gradually thickening towards base, 8.0–17 mm thick at base. Stipe surface covered with small, white, evanescent fibrils.

Spores (7.5–)8.0–9.7(–10.5) × (4.0–)4.5–6.0 μm, Q = 1.5–2.0, amygdaliform in profile view, (4.5–)4.8–6.0(–6.3) μm broad, ovoid to elongate in face view, inamyloid, red-brown in water, brown in alkaline solution, fades in concentrated sulphuric acid, ornamentation up to 1.0 μm high, composed of irregular ridges and rarely verrucose, variable in length, partly connected, sometimes forming a zebroid pattern or closed meshes, suprahilar plage obvious, germ pore absent. Basidia (19–)22–29 × 9.5–12.0 μm, clavate, hyaline, 4- or 2-spored. Pseudoparaphyses abundant. Pleurocystidia absent. Cheilocystidia (37–)40–61(–68) × (9.5–)12–18(–22) μm, hyaline, utriform with obtuse to broadly obtuse apex, base tapering to a short or long stipe. Caulocystidia 50–90 × 6.0–14 μm, scattered or caespitose, various, mostly narrow clavate, hyaline. Trama of gills subparallel. Pileipellis hymeniderm, composed of a 1-cell-deep layer of pyriform cells, mixed with sparsely simple hairs, pyriform cells (35–)38–60 (–62) × (12–)14–23 μm, hairs hyphae, separate, 7.0–10 μm broad. Clamps present.

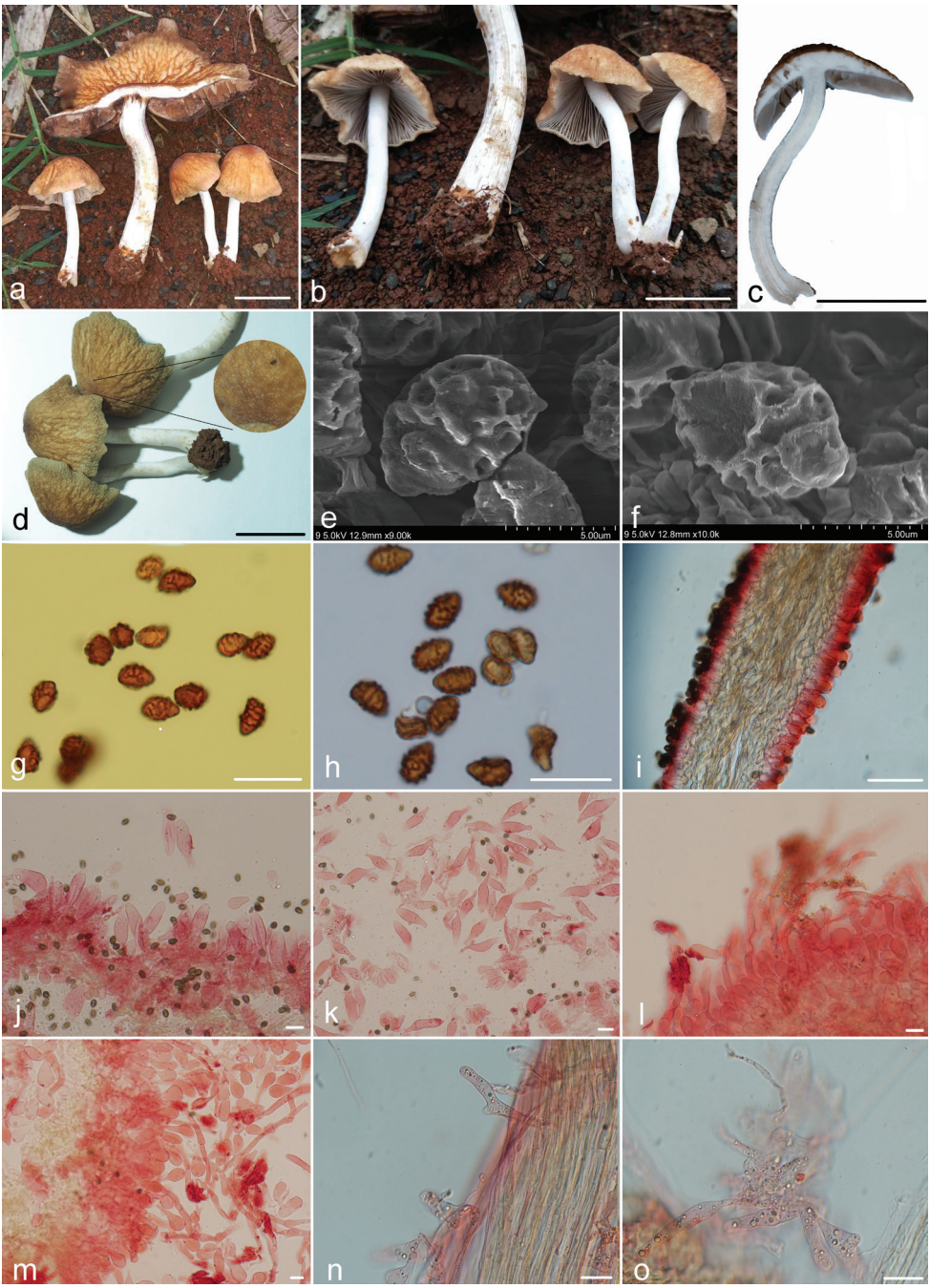

Figure 3. Macroscopic and microscopic structures of *Iugisporipsathyra reticulopilea* **a–d** Basidiomata **e, f** spores viewed by scanning electron microscopy **g** spores in Melzer's Reagent **h** spores in water **i** hymenophore **j, k** cheilocystidia **l, m** pileipellis and hairs hyphae **n, o** caulocystidia. Scale bars: 20 mm (**a–d**); 20 μm (**g–o**). Structures of **i–o** were observed in 5% KOH solution and Congo red was used as the stain.

Known distribution. Tropical China (Hainan Province).

Habit and habitat. Scattered or 2–3 caespitose on red soil of roadside under broadleaf tree.

Specimens examined. China. Hainan Province, Ding'an County, Longhu Town, 2 Jan 2019, Yu-Guang Fan, Jun-Qing Yan HFJAU 1352 (holotype); 4 Jan 2019, Jun-Qing Yan, Sheng-Nan Wang, HFJAU 3181, HFJAU 3182.

DNA sequence of type. ON207138 (ITS), ON207137 (LSU), ON210974 (β-*tub*).

Notes. Differs from other species in Psathyrellaceae by having ridge-ornamented spores with an obvious suprahilar plage.

Discussion

The discovery of *I. reticulopilea* has transformed our traditional understanding of Psathyrellaceae. The species is unique amongst Psathyrellaceae in producing ridge-ornamented spores with an obvious suprahilar plage. This feature is so unusual that it seems difficult to associate it with Psathyrellaceae. However, the characteristic of the spores of fading in concentrated sulphuric acid is in common with other species in this family (Singer 1986; Kirk et al. 2008; Padamsee et al. 2008; Nagy et al. 2013; Örstadius et al. 2015; Wächter and Melzer 2020).

Macroscopically, the psathyrelloid basidiomata of *I. reticulopilea* enables ready discrimination from the coprinoid taxa of Psathyrellaceae. *Gasteroagaricoides* spp. have a densely granular-warty pileus and *Macrometrula* spp. have a volva (Singer 1948; Reid 1986). *Iugisporipsathyra reticulopilea* can be distinguished from these species by the smooth pileus and absence of a volva. Amongst the abundant psathyrelloid taxa of Psathyrellaceae, only the species of *Typhrasa* have slight to distinct ridge-like folds on the pileus. However, no species has a reticulate-ridged pileus similar to that of *I. reticulopilea*. In addition, the pileus surface of *I. reticulopilea* is covered by a white, inconspicuous, but persistent villus. This feature also readily distinguishes *I. reticulopilea* from known species of *Typhrasa* (Örstadius et al. 2015; Wang et al. 2021).

Microscopically, almost all species of Psathyrellaceae have smooth spores. Granulose spores are observed only in *Coprinopsis*, *Coprinellus* and *Psathyrella*, but are extremely rare. Verrucose spores are known only in *Lacrymaria*. No species has an obvious suprahilar plage as in *I. reticulopilea* (Guzmán et al. 1990; Örstadius and Knudsen 2012; Örstadius et al. 2015). In the classification system of Smith (Smith 1972), some species with ornamented spores were classified in *Psathyrella* subg. *Panaeolina* (Maire) A.H. Smith. Those species are now excluded from the Psathyrellaceae and are classified in *Panaeolina* Maire, based on phylogenetic relationships and spores that do not fade in concentrated sulphuric acid (Kirk et al. 2013; Zhao et al. 2017). Detailed morphological comparison of *Iugisporipsathyra* and psathyrelloid genera of Psathyrellaceae is presented in Table 2.

Table 2. Summary of morphological characteristics used to discriminate psathyrelloid genera in the Psathyrellaceae.

	Britzelmayria	*Candolleomyces*	*Cystoagaricus*	*Heterospathyrella*	*Homophron*	*Iugisporipsathyra*	*Kauffmania*	*Lacrymaria*	*Olotia*	*Psathyrella*	*Typhrasa*
Pileus surface	smooth	smooth	fibrillose, squamulose, spiny, or squarrose; hyphae	smooth	smooth	**non-obvious villus; hyphae**	smooth	tomentose; hyphae	smooth	smooth	slight to distinct ridge-like folds
Veil	wipeable; hyphae	wipeable; hyphae	absent	wipeable; hyphae	absent	**absent**	wipeable; hyphae	absent	wipeable; hyphae	wipeable; hyphae, rarely subglobose cells	wipeable; hyphae
Cap or lamellae	non-deliquescent	non-deliquescent	non-deliquescent	non-deliquescent	non-deliquescent	**non-deliquescent**	non-deliquescent	non-deliquescent	non-deliquescent	non-deliquescent	non-deliquescent
Spore surface	smooth	smooth	smooth	smooth	smooth	**ridges ornamentation with obvious suprahilar plage**	smooth	often warty	smooth	smooth, rarely granulose or with myxosporium	smooth
Basidia	monomorphic	monomorphic	monomorphic	monomorphic	monomorphic	**monomorphic**	monomorphic	mono- to dimorphic	monomorphic	monomorphic	monomorphic
Pseudoparaphyses	absent	absent	absent	present	absent	**present**	absent	absent	absent	rarely present	absent
Pileipellis	paraderm	hymeniderm to paraderm	paraderm	hymeniderm to paraderm, covered by a 1 cell deep layer of periclinal hyphae	hymeniderm to paraderm. simple hairs sometimes present	**Hymeniderm, mixes with sparsely simple hairs**	hymeniderm to paraderm	hymeniderm	hymeniderm to paraderm	hymeniderm, paraderm, rarely cutis	hymeniderm to paraderm
Pleurocystidia	thin-walled	absent	thin-walled	thin-walled	thick-walled	**absent**	thin-walled	thin-walled	predominantly spatula-shaped and strongly pediculated	thin-walled or rarely slight thick-walled	thin-walled, with intracellular oily drops or globules
Cheilocystidia	present	present	present	present	present	**present**	present	present	present	present	present
Pileocystidia	present	absent	absent	absent	absent	**absent**	absent	absent	absent	very rarely present	absent

Acknowledgements

This work was financed by the National Natural Science Foundation of China (31960008, 31860009), The Project of FAAS (XTCXGC2021007) and Jiangxi Provincial Natural Science Foundation (20202BABL213041). Sincere thanks to the anonymous reviewers of the manuscript.

References

Bas C (1969) Morphology and subdivision of *Amanita* and a monograph of its section *Lepidella*. Persoonia 5: 285–573.

Bau T, Yan J-Q (2021a) A new genus and four new species in the/Psathyrella s.l. clade from China. MycoKeys 80: 115–131. https://doi.org/10.3897/mycokeys.80.65123

Bau T, Yan J-Q (2021b) Two new rare species of *Candolleomyces* with pale spores from China. MycoKeys 80: 149–161. https://doi.org/10.3897/mycokeys.80.67166

Fries EM (1821) Systema mycologicum. Gryphiswaldiae, Sumtibus Ernesti Mauritii, 1–510.

Fries E (1838) Epicrisis Systematis Mycologici. seu synopsis Hymenomycetum. Typographia Academica, Uppsala, Sweden, 1–610.

Ge Y-P, Liu Z-W, Zeng H, Cheng X-H, Na Q (2021) Updated description of *Atheniella* (Mycenaceae, Agaricales), including three new species with brightly coloured pilei from Yunnan Province, southwest China. MycoKeys 81: 139–164. https://doi.org/10.3897/mycokeys.81.67773

Guzmán G, Bandala VM, Montoya L (1990) Observaciones taxonómicas sobre el género *Psathyrella* subgénero *Lacrymaria* en México y descripción de nuevos taxa (Basidiomycotina, Agaricales). Scientia Fungorum: 105–123.

Hawksworth DL, Sutton BC, Ainsworth GC (1983) Ainsworth and Bisby's Dictionary of the Fungi. Commonwealth mycological institute, Surrey, USA, 444 pp.

Hawksworth DL, Kirk PM, Sutton BC, Pegler DN (1995) Ainsworth & Bisby`s Dictionary of the Fungi. The Cambridge University Press, Cambridge, UK, 616 pp.

Hopple Jr JJ, Vilgalys R (1999) Phylogenetic relationships in the mushroom genus *Coprinus* and dark-spored allies based on sequence data from the nuclear gene coding for the large ribosomal subunit RNA: Divergent domains, outgroups, and monophyly. Molecular Phylogenetics and Evolution 13(1): 1–19. https://doi.org/10.1006/mpev.1999.0634

Horak E (2005) Röhrlinge und Blätterpilze in Europa: Bestimmungsschlüssel für Polyporales (pp), Boletales, Agaricales, Russulales. Elsevier, Munich, Germany, 1–555.

Katoh K, Rozewicki J, Yamada KD (2019) MAFFT online service: Multiple sequence alignment, interactive sequence choice and visualization. Briefings in Bioinformatics 20(4): 1160–1166. https://doi.org/10.1093/bib/bbx108

Kirk PM, Cannon PF, David J, Stalpers JA (2001) Ainsworth and Bisby's dictionary of the fungi. CABI publishing, 665 pp.

Kirk PM, Cannon PE, Minter DW, Stalpers JA (2008) Dictionary of the Fungi. CABI International, Wallingford, USA, 771 pp.

Kirk PM, Stalpers JA, Braun U, Crous PW, Hansen K, Hawksworth DL, Hyde KD, Lücking R, Lumbsch TH, Rossman AY, Seifert KA, Stadler M (2013) A without-prejudice list of generic names of fungi for protection under the International Code of Nomenclature for algae, fungi, and plants. IMA Fungus 4(2): 381–443. https://doi.org/10.5598/imafungus.2013.04.02.17

Kits van Waveren E (1985) The Dutch. French and British species of *Psathyrella.* Persoonia 2: 1–284.

Kornerup A, Wanscher JHK (1978) The methuen handbook of colour 3rd Edn. Eyre Methuen Ltd. Reprint., London, UK, 1–252.

Lanfear R, Frandsen PB, Wright AM, Senfeld T, Calcott B (2017) PartitionFinder 2: New methods for selecting partitioned models of evolution for molecular and morphological phylogenetic analyses. Molecular Biology and Evolution 34: 772–773. https://doi.org/10.1093/molbev/msw260

Na Q, Liu Z-W, Zeng H, Cheng X-H, Ge Y-P (2022) *Crepidotus yuanchui* sp. nov. and *C. caspari* found in subalpine areas of China. Mycoscience 63(1): 1–11. https://doi.org/10.47371/mycosci.2021.10.004

Nagy LG, Walther G, Házi J, Vágvölgyi C, Papp T (2011) Understanding the Evolutionary Processes of Fungal Fruiting Bodies: Correlated Evolution and Divergence Times in the Psathyrellaceae. Systematic Biology 60(3): 303–317. https://doi.org/10.1093/sysbio/syr005

Nagy LG, Vágvölgyi C, Papp T (2013) Morphological characterization of clades of the Psathyrellaceae (Agaricales) inferred from a multigene phylogeny. Mycological Progress 12(3): 505–517. https://doi.org/10.1007/s11557-012-0857-3

Nguyen LT, Schmidt HA, von Haeseler A, Minh BQ (2014) IQ-TREE: A fast and effective stochastic algorithm for estimating maximum-likelihood phylogenies. Molecular Biology and Evolution 32(1): 268–274. https://doi.org/10.1093/molbev/msu300

Örstadius L, Knudsen H (2012) *Psathyrella* (Fr.) Quél. In: Knudsen H, Vesterholt J (Eds) Funga Nordica Agaricoid, boletoid, cyphelloid and gasteroid genera. Nordsvamp, Copenhagen, Denmark, 586–623.

Örstadius L, Ryberg M, Larsson E (2015) Molecular phylogenetics and taxonomy in Psathyrellaceae (Agaricales) with focus on psathyrelloid species: Introduction of three new genera and 18 new species. Mycological Progress 14(5): 1–42. https://doi.org/10.1007/s11557-015-1047-x

Padamsee M, Matheny PB, Dentinger BT, McLaughlin DJ (2008) The mushroom family Psathyrellaceae: Evidence for large-scale polyphyly of the genus *Psathyrella.* Molecular Phylogenetics and Evolution 46(2): 415–429. https://doi.org/10.1016/j.ympev.2007.11.004

Persoon CH (1797) Tentamen dispositionis methodicae fungorum in classes, ordines, genera et familias. Cum supplemento adjecto. Arcum Caeci, Leipzig, Germany, 1–76. https://doi.org/10.5962/bhl.title.42674

Quélet L (1872) Les champignons du Jura et des vosges. Mémoires de la Société d'Émulation de Montbéliard 5: 43–332.

Redhead SA, Vilgalys R, Moncalvo JM, Johnson J, Hopple Jr JS (2001) *Coprinus* Pers. and the disposition of *Coprinus* species *sensu lato.* Taxon 50(1): 203–241. https://doi.org/10.2307/1224525

Reid DA (1986) New or interesting records of Australasian basidiomycetes: VI. Transactions of the British Mycological Society 86(3): 429–440. https://doi.org/10.1016/S0007-1536(86)80186-3

Ronquist F, Teslenko M, Van Der Mark P, Ayres DL, Darling A, Höhna S, Larget B, Liu L, Suchard MA, Huelsenbeck JP (2012) MrBayes 3.2: Efficient Bayesian phylogenetic inference and model choice across a large model space. Systematic Biology 61(3): 539–542. https://doi.org/10.1093/sysbio/sys029

Singer R (1948) New Genera of Fungi-IV. Mycologia 40(2): 262–264. https://doi.org/10.1080/00275514.1948.12017704

Singer R (1951) Type study on basidiomyceteV. Sydowia 5: 445–475.

Singer R (1975) The Agaricales in modern taxonomy. J. Cramer, Vaduz, Liechtenstein, 912 pp.

Singer R (1986) The Agaricales in Modern Taxonomy. 4 ed. Koeltz Scientific Books, Koenigstein, Federal Republic of Germany, 981 pp.

Smith AH (1972) The North American species of *Psathyrella.* The New York Botanical Garden 24: 1–633.

Vizzini A, Consiglio G, Marchetti M (2019) Mythicomycetaceae fam. nov. (Agaricineae, Agaricales) for accommodating the genera Mythicomyces and Stagnicola, and Simocybe parvispora reconsidered. Fungal Systematics and Evolution 3(1): 41–56. https://doi.org/10.3114/fuse.2019.03.05

Wächter D, Melzer A (2020) Proposal for a subdivision of the family Psathyrellaceae based on a taxon-rich phylogenetic analysis with iterative multigene guide tree. Mycological Progress 19(11): 1151–1265. https://doi.org/10.1007/s11557-020-01606-3

Wang S-N, Hu Y-P, Chen J-L, Qi L-L, Zeng H, Ding H, Huo G-H, Zhang L-P, Chen F-S, Yan J-Q (2021) First record of the rare genus *Typhrasa* (Psathyrellaceae, Agaricales) from China with description of two new species. MycoKeys 79: 119–128. https://doi.org/10.3897/mycokeys.79.63700

White TJ, Bruns TD, Lee SB, Taylor JW, Innis MA, Gelfand DH, Sninsky JJ (1990) Amplification and direct sequencing of Fungal Ribosomal RNA Genes for phylogenetics. In: Innis MA, Gelfand DH, Sninsky JJ, White TJ (Eds) PCR protocols: a guide to methods and applications. New York, USA, Academic Press, 315–322. https://doi.org/10.1016/B978-0-12-372180-8.50042-1

Yan JQ, Bau T (2017) New and newly recorded species of *Psathyrella* (Psathyrellaceae, Agaricales) from Northeast China. Phytotaxa 321(1): 139–150. https://doi.org/10.11646/phytotaxa.321.1.7

Yan JQ, Bau T (2018a) The Northeast Chinese species of *Psathyrella* (Agaricales, Psathyrellaceae). MycoKeys 33: 85–102. https://doi.org/10.3897/mycokeys.33.24704

Yan JQ, Bau T (2018b) *Psathyrella alpina* sp. nov. (Psathyrellaceae, Agaricales), a new species from China. Phytotaxa 349(1): 85–91. https://doi.org/10.11646/phytotaxa.349.1.11

Yan J-Q, Ge Y-P, Hu D-M, Zhou J-P, Huo G-H (2019) *Psathyrella tintinnabula* sp. nov. (Psathyrellaceae, Agaricales), a new species from southwest China. Phytotaxa 400(2): 64–70. https://doi.org/10.11646/phytotaxa.400.2.2

Yu W-J, Chang C, Qin L-W, Zeng N-K, Fan Y-G (2020) *Pseudosperma citrinostipes* (Inocybaceae), a new species associated with Keteleeria from southwestern China. Phytotaxa 450: 8–16. https://doi.org/10.11646/phytotaxa.450.1.2

Zhao R-L, Li G-J, Sanchez-Ramirez S, Stata M, Yang Z-L, Wu G, Dai Y-C, He S-H, Cui B-K, Zhou J-L, Wu F, He M-Q, Moncalvo J-M, Hyde KD (2017) A six-gene phylogenetic overview of Basidiomycota and allied phyla with estimated divergence times of higher taxa and a phyloproteomics perspective. Fungal Diversity 84(1): 43–74. https://doi.org/10.1007/s13225-017-0381-5

Supplementary material 1

***Iugisporipsathyra reticulopilea* gen. et sp. nov. (Agaricales, Psathyrellaceae) from Tropical China Produces Unique Ridge-ornamented Spores with an Obvious Suprahilar Plage**

Authors: Jun-Qing Yan, Yu-Guang Fan, Sheng-Nan Wang

Data type: phylogenetic

Explanation note: A nexus file contains alignment sequence and original tree of ML and Bayes.

Link: https://doi.org/10.3897/mycokeys.90.85690.suppl1

MycoKeys 90: 163–202 (2022)
doi: 10.3897/mycokeys.90.85267
https://mycokeys.pensoft.net

RESEARCH ARTICLE

A peer-reviewed open-access journal
MycoKeys
Launched to accelerate biodiversity research

Not (only) poison pies – *Hebeloma* (Agaricales, Hymenogastraceae) in Mexico

Ursula Eberhardt[1], Alejandro Kong[2], Adriana Montoya[2], Nicole Schütz[1], Peter Bartlett[3], Henry J. Beker[4,5,6]

1 *Staatliches Museum für Naturkunde Stuttgart, Rosenstein 1, 70191 Stuttgart, Germany* **2** *Centro de Investigación en Ciencias Biológicas, Universidad Autónoma de Tlaxcala, Km 10.5 carretera San Martín Texmelucan-Tlaxcala, San Felipe Ixtacuixtla, Tlaxcala, 90120, Mexico* **3** *La Baraka, Gorse Hill Road, Virginia Water, Surrey GU25 4AP, United Kingdom* **4** *Rue Père de Deken 19, B-1040 Bruxelles, Belgium* **5** *Royal Holloway College, University of London, Egham, UK* **6** *Plantentuin Meise, Nieuwelaan 38, B-1860 Meise, Belgium*

Corresponding author: Ursula Eberhardt (ursula.eberhardt@smns-bw.de)

Academic editor: Maria-Alice Neves | Received 12 April 2022 | Accepted 7 June 2022 | Published 30 June 2022

Citation: Eberhardt U, Kong A, Montoya A, Schütz N, Bartlett P, Beker HJ (2022) Not (only) poison pies – *Hebeloma* (Agaricales, Hymenogastraceae) in Mexico. MycoKeys 90: 163–202. https://doi.org/10.3897/mycokeys.90.85267

Abstract

The species of *Hebeloma* have been little studied in Mexico, but have received attention as edibles and in trials to enhance production of edible fungi and tree growth through inoculation of seedlings with ectomycorrhizal fungi. Here we describe three new species of *Hebeloma* that are currently known only from Mexico. These species belong to separate sections of the genus: *H. ambustiterranum* is a member of *H.* sect. *Hebeloma*, *H. cohaerens* belongs to *H.* sect. *Theobromina*, while *H. magnicystidiatum* belongs to *H.* sect. *Denudata.* All three species were collected from subtropical pine-oak woodland; all records of *H. cohaerens* came from altitudes above 2500 m. *Hebeloma ambustiterranum* is commonly sold in the local markets of Tlaxcala as a prized edible mushroom. An additional nine species are reported from Mexico, of which eight are new records for the country: *H. aanenii*, *H. eburneum*, *H. excedens*, *H. ingratum*, *H. neurophyllum*, *H. sordidulum*, *H. subaustrale* and *H. velutipes*. First modern descriptions of *H. neurophyllum* and *H. subaustrale*, originally described from the USA, are given here.

Keywords

barcodes, Basidiomycota, ectomycorrhizal fungi, edible fungi, 3 new species, type studies

Introduction

Arguably, the best recognized vernacular English name for the genus *Hebeloma* is poison pie, although this name is often reserved for *H. crustuliniforme*, and other species within the genus are qualified versions of this name, e.g. *H. mesophaeum* is the veiled poison pie and *H. pusillum* is the dwarf poison pie (https://www.britmycolsoc.org.uk/library/english-names, accessed 18 Nov 2021). The name poison pie suggests what is, certainly in Europe, believed to be true for all members of the genus: that they are poisonous, or even if they were not, all too easily mixed up with poisonous members of the genus. Collecting *Hebeloma* for human consumption is generally discouraged (Bresinsky and Besl 1990; Benjamin 1995).

In Mexico, the main interest in *Hebeloma* from the local community was either in the context of edibility (e.g., Montoya et al. 2008; Reyes-López et al. 2020) or with regard to the inoculation of trees of forest importance with ectomycorrhizal fungi (Pérez-Moreno et al. 2020 and references therein; Pérez-Moreno et al. 2021). A number of *Hebeloma* species were mentioned in these articles, including *H. alpinum*, *H. helodes*, *H. leucosarx* and *H. mesophaeum*.

We have not had the opportunity to examine the material used in the respective publications. Given the difficulty surrounding species concepts of this genus, the presence of these species in Mexico should be treated with caution. Both, with regard to the consumption of mushrooms and the inoculation of tree seedlings, it would be advantageous to have a clear understanding of the species involved and the morphological and molecular characters that define them to recognize or verify collections or strains.

To the best of our knowledge, *Hebeloma* are not included in commercial ectomycorrhizal fungi mixtures currently sold to enhance tree growth, but it is one of the few genera that have been used in numerous nursery trials and transplanting experiments (e.g., Castellano and Molina 1989; Barroetaveña and Rajchenberg 2005; Gagné et al. 2006; Oliveira et al. 2010 and see below). Owing to the difficulties delimiting and identifying *Hebeloma* species, members of the genus have often been treated as if they all shared the same ecological traits. This is clearly not the case (Beker et al. 2016).

From the taxonomic side, the *Hebeloma* of North America have been largely neglected since the work of Hesler and Smith in the 1970s and 1980s (Hesler 1977 and his unpublished manuscript on North American species of *Hebeloma*, Smith et al. 1983) and never extensively studied within Mexico. This lack of understanding of species concepts can be illustrated by reference to observation websites. For example, iNaturalist (https://www.inaturalist.org/observations?place_id=6793&taxon_id=192716 accessed on 12 March 2021) listed 41 *Hebeloma* observations for Mexico, but just six of these observations had species names attached: one was referred to *H. mesophaeum* and five were referred to *H. crustuliniforme*. Mushroom Observer (https://mushroomobserver.org/observer/advanced_search?q=1eMh6 accessed 12 March 2021) listed just eleven *Hebeloma* records from Mexico, none of which were identified to species level. The Global Biodiversity Information Facility GBIF.org (GBIF Occurrence Download https://doi.org/10.15468/dl.wd7f75 accessed 18 November 2021) gave

169 results for *Hebeloma* from Mexico, of which 60 were identified to species level: *H. alpinum* (1), *H. crustuliniforme* (17), *H. edurum* (1), *H. fastibile* (19), *H. mesophaeum* (16), *H. sacchariolens* (1) and *H. sinapizans* (5). MycoPortal (https://mycoportal.org/portal/collections/list.php accessed on 18 November 2021) gave 105 results for *Hebeloma* of Mexico. 100 of these records were from the National Herbarium of Mexico Fungal Collection (MEXU), four were from the Field Museum of Natural History (F) and one was from USDA, the United States National Fungus Collections (BPI). Of these 105 collections, 86 had no species name given, ten were identified as *H. fastibile*, five as *H. sinapizans*, three as *H. mesophaeum* and one as *H. sacchariolens*. There were, of course, overlaps between these databases, and one should be cautious of determinations given the historical confusion regarding species definitions, but all species records indicate just 6 species recorded: *H. alpinum*, *H. crustuliniforme*, *H. laterinum* (= *H. edurum*, *H. fastibile*), *H. mesophaeum*, *H. sacchariolens* and *H. sinapizans*.

Beker et al. (2016) published a monograph on *Hebeloma* of Europe to provide a new foundation for the understanding of species of this genus, on which future studies could be built. Although this monograph only addressed the genus within Europe, it has provided a base both morphologically and molecularly. Since the publication of that monograph, a number of papers have been published describing new species of *Hebeloma* as well as resurrecting long forgotten names that can now be confirmed as valid (e.g., Cripps et al. 2019; Eberhardt et al. 2020a, 2020b, 2021a, 2021b, 2022a, 2022b; Monedero and Alvarado 2020).

Within this paper, we present a list of *Hebeloma* species we have found during analysis of herbarium collections from Universidad Autónoma de Tlaxcala (TLXM). The 90 collections studied came from two principal areas in Chihuahua and Tlaxcala but also included a few collections from the regions of Mexico City and Puebla. Within this set, two species were rediscovered, *H. neurophyllum* (Atkinson 1909) and *H. subaustrale* (Murrill 1945), originally described from the US. The identifications were verified by morphological and molecular type studies. Three species new to science were discovered and are described below as *H. ambustiterranum*, *H. cohaerens* and *H. magnicystidiatum*. These species belong to separate sections of the genus and are described below.

Materials and methods

All the material studied were dried specimens from the Universidad Autónoma de Tlaxcala (TLXM). The collections sites are shown in Fig. 1. These collections were compared to material collected for the *Hebeloma* project (Beker et al. 2016). Coordinates were obtained in the field by GPS or were approximated from the collection data. Approximations of elevations (m above sea level), where not recorded at time of collection, were deduced using Google Earth (Google Earth Pro Version 7.3.4.8248).

Sequences were obtained from the dried basidiomes by direct sequencing. At least the ITS (barcode) locus was generated for all Mexican collections and, in a number

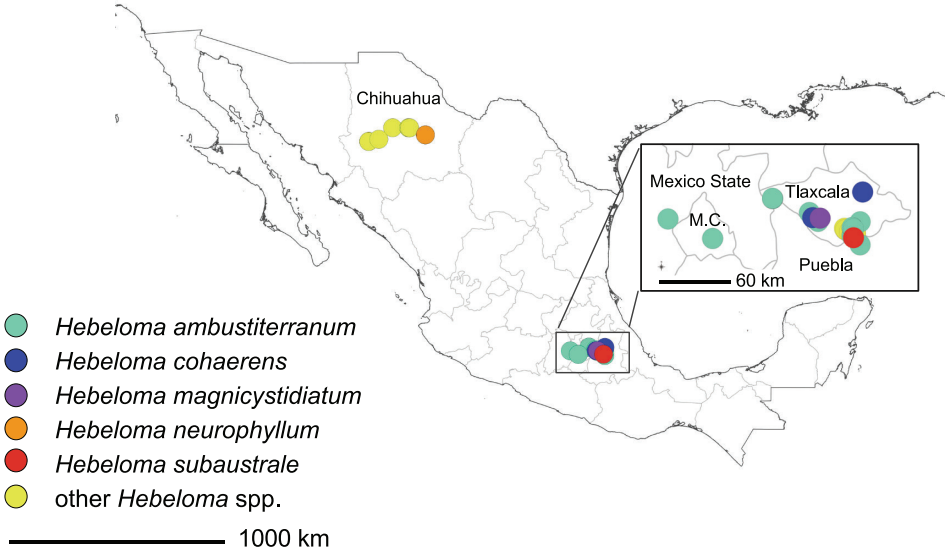

Figure 1. Collection sites of studied material. Scale bar 1000 km. The map was generated with QGIS version 3.16.15 using WGS84, EPDG: 4326 (QGIS Association, QGIS.org, 2022). Shapefiles were provided by the Database of Global Administrative Areas (GADM); Accessed April 2018 to March 2022.

of cases, additional loci were sequenced. Internal transcribed spacer sequences were generated following methods detailed in Eberhardt (2012) and Cripps et al. (2019); *MCM7* (minichromosome maintenance complex component 7, partial) data following Eberhardt et al. (2016a); *RPB2* and *TEF1*a sequences following Eberhardt et al. (2021a); and sequences of two variable regions (V6 and V9) of the mitochondrial SSU followed Gonzalez and Labarère (1998). Sequencing was carried out by LGC Genomics (Berlin, Germany). Sequences were edited using Sequencher vs. 4.9 (Gene Codes Corp., Ann Arbor, Michigan). Newly generated sequences were accessioned to GenBank (ON167764–ON167898, ON168958–ON168966, ON202494–ON202614 and ON237944–ON237985), Suppl. material 1: Table S1 summarizes all sequences used in the analyses, including those previously published in the context of a number of publications (Eberhardt et al. 2009, 2013, 2015, 2016a, 2016b, 2021a, 2022a, 2022b; Eberhardt and Beker 2010; Beker et al. 2010, 2013, 2016; Schoch et al. 2012; Cripps et al. 2019).

Sequence alignments were done online in MAFFT using the E-INS-i option (Katoh et al. 2005, 2019) or locally with the "Mafft-globalpair" setting of MAFFT 7.471 (Katoh and Standley 2013). Alignments were done, viewed and reformatted in ALIVIEW 1.27 (Larsson 2014). Phylogenetic analyses (ML) were run in IQ-TREE (Nguyen et al. 2015) online (Trifinopoulos et al. 2016). Model selection (Kalyaanamoorthy et al. 2017) was done using the BIC criterion, including FreeRate models and merging partitions if possible (protein coding loci were originally partitioned according to position, coding and non-coding). Branch support was obtained through 1000 replicates of ultrafast

bootstrap (ufb; Minh et al. 2013; Hoang et al. 2018) and SH-like approximate likelihood ratio tests (SH-aLRT; Guindon et al. 2010). Support values are given as (SH-aLRT [%]/ufb [%]), for SH-aLRT support ≥ 85% and ufb support ≥ 95%. Nexus files with alignments and trees, including all single locus trees, are available as Suppl. material 2.

Alignments were made for sections including new or rediscovered species, i.e., for *H.* sect. *Hebeloma*, *H.* sect. *Naviculospora*, *H.* sect. *Theobromina* and *H.* sect. *Velutipes*, including loci that were known to facilitate species recognition in the respective section (Beker et al. 2016). Sequences of types were included if available unless missing data (short sequences) had an adverse effect on the taxonomic resolution of the result. The selection of loci, additional species and taxa used for rooting was guided by previous results (Beker et al. 2016; Cripps et al. 2019; Eberhardt et al. 2021a, 2021b, 2022a, 2022b) – and by the loci that could be generated from the collections available. Prior to concatenation, single locus trees (see Suppl. material 2) were generated. Conflicts were detected using the principle by Kauff and Lutzoni (2002), assuming a conflict to be significant if two different relationships for the same set of taxa, one being monophyletic and the other non-monophyletic, were supported by SH-aLRT support ≥ 85% or ufb support ≥ 95%. Alignments of different loci were concatenated and analyzed, indicating branches with conflicting results from single locus analyses by dashed lines.

Distances between sequences were calculated from the alignments used for the ML analyses as p-distances with pairwise deletion of gaps in MegaX (Kumar et al. 2018; Stecher et al. 2020). The UNITE database (Kõljalg et al. 2013, 2020) and plutof (Abarenkov et al. 2010) were used for sequence searches, directly and via BLAST and for matching sequences to SH (species hypotheses).

Details of morphological analyses were provided in Beker et al. (2016). The amount of macroscopic detail available to us varied hugely from collection to collection as it was dependent on the detail provided by the collector. For recent collections where one of the authors was the collector, each specimen was photographed and observed both in the field when characters were still fresh, and later in the laboratory. Fresh basidiomes of each specimen were dried using a food dehydrator.

All microscopic analysis was carried out on dried material, using a Leica DMRZA2 microscope with a Leica DFC495 camera connected to a computer running Leica Application Suite (LAS) V4 software.

The basidiospores were first studied in Melzer's reagent to assess the shape, degree of dextrinoidity, ornamentation and the degree of loosening of the perispore. For the assessment of the degrees of ornamentation (O0, O1, O2, O3, O4), of the loosening perispore (P0, P1, P2, P3) and for the dextrinoidity (D0, D1, D2, D3, D4), we used Beker et al. (2016) and Vesterholt (2005). A number of photographs were taken of the basidiospores at ×500 and ×1600, which were then measured using the LAS software. For each collection, wherever possible, at least 50 basidiospores were measured in Melzer's reagent, excluding the apiculus. As discussed in Beker et al. (2016), the difference in *Hebeloma* basidiospore size from dried material, measured in Melzer's reagent and 5% KOH, is negligible. The maximum length and width of each spore was measured, and its Q value (ratio of length to width) calculated. Average length, width,

and Q value were calculated and recorded alongside the median, standard deviation, and 5% and 95% percentiles.

The material was then examined in 5% KOH. Photographs were taken of the basidiospores and also of the cheilocystidia (and pleurocystidia if any were present) and basidia at ×500 and ×1000. Because of the complex shapes of the cheilocystidia four measurements were made: length, width at apex (A), width at narrowest point in central region (M), and maximum width in lower half (B). The measurements were given in this order, and an average value was calculated for each of these measurements. The average width of the cheilocystidium in the vicinity of the apex appears to be an important character in the separation of species within *Hebeloma* (Vesterholt 2005). It is also important, when determining this average width near the apex, not to be selective with regard to the cystidia chosen for measurement. To determine the average width at the apex, about 100 cheilocystidia were measured on the lamella edge. For other measurements, some 20 cheilocystidia, separated from the lamella edge, were measured from each collection. For each cheilocystidium the ratios A/M, A/B, and B/M were calculated and averaged across all cheilocystidia measured. For all other details with regard to our methodology, see Beker et al. (2016).

Each collection studied has a database record number associated with that collection (beginning HJB); we give these numbers as we intend to make the database publicly available. If no other herbarium abbreviation or herbarium accession number is given, the HJB number is also the collection number within H.J. Beker's herbarium.

Species were identified considering morphological and molecular data. In cases in which molecular data were not conclusive (as e.g., for *H. eburneum* and *H. velutipes*, or could not be obtained, as for the type of *H. subaustrale*), species identification followed morphology. For species not discussed in detail here, please refer to species descriptions in Beker et al. (2016) and Eberhardt et al. (2021a, 2022a).

Results

It appears that all of the species found in our sample, other than *Hebeloma mesophaeum*, are new species records for Mexico. Fig. 1 shows the distribution of these fungal collections in Mexico; Suppl. material 1: Table S1 lists all collections utilized during this study, including those not specifically discussed in the Taxonomy part.

The analysis of taxa from *H.* sect. *Hebeloma* (from Mexico *H. ambustiterraneum*, *H. excedens* and *H. mesophaeum*) included ITS, *RPB2* and *Tef1a* data, and 67 collections from 13 species. *Hebeloma sordescens* (*H.* sect. *Hebeloma*) was used for rooting. *Hebeloma ambustiterranum* was monophyletic in all single locus results and received support in ITS (100/100%) and *RPB2* (85/98%). Conflicts between ITS and the other two loci were observed in relation to the position of *H. pubescens* (p.p.) and *H. subtortum* (ITS with *H. excedens*, *H. mesophaeum* and *H. psammophilum*; *RPB2* and *TEF1a* with *H. colvinii* and *H. velatum* [= *H. dunense*, Eberhardt et al. 2022a] and within *H. pubescens* [collection HJB12057]). Neither of these conflicts were considered rel-

evant in the current context. The concatenated alignment spanned 2205 positions. The clade of *H. ambustiterranum* (Fig. 2) received full (100/100%) support. This result supported morphology in that *H. ambustiterranum* is a good species new to science. Neither *H. excedens* nor *H. mesophaeum* were resolved (Fig. 2); the Mexican collections of these two species were placed among other members of *H. excedens* and *H. mesophaeum*.

The analysis for *H.* sect. *Denudata* (in Mexico *H. aanenii*, *H. eburneum*, *H. ingratum*, *H. magnicystidiatum* and *H. sordidulum*) was based on ITS, mitSSU V6 and V9 of 78 collections from 17 species. *Hebeloma echinosporum* and *H. populinum* (*H.* sect. *Denudata*, subsect. *Echinospora*) were used for rooting. In the ITS tree, *H. magnicystidiatum* was part of the *H. sordidulum* clade (90/–%), which was included in a weakly supported clade (90/–%) with all other members of *H.* subsect. *Clepsydroida* considered in the analysis. Neither of the mitSSU results contradicted this relationship with any support, but there were conflicts between the ITS and mitSSU results and between the two mitSSU results in relation to the limits of the subsections and the relationship of *H. hiemale* (*H.* subsect. *Hiemalia*) and *H.* subsect. *Clepsydroida* and *H.* subsect. *Crustuliniformia*. In spite of this, the alignments were concatenated. The resulting phylogenetic hypothesis (Fig. 3) showed *H. magnicystidiatum* outside the clade of *H. sordidulum* (which was only weakly supported, 85/–%), but on a relatively long branch, thus supporting morphology that *H. magnicystidiatum* is a separate species. Because of existing conflicts, molecular data could not resolve the position of *H. magnicystidiatum* in any of *H.* subsects. *Clepsydroida*, *Crustuliniformia* or *Hiemalia*.

The Mexican collections of *H. aanenii* clustered with their conspecifics from other countries, while the Mexican collections of *H. eburneum* were not in the same clade as *H. eburneum* collections from other countries, both clades received some support, one by ufb, the other by SH-aLRT (see Fig. 3). The only single locus tree showing a Mexican *H. eburneum* clade is mitSSU V6 (86/95% support). Both *H. eburneum* clades were, as well as *H. aanenii*, in what Beker et al. (2016) termed the *H. alpinum*-complex (94/97% support). The Mexican collection of *H. ingratum* was included in the *H. ingratum* clade (93/98% support); the Mexican collection of *H. sordidulum* was included in the respective species clade, which only received 87/– support.

The analysis for *H.* sect. *Velutipes* (in Mexico *H. neurophyllum* and *H. velutipes*) was based on ITS, *RPB2*, *TEF1a* and mitSSU V6 of 59 collections from 12 species. *Hebeloma bulbiferum* and *H. sinapizans* (*H.* sect. *Sinapizantia*) were used for rooting. *Hebeloma neurophyllum* received good support (95/95%) in the ITS result, and is paraphyletic in relation to *H. erebium* in the *RPB2* and *TEF1a* results, and in relation to *H. celatum* in the mitSSU V6 result. In spite of a number of conflicts concerning interspecific relationships within *H.* sect. *Velutipes*—intraspecific conflicts were not detected—the different single locus alignments were concatenated. The alignment included 2670 positions. In the analysis of the concatenated dataset (Fig. 4), *H. neurophyllum* was well supported (97/99%), as were *H. celatum* (97/ 99%) and *H. erebium* (98/100%). Thus, molecular data as well as morphological characters (see below) supported *H. neurophyllum* as a good species.

Hebeloma velutipes was paraphyletic in relation to the other member species of the *H. velutipes* complex clade (*H. incarnatulum*, *H. leucosarx* and *H. subconcolor*). The

Figure 2. ML topology of concatenated ITS, *RPB2* and *TEF1a* sequences of *Hebeloma* sect. *Hebeloma*. Branch support was obtained through 1000 replicates of SH-like approximate likelihood ratio tests and ultrafast bootstrap annotated SH-aLRT/ufb at the branches for ≥ 85% SH-aLRT and ≥ 95% for ufb support. Dotted lines indicate parts of the tree where conflicts between single locus results were observed. *Hebeloma sordescens* (*H.* sect. *Hebeloma*) was used for rooting. Collections indicated with * are types; clade names indicated by * include type sequences. Collections and species names in red refer to Mexican material.

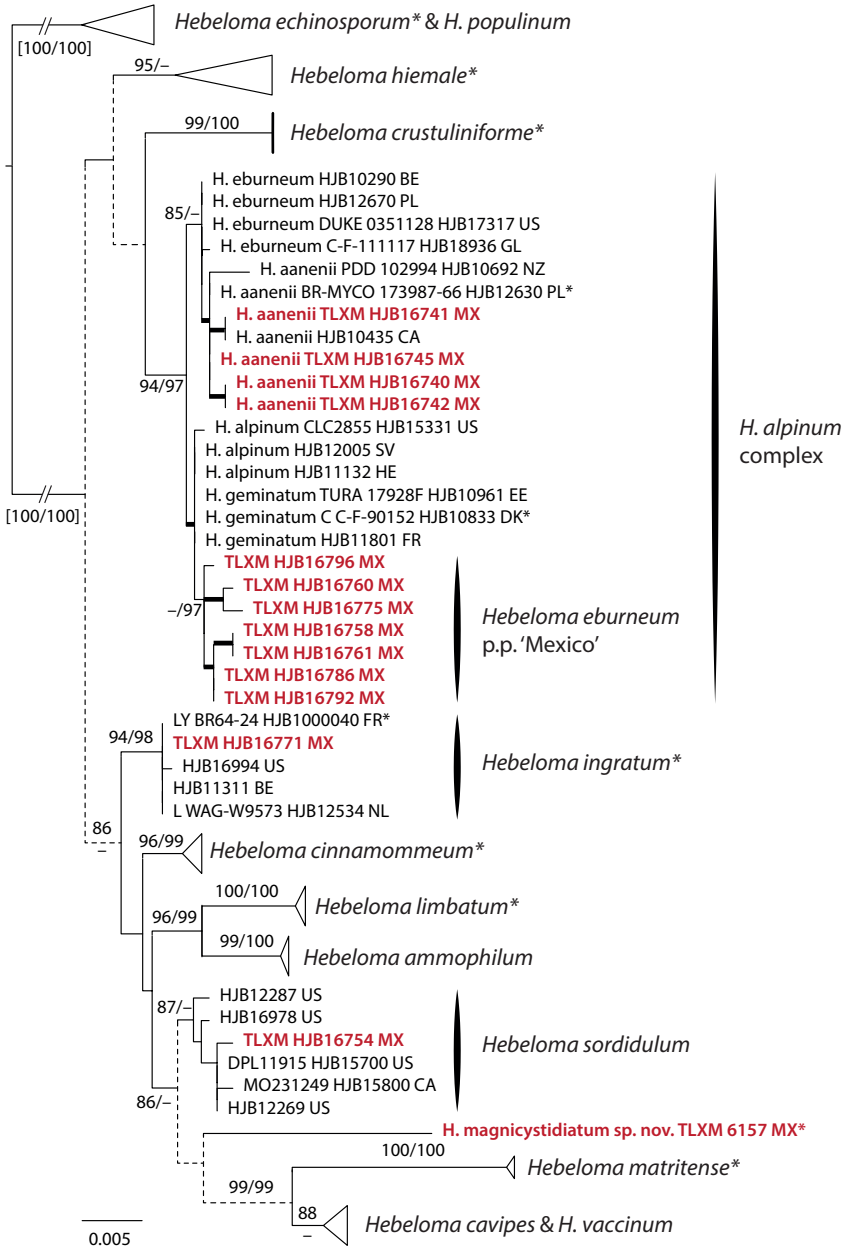

Figure 3. ML topology of concatenated ITS, mitSSU V6 and V9 sequences of *Hebeloma* sect. *Denudata*. Branch support was obtained through 1000 replicates of SH-like approximate likelihood ratio tests and ultrafast bootstrap annotated SH-aLRT/ufb at the branches for ≥ 85% SH-aLRT and ≥ 95% for ufb support or by thick lines in the case that at least one of the support values is equal to or exceeds the limits. Dotted lines indicate parts of the tree where conflicts between single locus results were observed. *Hebeloma echinosporum* and *H. populinum* (*H.* subsect. *Echinospora* of *H.* sect. *Denudata*) were used for rooting. Collections indicated with * are types; clade names indicated by * include type sequences. Collections in red refer to Mexican material.

position of the Mexican collections of *H. velutipes* in a separate clade (97/99%) was only supported by the mitSSU V6 data.

The analysis for *H.* sect. *Theobromina* (in Mexico *H. cohaerens*) was based on ITS, *MCM7* and *RPB2* of 32 collections from nine species. *Hebeloma sinapizans* was used for rooting. *Hebeloma cohaerens* was supported by all three single locus analyses (96–97/95–100%) and received full (100/100%) support in the analysis of the concatenated data (2152 bp) (Fig. 5A). No conflicts were found between the single locus results. Thus, both molecular results and morphology supported *H. cohaerens* as a new species.

The analysis for *H.* sect. *Naviculospor*a (in Mexico *H. subaustrale*) was based on the ITS of 24 collections of eight species and included 703 positions. *Hebeloma islandicum*, provisionally placed by Beker et al. (2016) in *H.* sect. *Naviculospora* to avoid creating a monospecific section for the species, was used for rooting. Holotype sequences generated by P.B. Matheny and A.D. Wolfenbarger of *H. angustisporium* (NR_119890, Schoch et al. 2014) and of *H. perangustisporium* (HQ179680, unpublished, submitted 23 Aug 2010) and by H. Gordon of *H. pungens* (MW412387, unpublished, submitted 28 Dec 2020) were identical or almost identical with our sequences but had shorter read length in the analyzed region. Thus, only the sequences generated by us were considered in the analysis. The holotype sequences of *H. angustisporium* and *H. perangustisporium*, as well as three morphologically matching collections formed a clade supported by 97/97% among all other recognized members of *H.* sect. *Naviculospora*. Morphologically, the *H. angustisporium* and *H. perangustisporium* agree with *H. subaustrale*, which is the oldest of the three names. Thus, although no sequence data could be obtained for the type of *H. subaustrale*, the clade is referred to as *H. subaustrale* in Fig. 5B, and *H. subaustrale* is accepted and described below.

Taxonomy

For species described from Europe please refer to Beker et al. (2016); for *H. excedens* and *H. sordidulum* to Eberhardt et al. (2022a) and for *H. excedens* also to Cripps et al. (2019).

Hebeloma ambustiterranum **A. Kong & Beker, sp. nov.**

MycoBank No: 842826
Figs 6–7

Type. Mexico. Tlaxcala: La Malinche National Park, 19.2749°N, 97.9825°W, alt. approx. 2800 m, on burnt soil in coniferous woodland under *Pinus montezumae* and *P. teocote*, 8 Jul 2017, H.J. Beker HJB16802 (holotype TLXM 6155; isotype BR 5020224874626V); GenBank ITS ON202501.

Diagnosis. The small ellipsoid, non-dextrinoid, almost smooth basidiospores (on average 8.0–10.2 × 5.6–6.5 µm) and at least 50 full length lamellae distinguish this species from all other known North American *Hebeloma* species and the ITS sequence differentiates this species from all other known species, worldwide.

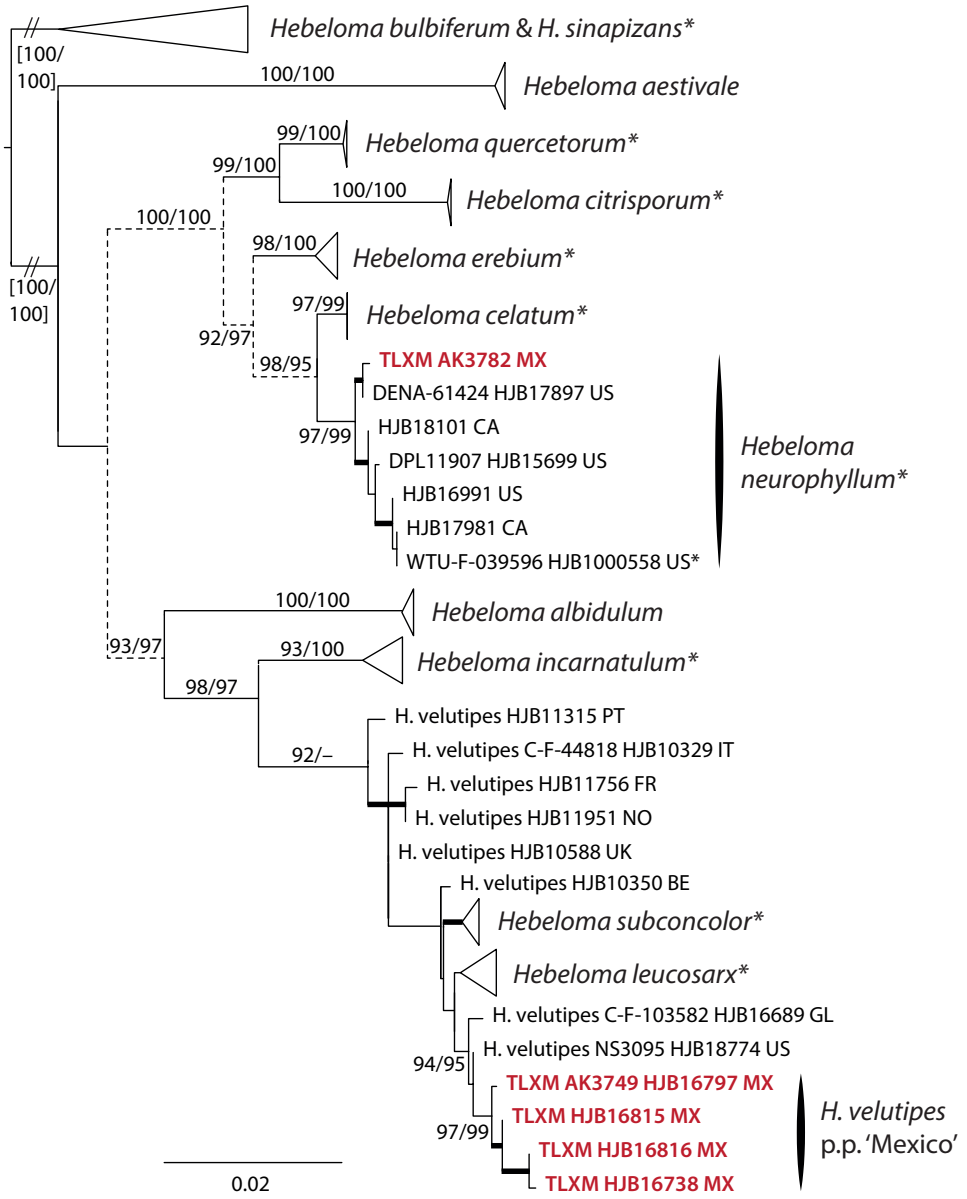

Figure 4. ML topology of concatenated ITS, *RPB2* and *TEF1a* and mitSSU V6 sequences of *Hebeloma* sect. *Velutipes*. Branch support was obtained through 1000 replicates of SH-like approximate likelihood ratio tests and ultrafast bootstrap annotated SH-aLRT/ufb at the branches for ≥ 85% SH-aLRT and ≥ 95% for ufb support or by thick lines in the case that at least one of the support values is equal to or exceeds the limits. Dotted lines indicate parts of the tree where conflicts between single locus results were observed. *Hebeloma bulbiferum* and *H. sinapizans* (*H.* sect. *Sinapizantia*) were used for rooting. Collections indicated with * are types; clade names indicated by * include type sequences. Collections in red refer to Mexican material.

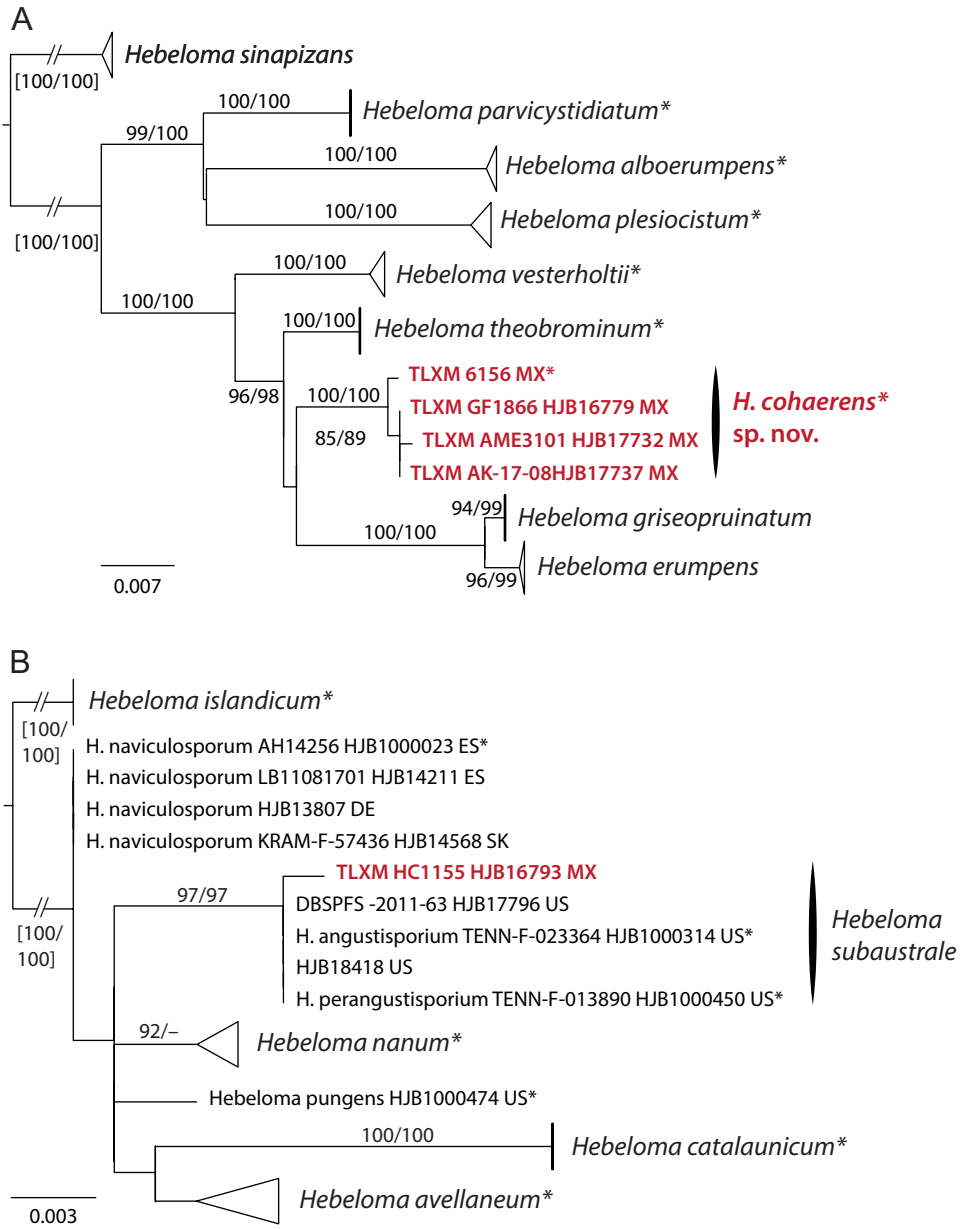

Figure 5. ML topologies with branch support obtained through 1000 replicates of SH-like approximate likelihood ratio tests and ultrafast bootstrap annotated SH-aLRT/ufb at the branches for ≥ 85% SH-aLRT and ≥ 95% for ufb support. Collections indicated with * are types; clade names indicated by * include type sequences. Collections in red refer to Mexican material **A** concatenated ITS, *MCM7* and *RPB2* sequences of *Hebeloma* sect. *Theobromina*, rooted with *H. sinapizans* (*H.* sect. *Sinapizantia*) **B** ITS sequences of *H.* sect. *Naviculospora*, rooted with *H. islandicum* (*H.* sect. *Naviculospora*).

Etymology. From *ambustus* (Latin adj.) meaning scorched, *terra* (Latin n.) meaning soil and the Latin suffix *-anum* indicating position to indicate growing on scorched soil. In Mexico, the local people burn the ground in the pine forests to encourage the growth of this mushroom, which they regard as an excellent edible mushroom. The local people refer to it in Nahuatl as the xolete de ocoxal (or ocoxalnanacatl), the mushroom of the pine needles from Chamusquinero, meaning from burnt ground.

Description. Pileus (12) 16–45 (52) mm diameter, usually umbonate or subumbonate, rarely convex or applanate; margin usually entire, sometimes involute particularly when young, often with remains of the universal veil, occasionally spotting, not hygrophanous; usually almost unicolored with color at center usually cream to ochraceous or clay-buff but may occasionally be darker, honey to sepia or umber, usually a little paler at the margin. Lamellae emarginate, white, cream to brown, with a weak white fimbriate edge sometimes visible and without droplets, number of full-length lamellae 50–74. Stipe (23) 24–60 (75) mm long, 3–8 (10) mm diameter at median, cylindrical, surface cream, ivory to pale brown but occasionally discoloring from the base upwards, sometimes strongly, fibrillose, at apex pruinose; base with white mycelium. Partial veil present on young specimens, whitish at first, before basidiospores mature, and often clear fibrils remaining on the stipe and pileus. Context in pileus white to cream, firm, in stipe stuffed, becoming hollow with age; taste not recorded, smell occasionally odorless but usually raphanoid, sometimes strongly so or with cacao components. Spore deposit color clay-buff.

Basidiospores based on n = 146 spores of the holotype, 5% to 95% percentile range 7.7–9.8 × 5.5–7.0 µm, with median 8.9 × 5.9 µm and av. 8.9 × 6.0 µm with S.D. length 0.68 µm and width 0.44 µm; Q value 5% to 95% percentile range 1.25–1.63, with median 1.48 and av. 1.47 with S.D. 0.11; spore size based on 33 collections medians 7.8–10.3 × 5.5–6.4 µm and av. 8.0–10.2 × 5.6–6.5 µm with av. S.D. length 0.61 µm and width 0.35 µm, av. Q 1.36 –1.61, ellipsoid or ovoid, with small apiculus, apex round or subacute, with a distinct thinning of the apical wall, guttulate with one or sometimes more oily drops, usually almost smooth even under immersion, with perispore not loosening, almost totally non-dextrinoid with just an indistinct brownish tint in Melzer's reagent (O1; P0; D1); pale yellow to brown in KOH. Basidia 25–34 × 6–8 µm, with av. Q 3.7–4.4, cylindrical to clavate, hyaline, 4-spored. Cheilocystidium width near apex holotype 5% to 95% percentile range 3.5–5.3 µm, with median 4.3 µm and av. 4.3 µm with S.D. 0.63 µm; across 33 collections median 4.1–5.4 µm and av. 4.1–5.1 µm; examining approx. 20 selected cheilocystidia of each of the 33 collections yields a range for the avs. of 35–55 × 4.1–5.1 × 4.2–5.1 × 7.1–9.9 µm and 35 × 4.3 × 4.2 × 7.3 µm av. for holotype; av. ratios A/M: 0.96–1.15, A/B: 0.51–0.70, B/M: 1.55–2.31, mainly swollen in the lower half, some ventricose or lageniform, often with one or two septa, rarely geniculate or with some thickening of the median wall, hyaline. Pleurocystidia absent. Caulocystidia similar to cheilocystidia but more cylindrical and larger, up to 140 µm. Pileipellis an ixocutis; epicutis up to 100 µm thick, with gelatinized, often encrusted hyphae up to 6 µm wide; subcutis yellow and

Figure 6. *Hebeloma ambustiterranum* **A–C** basidiomata **A** holotype TLXM 6155 (HJB16802) **B** TLXM HJB16803. **C** TLXM HJB16805 **D** mushroom vendor in the market of Tlaxcala City **E** *H. ambustiterranum* sold in the market of Tlaxcala City. Photos **A–D** H.J. Beker **E** A. Montoya.

the trama below the cutis made up of cylindrical or occasionally ellipsoid cells up to 14 µm wide. Clamp connections present throughout the basidiome.

Ecology and distribution. In temperate coniferous woodlands on burnt ground with *Pinus* and *Quercus*. Growth habit usually scattered, rarely solitary or caespitose. To date, all collections of *Hebeloma ambustiterranum* recorded from Mexico at latitudes between 19°N and 20°N and altitudes above 2000 m.

Additional collections examined. Mexico. **Mexico City:** Municipality of Milpa Alta, approx. 19.1942°N, 99.0267°W, alt. approx. 2400 m, 4 Jul 2011, R. Vanegas-Enriquez (TLXM RVE042, HJB17734). Municipality of Milpa Alta, approx. 19.1942°N, 99.0267°W, alt. approx. 2400 m, 16 Jul 2011, R. Vanegas-Enriquez (TLXM RVE049, HJB17735). Municipality of Milpa Alta, approx. 19.1942°N, 99.0267°W, alt. approx. 2400 m, 21 May 2013, A.C. López (TLXM ACL-MA-085, HJB17736). **Puebla:** Municipality of Acajete, La Malinche National Park, north of Santa Isabel Tepetzala, approx. 19.1471°N, 97.924°W, alt. approx. 2600 m, on soil in woodland under *Pinus* sp., 15 Jul 1998, R. Reyes-Lopez (TLXM RL1-01, HJB16780). Municipality of Acajete, La Malinche National Park, 4 km north of Santa Isabel Tepetzala, approx. 19.1471°N, 97.9239°W, alt. approx. 2600 m, on soil in woodland under *Pinus* sp., 29 Jul 1998, R. Reyes-López (TLXM RL2-7, HJB16765). **Tlaxcala:** La Malinche National Park, 19.2742°N, 97.9833°W, alt. approx. 2850 m), on burnt soil in coniferous woodland under *Pinus montezumae* and *Pinus teocote*, 8 Jul 2017, Forayer (TLXM HJB16799).

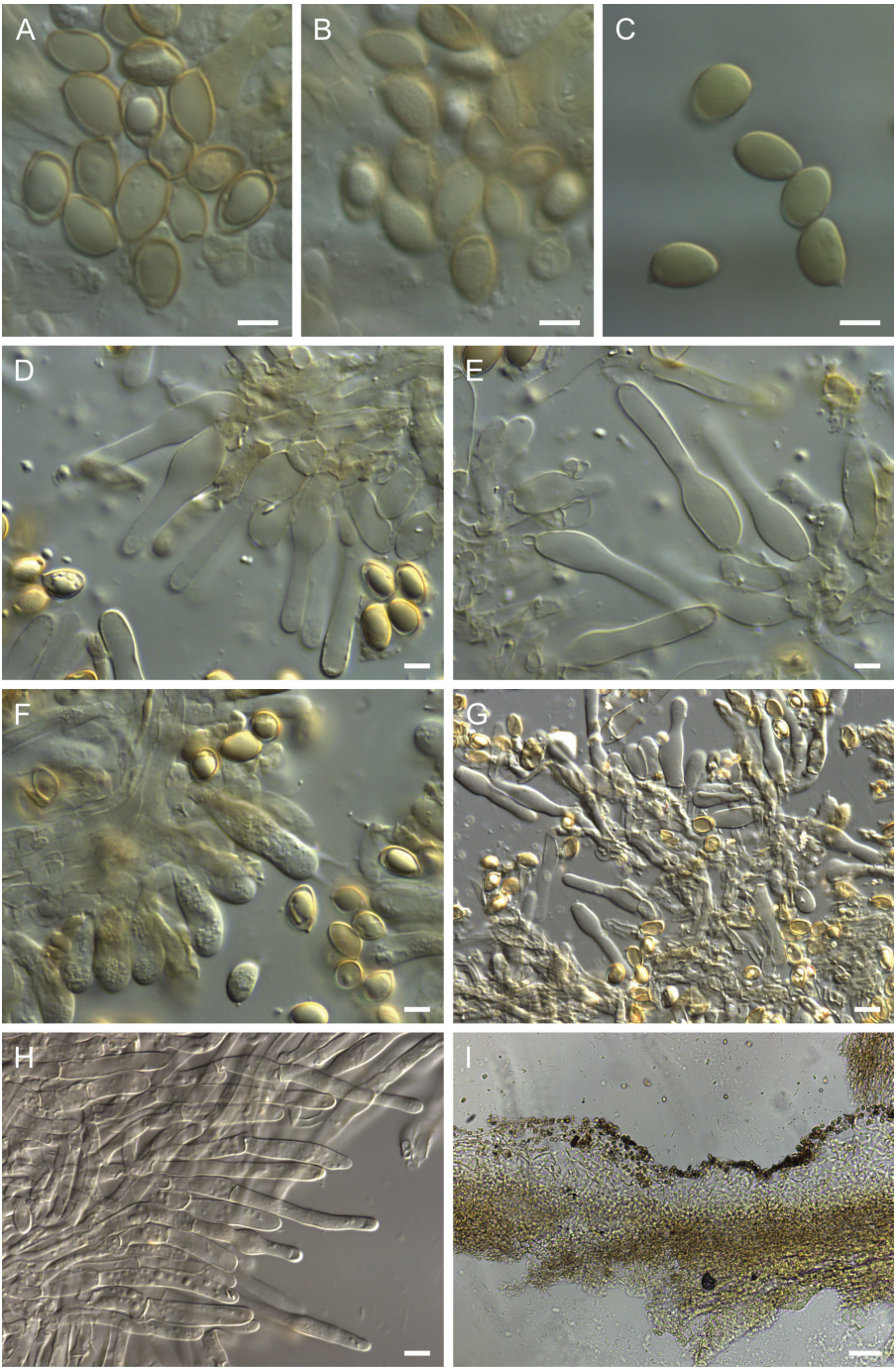

Figure 7. Holotype of *Hebeloma ambustiterranum* TLXM 6155 (HJB16802) **A** basidiospores ×1600 **B** spore ornamentation ×1600 **C** basidiospores in Melzer's reagent ×1600 **D–E** cheilocystidia ×1000 **F** basidia ×1000 **G** cheilocystidia on lamella edge ×500 **H** caulocystidia ×500 **I** Cutis ×125. All in KOH, except **C**. Scale bars: 5 µm (**A–F**); 10 µm (**G–J**); 50 µm (**K**). Photos H.J. Beker.

La Malinche National Park, 19.2744°N, 97.9831°W, alt. approx. 2850 m, on burnt soil in coniferous woodland under *Pinus montezumae* and *Pinus teocote*, 8 Jul 2017, L. Davies (TLXM HJB16800). La Malinche National Park, 19.2743°N, 97.9829°W, alt. approx. 2840 m 8 Jul 2017, L. Davies (TLXM HJB16801), on burnt soil in coniferous woodland under *Pinus montezumae* and *Pinus teocote*. La Malinche National Park, 19.2749°N, 97.9820°W, alt. approx. 2830 m, 8 Jul. 2017, A. Montoya-Esquivel, A. Kong (TLXM HJB16803), on burnt soil in coniferous woodland under *Pinus montezumae* and *Pinus teocote*. La Malinche National Park, 19.2752°N, 97.9820°W, alt. approx. 2830 m, on burnt soil in coniferous woodland under *Pinus montezumae* and *Pinus teocote*, 8 Jul 2017, A. Kong (TLXM HJB16804). La Malinche National Park, 19.2753°N, 97.9823°W, alt. approx. 2830 m, on burnt soil in coniferous woodland under *Pinus montezumae* and *Pinus teocote*, 8 Jul. 2017, A. Montoya-Esquivel, A. Kong (TLXM HJB16805). La Malinche National Park, 19.2751°N, 97.9825°W, alt. approx. 2830 m, on burnt soil in coniferous woodland under *Pinus montezumae* and *Pinus teocote*, 8 Jul 2017, A. Montoya-Esquivel, A. Kong (TLXM HJB16806). La Malinche National Park, 19.2754°N, 97.9824°W, alt. approx. 2830 m, on burnt soil in coniferous woodland under *Pinus montezumae* and *Pinus teocote*, 8 Jul 2017, H.J. Beker (TLXM HJB16807). La Malinche National Park, 19.2755°N, 97.983°W, alt. approx. 2830 m, on burnt soil in coniferous woodland under *Pinus montezumae* and *Pinus teocote*, 8 Jul 2017, A. Montoya-Esquivel, A. Kong (TLXM HJB16808). La Malinche National Park, 19.2652°N, 97.9744°W, alt. approx. 2825 m, on soil in coniferous woodland ditch under *Pinus teocote*, 9 Jul 2017, A. Montoya-Esquivel (TLXM HJB16818). Municipality of Huamantla, La Malinche National Park, Los Pilares, approx. 19.3184°N, 97.9233°W, alt. approx. 2500 m, on soil in woodland under *Pinus* sp., 2 Aug 1991, A. Montoya-Esquivel (TLXM AME1048, HJB16788). Municipality of Nanacamilpa, 19.4925°N, 98.5778°W, alt. approx. 2725 m, on burnt soil and litter in coniferous woodland under *Pinus montezumae*, 6 Jul 2017, Forayer (TLXM HJB16747). Municipality of Nanacamilpa, 19.4923°N, 98.5783°W, alt. approx. 2730 m, on burnt soil and litter in coniferous woodland under *Pinus montezumae*, 6 Jul 2017, A. Kong (TLXM HJB16748). Municipality of Nanacamilpa, road from Nanacamilpa to Tepuente, 19.4922°N, 98.5783°W, alt. approx. 2730 m, on burnt soil and litter in coniferous woodland under *Pinus montezumae*, 6 Jul 2017, A. Montoya-Esquivel (TLXM HJB16749). Municipality of Nanacamilpa, road from Nanacamilpa to Tepuente, 19.4928°N, 98.5792°W, alt. approx. 2725 m, on burnt soil and litter in coniferous woodland under *Pinus montezumae*, 6 Jul 2017, L. Davies (TLXM HJB16750). Municipality of Nanacamilpa, 19.4928°N, 98.5792°W, alt. approx. 2725 m, on burnt soil and litter in coniferous woodland under *Pinus montezumae*, 6 Jul 2017, L. Davies (TLXM HJB16751). Municipality of Nanacamilpa, 19.4933°N, 98.5791°W, alt. approx. 2725 m, on burnt soil and litter in coniferous woodland under *Pinus montezumae*, 6 Jul 2017, L. Davies (TLXM HJB16752). Municipality of Nanacamilpa, 19.4935°N, 98.579°W, alt. approx. 2725 m, on burnt soil and litter in coniferous woodland under *Pinus montezumae*, 6 Jul 2017, L. Davies (TLXM HJB16753). Municipality of Panotla, San Mateo, Huexoyucan, 19.3874°N,

98.3028°W, alt. approx. 2485 m, on soil in deciduous woodland under *Quercus* sp., 10 Jul 2017, H.J. Beker (TLXM HJB16820). Municipality of Santa Ana Chiahutempan, La Malinche National Park, Surroundings of San Pedro Tlalcuapan, approx. 19.2152°N, 97.9841°W, alt. approx. 3100 m, on soil, 18 Jul 1998, A. Montoya-Esquivel (TLXM AME1652, HJB16766). Municipality of Tlaxco, north of El Rosario, El Rodeo, approx. 19.3395°N, 99.3605°W, alt. approx. 3100 m, on soil in woodland under *Pinus* sp. and *Quercus* sp., Jun 1991, A. Kong (TLXM AK1925, HJB16787). Municipality of Tlaxco, north of El Rosario, El Rodeo, approx. 19.2153°N, 97.9841°W, alt. approx. 3100 m, on soil in woodland under *Pinus* sp. and *Quercus* sp., 10 Jul 1991, A. Kong (TLXM AK1972, HJB16790). Municipality of Trinidad Sánchez Santos, La Malinche National Park, east of Javier Mina, approx. 19.2152°N, 97.9841°W, alt. approx. 3100 m, on soil, 21 May 1994, Hernandez-Valencia (TLXM HV6, HJB16778). Municipality of Trinidad Sánchez Santos, La Malinche National Park, east of Javier Mina, approx. 19.2153°N, 97.9841°W, alt. approx. 3100 m, on soil in woodland under *Alnus* sp. and *Pinus* sp., 3 Jul 1998, A. Montoya-Esquivel (TLXM AME1643, HJB16781). Tlaxcala City, mushrooms bought at the Tlaxcala market, 10 Jul 1999, A. Montoya-Esquivel (TLXM AME1713, HJB16764). Tlaxcala City, bought in market at Tlaxcala, collected from La Malinche National Park, 19.3218°N, 98.2387°W, alt. approx. 2160 m, 8 Jul 2017, M.F.M. Aguilar (TLXM HJB16809). Tlaxcala City, bought in market at Tlaxcala, collected from La Malinche National Park, 19.3218°N, 98.2388°W, alt. approx. 2160 m, 8 Jul 2017, M.F.M. Aguilar (TLXM HJB16810).

Remarks. With its small ellipsoid, non-dextrinoid basidiospores and cheilocystidia swollen in the lower half, often lageniform or ventricose, this taxon clearly belongs to *Hebeloma* sect. *Hebeloma* and is closely related to the complex of species around *H. mesophaeum*. The close, but not crowded, lamellae with more than 50 full length lamellae rules out *H. excedens* and *H. mesophaeum*, both of which are widespread throughout North America (Eberhardt et al. 2022a). Indeed, were this mushroom collected in Europe, and the key of Beker et al. (2016) applied, this would key out to *H. subtortum*. *Hebeloma subtortum* is most common in southern Europe, growing with lowland pines, and not known from North America. Within North America, no known taxon in *H.* sect. *Hebeloma* with such small ellipsoid spores has this number of full-length lamellae, making these characters sufficient for its determination.

Fig. 6D–E show this mushroom for sale in local markets of Tlaxcala, where it is regarded as a prized edible mushroom known as hongo de ocote (ocote mushroom) in Spanish (Montoya et al. 2002). It is gathered from the temperate pine woodlands at altitudes of 2000 m and above. The local people burn the ground in the pine forests, ahead of the growing season, to encourage the growth of this mushroom. Frequent, controlled fires prevent the development of hot fires that would also damage the pines and pine roots, which are required for the fungi to grow. It is referred to in Nahuatl by several names, for example as the Xolete de ocō-xāl or ocō-xāl-nanácatl (ocō-xālli = pine-litter; mushroom growing in ocō-xāl - the mushroom of the pine needles), rastrojo-nanácatl (mushroom growing on stubble), ocochalero, ocotero, ocoxal, ocochal, cholete de ocote, nixtamalero or as chamusquinero, mean-

ing from burnt ground (Estrada-Martínez et al. 2009; Reyes-López et al. 2020; Viveros-Assad et al. 2019). It is likely the same species as mentioned by Guzmán (1977) as "joletes" in Spanish, described as commonly sold in the Amecameca market, where it is recommended to boil them and then discard the water so that they are safe for consumption.

Hebeloma cohaerens A. Montoya & Beker, sp. nov.

MycoBank No: 842828
Figs 8–9

Type. Mexico. Tlaxcala: Municipality of Panotla, 1 km al este de San Francisco Temezontla, approx. 19.3496°N, 98.2784°W, alt. approx. 2600 m, in deciduous woodland under *Quercus* sp., 23 Jul 2017, A. Montoya-Esquivel AME3102 (holotype TLXM 6156; isotype BR 5020224875654V; HJB17733); Genbank ITS ON202511.

Diagnosis. The short clavate-ventricose cheilocystidia, with average apical width less 6.5 µm, the small (on average less than 10 × 5.5 µm), weakly ornamented but rather strongly dextrinoid basidiospores and the whitish to cream or buff color of the pileus, differentiate this species from other *Hebeloma* species.

Etymology. From *cohaerens* (adj. Latin) meaning united or joined together, to emphasize the connate habitus.

Description. Pileus (22) 32–38 (47) mm diameter, convex, often applanate, occasionally umbonate; margin smooth, often involute, particularly when young, occasionally eroded, not hygrophanous; usually almost unicolored, usually cream or buff, sometimes slightly paler towards margin. Lamellae often adnate or adnexed, occasionally emarginate, depth up to 4 mm, white, cream to brown, with white fimbriate edge but without droplets on the lamella edge, number of full-length lamellae 70–80. Stipe (31) 37–46 (48) mm long, (5) 7–8 (10) mm diameter at median, usually cylindrical but sometimes with a clavate base, surface cream, ivory, not discoloring, fibrillose, pruinose, particularly towards apex; base with white mycelium. Context in pileus and stipe white to cream, firm, in stipe stuffed; taste not recorded, smell earthy. Spore deposit color not recorded.

Basidiospores based on n = 64 spores of the holotype, 5% to 95% percentile range 8.6–10.5 × 4.9–5.7 µm, with median 9.4 × 5.3 µm and av. 9.5 × 5.3 µm with S.D. length 0.57 µm and width 0.26 µm; Q value 5% to 95% percentile range 1.64–1.95, with median 1.79 and av. 1.78 with S.D. 0.10; spore size based on four collections medians 9.1–9.5 × 5.3–5.6 µm and av. 9.1–9.5 × 5.3–5.5 µm with av. S.D. length 0.50 µm and width 0.30 µm, av. Q 1.65–1.78, amygdaloid, occasionally limoniform, with small apiculus and rounded apically, often subacute, with a distinct thinning of the apical wall and sometimes a papilla, usually guttulate with one or sometimes more oily drops, at most weakly ornamented (ornamentation only visible under immersion), with a perispore hardly loosening, rather strongly dextrinoid, becoming medium reddish brown in Melzer's reagent (O1/2; P0; D3); yellow brown in KOH. Basidia

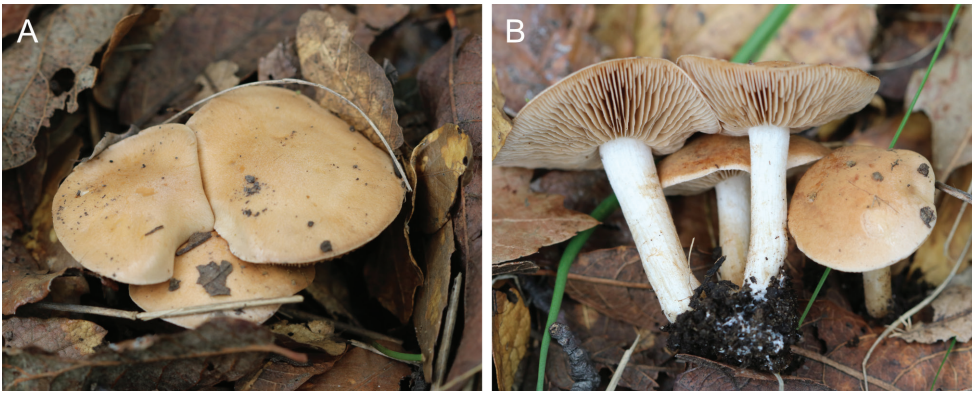

Figure 8. A–B basidiomata, holotype of *Hebeloma cohaerens* TLXM 6156 (HJB17733). Photos A. Kong.

22–27 × 5–7 µm, with av. Q 3.7–3.8 µm, cylindrical to clavate, hyaline, 4–spored. Cheilocystidium width near apex holotype 5% to 95% percentile range 4.7–7.7 µm, with median 6.0 µm and av. 6.1 µm with S.D. 1.0 µm; across four collections median 5.6–6.4 µm and av. 5.5–6.3 µm; examining approx. 20 selected cheilocystidia of each of the four collections yields a range for the avs. of 33–36 × 5.5–6.3 × 3.5–4.1 × 5.5–6.6 µm and 33 × 6.1 × 4.1 × 6.5 µm av. for holotype. Cheilocystidium av. ratios A/M: 1.49–1.63, A/B: 0.86–1.03, B/M: 1.59–1.88, mainly clavate-ventricose, often with one or two septa. Pleurocystidia absent. Caulocystidia similar to cheilocystidia but larger, up to 90 µm long. Pileipellis an ixocutis with an epicutis up to 110 µm thick, with gelatinized, hyphae up to 6 µm wide; subcutis cream to pale yellow, and the trama below the cutis made up of cylindrical, often ellipsoid cells, up to 14 µm wide. Clamp connections present throughout the basidiome.

Ecology and distribution. In deciduous or mixed woodlands apparently associated with *Quercus* or *Pseudotsuga*. Growth habit mainly caespitose, sometimes with a few scattered basidiomes. To date, all collections of *Hebeloma cohaerens* recorded from Tlaxcala at altitudes of 2600 m or more.

Additional collections examined. Mexico. **Tlaxcala**: Municipality of Panotla, 1 km al este de San Francisco Temezontla, approx. 19.3496°N, 98.2784°W, alt. approx. 2600 m, in deciduous woodland under *Quercus* sp., 23 Jul 2017, A. Montoya-Esquivel (TLXM AME3101, HJB17732). Municipality of Panotla, 1 km al este de San Francisco Temezontla, approx. 19.3496°N, 98.2784°W, alt. approx. 2600 m, in deciduous woodland under *Quercus* sp., 23 Jul 2017, A. Kong (TLXM AK17-08, HJB17737). Municipality of Terrenate, Rancho el pozo, approx. 19.5407°N, 97.9046°W, alt. approx. 2900 m, on soil in woodland under *Pseudotsuga* sp., 13 Jul 1995, Galindo-Flores (TLXM GF1866, HJB16779).

Remarks. The small, short clavate-ventricose cheilocystidia, together with the small rather smooth, rather strongly dextrinoid basidiospores, support the placement of this species within *Hebeloma* sect. *Theobromina*. Within this section the pale cream to buff pileus color together with the caespitose habitus is unique.

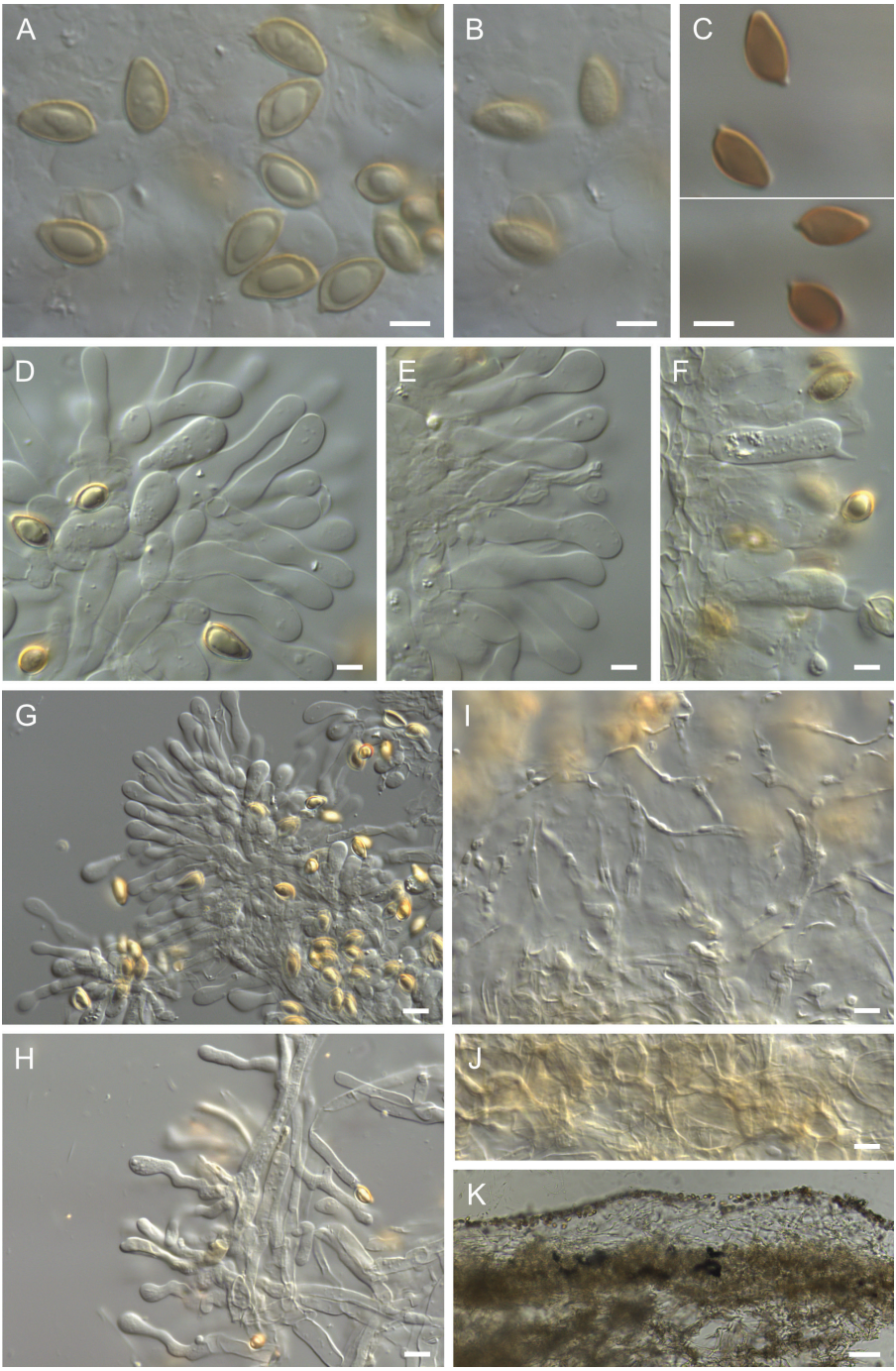

Figure 9. Holotype of *Hebeloma cohaerens* TLXM 6156 (HJB17733) **A** basidiospores ×1600– **B** spore ornamentation ×1600 **C** basidiospores in Melzer's reagent ×1600 **D–E** cheilocystidia ×1000 **F** basidia ×1000 **G** cheilocystidia ×500 **H** caulocystidia ×500 **I** epicutis hyphae ×1000 **J** subcutis ×1000 **K** cutis ×125. All in KOH, except **C**. Scale bars: 5 µm (**A–F**); 10 µm (**G–J**); 50 µm (**K**). Photos H.J. Beker.

The description was based on just four collections all from the same region of Mexico, and is not known from any other location. More records for this species will help to define better its morphological characters and its biogeographic preferences.

The minimum interspecific distance between the ITS sequences of *H. cohaerens* and sequences from other species is around 1.2%. The BLAST result of the type sequence of *H. cohaerens* against UNITE resulted in a hit of a soil sample sequence, pointing towards UNITE SH1563973.08FU (98.5% level). This SH includes two independently generated sequences from California (UDB0767851, soil sample, Tedersoo et al. 2021; DQ822802, basidiome, Point Reyes National Seashore Reserve, under *Pinus muricata*, Peay et al. 2007) that differ by around 0.5% from the sequences assigned to *H. cohaerens*, but match no other species. These results suggest that *H. cohaerens* may occur in the US (California) and the UNITE SH corresponding to *H. cohaerens* is likely to be SH1563973.08FU.

***Hebeloma magnicystidiatum* A. Kong & Beker, sp. nov.**
MycoBank No: 842829
Fig. 10

Type. Mexico. Tlaxcala: Municipality of Totolac, Tepeticpac, 19.3457°N, 98.2226°W, alt. approx. 2400 m, on the ground in woodland under *Pinus* sp. and *Quercus* sp., 29 Aug. 1990, A. Estrada-Torres AET3093 (holotype TLXM 6157; isotype BR 5020224873599V; HJB16795); GenBank ITS ON202534.

Diagnosis. The amygdaloid, non-dextrinoid, rather strongly ornamented spores with average Q value less than 1.6 and the capitate-stipitate cheilocystidia with average width at the apex greater than 9.5 µm distinguish this species from all other known *Hebeloma* species.

Etymology. From *magni-* (Latin, composite) meaning large and *cystidiatus* to emphasize the large capitate-stipitate cheilocystidia.

Description. Pileus 19–26 mm diameter, convex, surface dry, finely tomentose, cuticle separable, reddish yellow to brown in the center, and pale orange towards the margin. Lamellae emarginate, white, cream to orange brown as the spores mature, with a white fimbriate edge, and about 60 full-length lamellae. Stipe 10–21 mm long, 4–6 mm diameter at median, cylindrical, surface whitish but discoloring brown from the base upwards, with age or handling, fibrillose, at apex pruinose. Context in pileus white to cream, firm, in stipe stuffed, initially white to cream but becoming brown with age and handling, becoming hollow with age; taste fungal to sweet, smell raphanoid. Spore deposit not recorded.

Basidiospores based on n = 44 spores of the holotype, 5% to 95% percentile range 9.7–11.6 × 6.4–7.6 µm, with median 10.5 × 7.0 µm and av. 10.5 × 7.0 µm with S.D. length 0.62 µm and width 0.42 µm; Q value 5% to 95% percentile range 1.40–1.62, with median 1.49 and av. 1.50 with S.D. 0.07; amygdaloid, often limoniform, with small apiculus and rounded apically, often subacute to acute, with a distinct thinning of the apical wall and sometimes a clearly visible papilla, not guttulate, usually rather

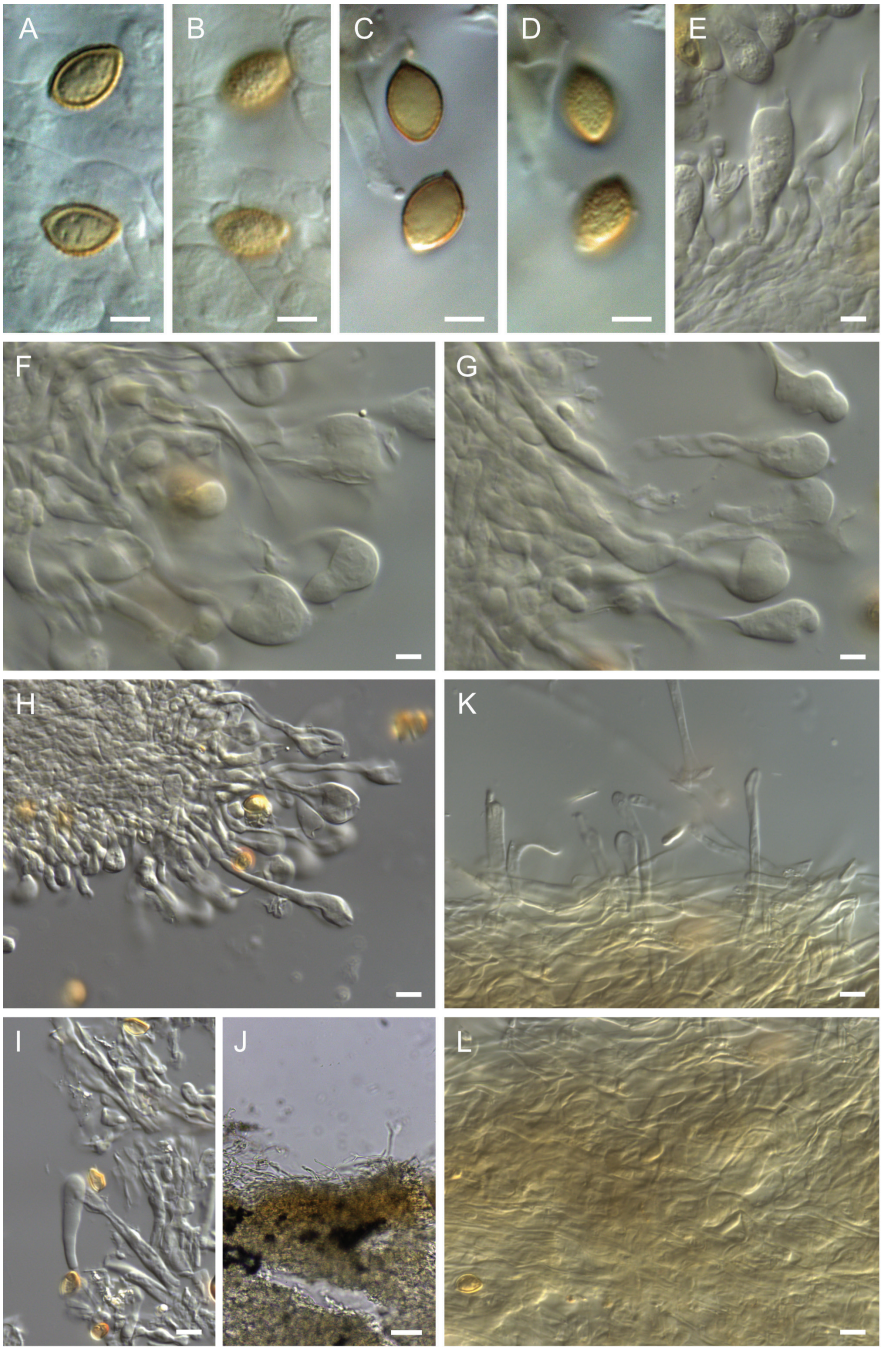

Figure 10. Holotype of *Hebeloma magnicystidiatum* TLXM 6157 (HJB16795) **A** Basidiospores ×1600 **B** spore ornamentation ×1600 **C** basidiospores and **D** spore ornamentation in Melzer's reagent ×1600 **E** basidium ×1000 **F–H** cheilocystidia ×1000 **H** cheilocystidia ×500 **I** caulocystidia ×500 **J** cutis ×125 **K** epicutis hyphae ×500 **L** subcutis ×500. All in KOH, except **C–D**. Scale bars: 5 µm (**A–G**); 10 µm (**H–I, K–L**); 50 µm (**J**). Photos H.J. Beker.

strongly ornamented, ornamentation visible even without immersion, with perispore at most somewhat loosening in a few spores, an indistinct brownish tint in Melzer's reagent (O3; P1; D1); yellow-brown in KOH. Basidia 27.5–35 × 7.5–9 µm, with av. Q 3.9, cylindrical to clavate, without pigmentation, 4-spored. Cheilocystidium width near apex holotype 5% to 95% percentile range 6.1–14.3 µm, with median 9.1 µm and av. 9.7 µm with S.D. 2.61 µm; examining approx. 20 selected cheilocystidia of the holotype yields a range for the avs. of 55 × 9.7 × 7.3 × 4.3 µm av. and cheilocystidium av. ratios A/M: 2.58, A/B: 2.67, B/M: 0.95; mainly capitate-stipitate, unfortunately many collapsed in exsiccata. Pleurocystidia absent. Caulocystidia similar to cheilocystidia but larger, up to 80 µm long. Pileipellis an ixocutis; epicutis up to 110 µm thick, with gelatinized hyphae up to 7 µm wide; subcutis yellow; and the trama below the cutis made up of cylindrical or occasionally ellipsoid cells up to 17 µm wide. Clamp connections present throughout the basidiome.

Ecology and distribution. In woodland on the ground with *Comarostaphylis* and *Quercus*. Growth habit scattered. To date, with only one collection of this species, not possible to describe its distribution and ecology.

Remarks. With its amygdaloid, hardly dextrinoid basidiospores and capitate-stipitate cheilocystidia, morphologically this taxon clearly belongs to *Hebeloma* sect. *Denudata* and there to *H*. subsect. *Crustuliniformia*. The amygdaloid spores with rather small average Q value separate this species from all other studied *Hebeloma* from our database with more than 10,000 collections. While this may suggest that this is a rare species, we have insufficient *Hebeloma* collections from Mexico to reach such a conclusion. The single collection was collected in the 1990s, thus the only loci we could amplify were ITS and mitSSU variable regions V6 and V9.

The phylogenetic placement of *H. magnicystidiatum* within *H*. sect. *Denudata* is unresolved. As pointed out before (e.g. Eberhardt et al. 2016, 2022b; Beker et al. 2016), the more species rich subsections of *H*. sect. *Denudata* (*H*. subsects *Clepsydroida* and *Crustuliniformia*) are not supported molecularly. In terms of ITS, the most similar species was *H. sordidulum* (*H.* subsect. *Clepsydroida*) with similarity values ≤ 98.7%. Possibly *H. magnicystidiatum* will correspond to a UNITE SH at the 99% or 98.5% level once sequences of this species are included in the system. Morphologically, the capitate-stipitate cheilocystidia together with the amygdaloid spores with av. Q less than 1.6 are sufficient characters to separate this species from members of *H*. sect. *Clepsydroida*, such as *H. cavipes*, *H. matritense*, *H. sordidulum* and *H. vaccinum*.

***Hebeloma neurophyllum* G.F. Atk., Annales Mycologici 7(4): 370 (1909)**
Figs 11–12

Type. USA. New York: Coy Glen, Ithaca, approx. 42.4272°N, 76.5241°W, alt. approx. 125 m, on soil in woodland, 18 Oct 1906, N. Coil (holotype CUP-A-021514; isotype TENN-F-037531, HJB1000453, isotype WTU-F-039596, HJB1000558).

Diagnosis. Gregarium 7–8 cm altum, pileo 5–6 cm lato, stipite 5–6 mm crasso: Pileo ochraceo-cremeo vel fulvo-ochraceo, leviter viscido. Lamellis 8 mm latis, pallide cinnamomeo-rufis, late sinuatis, adnexis, costatis. Basidiis 4-sporis. Sporis subfusoideis, 12–15 × 7–8 μ[m]. Ad terram in silvis, Ithacae, N. Y. Stipite albo, fibroso-striato, cavo vel subfarcto.

English translation of diagnosis. Gregarious 7–8 cm high, pileus 5–6 cm broad, stipe 5–6 mm thick: pileus ochraceous-cream or fulvous-ochraceous, slightly viscid. Lamellae 8 mm broad, pale cinnamon-reddish, broadly sinuate, adnexed, intervenose. Basidia four-spored. Spores subfusoid, 12–15 × 7–8 μm. On the ground in woodland, New York. Stipe white, fibrous-striate, fistulose or almost stuffed.

Description. Pileus (26) 30–55 (60) mm diameter, convex, occasionally umbonate or broadly umbonate; margin often smooth, occasionally involute or wavy, not hygrophanous; usually unicolor, occasionally two colors, at center occasionally yellowish brown, ochraceous or cream, rarely fawn, cinnamon or clay-buff, sometimes slightly paler towards margin. Lamellae usually emarginate, occasionally adnexed, depth up to 9 mm, white, cream to brown, usually with white fimbriate edge, usually without droplets on the lamella edge but rarely some drops may be visible, number of full-length lamellae 70–94. Stipe (25) 31–75 (80) mm long, 5–14 (16) mm diameter at median, often clavate or bulbous, occasionally cylindrical, (7) 9–16 (18) mm wide at base, surface cream, ivory, rarely discoloring, occasionally velutinous, floccose or fibrillose, often pruinose, particularly towards apex. Veil not observed. Context in pileus white to cream, firm, in stipe usually hollow, rarely with superior hanging wick; taste mild, smell occasionally raphanoid or odorless, rarely fruity or earthy. Spore deposit yellowish brown to brownish olive.

Basidiospores based on n = 70 spores of the holotype, 5% to 95% percentile range 12.7–15.6 × 7.2–9.0 μm, with median 14.2 × 8.2 μm and av. 14.2 × 8.2 μm with S.D. length 0.93 μm and width 0.54 μm; Q value 5% to 95% percentile range 1.52–1.91, with median 1.74 and av. 1.73 with S.D. 0.12; spore size based on 47 collections medians 11.6–14.3 × 7.2–8.2 μm and av. 11.7–14.2 × 7.5–8.3 μm with av. S.D. length 0.898 μm and width 0.459 μm, av. Q 1.53–1.78, amygdaloid, usually limoniform, with small apiculus and rounded apically, often subacute to acute, with a distinct thinning of the apical wall and a clear papilla, occasionally guttulate with one or sometimes more oily drops, distinctly to strongly ornamented (ornamentation visible without immersion), with a perispore somewhat to distinctly loosening, at least in a few spores, strongly dextrinoid, becoming at least medium brown and often intensely red-brown in Melzer's reagent (O3/4; P1/2; D3/4); yellow to brown in KOH. Basidia 20–43 × 7–10 μm, with av. Q 2.7–3.8 μm, cylindrical to clavate, with a median constriction, hyaline, 4-spored. Cheilocystidium width near apex holotype 5% to 95% percentile range 4.9–9.0 μm, with median 6.5 μm and av. 6.7 μm with S.D. 1.27 μm; across 47 collections median 4.5–6.8 μm and av. 4.6–6.7 μm; examining approx. 20 selected cheilocystidia of each of the 47 collections yields a range for the avs of 40–59 × 4.6–6.7 × 4.4–5.7 × 5.6–8.4 μm and 49 × 6.7 × 5.6 × 6.7 μm av. for the holotype. Cheilocystidium av. ratios A/M: 1.01–1.41, A/B: 0.68–1.23, B/M: 1.16–1.58, mainly gently clavate or ventricose, occasionally cylindrical, lageniform or clavate-lageniform

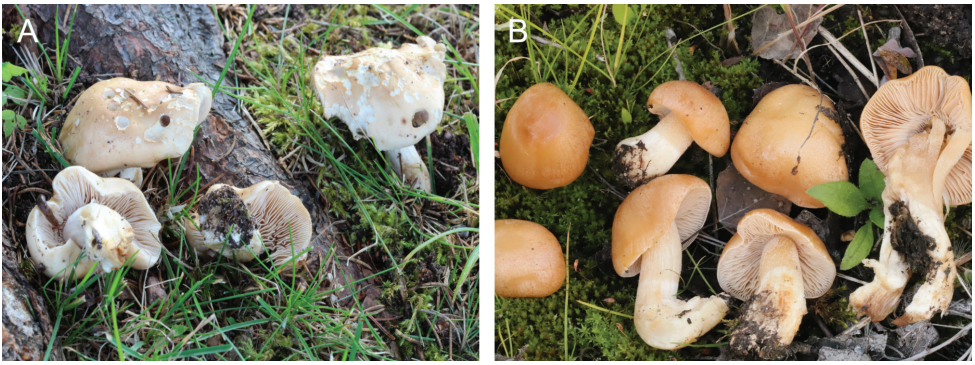

Figure 11. *Hebeloma neurophyllum*, basidiomata **A** HJB16991 **B** HJB18101. Photos H.J. Beker.

or clavate-ventricose, often with one or two septa, sometimes clamped, often with plaques on the cystidial walls, occasionally geniculate or with basal wall thickening, rarely bifurcate, hyaline, rarely with yellow contents. Pleurocystidia absent. Caulocystidia similar to cheilocystidia but larger, up to 115 µm long. Pileipellis an ixocutis, epicutis up to 90 µm thick, with gelatinized, hyphae up to 6 µm wide; subcutis pale yellow to brownish yellow, and the trama below the cutis made up of cylindrical, often ellipsoid cells, up to 16 µm wide. Clamp connections present throughout the basidiome.

Habitat and distribution. Based on almost 50 collections, where only one possible associate was recorded, the most commonly recorded associates were *Picea* and *Quercus*, but *Populus*, *Salix* and *Tilia* were also recorded; the most commonly recorded families were Fagaceae, Pinaceae and Salicaceae, but Betulaceae and Malvaceae were also recorded. We have additional records where *Alnus*, *Arctostaphylos*, *Betula*, *Dryas*, *Pinus* and *Polygonum* were recorded as possible associates, but in each of these cases a number of possible associates were mentioned. All records of *H. neurophyllum* are from Northern America, where it is widespread across the region but primarily collected in temperate to boreal woodland, occasionally in urban areas.

Additional material examined. Canada. **Alberta**: Moose Hill, Breton, Edmonton, 53.1418°N, 114.6097°W, alt. approx. 810 m, on soil in mixed woodland under *Picea mariana*, 12 Aug 2017, H.J. Beker (HJB16856). **Northwest Territories**: Highway 3, between Yellowknife and Behchoko, 62.5198°N, 114.897°W, alt. approx. 165 m, on mossy soil in boreal, calcareous woodland roadside under *Betula* sp. and *Salix* sp., 7 Sep 2018, H.J. Beker, L. Davies (HJB18101). **Yukon**: Railway Station, Whitehorse, 60.7214°N, 135.0505°W, alt. approx. 665 m, on soil and litter in boreal shrubland riverside under *Populus tremuloides* and *Salix* sp., 31 Aug 2018, H.J. Beker, L. Davies (HJB17975). 3rd Avenue near Wood St intersection, Whitehorse, 60.7212°N, 135.0555°W, alt. approx. 665 m, on grassy, mossy soil in boreal urban roadside under *Populus* sp., 1 Sep 2018, H.J. Beker, L. Davies (HJB17981). MEXICO. **Chihuahua**: El Ranchito, approx. 28.3387°N, 105.4076°W, alt. approx. 1150 m, on soil in montane, subtropical woodland, 18 Aug 2001, A. Kong 3782 (TLXM AK3782, HJB16773). UNITED STATES. **Alaska**: Kantishna Roadhouse Nature Trail, Denali National Park,

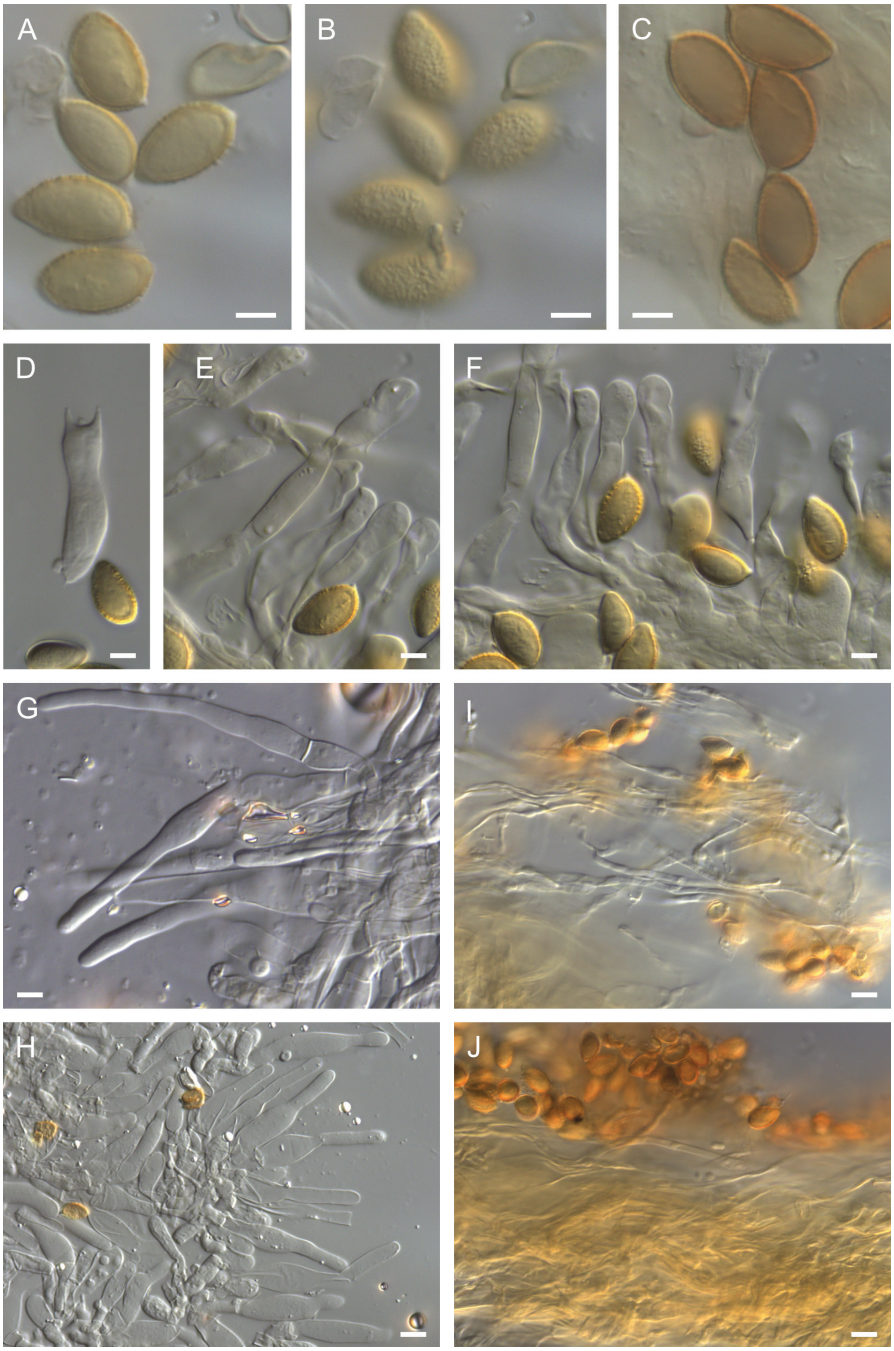

Figure 12. *Hebeloma neurophyllum* **A** basidiospores and **B** spore ornamentation of isotype TENN-F-037531 (HJB1000453) ×1600 **C** basidiospores of HJB17897 in Melzer's reagent ×1600 **D** basidium of isotype ×1000 **E–F** cheilocystidia of isotype ×1000 **G** caulocystidia of HJB17975 ×500 **H** caulocystidia of HJB16856 ×500 **I** epicutis hyphae and **J** subcutis of isotype ×500. All in KOH, except **C**. Scale bars: 5 µm (**A–F**); 10 µm (**G–J**). Photos H.J. Beker.

63.5243°N, 150.9625°W, alt. approx. 490 m, on sandy soil in boreal, mixed but mainly coniferous woodland pathside under *Alnus* sp., *Betula* sp. and *Salix* sp., 18 Aug 2018, H.J. Beker, L. Davies (DENA-61424, HJB17897). **Texas**: Jefferson County, Beaumont, residence of Penny Clark, approx. 30.0788°N, 94.1372°W, alt. approx. 0 m, in garden under *Quercus fusiformis*, 4 Dec 2015, D. Lewis DPL11907 (HJB15699). **Wisconsin**: Bark Point Road, near Bark Bay, 46.8353°N, 91.2594°W, alt. approx. 185 m, on grassy soil in coniferous garden under *Picea glauca*, 13 Sep 2017, L. Davies, H.J. Beker (HJB16991).

Remarks. With the mixture of gently clavate and ventricose cystidia alongside the strongly dextrinoid basidiospores, this species belongs within *Hebeloma* sect. *Velutipes*. Within this section the combination of spores with minimum average width 7.5 µm and a distinctly loosening perispore in at least some spores, together with the absence of pleurocystidia, defines this species. The collection of *H. neurophyllum* from Mexico, gathered at El Ranchito in Chihuahua, matches well with other collections of this species. We are not aware of any synonyms for this species.

In terms of ITS, the most similar to *H. neurophyllum* were *H. celatum*, *H. erebium* and *H. quercetorum*, the ITS sequences of which were around 99% similar (99.2–98.6%) to those of *H. neurophyllum*. *Hebeloma neurophyllum* appears to correspond to UNITE SH1733487.08FU (99%). Intriguingly, this species hypothesis includes a number of soil sample sequences from Estonia, suggesting that either *H. neurophyllum* occurs in Europe, too, or that species known to occur in Europe also contain ITS copies corresponding to *H. neurophyllum* below the detection limit of Sanger sequencing.

Hebeloma subaustrale **Murrill, Lloydia 8: 287 (1946) [1945]**
Fig. 13

= *Hebeloma angustisporium* Hesler, Kew Bulletin 32(3): 471 (1977)
= *Hebeloma perangustisporium* Hesler, Kew Bulletin 32(3): 478 (1977)

Type. USA. Florida: Gainesville, Alachua Co., approx. 29.651634°N, 82.324826°W, alt. approx. 50 m, on grassy, shady soil in lawn, 30 Oct 1941, G.F. Weber (holotype FLAS-F-19345, HJB1000402; isotype TENN-F-021177, HJB1000447).

Diagnosis. Pileo convexo-expanso, 3–4 cm. lato, subviscido, glabro, pallido-roseo, raphanico; lamellis sinuatis, latis, confertis; sporis subovoidcis, pallidis, levibus, 8–10 × 4–4.5 µ[m]; stipite acquali, pallido, 3 × 0.5 cm.

English translation of diagnosis. Pileus convex to applanate, 3–4 cm broad, slightly viscid, glabrous, pale pink, with raphanoid smell; lamellae sinuate, broad, crowded; spores subovoid, pale, smooth, 8–10 × 4–4.5 µ[m]; stipe equal, pale, 3 × 0.5 cm.

Description. Pileus (20) 32–45 (46) mm diameter, usually convex, occasionally umbonate; occasionally with remains of universal veil; margin often smooth, occasionally scalloped, not hygrophanous; usually unicolor, occasionally two colors, at center cream to buff to ochraceous, often becoming paler towards the margin. Lamellae usu-

ally emarginate, occasionally adnate or adnexed; white, cream to brown, usually with white fimbriate edge, without droplets on the lamella edge, number of full-length lamellae 80–92. Stipe 30–56 (70) mm long, 5–10 (11) mm diameter at median, often clavate or cylindrical, 5–13 (14) mm wide at base, surface cream, ivory to white rarely discoloring, pruinose, particularly towards apex. Context in pileus white to cream, firm, similar color in stipe, becoming hollow with age; taste raphanoid, smell raphanoid, occasionally earthy. Spore deposit cinnamon color.

Basidiospores based on n = 63 spores of the holotype, 5% to 95% percentile range 8.4–9.8 × 4.6–5.2 µm, with median 9.0 × 4.8 µm and av. 9.0 × 4.9 µm with S.D. length 0.51 µm and width 0.18 µm; Q value 5% to 95% percentile range 1.65–2.03, with median 1.88 and av. 1.85 with S.D. 0.12; spore size based on seven collections medians 8.5–10.2 × 4.6–5.3 µm and av. 8.6–9.9 × 4.6–5.3 µm with av. S.D. length 0.657 µm and width 0.271 µm, av. Q 1.73–2.09, amygdaloid, usually fusoid, rarely navicular, with small apiculus and rounded apically, often subacute to acute, with a distinct thinning of the apical wall and no papilla, occasionally guttulate with one or sometimes more oily drops, very weakly ornamented (ornamentation only visible under immersion), with a perispore somewhat loosening, in at most a few spores, rarely not loosening or distinctly loosening, distinctly to rather strongly dextrinoid, becoming yellow brown to medium brown in Melzer's reagent (O1/2; P0/1/2; D2/3); yellow in KOH. Basidia 19–32 × 5–7 µm, with av. Q 3.8–4.6 µm, cylindrical to clavate, hyaline, 4-spored. Cheilocystidium width near apex holotype 5% to 95% percentile range 4.5–6.8 µm, with median 5.8 µm and av. 5.7 µm with S.D. 0.85 µm; across seven collections median 4.4–6.3 µm and av. 4.5–6.3 µm; examining approx. 20 selected cheilocystidia of each of the seven collections yields a range for the avs of 29–43 × 4.5–6.3 × 3.9–5.1 × 4.8–6.8 µm and 33 × 5.7 × 4.3 × 5.6 µm av. for the holotype. Cheilocystidium av. ratios A/M: 1.04–1.48, A/B: 0.84–1.31, B/M: 1.20–1.36, irregular but mainly cylindrical, often ventricose, often clavate, occasionally clavate-lageniform or clavate-ventricose or gently clavate, rarely capitate stipitate or clavate stipitate, often with one or two septa, occasionally with apical wall thickening. Pleurocystidia absent. Caulocystidia similar to cheilocystidia but larger, up to 100 µm. Pileipellis an ixocutis, epicutis up to 100 µm thick, with gelatinized, hyphae up to 7 µm wide, often encrusted; subcutis pale yellow; and the trama below the cutis made up of ellipsoid or thickly sausage-shaped, often cylindrical cells up to 13 µm wide. Clamp connections present throughout the basidiome.

Habitat and distribution. Where only one possible associate was recorded, that associate has always been *Quercus* (Fagaceae). We have additional records where *Pinus*, *Abies* and *Fagus* were recorded as possible associates, but in each of these cases a number of possible associates were mentioned by the collector. We are only aware of five collections other than that from Mexico. These are all from the eastern half of the United States: Ohio, Pennsylvania and Tennessee.

Additional material examined. Mexico. **Tlaxcala**: Municipality of Huamantla, La Malinche National Park, Cañada Grande, east side of La Malintzi volcano, approx. 19.1999°N, 97.9729°W, alt. approx. 3000 m, on soil in montane, temperate woodland under *Abies* sp. and *Pinus* sp., 25 Jul 1990, H. Cuevas HC1155 (TLXM

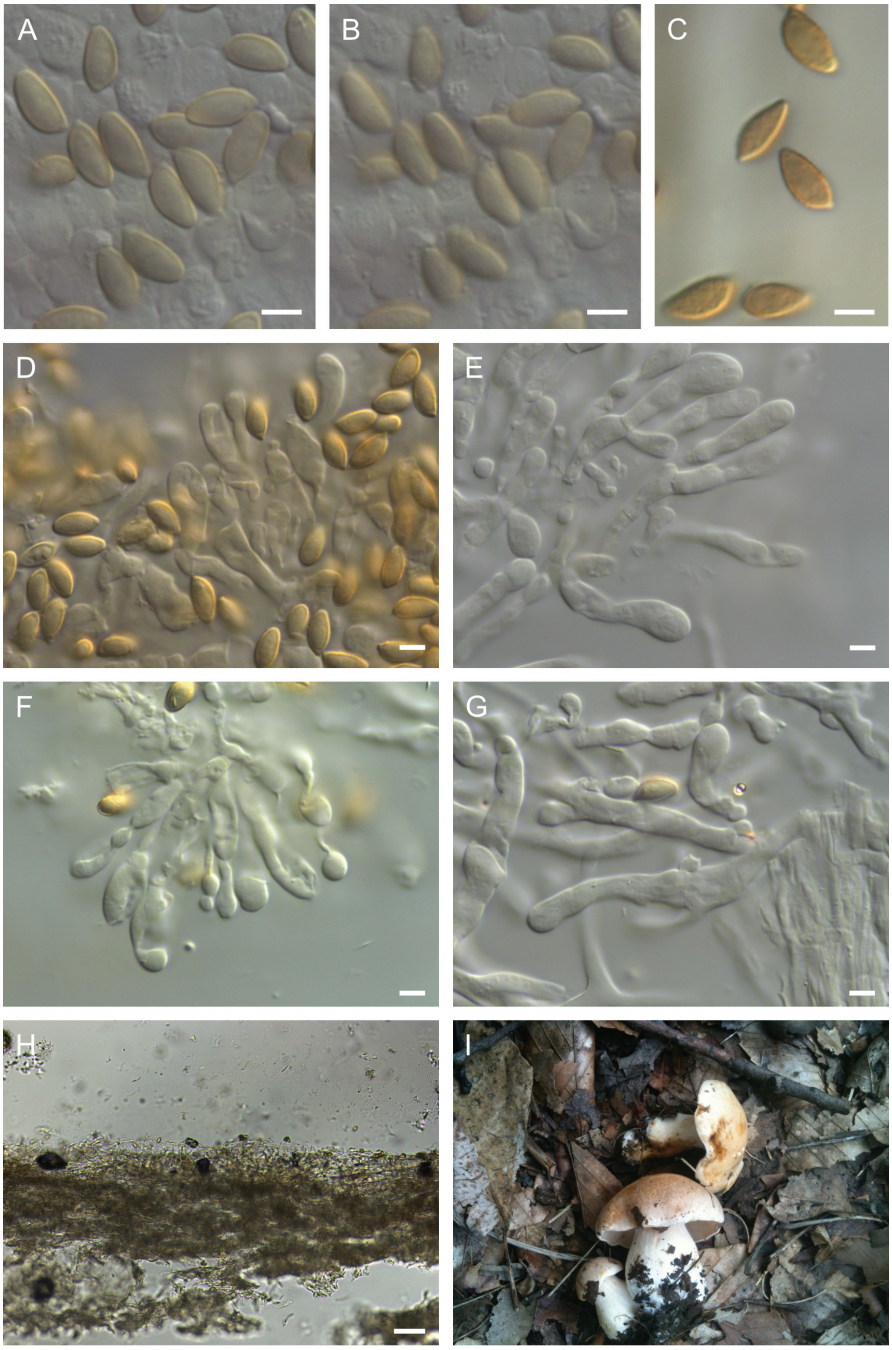

Figure 13. *Hebeloma subaustrale* **A** basidiospores and **B** spore ornamentation of holotype FLAS-F-19345 ×1600 **C** spores of SPFS-2011-63 (HJB17796) in Melzer's reagent ×1600 **D** spores and cheilocystidia of holotype ×1000 **E** cheilocystidia of isotype TENN-F-021177 ×1000 **F** cheilocystidia of holotype ×1000 **G** caulocystidia of isotype ×1000 **H** cutis of SPFS-2011-63 ×125. All in KOH, except **C**. **I** basidiomata of collection SPFS-2011-63. Scale bars: 5 µm (**A–G**); 50 µm (**H**). Photos **A–G** H.J. Beker **H** D. Bartholow.

Table 1. Comparison of the most taxonomically important holotype characters of *Hebeloma subaustrale* and its synonyms. Macroscopic data from the original descriptions and microscopic measures from own studies.

Species	*Hebeloma angustisporium*	*Hebeloma perangustisporium*	*Hebeloma subaustrale*
Number of complete lamellae	86	80	88
Spore ornamentation	O1; O2	O2	O1
Spore perispore loosening	P1	P1; P2	P0; P1
Spore dextrinoidity	D2; D3	D1; D2	D2
Spore length av. (µm)	8.6	9.9	9
Spore width av. (µm)	5	5.3	4.9
Spore Q av.	1.73	1.87	1.85
Cheilocystidia length av. (µm)	29	39	33
Cheilocystidia apex on gill edge av. (µm)	4.5	4.6	5.7
Cheilocystidia av. Q1, A/M	1.04	1.12	1.38
Cheilocystidia av. Q2, A/B	0.86	0.84	1.06
Cheilocystidia av. Q3, B/M	1.24	1.36	1.44
Basidia Q av.	4.3	3.8	3.8
Pileus diameter (mm)	25–40	20–45	30–40
Stipe median width (mm)	9–10	9–11	5

HC1155, HJB16793). USA. **Ohio**: Shaker Parklands, Doan Brook Gorge, approx. 41.495°N, 81.5953°W, alt. approx. 275 m, on grassy soil under *Fagus* sp. and *Quercus* sp., 26 Sep 2011, D. Bartholow SPFS-2011-63 (HJB17796). **Pennsylvania**: Fort Washington Park, Parking Lot 5, approx. 40.1208°N, 75.2232°W, alt. approx. 80 m, on soil in mixed woodland under *Quercus* sp., 23 Oct 2018, T. Deluce (HJB18418). **Tennessee**: Gatlinburg, Great Smoky Mountains National Park, Indian Gap, approx. 35.6108°N, 83.4386°W, alt. approx. 1650 m, 29 Jul 1941, L.R. Hesler LRH13890 (holotype of *Hebeloma perangustisporium* TENN-F-013890, HJB1000450). Blount, Townsend, Great Smoky Mountains National Park, Cades Cove, approx. 35.6019°N, 83.8113°W, alt. approx. 550 m, 23 Aug 1959, L.R. Hesler LRH23364 (holotype of *Hebeloma angustisporium* TENN-F-023364, HJB1000314).

Remarks. The small weakly ornamented basidiospores together with the short irregular cheilocystidia, often cylindrical but also both ventricose and clavate, suggest *Hebeloma* sect. *Naviculospora*, which is supported by molecular data. Within this section *H. subaustrale* is differentiated from other Northern American species of this section by the average basidiospore length (a maximum of 10 µm), and average spore Q greater than 1.7, together with the cheilocystidia that have a maximum average A/B ratio of 1.5 and a minimum average B/M ratio of 1.2.

We were not able to generate any sequence data from the type of *H. subaustrale*. However, our morphological study of the type, and of a number of other species within *H.* sect. *Naviculospora*, leaves us in no doubt that this is a conspecific of both *H. angustisporium* and *H. perangustisporium*. For these latter two species types we have good morphological and molecular data. Table 1 shows a comparison of the most important taxonomic parameters for the holotypes of these three species. The spore size and the average cheilocystidium shape, despite their irregularity, are key to differentiating species within this section. The Mexican collection corresponded well with this type material and other recent collections from the USA.

Hebeloma subaustrale formed a reasonably well supported clade in the ITS analysis (Fig. 5B), thus it is expected to be identifiable by its barcode. Although the maximum intraspecific distance of the sequences in the analysis is only 0.14%, the minimum distance to other species of the section is 0.7%. At this time (4 Feb 2022), there is no multi-sequence UNITE SH that represents the species; the published sequence of the holotype of *H. angustisporium* (NR_119890 = HQ179674) formed a singleton SH at the 99% level and the respective SH at the next level included several species.

Discussion

The systematic position of the discussed species, three new (*H. ambustiterranum*, *H. cohaerens* and *H. magnicystidiatum*) and two neglected and rediscovered (*H. neurophyllum*, *H. subaustrale*), are unambiguous and supported by morphological and molecular results. All species can be placed in previously described sections of *Hebeloma*. Based on our current knowledge, all species are easy to delimit molecularly and are recognizable by their ITS-barcodes.

Garibay-Orijel et al. (2013) identified *H. albocolossum* (synonymized with *H. eburneum* by Beker et al. 2016), *H. helodes*, *H. leucosarx* and *H. mesophaeum* from ectomycorrhizal root tips of *Pinus montezumae* from the Transmexican Volcanic Belt, based on the sequences available in GenBank at the time. The sequences of Garibay-Orijel et al. (2013) were not included in the tree analyses, because ITS only entries would have negatively influenced the phylogenetic resolution of the respective analyses. Based on currently available sequence data, we would tend to identify the sequences obtained in that study as *H. eburneum* (JN704820; species in Fig. 3), *H. excedens* or *H. mesophaeum* (JN704814; species in Fig. 2), *H. velutipes* (JN704825; species in Fig. 5), and *H. sordidulum* (JN704810; species in Fig. 3). These species are treated in detail by Beker et al. (2016) and Eberhardt et al. (2021a, 2022a). Given that these identifications are based only on ITS sequence data, they have to be treated with caution.

Many of the issues such as conflicting phylogenetic hypotheses or lack of species resolution in phylogenetic analyses have been encountered and discussed before for *H.* sect. *Denudata* (Eberhardt et al. 2015, 2016a; Beker et al. 2016), for H. sect. *Velutipes* (Aanen et al. 2001; Grilli et al. 2016; Beker et al. 2016) and *H.* sect. *Hebeloma* (Beker et al. 2016; Eberhardt et al. 2022a). For the delimitation and recognition of the species described in detail here, *H. ambustiterranum*, *H. cohaerens*, *H. magnicystidiatum*, *H. neurophyllum* and *H. subaustrale*, these are non-issues. For *H. magnicystidiatum* the conflicts between the different loci used imply that there was no molecular support for the assignment to subsection. However, already Eberhardt et al. (2016a) showed that even when using additional loci such as *RPB2*, *TEF1a* and *MCM7* support for *H.* subsects. *Clepsydroida* and *Crustuliniformia* was lacking and their relation to *H.* subsect. *Hiemalia* was unresolved. Likewise, Grilli et al. (2016) showed that the phylogenetic relationship between *H. celatum*, *H. erebium* and *H. quercetorum* could not be resolved based on five loci. Here, *H. neurophyllum* is presented as a fourth species in this group the evolutionary history of which could not be reconstructed based on four loci.

Other questions arising from the presented results will have to be tackled in a wider context with more samples, more loci and geographically wider sampling. These include whether *H. excedens* and *H. mesophaeum* should be treated as a single species (see also Eberhardt et al. 2022a), or whether to attach any importance to the somewhat isolated position of the Mexican *H. eburneum* in relation to other *H. eburneum* sequences in the analysis, or the divergent mitSSU V6 sequences of Mexican *H. velutipes*. Eberhardt and co-workers (2016) showed that member species of the *H. alpinum* complex varying in their mitSSU variable regions are likely to belong to different mating groups defined by Aanen and Kuyper (1999). Using the same reasoning, if the mitSSU V6 differences of the Mexican *H. eburneum* or *H. velutipes* had been accompanied by morphological differences, we would have had to recognize them as a distinct species. There were no differences found, thus the collections are here addressed as *H. eburneum* and *H. velutipes*, respectively, although the suspicion remains that the mitSSU results point towards mating groups—and possibly species—so far not sampled outside Mexico. Or, alternatively, that our current concept recognizes too many species in the respective groups.

There have been reports of edible *Hebeloma* species from other regions of the world, for example from Guatemala, Laos and Nigeria (Aremu et al. 2009; Carrasco-Hernández et al. 2015; Eberhardt et al. 2020a; Flores-Arzú 2020), where, for example, Eberhardt and colleagues reported that in Laos *H. parvisporum* is sold in markets and on roadsides as edible and that it is called "wai khom," which refers to its bitter taste, which, apparently, remains, at least to some degree, after cooking.

From their literature review, Carrasco-Hernández et al. (2015) found that cytotoxic triterpenes, lanostanetype triterpene esters, neurotoxic cucurbitane-type glycosides and 6,7-seco-caryophyllenes, and related sesquiterpenoids may be the cause of *Hebeloma* toxicity. It is reported that *Hebeloma* poisonings typically cause gastrointestinal symptoms in humans that pass after several days. It is not known which species of *Hebeloma* are poisonous, but, as said above, their consumption is strongly discouraged (Bresinsky and Besl 1990, Benjamin 1995). It was pointed out (Beker et al. 2016; Eberhardt et al. 2020a) that, given the difficulty of species identification within the genus, one could not be certain which toxic compounds referred to which species.

Carrasco-Hernández et al. (2015) described *Hebeloma* spp. obtained from the Ozumba market, thus presumably intended for human consumption. They recognize three different species, identified as *H. alpinum*, *H. leucosarx* and *H. mesophaeum*. These identifications have to be treated with caution. Certainly, the basidiospore measures they give for *H. alpinum* and *H. leucosarx* would appear too small for those species as we interpret them today. The fact that the spore sizes they give for all three species differ considerably from the spore size of *H. ambustiterranum* would suggest that more than one species of *Hebeloma* is consumed in Mexico.

Hebeloma ambustiterranum is a species of great cultural significance in central Mexico, since it is used as food for the preparation of several local recipes. It is commonly and widely sold in local food markets. Traditional management practices are carried out to encourage the production of basidiomes, such as the use of fire. Traditional names have been assigned to the edible taxa of the genus, and it appears that their dis-

tribution is wide. However, the analysis of a far greater number of samples is required before the real diversity of this group of species may be known and the knowledge of the edible mushrooms of Mexico expanded.

Hebeloma species have been considered as "early-stage [ectomycorrhizal] fungi" (Deacon et al. 1983; Mason et al. 1983; Gryta et al. 1997) and gained a reputation as nursery fungi (e.g., Castellano and Molina 1989; Menkis and Vasaitis 2011). There are other species in the genus, further to *H. ambustiterranum*, known to associate with burnt ground (Beker et al. 2016). High pH and nutrient levels are associated both with nurseries and burnt ground. It is not clear whether *H. ambustiterranum* occurs in nurseries. However, should *H. ambustiterranum* be considered for nursery typo utilizing edibles, knowing about the fire ecology should be helpful in establishing inoculum production and stabilizing *H. ambustiterranum* populations in the long-term.

While this study was limited with regard to collecting sites and the number of collections studied, nevertheless, with eleven species new to Mexico, it provides an important step in the understanding of the *Hebeloma* of Mexico and a basis for further development. Given how little we know about *Hebeloma* of Mexico, it appears premature to attempt a key. In lieu of a key for *Hebeloma* in Mexico (which would be deficient, based on too few collections), we refer to an interactive identification tool for *Hebeloma* that is currently under development (Bartlett et al. 2021, accepted).

Acknowledgements

We are very much obliged to A. Bogaerts and P. Ballings of the Botanic Garden Meise (BR) for help with handling various loans from a variety of herbaria. We also thank these herbaria for their help: AH, C, DAOM, DBG, DENA, DUKE, G, H, K, KRAM, L, LIP, LOD, LY, MAK, MICH, MONT, NY, PDD, PRM, ROHB, SWGC, TENN, TLXM, TNS, TURA, UPS and WTU. We are indebted to the staff at TLXM for supplying us with interesting and exciting *Hebeloma* collections. We thank E. Grilli for help with Latin translations. This work was partially supported by CONABIO Project X001 in the collection of specimens from Chihuahua. Roberto Garibay-Orijel and Laura Guzmán-Davalos are thanked for all the thought and work they put into reviewing and improving our manuscript. We thank Maria-Alice Neves for taking on this article as editor.

References

Aanen DK, Kuyper TW (1999) Intercompatibility tests in the *Hebeloma crustuliniforme* complex in northwestern Europe. Mycologia 91(5): 783–795. https://doi.org/10.1080/00275514.1999.12061084

Aanen DK, Kuyper TW, Hoekstra RF (2001) A widely distributed ITS polymorphism within a biological species of the ectomycorrhizal fungus *Hebeloma velutipes*. Mycological Research 105(3): 284–290. https://doi.org/10.1017/S0953756201003628

Abarenkov K, Tedersoo L, Nilsson RH, Vellak K, Saar I, Veldre V, Parmasto E, Prous M, Aan A, Ots M, Kurina O, Ostonen I, Jõgeva J, Halapuu S, Põldmaa K, Toots M, Truu J, Larsson K-H, Kõljalg U (2010) PlutoF – a Web based workbench for ecological and taxonomic research, with an online implementation for fungal ITS sequences. Evolutionary Bioinformatics Online 6: 189–196. https://doi.org/10.4137/EBO.S6271

Aremu MO, Basu SK, Gyar SD, Goyal A, Bhowmik PK, Datta Banik S (2009) Proximate composition and functional properties of mushroom flours from *Ganoderma* spp., *Omphalotus olearius* (DC.) Sing. and *Hebeloma mesophaeum* (Pers.) Quél. used in Nasarawa State, Nigeria. Malaysian Journal of Nutrition 15: 233–241.

Atkinson GF (1909) Preliminary notes on some new species of Agaricaceae and *Clavaria*. Annales Mycologici 7: 365–376.

Barroetaveña C, Rajchenberg MC (2005) Mycorrhizal fungi in *Pinus ponderosa* introduced in Central Patagonia (Argentina). Nova Hedwigia 80(3–4): 453–464. https://doi.org/10.1127/0029-5035/2005/0080-0453

Bartlett P, Eberhardt U, Schütz N, Beker HJ (2021) Machine learning for species identification: The *Hebeloma* project from database to website. Biodiversity Information Science and Standards 5: e73972. https://doi.org/10.3897/biss.5.73972

Beker HJ, Eberhardt U, Vesterholt J (2010) *Hebeloma hiemale* Bres. in arctic/alpine habitats. North American Fungi 5: 51–65.

Beker HJ, Eberhardt U, Vesterholt J, Hawksworth DL (2013) Proposal to conserve the name *Agaricus laterinus* (*Hebeloma laterinum*) against the sanctioned *Agaricus fastibilis* (*Hebeloma fastibile*) (Basidiomycota: Agaricales: Strophariaceae). Taxon 62: 1059–1060. https://doi.org/10.12705/625.27

Beker HJ, Eberhardt U, Vesterholt J (2016) *Hebeloma* (Fr.) P. Kumm. Fungi Europaei 13. Edizioni Tecnografica, Lomazzo, Italy, 1232 pp.

Benjamin DR (1995) Mushrooms, Poisons and Panaceas. W.H. Freeman and Company, New York.

Bresinsky A, Besl H (1990) A Colour Atlas of Poisonous Fungi. Wolfe, London, 295 pp.

Carrasco-Hernández V, Pérez-Moreno J, Quintero-Lizaola R, Espinosa-Solares T, Lorenzana-Fernández A, Espinosa-Hernández V (2015) Edible species of the fungal genus *Hebeloma* and two neotropical pines. Pakistan Journal of Botany 47: 319–326.

Castellano MA, Molina R (1989) Mycorrhizae. In: McDonald SE, Barnett JP (Eds) The Container Tree Nursery Manual, vol 5 Agricultural Handbook 674. U.S. Department of Agriculture, Forest Service, Washington D.C., 101–167.

Cripps C, Eberhardt U, Schütz N, Beker HJ, Evenson VS, Horak E (2019) The genus *Hebeloma* in the Rocky Mountain alpine zone. MycoKeys 46: 1–54. https://doi.org/10.3897/mycokeys.46.32823

Deacon JW, Donaldson SJ, Last FT (1983) Sequences and interactions of mycorrhizal fungi on birch. Plant and Soil 71(1–3): 257–262. https://doi.org/10.1007/BF02182660

Eberhardt U (2012) Methods for DNA barcoding fungi. In: Kress JW, Erickson DL (Eds) DNA Barcodes: Methods and Protocols. Humana Press Imprint (Springer), New York, 183–205. https://doi.org/10.1007/978-1-61779-591-6_9

Eberhardt U, Beker HJ (2010) *Hebeloma vesterholtii*, a new species in section *Theobromina*. Mycological Progress 9(2): 215–223. https://doi.org/10.1007/s11557-009-0627-z

Eberhardt U, Beker HJ, Vila J, Vesterholt J, Llimona X, Gadjieva R (2009) *Hebeloma* species associated with *Cistus*. Mycological Research 113(1): 153–162. https://doi.org/10.1016/j.mycres.2008.09.007

Eberhardt U, Beker HJ, Vesterholt J, Dukik K, Walther G, Vila J, Fernández Brime S (2013) European species of *Hebeloma* section *Theobromina*. Fungal Diversity 58(1): 103–126. https://doi.org/10.1007/s13225-012-0188-3

Eberhardt U, Beker HJ, Vesterholt J (2015) Decrypting the *Hebeloma crustuliniforme* complex: European species of *Hebeloma* section *Denudata* subsection *Denudata*. Persoonia 35: 101–147. https://doi.org/10.3767/003158515X687704

Eberhardt U, Beker HJ, Vesterholt J, Schütz N (2016a) The taxonomy of the European species of *Hebeloma* section *Denudata* subsections *Hiemalia*, *Echinospora* subsect. nov. and *Clepsydroida* subsect. nov. and five new species. Fungal Biology 120(1): 72–103. https://doi.org/10.1016/j.funbio.2015.09.014

Eberhardt U, Ronikier A, Schütz N, Beker HJ (2016b) The genus *Hebeloma* in the alpine belt of the Carpathians including two new species. Mycologia 107(6): 1285–1303. https://doi.org/10.3852/15-097

Eberhardt U, Beker HJ, Schütz N, Pedersen OS, Sysouphanthong P, Læssøe T (2020a) Adventurous cuisine in Laos: *Hebeloma parvisporum*, a new species in *Hebeloma* section *Porphyrospora*. Mycologia 112(1): 172–184. https://doi.org/10.1080/00275514.2019.1680220

Eberhardt U, Beker HJ, Schütz N, Mikami M, Kasuya T (2020b) Rooting Hebelomas: The Japanese '*Hebeloma radicosum*' is a distinct species, *Hebeloma sagarae* sp. nov. (Hymenogastraceae, *Agaricales*). Phytotaxa 456(2): 125–144. https://doi.org/10.11646/phytotaxa.456.2.1

Eberhardt U, Beker HJ, Borgen T, Knudsen H, Schütz N, Elborne SA (2021a) A survey of *Hebeloma* (Hymenogastraceae) in Greenland. MycoKeys 79: 17–118. https://doi.org/10.3897/mycokeys.79.63363

Eberhardt U, Schütz N, Beker HJ, Lee S, Horak E (2021b) *Hebeloma* in the Malay Peninsula: Masquerading within *Psathyrella*. MycoKeys 77: 117–141. https://doi.org/10.3897/mycokeys.77.57394

Eberhardt U, Schütz N, Bartlett P, Beker HJ (2022a) 96 North American taxa sorted – Peck's *Hebeloma* revisited. Mycologia online early. https://doi.org/10.1080/00275514.2021.2012063

Eberhardt U, Schütz N, Bartlett P, Hosaka K, Kasuya T, Beker HJ (2022b) Revisiting *Hebeloma* (Hymenogastraceae, Agaricales) in Japan: Four species recombined into other genera but three new species discovered. Mycological Progress 21(1): 447–472. https://doi.org/10.1007/s11557-021-01757-x

Estrada-Martínez E, Guzmán G, Tovar DC, Ortega Paczka R (2009) Contribución al conocimiento etnomicológico de los hongos comestibles silvestres de mercados regionales y comunidades de la Sierra Nevada (México). Interciencia 34: 25–33.

Flores Arzú R (2020) Diversity and importance of edible ectomycorrhizal fungi in Guatemala. In: Pérez-Moreno J, Guerin-Laguette A, Flores Arzú R, Yu F-Q (Eds) Mushrooms, Humans and Nature in a Changing World. Springer, Cham, 101–140. https://doi.org/10.1007/978-3-030-37378-8_4

Gagné A, Jean-Luc Jany J-L, Bousquet J, Khasa DP (2006) Ectomycorrhizal fungal communities of nursery-inoculated seedlings outplanted on clear-cut sites in northern Alberta. Canadian Journal of Forest Research 36(7): 1684–1694. https://doi.org/10.1139/x06-063

Garibay-Orijel R, Morales-Marañon E, Domínguez-Gutiérrey M, Flores-García A (2013) Caracterización morfológica y genética de las ectomicorrizas formadas entre *Pinus montezumae* y los hongos presentes en los bancos de esporas en la Faja Volcánica Transmexicana. Revista Mexicana de Biodiversidad 84(1): 153–169. https://doi.org/10.7550/rmb.29839

Gonzalez P, Labarère J (1998) Sequence and secondary structure of the mitochondrial small-subunit rRNA V4, V6, and V9 domains reveal highly species-specific variations within the genus *Agrocybe*. Applied and Environmental Microbiology 64(11): 4149–4160. https://doi.org/10.1128/AEM.64.11.4149-4160.1998

Grilli E, Beker HJ, Eberhardt U, Schütz N, Leonardi M, Vizzini A (2016) Unexpected species diversity and contrasting evolutionary hypotheses in *Hebeloma* sections *Sinapizantia* and *Velutipes* in Europe. Mycological Progress 15(1): 1–46. https://doi.org/10.1007/s11557-015-1148-6

Gryta H, Debaud J-C, Effosse G, Marmeisse R (1997) Fine scale structure of populations of the ectomycorrhizal fungus *Hebeloma cylindrosporum* in coastal sand dune forest ecosystems. Molecular Ecology 6(4): 353–364. https://doi.org/10.1046/j.1365-294X.1997.00200.x

Guindon S, Dufayard J-F, Lefort V, Anisimova M, Hordijk W, Gascuel O (2010) New algorithms and methods to estimate Maximum-Likelihood phylogenies: Assessing the performance of PhyML 3.0. Systematic Biology 59(3): 307–321. https://doi.org/10.1093/sysbio/syq010

Guzmán G (1977) Identificación de Los Hongos: Comestibles, Venenosos, Alucinantes y Destructores de La Madera. Editorial Limusa, Mexico City, 236 pp.

Hesler LR (1977) New species of Hebeloma. Kew Bulletin 31(3): 471–480. https://doi.org/10.2307/4119390

Hoang DT, Chernomor O, von Haeseler A, Minh BQ, Vinh LS (2018) UFBoot2: Improving the ultrafast bootstrap approximation. Molecular Biology and Evolution 35(2): 518–522. https://doi.org/10.1093/molbev/msx281

Kalyaanamoorthy S, Minh BQ, Wong TKF, von Haeseler A, Jermiin LS (2017) Fast model selection for accurate phylogenetic estimates. Nature Methods 14(6): 587–589. https://doi.org/10.1038/nmeth.4285

Katoh K, Standley DM (2013) MAFFT multiple sequence alignment software version 7: Improvements in performance and usability. Molecular Biology and Evolution 30(4): 772–780. https://doi.org/10.1093/molbev/mst010

Katoh K, Kuma K, Toh H, Miyata T (2005) MAFFT version 5: Improvement in accuracy of multiple sequence alignment. Nucleic Acids Research 33(2): 511–518. https://doi.org/10.1093/nar/gki198

Katoh K, Rozewicki J, Yamada KD (2019) MAFFT online service: Multiple sequence alignment, interactive sequence choice and visualization. Briefings in Bioinformatics 20(4): 1160–1166. https://doi.org/10.1093/bib/bbx108

Kauff F, Lutzoni F (2002) Phylogeny of the Gyalectales and Ostropales (Ascomycota, Fungi): Among and within order relationships based on nuclear ribosomal RNA small and large subunits. Molecular Phylogenetics and Evolution 25(1): 138–156. https://doi.org/10.1016/S1055-7903(02)00214-2

Kõljalg U, Nilsson RH, Abarenkov K, Tedersoo L, Taylor AFS, Bahram M, Bates ST, Bruns TD, Bengtsson-Palme J, Callaghan TM, Douglas B, Drenkhan T, Eberhardt U, Dueñas M, Grebenc T, Griffith GW, Hartmann M, Kirk PM, Kohout P, Larsson E, Lindahl BD, Lücking R, Martín MP, Matheny PB, Nguyen NH, Niskanen T, Oja J, Peay KG, Peintner U, Peterson M, Põldmaa K, Saag L, Saar I, Schüßler A, Scott JA, Senés C, Smith ME, Suija A, Taylor DL, Telleria MT, Weiß M, Larsson K-H (2013) Towards a unified paradigm for sequence-based identification of Fungi. Molecular Ecology 22(21): 5271–5277. https://doi.org/10.1111/mec.12481

Kõljalg U, Nilsson HR, Schigel D, Tedersoo L, Larsson K-H, May TW, Taylor AFS, Jeppesen TS, Frøslev TG, Lindahl BD, Põldmaa K, Saar I, Suija A, Savchenko A, Yatsiuk I, Adojaan K, Ivanov F, Piirmann T, Pöhönen R, Zirk A, Abarenkov K (2020) The taxon hypothesis paradigm—On the unambiguous detection and communication of taxa. Microorganisms 8(12): 1910. https://doi.org/10.3390/microorganisms8121910

Kumar S, Stecher G, Li M, Knyaz C, Tamura K (2018) MEGA X: Molecular Evolutionary Genetics Analysis across computing platforms. Molecular Ecology and Evolution 35(6): 1547–1549. https://doi.org/10.1093/molbev/msy096

Larsson A (2014) AliView: A fast and lightweight alignment viewer and editor for large data sets. Bioinformatics (Oxford, England) 30(22): 3276–3278. https://doi.org/10.1093/bioinformatics/btu531

Mason PA, Wilson J, Last FT, Walker C (1983) The concept of succession in relation to the spread of sheathing mycorrhizal fungi on inocculated tree seedlings growing in unsterile soils. Plant and Soil 71(1–3): 247–256. https://doi.org/10.1007/BF02182659

Menkis A, Vasaitis R (2011) Fungi in roots of nursery grown *Pinus sylvestris*: Ectomycorrhizal colonialization, genetic diversity and spatial distribution. Microbial Ecology 61(1): 52–63. https://doi.org/10.1007/s00248-010-9676-8

Minh BQ, Nguyen MAT, von Haeseler A (2013) Ultrafast approximation for phylogenetic bootstrap. Molecular Biology and Evolution 30(5): 1188–1195. https://doi.org/10.1093/molbev/mst024

Monedero LC, Alvarado P (2020) *Hebeloma adherens*: Una nueva especie de la sección *Adherentia* sect. nov. Yesca 32: 56–67.

Montoya A, Estrada-Torres A, Caballero J (2002) Comparative ethonomycological survey of three localities from La Malinche volcano, Mexico. Journal of Ethnobiology 22: 103–133.

Montoya A, Hernández N, Mapes C, Kong A, Estrada-Torres A (2008) The collection and sale of wild mushrooms in a community of Tlaxcala, Mexico. Economic Botany 62(3): 413–424. https://doi.org/10.1007/s12231-008-9021-z

Murrill WA (1945) More Florida fungi. Lloydia 8: 263–290.

Nguyen L-T, Schmidt HA, von Haeseler A, Minh BQ (2015) IQ-TREE: A fast and effective stochastic algorithm for estimating maximum likelihood phylogenies. Molecular Biology and Evolution 32(1): 268–274. https://doi.org/10.1093/molbev/msu300

Oliveira RS, Franco AR, Vosátka M, Castro PML (2010) Management of nursery practices for efficient ectomycorrhizal fungi application in the production of *Quercus ilex*. Symbiosis 52(2–3): 125–131. https://doi.org/10.1007/s13199-010-0092-0

Peay KG, Bruns TD, Kennedy PG, Bergemann SE, Garbelotto M (2007) A strong species-area relationship for eukaryotic soil microbes: Island size matters for ectomycorrhizal fungi. Ecology Letters 10(6): 470–480. https://doi.org/10.1111/j.1461-0248.2007.01035.x

Pérez-Moreno J, Martínez-Reyes M, Hernández-Santiago F, Ortiz-Lopez I (2020) Climate change, biotechnology, and Mexican neotropical edible ectomycorrhizal mushrooms. In: Pérez-Moreno J, Guerin-Laguette A, Flores Arzú R, Yu F-Q (Eds) Mushrooms, Humans and Nature in a Changing World. Springer, Cham, 61–99. https://doi.org/10.1007/978-3-030-37378-8_3

Pérez-Moreno J, Guerin-Laguette A, Rinaldi AC, Yu F, Verbeken A, Hernández-Santiago F, Martínez-Reyes M (2021) Edible mycorrhizal fungi of the world: What is their role in forest sustainability, food security, biocultural conservation and climate change? Plants People Planet 3(5): 471–490. https://doi.org/10.1002/ppp3.10199

Reyes-López RC, Montoya A, Kong A, Cruz-Campuzano EA, Caballero-Nieto J (2020) Folk classification of wild mushrooms from San Isidro Buensuceso, Tlaxcala, Central Mexico. Journal of Ethnobiology and Ethnomedicine 16(53): 1–21. https://doi.org/10.1186/s13002-020-00408-x

Schoch CL, Seifert KA, Huhndorf S, Robert V, Spouge JL, Levesque CA, Chen W, Bolchacova E, Voigt K, Crous PW, Miller AN, Wingfield MJ, Aime MC, An K-D, Bai F-Y, Barreto RW, Begerow D, Bergeron M-J, Blackwell M, Boekhout T, Bogale M, Boonyuen N, Burgaz AR, Buyck B, Cai L, Cai Q, Cardinali G, Chaverri P, Coppins BJ, Crespo A, Cubas P, Cummings C, Damm U, de Beer ZW, de Hoog GS, Del-Prado R, Dentinger B, Diéguez-Uribeondo J, Divakar PK, Douglas B, Dueñas M, Duong TA, Eberhardt U, Edwards JE, Elshahed MS, Fliegerova K, Furtado M, García MA, Ge Z-W, Griffith GW, Griffiths K, Groenewald JZ, Groenewald M, Grube M, Gryzenhout M, Guo L-D, Hagen F, Hambleton S, Hamelin RC, Hansen K, Harrold P, Heller G, Herrera C, Hirayama K, Hirooka Y, Ho H-M, Hoffmann K, Hofstetter V, Högnabba F, Hollingsworth PM, Hong S-B, Hosaka K, Houbraken J, Hughes K, Huhtinen S, Hyde KD, James T, Johnson EM, Johnson JE, Johnston PR, Jones EBG, Kelly LJ, Kirk PM, Knapp DG, Kõljalg U, Kovács GM, Kurtzman CP, Landvik S, Leavitt SD, Liggenstoffer AS, Liimatainen K, Lombard L, Luangsa-ard JJ, Lumbsch HT, Maganti H, Maharachchikumbura SSN, Martin MP, May TW, McTaggart AR, Methven AS, Meyer W, Moncalvo J-M, Mongkolsamrit S, Nagy LG, Nilsson RH, Niskanen T, Nyilasi I, Okada G, Okane I, Olariaga I, Otte J, Papp T, Park D, Petkovits T, Pino-Bodas R, Quaedvlieg W, Raja HA, Redecker D, Rintoul TL, Ruibal C, Sarmiento-Ramírez JM, Schmitt I, Schüßler A, Shearer C, Sotome K, Stefani FOP, Stenroos S, Stielow B, Stockinger H, Suetrong S, Suh S-O, Sung G-H, Suzuki M, Tanaka K, Tedersoo L, Telleria MT, Tretter E, Untereiner WA, Urbina H, Vágvölgyi C, Vialle A, Vu TD, Walther G, Wang Q-M, Wang Y, Weir BS, Weiß M, White MM, Xu J, Yahr R, Yang ZL, Yurkov A, Zamora J-C, Zhang N, Zhuang W-Y, Schindel D, Fungal Barcoding Consortium (2012) Nuclear ribosomal internal transcribed spacer (ITS) region as a universal DNA barcode marker for Fungi. Proceedings of the National Academy of Sciences of the United States of America 109(16): 6241–6246. https://doi.org/10.1073/pnas.1117018109

Schoch CL, Robbertse B, Robert V, Vu D, Cardinali G, Irinyi L, Meyer W, Nilsson RH, Hughes KW, Miller AN, Kirk PM, Abarenkov K, Aime MC, Ariyawansa HA, Bidartondo MI, Boekhout T, Buyck B, Cai Q, Chen J, Crespo A, Crous PW, Damm U, De Beer ZW,

Dentinger BTM, Divakar APK, Duen M, Feau N, Fliegerova K, Garcıa MA, Ge ZW, Griffith GW, Groenewald JZ, Groenewald M, Grube M, Gryzenhout M, Gueidan C, Guo L, Hambleton S, Hamelin R, Hansen K, Hofstetter V, Seung-Beom Hong S-B, Houbraken J, Hyde KD, Inderbitzin P, Johnston PR, Karunarathna SC, Kõljalg U, Kovács GM, Kraichak E, Krizsan K, Kurtzman CP, Larsson K-H, Leavitt S, Letcher PM, Liimatainen K, Liu J-K, Lodge DJ, Luangsa-ard JJ, Lumbsch HT, Maharachchikumbura SSN, Manamgoda D, Martín MP, Minnis AM, Moncalvo J-M, Mulé G, Nakasone KK, Niskanen T, Olariaga I, Papp T, Petkovits T, Pino-Bodas R, Powell MJ, Raja HA, Redecker D, Sarmiento-Ramirez JM, Seifert KA, Shrestha B, Stenroos S, Stielow B, Suh S-O, Tanaka K, Tedersoo L, Telleria MT, Dhanushka Udayanga D, Untereiner WA, Uribeondo JD, Subbarao KV (2014) lgyi CV, Visagie C, Voigt K, Walker DM, Weir BS, Weiß M, Wijayawardene NN, Wingfield MJ, Xu JP, Yang ZL, Zhang N, Zhuang W-Y, Federhen S (2014) Finding needles in haystacks: Linking scientific names, reference specimens and molecular data for Fungi. Database (Oxford): 1–21. https://doi.org/10.1093/database/bau061/2634542

Smith AH, Evenson VS, Mitchel DH (1983) The Veiled Species of *Hebeloma* in the Western United States. University of Michigan Press, Ann Arbor, Michigan, 219 pp. https://doi.org/10.3998/mpub.12590

Stecher G, Tamura K, Kumar S (2020) Molecular Evolutionary Genetics Analysis (MEGA) for macOS. Molecular Biology and Evolution 37(4): 1237–1239. https://doi.org/10.1093/molbev/msz312

Tedersoo L, Mikryukov V, Anslan S, Bahram M, Khalid AN, Corrales A, Agan A, Vasco-Palacios A-M, Saitta A, Antonelli A, Rinaldi AC, Verbeken A, Sulistyo BP, Tamgnoue B, Furneaux B, Ritter CD, Nyamukondiwa C, Sharp C, Marín C, Dai DQ, Gohar D, Sharmah D, Biersma EM, Cameron EK, De Crop E, Otsing E, Davydov EA, Albornoz FE, Brearley FQ, Buegger F, Gates G, Zahn G, Bonito G, Hiiesalu I, Hiiesalu I, Zettur I, Barrio IC, Pärn J, Heilmann-Clausen J, Ankuda J, Kupagme JY, Sarapuu J, Maciá-Vicente JG, Fovo JD, Geml J, Alatalo JM, Alvarez-Manjarrez J, Monkai J, Põldmaa K, Runnel K, Adamson K, Bråthen KA, Pritsch K, Tchan KI, Armolaitis K, Hyde KD, Newsham KK, Panksep K, Adebola LA, Lamit LJ, Saba M, da Silva Cáceres ME, Tuomi M, Gryzenhout M, Bauters M, Bálint M, Wijayawardene N, Hagh-Doust N, Yorou NS, Kurina O, Mortimer PE, Meidl P, Nilsson RH, Puusepp R, Casique-Valdés R, Drenkhan R, Garibay-Orijel R, Godoy R, Alfarraj S, Rahimlou S, Põlme S, Dudov SV, Mundra S, Ahmed T, Netherway T, Henkel TW, Roslin T, Fedosov VE, Onipchenko VG, Yasanthika WAE, Lim YW, Piepenbring M, Klavina D, Kõljalg U, Abarenkov K (2021) The Global Soil Mycobiome consortium dataset for boosting fungal diversity research. Fungal Diversity 111(1): 573–588. https://doi.org/10.1007/s13225-021-00493-7

Trifinopoulos J, Nguyen LT, von Haeseler A, Minh B (2016) W-IQ-TREE: A fast online phylogenetic tool for maximum likelihood analysis. Nucleic Acids Research 44(W1): W232–W235. https://doi.org/10.1093/nar/gkw256

Vesterholt J (2005) The Genus *Hebeloma*. Fungi of Northern Europe 3. Svampetryk, Tilst, Denmark, 146 pp.

Viveros-Assad LJ, Flores-Encarnación M, Carreño-López R, Munguía-Pérez R, Santiesteban NA, García-García SMC (2019) Etnomicología de la Sierra Nevada. RD ICUAP 5(15). http://rd.buap.mx/ojs-dm/index.php/rdicuap/article/view/393 [accessed 19 Jan 2021]

Supplementary material 1

Sequences used in the analyse

Authors: Ursula Eberhardt, Alejandro Kong, Adriana Montoya, Nicole Schütz, Peter Bartlett, Henry J. Beker

Data type: Docx file.

Explanation note: Sequences used in the analyses. Herbarium abbreviations follow Index Herbariorum (http://sweetgum.nybg.org/science/ih/) and are separated from the specimen numbers by a space or by a hyphen. MuOb, Mushroom Observer https://mushroomobserver.org/. HJB, personal collection of H.J. Beker unless preceded by an herbarium abbreviation.

Link: https://doi.org/10.3897/mycokeys.90.85267.suppl1

Supplementary material 2

Alignments and trees

Authors: Ursula Eberhardt, Alejandro Kong, Adriana Montoya, Nicole Schütz, Peter Bartlett, Henry J. Beker

Data type: Txt file.

Explanation note: This file includes all alignments and trees, including single locus trees associated with Eberhardt et al. (2022) Not (only) poison pies – *Hebeloma* (Hymenogastraceae, Agaricales) in Mexico.

Link: https://doi.org/10.3897/mycokeys.90.85267.suppl2

MycoKeys 90: 203–213 (2022)
doi: 10.3897/mycokeys.90.84866
https://mycokeys.pensoft.net

SHORT COMMUNICATION

A peer-reviewed open-access journal
MycoKeys
Launched to accelerate biodiversity research

Evidence for further non-coding RNA genes in the fungal rDNA region

Magnus Alm Rosenblad[1], Ellen Larsson[2], Arttapon Walker[3,4], Naritsada Thongklang[3,4], Christian Wurzbacher[5], R. Henrik Nilsson[2]

1 *Department of Chemistry and Molecular Biology, National Infrastructure of Bioinformatics (NBIS), Lundberg laboratory, University of Gothenburg, Gothenburg, Sweden* **2** *Gothenburg Global Biodiversity Centre, Department of Biological and Environmental Sciences, University of Gothenburg, Box 461, 405 30 Gothenburg, Sweden* **3** *Center of Excellence in Fungal Research, Mae Fah Luang University, Chiang Rai 57100, Thailand* **4** *School of Science, Mae Fah Luang University, Chiang Rai 57100, Thailand* **5** *Chair of Urban Water Systems Engineering, Technical University of Munich, Am Coulombwall 3, 85748 Garching, Germany*

Corresponding author: R. Henrik Nilsson (henrik.nilsson@bioenv.gu.se)

Academic editor: Francesco Dal Grande | Received 4 April 2022 | Accepted 14 June 2022 | Published 30 June 2022

Citation: Alm Rosenblad M, Larsson E, Walker A, Thongklang N, Wurzbacher C, Nilsson RH (2022) Evidence for further non-coding RNA genes in the fungal rDNA region. MycoKeys 90: 203–213. https://doi.org/10.3897/mycokeys.90.84866

Abstract

Non-coding RNA (ncRNA) genes play important, but incompletely understood, roles in various cellular processes, notably translation and gene regulation. A recent report on the detection of the ncRNA Signal Recognition Particle gene in the nuclear ribosomal internal transcribed spacer region of several species of three genera of ectomycorrhizal basidiomycetes prompted a more thorough bioinformatics search for additional ncRNA genes in the full fungal ribosomal operon. This study reports on the detection of three ncRNA genes hitherto not known from the fungal ribosomal region: nuclear RNase P RNA, RNase MRP RNA, and a possible snoRNA U14 in a total of five species of *Auricularia* and *Inocybe*. We verified their presence through resequencing of independent specimens. Two completed *Auricularia* genomes were found to lack these ncRNAs elsewhere than in the ribosomal operon, suggesting that these are functional genes. It seems clear that ncRNA genes play a larger role in fungal ribosomal genetics than hitherto thought.

Keywords

Basidiomycetes, IGS, ITS, MRP, non-coding RNA, RNase MRP, RNase P, SRP

Introduction

Non-coding RNA (ncRNA) are stretches of RNA – typically thought of as genes – that are not translated into proteins through translation. A range of functions has been ascribed to the various groups of ncRNAs known to date, including important roles in translation, gene regulation, and chromosome inactivation (Cech and Steitz 2014). The number of ncRNA genes in the human genome alone is believed to run in the thousands, although relatively few have been characterised to any satisfactory level (Li and Liu 2019). Knowledge of ncRNAs in fungal genomes is rudimentary by comparison, but ncRNAs appear to play important cellular roles in the relatively few fungi examined to date (Li et al. 2021). The ncRNAs identified in the present study are, with few exceptions, all ubiquitous in eukaryotes and there are as yet no examples of them missing in fungi. They play important roles in tRNA processing (RNase P RNA), rRNA maturation (RNase MRP RNA), and ER targeting of proteins (SRP RNA), and they constitute the RNA component of the respective ribonucleoprotein (RNP) particles (López et al. 2009; Akopian et al. 2013).

Alm Rosenblad et al. (2016) unexpectedly found sequence analysis-derived evidence of the ncRNA Signal Recognition Particle (SRP) RNAs in the nuclear ribosomal ITS1 region of 11 species in three ectomycorrhizal genera of the Basidiomycota: *Astraeus*, *Russula*, and *Lactarius*. Indirect evidence furthermore suggested that these SRP RNAs could be functional. Queries in the GenBank (Sayers et al. 2021) and UNITE (Nilsson et al. 2019; Abarenkov et al. 2022) databases failed to produce any other fungi with SRP RNA in their ITS region, raising questions as to why such a rare genetic element would have been gained several times independently in the ITS1 region of a set of three relatively closely related genera.

The recent trend of employing various high-throughput sequencing technologies to generate longer stretches of the fungal ribosomal operon than just the ITS region (Wurzbacher et al. 2019) offers a possibility to extend the search for fungal ncRNAs beyond the ITS region. The present study reports on a broadening of the search of Alm Rosenblad et al. (2016) to include a wider selection of ncRNAs and to cover the full nuclear ribosomal operon. We recovered and verified three to four different ncRNAs from the ribosomal intergenic spacer 1 (IGS1) region of a set of *Auricularia* and *Inocybe* species, and we submit that ncRNAs are elements that can no longer be disregarded in the context of fungal ribosomal biology.

Materials and methods

Sequence query

Since ncRNAs are conserved primarily on the secondary structure level rather than the primary sequence level, we queried GenBank for fungal ribosomal ncRNAs using the secondary structure covariance models from the Rfam database (Nawrocki et al. 2014)

and Dumesic et al. (2015) through the cmsearch and cmscan commands of the INFERNAL v1.1 package (Nawrocki and Eddy 2013). As a part of an ongoing phylogenetic study of the basidiomycete genus *Inocybe*, we also sequenced the full ribosomal operon of four *Inocybe* species: *Inocybe cincinnata*, *Inocybe flocculosa*, *Inocybe leiocephala*, and *Inocybe phaeocystidiosa*. We queried these, too, for any new ncRNAs. We considered only highly significant matches that passed the Rfam E-value threshold applied for each gene. We then double-checked all matches by detailed manual examination of all conserved motifs as well as the secondary structure to filter out any partial or spurious candidates.

Verification of ncRNA matches

After quality control filtering, our GenBank query produced more than 30 highly significant ncRNA matches belonging to four different ncRNA genes in the IGS1 region of several *Auricularia* species from Li et al. (2011). Attempts at locating the underlying fungal specimens through the publication were unsuccessful. However, other Asian specimens from the same and related species were located in the Mae Fah Luang University herbarium (Table 1). To rule out sequencing or assembly error by the initial sequence authors, we thus ordered and sequenced those specimens for the full ribosomal operon.

We targeted two species of *Auricularia* and four species of *Inocybe* for sequencing of the full ribosomal operon. The fungal DNA was extracted using a DNA plant Mini Kit (Qiagen) and subsequently amplified using the primers NS1rc and RCA95rc or Fun-rOP-F/Fun-rOP-R as detailed in Wurzbacher et al. (2019). Briefly, the long-range PCR was performed using the PrimeStar GLX polymerase (Takara) with a 2.5 min elongation time for the first primer pair, and a 4 min elongation time for the second primer pair for 36 cycles. The samples were subsequently barcoded by an index PCR with 10 additional cycles. The amplicons were then sequenced with either a MinION instrument (Oxford Nanopore Technologies; LSK-308 library preparation; R9.5 flow cell) or sequenced in circular consensus mode with a PacBio RSII (Pacific Biosciences). The generated sequence data were processed as outlined in Wurzbacher et al. (2019; Suppl. material 1) using a quality filtering step, demultiplexing, alignment, clustering, and consensus generation. The newly generated *Auricularia* and *Inocybe* consensus sequences were queried for the presence of ncRNAs as detailed above.

Assessment of ncRNA functionality in *Auricularia*

An opportunity to at least partially assess whether the ncRNAs found in the *Auricularia* specimens may be functional – rather than pseudogenes – presented itself through the draft genome assemblies of *Auricularia heimuer* (strain Dai 13782; NCBI WGS accession NEKD01; Fang et al. 2020) and *Auricularia cornea* (strain CCMJ2827, WGS RJDY01; Dai et al. 2019). If these genomes, too, were found to contain these ncRNAs in the ribosomal operon, but nowhere else in the genome, then that would suggest that those ncRNA copies are functional. The draft assemblies were queried with the Rfam covariance models as above.

Table 1. List of specimens/sequences with at least one ncRNA beyond the ordinary rRNA genes. GenBank and collection/herbarium accession numbers are shown. The columns SRP, nuclear RNase P, RNase MRP, and U14 indicate whether these genes were recovered in the ribosomal operon of the specimen/sequence in question. The majority of the *Auricularia auricula-judae* sequences are from Li et al. (2014). a) For entry WGS:NEKD01, the contig NEKD01000094 contains four operons covering SSU-5S. b) For entry WGS:AFVO01, no rRNA operon could be found in the assembly. c) For entry WGS:QFEN01, the ncRNA genes were found on separate contigs (viz. nuclear RNase P in QFEN01000681, RNase MRP in QFEN01000187, and SRP in QFEN01000909). d) For entry WGS:RJDY01, the ncRNA genes are found in the three operons in RJDY01000048. Accession numbers given in bold were produced as part of this study. WGS project identifiers refer to the NCBI Whole Genome Shotgun assembly database.

GenBank	Species name	Voucher specimen	nuclear RNase P	RNase MRP	SRP	U14
OM964555	*Inocybe cincinnata*	EL113-16	Y	N	N	Y
OM964556	*Inocybe flocculosa*	EL168-16	Y	N	N	Y
OM964554	*Inocybe leiocephala*	EL85-16	Y	N	N	Y
OM964557	*Inocybe phaeocystidiosa*	EL23-16	N	N	N	N
OM964558	*Auricularia cornea*	MFLU16-2108	Y	Y	Y	Y
OM964559	*Auricularia delicata*	MFLU16-2118	Y	Y	Y	Y
WGS:NEKD01	*Auricularia heimuer* (a)	Dai 13782	Y	Y	Y	Y
WGS:AFVO01	*Auricularia subglabra* (b)	TFB-10046 SS5	N	N	N	N
WGS:QFEN01	*Auricularia polytricha* (c)	MG66	Y	Y	Y	N
JF440699.1	*Auricularia polytricha*	AP112	Y	Y	Y	Y
JF440698.1	*Auricularia polytricha*	APFJ	Y	Y	Y	Y
JF440701.1	*Auricularia delicata*	ADFJ	Y	Y	Y	Y
JF440702.1	*Auricularia delicata*	AD5424	Y	Y	Y	Y
JF440697.1	*Auricularia fuscosuccinea*	AFJLH	Y	Y	Y	Y
JF440700.1	*Auricularia peltata*	APLME	Y	Y	Y	Y
MN156315	*Auricularia cornea*	B02	Y	Y	Y	Y
WGS:RJDY01	*Auricularia cornea* (d)	CCMJ2827	Y	Y	Y	Y
HQ414239.1	*Auricularia auricula-judae*	XK-1	Y	Y	Y	Y
HQ414240.1	*Auricularia auricula-judae*	HE-1	Y	Y	Y	Y
HQ414241.1	*Auricularia auricula-judae*	DP-5	Y	Y	Y	Y
HQ414242.1	*Auricularia auricula-judae*	XE-987	Y	Y	Y	Y
HQ414243.1	*Auricularia auricula-judae*	ZHI-5	Y	Y	Y	Y
JF440694.1	*Auricularia auricula-judae*	HW5D31	Y	Y	Y	Y
JF440695.1	*Auricularia auricula-judae*	5L0109	Y	Y	Y	Y
JF440696.1	*Auricularia auricula-judae*	5L0096	Y	Y	Y	Y
JF440735.1	*Auricularia auricula-judae*	9809	Y	Y	Y	Y
JF440737.1	*Auricularia auricula-judae*	HE-9	Y	Y	Y	Y
JF440738.1	*Auricularia auricula-judae*	ME-6	Y	Y	Y	Y
JF440739.1	*Auricularia auricula-judae*	XE-887	Y	Y	Y	Y
JF440740.1	*Auricularia auricula-judae*	HE-3	Y	Y	Y	Y
JF440741.1	*Auricularia auricula-judae*	SHAN-1	Y	Y	Y	Y
JF440742.1	*Auricularia auricula-judae*	8129	Y	Y	Y	Y
JF440743.1	*Auricularia auricula-judae*	DA-2	Y	Y	Y	Y
JF440744.1	*Auricularia auricula-judae*	173	Y	Y	Y	Y
JF440745.1	*Auricularia auricula-judae*	HME-1	Y	Y	Y	Y
JF440746.1	*Auricularia auricula-judae*	139	Y	Y	Y	Y
JF440747.1	*Auricularia auricula-judae*	186	Y	Y	Y	Y
JF440748.1	*Auricularia auricula-judae*	C21	Y	Y	Y	Y
JF440749.1	*Auricularia auricula-judae*	CBS-7	Y	Y	Y	Y
JF440750.1	*Auricularia auricula-judae*	DZ-1	Y	Y	Y	Y
JF440751.1	*Auricularia auricula-judae*	HEI-29	Y	Y	Y	Y
JF440752.1	*Auricularia auricula-judae*	SN-A8	Y	Y	Y	Y
JF440753.1	*Auricularia auricula-judae*	XP-10	Y	Y	Y	Y
JF440754.1	*Auricularia auricula-judae*	YM-1	Y	Y	Y	Y

GenBank	Species name	Voucher specimen	nuclear RNase P	RNase MRP	SRP	U14
JF440755.1	*Auricularia auricula-judae*	8808	Y	Y	Y	Y
JF440756.1	*Auricularia auricula-judae*	35431	Y	Y	Y	Y
JF440757.1	*Auricularia auricula-judae*	DA-1	Y	Y	Y	Y
JF440758.1	*Auricularia auricula-judae*	DA-3	Y	Y	Y	Y
JF440759.1	*Auricularia auricula-judae*	JY-1	Y	Y	Y	Y
JF440760.1	*Auricularia auricula-judae*	ZJ-310	Y	Y	Y	Y
JF440761.1	*Auricularia auricula-judae*	YE-K3	Y	Y	Y	Y
JF440762.1	*Auricularia auricula-judae*	HEI-916	Y	Y	Y	Y
JN712676.1	*Auricularia auricula-judae*	AU110	Y	Y	Y	Y

Results

Sequence query and verification of ncRNA matches

Our GenBank query produced more than 30 highly significant ncRNA matches (belonging to the four different ncRNA genes SRP RNA, nuclear RNase P RNA, RNase MRP RNA, and a possible U14) in the IGS1 region of several *Auricularia* species in GenBank (Fig. 1; Table 1; Suppl. material 2). We re-sequenced the full ribosomal operon of two of these *Auricularia* species plus four *Inocybe* species. An ncRNA query of the newly generated sequences verified that the same ncRNAs were present in the same order in these independent specimens, showing that the original GenBank sequences did not represent mis-assemblies or otherwise artifactual sequence data. Interestingly, another *Auricularia* species – *Auricularia polytricha* strain MG66 – was found to lack these ncRNAs altogether in the ribosomal operon. Similarly, we found a different combination of ncRNAs (nuclear RNase P and U14) in the IGS1 of *Inocybe cincinnata*, *Inocybe flocculosa*, and *Inocybe leiocephala*; however, *Inocybe phaeocystidiosa* was found to lack all of the above ncRNAs in the ribosomal operon (Fig. 1, Table 1).

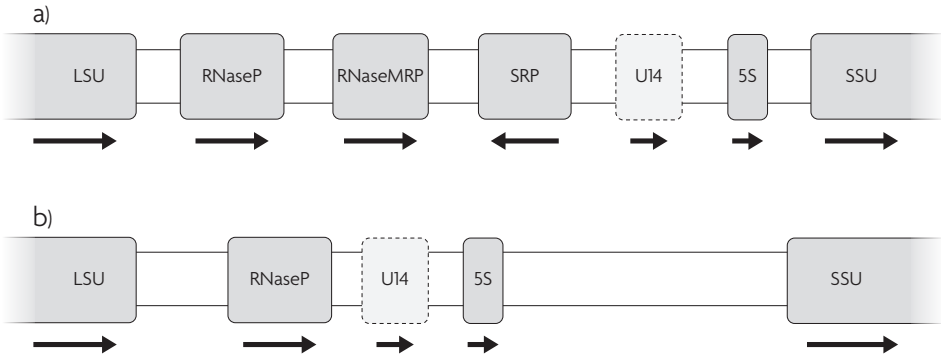

Figure 1. Schematic illustration of the fungal IGS region and neighbouring genes. Shown are **a** *Auricularia cornea* and **b** *Inocybe leiocephala*. The four ncRNA elements SRP RNA, nuclear RNase P RNA, RNase MRP RNA, and U14 are shown. U14 is shown in dashed outline to indicate its somewhat hypothetical nature. The arrows indicate strand. This schematic figure is not fully drawn to scale. The distance between LSU and SSU is approximately 5,000 bases, the length of U14 is approximately 200 bases, and the length of the other ncRNAs is approximately 300 bases.

Functional assessment

One of the contigs of the draft genome of *Auricularia heimuer* (NEKD01000094) was found to contain a ribosomal stretch comprising the expected rRNA genes nuclear small-subunit (nSSU), 5.8S in the ITS region, nuclear large-subunit (nLSU), and 5S but also the RNase P, MRP, and SRP genes, plus a putative U14/SNORD14 ncRNA copy. The result was the same for *Auricularia cornea.* No other copies of these ncRNAs were found in any other part of the genome assembly. *Auricularia subglabra* strain TFB-10046 SS5 (AFVO01) produced a similar result: we could not identify any of the ncRNAs in the genome assembly. Unfortunately, for this species the rDNA region was not included in the assembly or available elsewhere, but it seems probable that these ubiquitous ncRNAs would be located in the same region as in *A. heimuer*. The same result was obtained for *Auricularia auricula-judae* strain B14-8 (NCVV01). However, in the genome assembly of *Auricularia polytricha* strain MG66 (QFEN01), these ncRNAs were found on different contigs and none of these contigs contained any rRNA, implying those are the functional copies should additional ones exist also in the rDNA region. Interestingly, the *A. polytricha* strains AP112 and APFJ do have these ncRNAs in the IGS1 region, but there is no genome assembly available for either AP112 or APFJ.

Discussion

Alm Rosenblad et al. (2016) provided the first observation of an ncRNA other than the standard SSU, 5.8S, LSU, and 5S genes – namely the SRP RNA – in the ITS region of fungi. We expand on those findings by highlighting not only the SRP RNA gene but also an additional three ncRNA genes – nuclear RNase P RNA, RNase MRP RNA, and a possible U14 – in the IGS region of several *Auricularia* species. We verified the presence of these IGS ncRNAs through DNA sequencing of conspecific specimens. We furthermore used sequencing to recover the SRP RNA and a putative copy of the U14 gene in the IGS region of three *Inocybe* species. Our findings suggest that the SRP RNA results of Alm Rosenblad et al. (2016) were not isolated occurrences of limited interest to mycology and RNA biology. On the contrary, the SRP RNA gene seems to have been independently and repeatedly incorporated into the ribosomal operon of numerous fungi. This certainly warrants further investigation.

In addition to the SRP RNA, we also found strong evidence for two other ncRNAs in the IGS1 of both *Auricularia* specimens we sequenced – *Auricularia delicata* (MFLU16-2118) and *Auricularia cornea* (MFLU16-2108) – namely RNase P RNA and RNase MRP RNA. These genes correspond to important components for the maturation of tRNAs and rRNAs, respectively (López et al. 2009). While there are examples of a different type of nuclear RNase P in some organisms, all fungi use the standard RNP-type RNase P (Klemm et al. 2016). For the RNase MRP, there are, as yet, no examples of species lacking this RNP, although the exact composition of its protein subunits is unclear in some groups (Alm Rosenblad et al. 2021). Regarding the

U14 snoRNA, which also plays a part in the rRNA maturation process, the prediction score did pass the Rfam threshold, but since a thorough analysis of this ncRNA gene has not yet been made for basidiomycetes, we consider the predictions to be interesting candidates pending further analysis.

The fact that draft genome assemblies of *Auricularia heimuer* and *A. cornea* contain these RNAs in their ribosomal operon, but not elsewhere in the genome, suggests that these ncRNA genes are functional. Our approach does not enable us to prove that these ncRNAs indeed are functional, but the case for them as functional must be considered strengthened. The RNase P RNA and the RNase MRP RNA genes have been identified in introns of protein coding genes in metazoans such as *Caenorhabditis* and *Drosophila* (López et al. 2009), but there is no example of them from ribosomal operons. However, it has been shown in insects that the RNase P RNA, which is usually transcribed by pol III, is dependent on the recipient gene's pol II promoter and that splicing is not required for producing a mature RNase P RNA (Manivannan et al. 2015).

Interestingly, whereas our former study found SRP RNAs in the ITS1 region of strictly ectomycorrhizal species, this study reveals the presence of ncRNAs – including the SRP RNA – also in the non-ectomycorrhizal (but instead saprotrophic) basidiomycete genus *Auricularia*. This suggests that fungal nutritional mode may not determine or require the presence of these ncRNAs in the ribosomal operon, something that would be interesting to pursue in light of further data. It should nevertheless be pointed out that all five fungal genera from which ribosomal operon ncRNAs have been reported - *Astraeus*, *Russula*, *Lactarius, Inocybe,* and *Auricularia* – belong to the class Agaricomycetes of the Basidiomycota. The significance of this is unclear, but even a cursory glance at the finer levels of the Basidiomycota phylogeny shows that multiple independent gains/losses are needed to explain the observed ncRNA distribution. The fact that a single fungal class has seen a multitude of these events, whereas no other fungal class seems to have seen even a single one, certainly calls for an explanation.

It seems clear that ncRNAs must be taken into consideration in fungal ribosomal genetics. Four different ncRNAs are now known from the fungal ribosomal operon, and further research should screen genome and RNA operon sequences to determine how widespread ncRNAs are in fungi. Indeed, as databases accumulate a steadily increasing number of fungal ribosomal sequences that go far beyond the ITS region, there is every reason to think that additional ncRNAs will be recovered, presumably from non-Agaricomycetes fungi at that. The ribosomal operon is routinely excluded from many genome assemblies due to assembly difficulties (Hibbett et al. 2016), but our findings stress the importance of including it to enable research efforts like the present one. This study seeks to alert our fellow mycologists and RNA biologists to the presence of these ncRNAs in genetic regions where they up until recently were not expected to be, and we certainly hope that the evolutionary history of these ncRNAs and their presence in the fungal ribosomal operon will prove amenable to scientific explanation within not too long. *Auricularia* mycology primarily relies on genetic markers and genes such as the ITS region, nLSU, and RPB2 (Yuan et al. 2018; Wu et al. 2021), but several studies have explored the *Auricularia* IGS region for mycological usefulness

(e.g., Li et al. 2011 and Li et al. 2019). The present study suggests that caution is warranted when aligning the IGS region of *Auricularia* and possibly also other fungi due to the potential presence of these ncRNAs. Uncritical alignments may violate homology assumptions and may give rise to noisy multiple sequence alignments and skewed phylogenetic signals.

Conclusions

This study reports on the detection of three non-coding RNA genes hitherto not known from the fungal ribosomal region: nuclear RNase P RNA, RNase MRP RNA, and a possible snoRNA U14 in a total of five species of *Auricularia* and *Inocybe*. This expands on the recent finding of another non-coding RNA gene – the Signal Recognition Particle (SRP) RNA – in the internal transcribed spacer (ITS) region of three ectomycorrhizal genera of basidiomycetes. There are indications that these are functional genes rather than pseudogenes. The occurrence of these non-coding RNAs and their distribution in the fungal tree of life calls for further research attention but also caution in, e.g., multiple sequence alignment-based phylogenetic inference efforts involving the ribosomal regions of these fungi.

Acknowledgements

CW gratefully acknowledge funding from the German Research Foundation (DFG: WU890/2–1), and MAR gratefully acknowledges funding from Wilhelm and Martina Lundgrens Vetenskapsfond.

References

Abarenkov K, Kristiansson E, Ryberg M, Nogal-Prata S, Gómez-Martínez D, Stüer-Patowsky K, Jansson T, Põlme S, Ghobad-Nejhad M, Corcoll N, Scharn R, Sánchez-García M, Khomich M, Wurzbacher C, Nilsson RH (2022) The curse of the uncultured fungus. MycoKeys 86: 177–194. https://doi.org/10.3897/mycokeys.86.76053

Akopian D, Shen K, Zhang X, Shan S (2013) Signal recognition particle: An essential protein-targeting machine. Annual Review of Biochemistry 82(1): 693–721. https://doi.org/10.1146/annurev-biochem-072711-164732

Alm Rosenblad M, Martín MP, Tedersoo L, Ryberg M, Larsson E, Wurzbacher C, Abarenkov K, Nilsson RH (2016) Detection of signal recognition particle (SRP) RNAs in the nuclear ribosomal internal transcribed spacer 1 (ITS1) of three lineages of ectomycorrhizal fungi (Agaricomycetes, Basidiomycota). MycoKeys 13: 21–33. https://doi.org/10.3897/mycokeys.13.8579

Alm Rosenblad M, López MD, Samuelsson T (2021) The enigmatic RNase MRP of kinetoplastids. RNA Biology 25: 1–9. https://doi.org/10.1080/15476286.2021.1952758

Cech TR, Steitz JA (2014) The noncoding RNA revolution - trashing old rules to forge new ones. Cell 157(1): 77–94. https://doi.org/10.1016/j.cell.2014.03.008

Dai Y, Li X, Song B, Sun L, Yang C, Zhang X, Wang Y, Zhang Z, Fu Y, Li Y (2019) Genomic analyses provide insights into the evolutionary history and genetic diversity of *Auricularia* species. Frontiers in Microbiology 10: e2255. https://doi.org/10.3389/fmicb.2019.02255

Dumesic PA, Rosenblad MA, Samuelsson T, Nguyen T, Moresco JJ, Yates III JR, Madhani HD (2015) Noncanoncial signal recognition particle RNAs in a major eukaryotic phylum revealed by purification of SRP from the human pathogen *Cryptococcus neoformans.* Nucleic Acids Research 43(18): 9017–9027. https://doi.org/10.1093/nar/gkv819

Fang M, Wang X, Chen Y, Wang P, Lu L, Lu J, Yao F, Zhang Y (2020) Genome sequence analysis of *Auricularia heimuer* combined with genetic linkage map. Journal of Fungi 6(1): e37. https://doi.org/10.3390/jof6010037

Hibbett D, Abarenkov K, Kõljalg U, Öpik M, Chai B, Cole JR, Wang Q, Crous PW, Robert VARG, Helgason T, Herr J, Kirk P, Lueschow S, O'Donnell K, Nilsson RH, Oono R, Schoch CL, Smyth C, Walker D, Porras-Alfaro A, Taylor JW, Geiser DM (2016) Sequence-based classification and identification of Fungi. Mycologia 108: 1049–1068. https://doi.org/10.3852/16-130

Klemm BP, Wu N, Chen Y, Liu X, Kaitany KJ, Howard MJ, Fierke CA (2016) The diversity of ribonuclease P: Protein and RNA catalysts with analogous biological functions. Biomolecules 6(2): e27. https://doi.org/10.3390/biom6020027

Li J, Liu C (2019) Coding or noncoding, the converging concepts of RNAs. Frontiers in Genetics 10: e496. https://doi.org/10.3389/fgene.2019.00496

Li L, Liu W, Bian YB, Xiao Y (2011) Development of species-specific primers for identifying *Auricularia auricula-judae* using intergenic spacer 1 (IGS1) sequences. African Journal of Biotechnology 10(69): 15494–15500. https://doi.org/10.5897/AJB11.2433

Li L, Zhong CH, Bian YB (2014) The molecular diversity analysis of *Auricularia auricula-judae* in China by nuclear ribosomal DNA intergenic spacer. Electronic Journal of Biotechnology 17(1): 27–33. https://doi.org/10.1016/j.ejbt.2013.12.005

Li B-Y, Deng Y-J, Huang R-M, Zhao C, Wen Z-H, Xu W-N, Xie B-G (2019) Analyses of rDNA structure and preliminary evaluation of strains of *Auricularia* cornea based on IGS sequence. Junwu Xuebao 38: 2214–2220. https://doi.org/10.13346/j.mycosystema.190320

Li J, Liu X, Yin Z, Hu Z, Zhang KQ (2021) An overview on identification and regulatory mechanisms of long non-coding RNAs in fungi. Frontiers in Microbiology 12: e638617. https://doi.org/10.3389/fmicb.2021.638617

López MD, Rosenblad MA, Samuelsson T (2009) Conserved and variable domains of RNase MRP RNA. RNA Biology 6(3): 208–221. https://doi.org/10.4161/rna.6.3.8584

Manivannan SN, Lai LB, Gopalan V, Simcox A (2015) Transcriptional control of an essential ribozyme in Drosophila reveals an ancient evolutionary divide in animals. PLoS Genet 11(1): e1004893. https://doi.org/10.1371/journal.pgen.1004893

Nawrocki EP, Eddy SR (2013) Infernal 1.1: 100-fold faster RNA homology searches. Bioinformatics 29(22): 2933–2935. https://doi.org/10.1093/bioinformatics/btt509

Nawrocki EP, Burge SW, Bateman A, Daub J, Eberhardt RY, Eddy SR, Floden EW, Gardner PP, Jones TA, Tate J, Finn RD (2014) Rfam 12.0: Updates to the RNA families database. Nucleic Acids Research 43(D1): D130–D1373. https://doi.org/10.1093/nar/gku1063

Nilsson RH, Larsson K-H, Taylor AFS, Bengtsson-Palme J, Jeppesen TS, Schigel D, Kennedy P, Picard K, Glöckner FO, Tedersoo L, Saar I, Kõljalg U, Abarenkov K (2019) The UNITE database for molecular identification of fungi: Handling dark taxa and parallel taxonomic classifications. Nucleic Acids Research 47(D1): D259–D264. https://doi.org/10.1093/nar/gky1022

Sayers EW, Cavanaugh M, Clark K, Pruitt KD, Schoch CL, Sherry ST, Karsch-Mizrachi I (2021) GenBank. Nucleic Acids Research 49(D1): D92–D96. https://doi.org/10.1093/nar/gkaa1023

Wu F, Tohtirjap A, Fan LF, Zhou LW, Alvarenga RLM, Gibertoni TB, Dai YC (2021) Global diversity and updated phylogeny of *Auricularia* (Auriculariales, Basidiomycota). Journal of Fungi (Basel, Switzerland) 7(11): e933. https://doi.org/10.3390/jof7110933

Wurzbacher C, Larsson E, Bengtsson-Palme J, Van den Wyngaert S, Svantesson S, Kristiansson E, Kagami M, Nilsson RH (2019) Introducing ribosomal tandem repeat barcoding for fungi. Molecular Ecology Resources 19(1): 118–127. https://doi.org/10.1111/1755-0998.12944

Yuan H-S, Lu X, Decock C (2018) Molecular and morphological evidence reveal a new genus and species in Auriculariales from tropical China. MycoKeys 35: 27–39. https://doi.org/10.3897/mycokeys.35.25271

Supplementary material 1

Details of the sequence processing steps.

Authors: Magnus Alm Rosenblad, Ellen Larsson, Arttapon Walker, Naritsada Thongklang, Christian Wurzbacher, R. Henrik Nilsson

Data type: pdf file

Explanation note: Details of the sequence processing steps.

Link: https://doi.org/10.3897/mycokeys.90.84866.suppl1

Supplementary material 2

List of absolute positions of the rRNA and ncRNA genes in the six sequences released with this study

Authors: Magnus Alm Rosenblad, Ellen Larsson, Arttapon Walker, Naritsada Thongklang, Christian Wurzbacher, R. Henrik Nilsson

Data type: pdf file

Explanation note: List of absolute positions of the rRNA and ncRNA genes in the six sequences released with this study. The positions listed are from Infernal cmscan searches and the names are those used by Rfam. For *Auricularia*, the special model for basidiomycete SRP RNA from Dumesic et al. (2015) was used. Positions for the WGS contig of *Auricularia heimuer* mentioned in the text has been added below the sequences from this study. Note that the contig has been reverse-complemented before annotation to aid comparison. The contig contains four rRNA operons.

Link: https://doi.org/10.3897/mycokeys.90.84866.suppl2